FUNCTIONAL CHARACTERIZATION OF HGF AND ITS RECEPTOR C-MET IN ZEBRAFISH DEVELOPMENT

SHENG DONGLAI

(B. Sc.)

A THESIS SUBMITTED

FOR THE DEGREE OF DOCTOR OF PHILOSOPHY

DEPARTMENT OF BIOLOGICAL SCIENCES

NATIONAL UNIVERSITY OF SINGAPORE

2007

ACKNOWLEDGEMENTS

First of all, my deepest gratitude goes to my supervisor, Associate Professor Ge Ruowen, not only for giving me the opportunity to undertake this interesting project but also for her patience, encouragement, practical and professional guidance throughout my Ph. D candidature.

Secondly, I would like to express my heartfelt gratitude to A/P Gong Zhiyuan and A/P Low Boon Chuan for their guidance with the facilities and advice on my research project.

Thirdly, I would like to thank Mok Siew Li, Wang Xiaorui for their contribution for this study.

I would also like to thank the following friends and members in my laboratory who have helped me in one way or another: Liang Dong, Tan Lu Wee, Muhammad Farooq, Zhang Wei, Jiang Xia, Zhang Jianhua, Fan Huapeng, Ke Zhiyuan, Xiang Wei, Nilesh Kumar Mahajan, Jiang Junhui, Sulochana R, Sun Wei, Jia Jinghui, Lan Tian etc.

I want to thank the friends from other laboratories who assisted me in many ways and spent happy time with me such as Qian Zhuolei, Yu Hongbing, Li Mo, Tung Siew Lai, Wang Xiaoxing, Luo Min and Hu Yi etc.

More over, I must thank my parents, for their support in my career and life.

Finally, I thank the National University of Singapore for awarding me a research scholarship to carry out this interesting project.

TABLE OF CONTENTS

LIST OF PUBLICATIONS RELATED TO THIS STUDY

Sheng Donglai, Muhammad Farooq, Ge Ruowen. 2007. Characterizing HGF and its receptor c-met's role in zebrafish development (Manuscript in preparation).

LIST OF FIGURES

LIST OF ABBREVIATIONS

BCIP	5-bromo-3-chloro-3-indolyl phosphate
bp	base pair
BSA	bovine serum albumin
cDNA	DNA complementary to RNA
ddH2O	double distilled water
DEPC	diethyl pyrocarbonate
DIG	digoxigenin
DMSO	dimethylsulphoxide
DNA	deoxyribonucleic acid
dNTP	deoxyribonucleotide triphosphate
ECM	extracellular matrix
EDTA	ethylene diaminetetraacetic acid
EST	expressed sequence tag
EtOH	ethanol
GFP	green flurorescent protein
H2O	water
HCl	hydrochloric acid
hpf	hours post fertilization
kb	kilo base pair
KCl	potassium chloride
LB	Luria-Bertani medium
LiCl	lithium chloride
MgCl2	magnesium chloride
MgSO4	magnesium sulphate
MO	morpholino
mRNA	messenger ribonucleic acid
Na2HPO4	disodium hydrogen phosphate
NaCl	sodium chloride
NaOAc	sodium acetate
NaOH	sodium hydroxide
NBT	nitroblue tetrazolium
NCBI	national centre for biotechnology information
OD	optical density
PBS	phosphate-buffered saline
PBST	phosphate-buffered saline with 10% tween-20
PCR	polymerase chain reaction
PFA	paraformaldehyde
RACE	rapid amplification of cDNA ends
RNA	ribonucleic acid
rpm	revolution per minute
RT-PCR	reverse transcriptase-polymerase chain reaction
SDS	sodium dodecylsulfate
SSC	sodium chloride-trisodium citrate solution
SSCT	sodium chloride-trisodium citrate solution with 10% tween-20
tRNA	transfer ribonucleic acid
UTR	untranslated region
WISH	whole-mount in situ hybridization
ZFIN	zebrafish information network

Summary

Hepatocyte Growth Factor (HGF) is a pleiotropic factor that affects many aspects of biological functions through activation of its transmembrane tyrosine kinase receptor c-Met. This ligand/receptor pair has been shown to be essential for the development of several epithelial organs in mouse. However, many aspects of its function as well as the mechanisms of action are still unclear due to the early embryonic lethality of the knockout mice. In this study, we used zebrafish as a vertebrate model to study the developmental role of *hgf* and its receptor *c-met*. Full length cDNA of the two *hgf* genes *hgfa*, *hgfb* and the receptor *c-met* were cloned by PCR and their Expression analyzed by qRT-PCR as well as whole mount in situ hybridization. *hgfa* is mainly expressed in the somite during somitogenesis stage, indicating its role in somitogenesis. *hgfb* is expressed in liver mesenchyme while c-met was detected in hepatocytes, indicating their paracrine signaling in liver development. The co-expression of *hgfa* and *c-met* in pectoral fin, *hgfb* and *c-met* in proneprhic duct also indicate their paracrine signaling in the development of these organs in zebrafish.

Knockdown *hgfa* by morpholino antisense oligonucleotides resulted in curved truck and altered *myoD*, *fgf8* and *aldh1a2* expression patterns in somites, indicating roles of *hgfa* in zebrafish somitogenesis and myogenesis. In addition, the intersegmental vessel sprouting, especially the dorsal part is also affected in the *hgfa* morphants. Although *hgfa* is not expressed in liver or pancreas, knockdown of *hgfa* expression caused the left-right positional shift of these two organs and this shift is correlated with the curved trunk phenotype.

Knockdown of *hgfb* or *c-met* caused reduction in liver size which are dependent on

the extent of gene expression knockdown. Smaller liver correlated with lower level of endogenous *hgfb* or *c-met* expression in the *hgfb* morphants. Since the reduced liver size in *hgfb* or *c-met* morphants is only discernable after 4 dpf, and there is no change in the hepatocyte proliferation rate in morphants, it is likely that accelerated liver cell apoptosis is responsible.

These results indicate distinct expression and function of the two *hgfs* in zebrafish most likely through a shared receptor c-Met. The distinct function is mainly generated through differential gene expression both temporally as well as spatially. These studies expanded our understanding of HGF/c-Met in vertebrate development and established the foundation for further studies of their molecular mechanisms of action in various organs as well as their regulation of expression.

Chapter 1. Introduction

1.1 Discovery of HGF and its receptor c-met

1.1.1. Discovery of HGF

Hepatocyte growth factor (HGF) and scatter factor (SF) were originally identified as distinct cytokines that promote the growth or motility of epithelial cells, respectively. HGF was identified in the serum of partially hepatectomized rats as a potent mitogen for cultured rat hepatocytes (Michalopoulos et al., 1984; Nakamura et al., 1984). It was isolated from rat platelets (Nakamura et al., 1986), human plasma (Gohda et al., 1988), human serum (Zarnegar and Michalopoulos, 1989), and rat liver (Asami et al., 1991). The HGF cDNA has been cloned and sequenced (Miyazawa et al., 1989; Nakamura et al., 1989; Rubin et al., 1991; Tashiro et al., 1990). Scatter factor was originally described as a secretory product of fibroblasts that dissociate normal and malignant epithelial cells in vitro, increasing their motility and invasiveness (Gherardi et al., 1989; Stoker et al., 1987; Weidner et al., 1990). Sequence analysis (Gherardi and Stoker, 1990) and cDNA cloning from fibroblasts, placenta, and liver showed that HGF and scatter factor are identical (Naldini et al., 1991; Weidner et al., 1991). The molecular identity of the two cytokines has been further proven by their interchangeable activities in promoting hepatocyte growth, epithelial cell dissociation, and matrix invasion (Furlong et al., 1991; Naldini et al., 1991; Weidner et al., 1991). Nowdays people often name this protein as HGF/SF.

1.1.2. Discovery of c-met and identification of c-met as the receptor of HGF

In 1984, c-met was originally identified as a transforming gene from a chemically transformed human osteosarcoma-derived cell line (Cooper et al., 1984). In 1986, its cloning revealed that the oncogene encoded a truncated tyrosine kinase due to chromosomal rearrangement (Park et al., 1986). Although the oncogene product is predominantly a cytosolic kinase, the proto-oncogene product was identified as a transmembrane receptor-like protein (Park et al., 1987). In 1991, a 145kD tyrosyl phosphoprotein observed in rapid response to HGF treatment of intact target cells was identified by immunoblot analysis as the β subunit of the *c-met* proto-oncogene product, a membrane-spanning tyrosine kinsase (Bottaro et al., 1991). Covalent cross-linking of ^{125}I-labeled ligand to the cellular proteins of appropriate size recognized by c-met antibody established the c-met product as the cell-surface receptor for HGF (Bottaro et al., 1991).

1.2. Structure of HGF and c-met

1.2.1. Structure of HGF

HGF is a member of the plasminogen-related growth factor (PRGFs) family, thus is sometimes also referred as PRGF-1. Human *HGF* gene spans 70 kb on chromosome 7q21.1 and is initially produced as pro-HGF, a single chain precursor, which is subsequently cleaved by a protease to produce HGF which forms a two-chain heterodimer (Mars et al., 1993; Seki et al., 1991). The larger α chain (residues 1–494) contains a typical signal peptide, cleaved during secretion, followed by five distinct domains: an N-terminal (N) hairpin loop homologous to the activation peptide of plasminogen and four kringle (K) domains. The smaller β chain (residues 495–728) resembles a typical serine protease domain (Fig1.1).

1.2.2 Structure of c-met

The human *MET* gene is located on chromosome 7 band 7q21–q31 and spans more than 120 kb in length (Duh et al., 1997; Liu, 1998). In wild-type cells, the primary *MET* transcript produces a 150 kDa polypeptide that is partially glycosylated to produce a 170 kDa precursor protein. This 170 kDa precursor is further glycosylated and then cleaved into a 50 kDa α chain and a 140 kDa β chain, which are linked via disulfide bonds. The mature MET heterodimer thus consists of a highly glycosylated extracellular α subunit and a β subunit with a large extracellular region, a membrane spanning segment, and an intracellular tyrosine kinase domain (Fig1.1).

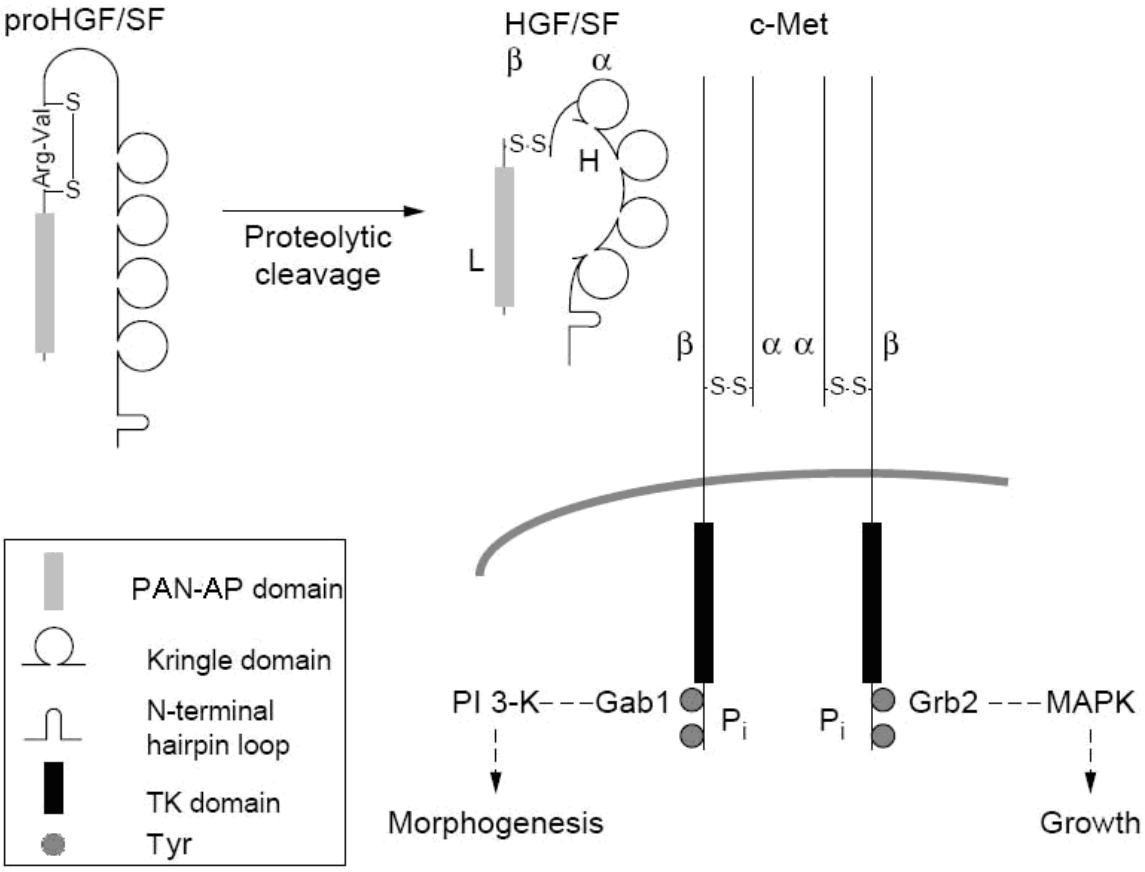

Fig.1.1 Schematic representation of proHGF/SF, HGF/SF and the c-Met receptor. Proteolytic cleavage of proHGF/SF generates the heavy (H) and light (L) chain of the active factor and is accompanied by a major conformational change. Active HGF/SF binds to c-Met, inducing receptor dimerization and activation.(from Birchmeier and Gherardi, 1998) (PAN-AP domain, divergent subfamily of APPLE domains, TK domain, Tyrosine kinase, catalytic domain)

1.3 HGF regulation by HGF activator (HGFA) and HGFA inhibitor (HAIs)

HGF/SF is a heparin-binding glycoprotein secreted by mesenchymal cells as an inactive single-chain precursor (also known as pro-HGF) with a molecular weight of around 94 kD. HGF/SF remains in this precursor single-chain form, probably associated with ECM in the producing tissue and/or with cellular surface proteoglycans (Matsumoto and Nakamura, 1996; Naldini et al., 1992). To generate biologically active HGF, the conversion of an inactive single-chain precursor form to a two-chain heterodimeric active form by a single proteolytic cleavage between Arg494 and Val495 is essential (Naka et al., 1992; Naldini et al., 1992). Activation of the inactive HGF is a highly regulated process that requires orchestration of a number of enzymes. One of the most powerful activators is the HGF activator, HGFA (Miyazawa et al., 1993; Shimomura et al., 1995). Other activators include urokinase-type plasminogen activator (Mars et al., 1993; Mars et al., 1996; Naldini et al., 1992); injurin, an inducer of expression of the gene for hepatocyte growth factor (Matsumoto et al., 1992); blood coagulation factor XIIa (Shimomura et al., 1995); membrane-type serine protease-1 (MT-SP1) (Lee et al., 2000); hepsin, a cell surface serine protease (Herter et al., 2005; Kirchhofer et al., 2005).

HGFA is a member of the Kringle-serine proteinase superfamily, and its molecular structure resembles that of the coagulation factor XII (Miyazawa et al., 1993). It is secreted mainly by the liver and circulates in the plasma as an inactive single-chain 96-kDa proform (proHGFA) (Miyazawa et al., 1993). Therefore, activation of proHGFA and efficient localization of mature HGFA to the desired tissue and cells

would be a prerequisite to utilize this potent enzyme in the pericellular activation of HGF. It has been shown that thrombin is responsible for the activation of proHGFA by cleavage at Arg407 in the presence of a negatively charged substance, resulting in an active two-chain heterodimeric form (Shimomura et al., 1993).

Mature HGFA is not inhibited by major serum proteinase inhibitors, and HGFA is, in fact, active in serum (Shimomura et al., 1992; Shimomura et al., 1995). Indeed, HGFA activity was initially identified in and purified from bovine serum (Shimomura et al., 1992). This evidence strongly suggests the existence of a regulatory system of HGFA activity in local tissue. This assumption led to the subsequent discovery of the HGFA inhibitor (HAI). The first endogenous HAI was purified from the culture-conditioned medium of an MKN45 gastric carcinoma cell line (Shimomura et al., 1997). Subsequently, a second type of HAI was purified from the same sample (Kawaguchi et al., 1997). These inhibitors were designated as HGFA inhibitor type 1 (HAI-1) and type 2 (HAI-2), respectively. Both HAI-1 and HAI-2 are Kunitz-type serine proteinase inhibitors. They have two Kunitz-type inhibitor domains that share a high degree of amino acid sequence identity. It is important to note that each HAI has a presumed transmembrane domain near the C-terminal end, suggesting that HAIs are type I transmembrane proteins. This unique structure would ensure their biological activities at the cellular surface in local tissues (Kataoka et al., 2002a). HAIs are also inhibitory against a number of other serine proteinases. Of particular interest is the observation in a study by Lin et al. (Lin et al., 1999) in which a secreted form of MT-SP1/matriptase was found to be complexed with HAI-1 in human milk. Therefore, MT-SP1/matriptase is a target proteinase of HAI-1 in vivo. HAI-1 also potently inhibits trypsin and plasmin in vitro (Denda et al., 2002; Kataoka et al., 2002a). HAI-2,

which appears to have broader inhibitory spectra against serine proteinases than HAI-1, inhibits plasma and tissue kallikreins, trypsin, plasmin and factor XIa very efficiently (Delaria et al., 1997).

.

Both HAI-1 and HAI-2 are synthesized as type I transmembrane proteins. However, only HAI-1 is a specific cellular inhibitor of active HGFA, which acts on the cell surface (Kataoka et al., 2000). Although the membrane-form HAI-2 is not acting as an HGFA inhibitor on the cell surface, the secreted-form HAI-2/PB generated by ectodomain shedding potently inhibits HGFA (Kataoka et al., 2002b; Kawaguchi et al., 1997; Qin et al., 1998).

1.4 HGF signaling pathways

HGF is known to be a paracrine factor that is produced by stromal and mesenchymal cells and acts on Met-expressing cells, mainly epithelial cells (Hayashi et al., 1996; Iwazawa et al., 1996; Nakashiro et al., 2000; Stella and Comoglio, 1999; Takai et al., 1997; Weimar et al., 1998; Yi et al., 1998). HGF/c-Met autocrine activation which lead to promotion of hepatocarcinogenesis has also been reported in HGF-transgenic mice (Horiguchi et al., 2002). A summary of HGF signaling pathway is shown in Fig.1.2.

c-Met signal transduction and regulation

c-Met is expressed by a variety of normal and malignant cells (Comoglio, 1993). Upon ligand binding, c-Met undergoes autophosphorylation of specific tyrosine residues within the intracellular region, which leads to the activation of the HGF/c-Met signaling pathway. Phosphorylation of Y1230, Y1234 and Y1235 located within the activation loop of the tyrosine kinase domain activates the intrinsic kinase activity of c-Met, whereas phosphorylated Y1313 is important in binding to PI3 kinase (PI3K) (with the YXXM motif). Phosphorylation of Y1349 and Y1356 in the C-terminus of c-Met activates the multisubstrate signal transducer docking site (Y1349VHVX3Y1356VNV) that can bind Src homology-2 (SH2) domains, phosphotyrosine binding (PTB) domains, and Met binding domains (MBD) of signal transducers and adapter proteins. Chimeric receptors containing this amino acid sequence can mediate cellular responses that are similar to those of Met, suggesting that this site is responsible for much of Met-mediated signal transduction. Mutational

analysis of the multisubstrate docking site suggests that Y1349 and Y1356 mediate the interactions with SHC, Src, and Gab1 while recruitment of Grb2, PI3-K, PLC-γ, and SHP2 is mediated by Y1356 (Furge et al., 2000). Regulation of morphogenesis of lung small cell carcinoma cell line is mediated via Y1365 (Maulik et al., 2002b). Within the juxtamembrane domain, the Y1003 residue has important role in binding to proteins such as c-Cbl, a protein binding to several activated tyrosine kinase receptors, acting either as a transducer or as a ubiquitin ligase, and thus has a role in receptor downregulation (Levkowitz et al., 1999; Thien and Langdon, 2001). Cbl binds and ubiquinates activated c-Met, promotes c-Met degredation. Moreover, by recruiting the endophilin-CIN85 complex, Cbl also regulates c-Met internalization. Internalization and subsequent degradation is a principal process regulating the duration and propagation of the signal initiated by c-Met, thereby preventing over-stimulation that could potentially lead to cellular transformation (Petrelli et al., 2002).

GAB1 pathway in c-Met mediated cell adhesion and migration

One of the major substrates of the activated c-Met is the adaptor protein GAB1 (GRB2-Associated Binding Protein-1). Phosphorylated GAB1 binds signal-relay molecules, such as the SH2-domain-containing proteins: SHP2 (Tyrosine Phosphatase-2), PI3K (Phosphatidylinositol-3 Kinase), PLC- γ (Phospholipase-C- γ), STAT3 (Signal Transducer and Activator of Transcription-3) and CrkL, through their SH2 domains. GAB1 interacts with CrkL, a protein with SH2 and SH3 protein interaction domains that couples to signaling further downstream (Fan et al., 2001). The actions of HGF on Pxn (Paxillin), DOCK1 (Dedicator of Cytokinesis-1) and Rap1 which alter cell motility are also mediated through GAB1. Through its SH3 domains, CrkL can associate with, and activate multiple effector proteins, like

DOCK1 C3G (Guanine Nucleotide Releasing Protein C3G), a GDP GTP exchange factor for Rap1. C3G is implicated in the activation of Rap1, which further activates FAK (Focal Adhesion Kinase) and Pxn, associated with Itg (Integrin). The activation of FAK induces the formation of focal adhesions, a preliminary step to increased cell motility and tissue invasion by transformed cells Paxillin phosphorylation may also alter cell adhesion of Met transformed cells (Birchmeier et al., 2003).

GRB2 pathway in c-Met mediated cytoskeletal regulation and motility

Activated Met can also recruit GRB2 (Growth Factor Receptor-Bound Protein-2), an adaptor protein that couples activated receptor tyrosine kinases to SOS (Son of Sevenless), promoting Ras activation (Schaeper et al., 2000). The activation and inactivation of Ras are regulated by GEPs (Guanine Exchange Proteins) and GAPs (GTPase-Activating Proteins). The major human GEP for Ras is SOS, which is constitutively associated with GRB2. Activation of Ras by HGF results in activation of Raf1, followed by the subsequent threonine and tyrosine phosphorylation of cytoplasmic dual specificity kinases, MEK1 (MAPK/ERK Kinase-1) and MEK2 (MAPK/ERK Kinase-2). The MEKs in turn activate the extracellular signal-regulated kinases: ERK1 and ERK2. The activation of these MAPKs is required for HGF-elicited cell scattering and tubulogenesis (Delehedde et al., 2001). Major substrates for ERKs are the transcription factors Elk1 and Ets, which upon activation, up-regulate the expression of immediate early response genes, such as c-Fos. The ERKs also stimulate the stress-responsive transcription factors: c-Jun and c-Fos, important for HGF-mediated survival. Regulation of Rac1 and CDC42 pathways in response to HGF contribute to cytoskeletal rearrangement and the subsequent changes in cellular

motility. HGF functions as a scattering factor for epithelial cells, and this ability is mediated through the activation of STAT3. Phosphorylation of STAT3 alters cellular transcription in addition to altering cell adhesion, proliferation and cell motility required for triggering differentiation for branching morphogenesis. Rac1 and CDC42, both are activated by phosphorylated Ras. DOCK1 also lies upstream of the Rac1 pathway (Gao and Vande Woude, 2005; Schaeper et al., 2000). Activation of the Rac1 pathway and the CDC42 pathway contributes to the regulation of cytoskeleton, thus culminating in cell polarity and cell motility.

PI3K in Met mediated cell survival and scattering

Protection of cells against DNA damage by HGF is mediated by a pathway from its receptor c-Met to PI3K through GAB1 to Akt and PAK1 (p21-Activated Kinase), resulting in enhanced DNA repair and decreased apoptosis (Xiao et al., 2001). Activation of PAK1 also inhibits Anoikis, a form of apoptosis which is induce by anchorage-dependent cells detaching from the surrouding extracellular matrix. The PI3K pathway is responsible for cell scattering by inducing the loss of intercellular junctions and cell migration. Akt, the downstream target of PI3K, exerts its anti-apoptotic effects in a variety of ways, including phosphorylation and activation of IKKs (I-KappaB Kinases). This results in I-KappaB degradation and allows NF-KappaB to enter the nucleus and activate transcription of anti-apoptotic genes. Another mechanism whereby Akt functions to promote survival is through phosphorylation of BAD. Akt also phosphorylates Procaspase9 and inhibits its protease activity, thus suppressing activation of Procaspase3 and promoting cell survival as Caspase3 activity has a reverse correlation with Akt activity (Delehedde et al., 2001). Activation of the Met receptor also results in an increase in receptor-

mediated activation of PLC-Gamma which catalyzes the generation of IP3 (Inositol 1,4,5-Trisphosphate) and DAG (Diacylglycerol) from PIP2 (Phosphatidylinositol 4,5-Bisphosphate), which act as second messenger molecules to mobilize intracellular Calcium and activate PKC (Protein Kinase-C) respectively. These signaling pathways act as important components of the cell survival and cell migratory response (Aoki et al., 2001).

Activation of transcription factors and cell cycle progresion

Activation of various transcription factors by HGF induces expression of several genes, involved in cell survival and cell cycle progression (Xiao et al., 2001). For example, CDK6 (Cyclin-Dependent Kinase-6), Rb (Retinoblastoma) and p27/p27(KIP1) (Cyclin Dependent Kinase Inhibitor-p27) are expressed, which act as positive regulators of cell cycle progression. The anti-apoptotic gene COX2 (Cyclooxygenase-2) is also induced by HGF in a c-Jun- and c-Fos-dependent manner (Ref.9). COX2 expression by HGF inhibits the process of Anoikis (also known as Suspension-Induced Apoptosis), is a term used to describe apoptosis of epithelial cells induced by loss of matrix attachment. This process is important for maintaining normal cell and tissue homeostasis (Zeng et al., 2002).

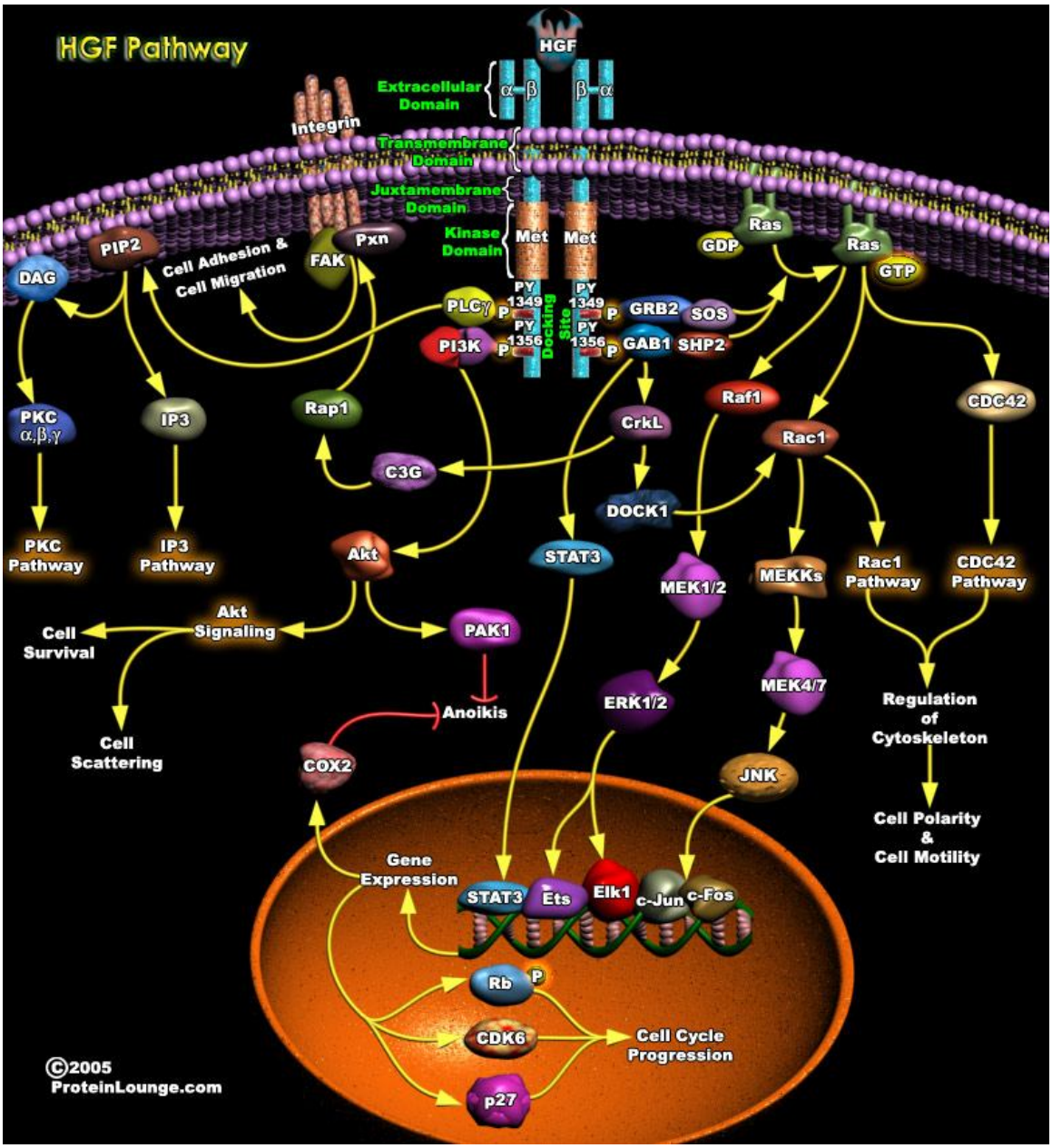

Fig.1.2 HGF signaling pathway. Active HGF/SF binds to c-Met, inducing receptor dimerization and activation. The multidocking site at the C-terminus of the c-Met is generated by phosphorylation of tyrosine residues (Tyr1349 and Tyr1356) upon HGF/SF binding. The multidocking site binds to various adaptor molecules that transmit the signals, which are essential for cell survival, cell scattering, cell cycle progression, cell polarity and cell motility. (from proteinlounge.com)

1.5 Biological functions of HGF and c-Met

1.5.1 Cell proliferation

HGF/c-Met signaling has been shown to promote proliferation of tumor cells derived from ovarian, gastric, glioma, lung adenocacinoma and squamous cell carcinoma, pancreatic, colorectal, prostate, and breast cancer patients. Activation of NF-kB has been shown to be essential for HGF-mediated proliferation and tubulogenesis in MLP29 liver cell line (Muller et al., 2002) and hepatic stem cells (Yao et al., 2004).

1.5.2 Cell survival

Dose-specific anti-apoptotic effects of HGF have been observed and, interestingly, high doses of HGF may be pro-apoptotic via a mechanism by which Met directly binds to and sequesters the death receptor Fas in hepatocytes. This interaction prevents Fas self-aggregation and Fas ligand binding, thus inhibiting Fas mediated apoptosis (Wang et al., 2002). c-Met activation by HGF induces tyrosine phosphorylation of focal adhesion kinase (p125FAK) at pY397 (autophosphorylation site, with binding to Src family SH2 and the p85 subunit of PI3-K) and pY861 (the major Src phosphorylation site) (Maulik et al., 2002a). p125FAK activation can be stimulated by integrin clustering as a result of integrin binding to extracellular matrix (ECM) ligands. Interestingly, p125FAK activation has been shown to promote cell proliferation, cell survival and migration. This anti-apoptotic effect would be important for tumor cells to survive during invasion and migration through ECM and distal tissues. Targets of FAK signaling implicated in the pro-survival pathways include RAS, RAC, PI3-K, ERK, and also CAS-CRK coupling.

1.5.3 Morphogenesis

Under physiological conditions, the HGF-Met signaling program activates a coordinated biological responses resulting in 'invasive growth' and 'branched morphogenesis'. The coordinated genetic control of the invasive program is believed to be essential in early embryonic development. Knock-out of either HGF or c-Met resulted in embryonic lethality in mice due to the severe defects in liver and placenta development in-utero (Birchmeier and Gherardi, 1998; Maina et al., 1996). A role of HGF in the nervous system development has also been suggested in these experiments, which have also been verified by other investigators and has been reviewed recently (Maina and Klein, 1999). More detailed information of developmental roles of HGF is reviewed in section 1.6.

1.5.4 Scattering

Scattering of adherent cells is a property of a variety of different cell types. The process of cell scattering can be divided into three phases, namely cell spreading, cell-cell dissociation, and cell migration. In order for epithelial cells to 'scatter', the attenuation of cell-cell adhesions is a prerequisite. Under physiological conditions, the assembly and maintenance of intercellular junctions is tightly regulated. Disassembly of these junctions occurs during normal development as well as tumor cell invasion/metastasis (Weisberg et al., 1997). HGF was discovered as a secreted product of fibroblasts and smooth muscle cells that induced dissociation and motility of epithelial cells (scatter factor). HGF is able to induce cell dissociation and mutual repulsion in a manner similar to semaphorins (Stella and Comoglio, 1999).

Cytoskeleton and focal adhesion regulation is required for scattering activity. The cytoskeleton is composed of a network of fibrous proteins within the cytoplasm of eukaryotic cells that plays pivotal structural and regulatory roles in the maintenance of cell structure and strength, cell division, proliferation, cell motility and invasion, as well as signaling functions. Cytoskeletal functions are mediated by a host of cytoskeletal proteins, the actin filament being the most abundant one. Other accessory proteins include cell surface adhesion receptor integrins, focal adhesion proteins, adapter proteins such as Crk and CRKL, non-receptor tyrosine kinases such as PI3-K, and cadherin/catenin complexes (Sattler et al., 2000; Sattler and Salgia, 1998). Receptor tyrosine kinase-generated signals can cause modification of phosphorylation of key cytoskeletal regulatory and structural proteins, as seen in the catalytically active p125FAK, SH2-containing tensin, and the multifunctional LIM domain-containing paxillin (Weisberg et al., 1997). The interactions of focal adhesion proteins, with each other and other proteins, may be altered after cellular transformation. Paxillin is a 68 kDa adapter protein containing several protein binding motifs for Srchomology2 (SH2) and SH3 domain-containing proteins such as Crk/CRKL and Src, five leucineand aspartate-rich (LD) domains, and four tandem-repeat double-zinc finger LIM domains that are employed to recruit signaling complexes to focal adhesions (Salgia et al., 1995; Sattler et al., 2000). Paxillin integrates adhesion- and growth factor-dependent signals with alterations in gene expression and actin reorganization. The ECM, β1- and β2-Integrin cross-linking, growth factor stimulation, and neuropeptide stimulation can induce tyrosine phosphorylation of paxillin. HGF/c-Met signaling has been shown to induce tyrosine phosphorylation of paxillin (Parr et al., 2001), and specifically at the tyrosine residue pY31 (the first CRKL bindingsite) but not pY118 or pY181 (Maulik et al., 2002a). Paxillin is known

to bind directly to focal adhesion kinase (p125FAK), as well as other molecules such as vinculin, clathrin and the tyrosine-phosphatase PEST (Turner, 2000a; Turner, 2000b). Paxillin signaling also converges with the Rho-dependent signaling pathway in the regulation of cell motility. Interestingly, paxillin has recently been shown to bind directly with schwannomin, the NF-2 gene product, at residue 50–70 (exon 2) where in-frame deletions and missense mutations have been identified, in mediating the dominant genetic disorder Neurofibromatosis type 2 (Fernandez-Valle et al., 2002). This interaction mediates the membrane localization of schwannomin to the plasma membrane, where it associates with β1-integrin and erbB2. p125FAK (focal adhesion kinase) is a 125 kDa protein, consisting of a N-terminus integrin-binding site, a central kinase domain, and a C-terminus focal adhesion targeting and paxillin-binding domains (Schaller and Sasaki, 1997). p125FAK family members include proteins such as PYK2 and FAK-B. p125FAK can interact with

integrins, paxillin, PI3-K, SH3 domain-containing adapter proteins, and other tyrosine kinases via an autophosphorylation site at tyrosine residue 397 (pY397). Its activation most likely occurs via tyrosine phosphorylation, which has been shown to be induced by HGF in SCLC (Maulik et al., 2002a). p125FAK was phosphorylated on pY397 (autophosphorylation site) and pY861 (the major Src phosphorylation site) in response to HGF. Overexpression of p125FAK in MDCK cells enhances the cell migration component of the HGF-induced cell scattering. Chan et al. has reported synergistic effect of FAK overexpression and HGF stimulation on cellular transformation in MDCK cells (Chan et al., 2002). Similarly, PYK2 was phosphorylated on pY402 (autophosphorylation site) and pY881 (Grb2 bindingsite) in response to HGF (Maulik et al., 2002a). The phosphorylation of the Grb2 binding site on PYK2 suggests a means to differentially activate the Ras/MAP kinase pathway.

1.5.5 Cell motility

Many studies have shown that HGF/c-Met signaling increases the motility of epithelial cells. Motility of small cell lung cancer (SCLC) cells is increased with HGF stimulation (Maulik et al., 2002a). Constitutively active c-Met induces the motility of Madin-Darby canine kidney cells (Jeffers et al., 1998). Cell motility comprises formation and retraction of filopodia/lamellipodia as well as uropod alteration in actin filament formation and cell migration (Weisberg et al., 1997). Cell motility is tightly controlled by the lipid kinase PI3-K and p21GTPases including Ras, Rac and Rho (Nobes and Hall, 1995a; Nobes and Hall, 1995b). PI3-K appears to be an important molecule in HGF-induced mito-, moto- and morpho-genesis, since inhibition of PI3-K by wortmannin leads to decreased branching formation on collagen matrix and chemotaxis of renal cells (Derman et al., 1995; Derman et al., 1996). In a recent study, HGF was found to induce transactivation of the EGFR in epithelial cells, and this is a prerequisite for induction of full motility (Spix et al., 2007).

1.5.6 Tumor invasion and metastasis

The concept of tumor invasion as a result of dysregulation of cell motility has gained much attention in recent years. Experimental evidence suggests that tumor invasion can be a distinct characteristic of tumor progression. In order for primary tumor cells to invade a tissue boundary and metastasize, they must degrade or remodel the surrounding extracellular matrix (ECM), which allows the tumor cells to eventually migrate through the ECM tissue boundary. Positive regulation of invasion and proteases by HGF/c-Met signaling has been shown. Mechanisms of the regulation

include upregulation of urokinase-type plasminogen activator (uPA), plasminogen activator inhibitor-1 (PAI-1), and matrix metalloproteases (MMPs) in tumor cells (Besser et al., 1997; Dunsmore et al., 1996; Wojta et al., 1994). In addition, consensus has been growing to believe that the rate-limiting step in invasion is cell migration. Reorganization of cytoskeletal scaffolds in the cell contributes to motility and migration. Both integrins (adhesion receptors) and growth factors/cytokines can modulate tumor cell motility, migration and hence invasion. Activation of PLCg, mobilizing actin-modifying proteins, was initially described as necessary for motility induced by EGF, PDGF, and IGF-1 (Gilmore and Burridge, 1996). Cell motility, as reflected by formation of membrane ruffles and filopodia, is well regulated by small GTPase and PI3-K. The actin cytoskeleton needs to be very dynamic for rapid alterations of cell shape, adhesion and de-adhesion during cell motility and migration. Ras-like GTPases of the Rho family, which includes Rho, Rac, and Cdc42, can reorganize actin.

The mechanism whereby HGF stimulation of c-Met leads to increased motility, migration and invasion is not well understood. c-Met signaling was first shown to be important in invasion when it was found that in mutant mice nullizygous for Met, muscles originating from dermomyotome cells that migrate to the limb, diaphragm and tip of the tongue fail to develop (Bladt et al., 1995). HGF/c-Met signaling is now known to be the main pathway mediating normal and malignant invasive growth. In addition, recent emerging data also point to the potential importance of other signaling molecules structurally related to c-Met, i.e. semaphorins and their receptors plexins.

With increased invasion, there is also increased metastasis seen in a variety of solid tumors (Maulik et al., 2002c). As an example, neoplastic cells harboring somatic activating mutations of c-Met, namely Y1230C and Y1235D, have been found to be selected, via clonal expansion, duringthe metastatic spread of head and neck squamous-cell carcinomas (Di Renzo et al., 2000). This is the first report providing evidence of a direct involvement of c-Met driving tumor cells metastasis in human malignancy. Moreover, a recent molecular profilingof metastatic murine squamous carcinoma cells by differential display and cDNA microarray revealed altered expression of multiple genes, notably including the RTK c-Met (up-regulated expression), during tumor progression (Dong et al., 2001). c-Met has been associated with metastatic progression in various tumors (Comoglio and Boccaccio, 2001; Jeffers et al., 1996). HGF/c-Met autocrine loop have been reported in various human primary and metastatic tumors, including breast cancer, osteosarcoma, glioblastoma and melanoma (Ferracini et al., 1995; Koochekpour et al., 1997; Li et al., 2001; Tuck et al., 1996). Using Tpr/Met as the oncogenic model, Giordano et al. (Giordano et al., 1997) reported a point mutation H1351N, located within the signal transducer docking site of Met, dissociated neoplastic transformation (increased) from metastasis (abrogated), implying the importance of this multifunctional docking site in mediating the metastatic potential of the oncogene. Bardelli et al. (Bardelli et al., 1999) have demonstrated concomitant activation of pathways downstream of Grb2 and PI3-K is a requirement for Met-mediated metastasis. More recently, Saucier et al. (Saucier et al., 2002) used Tpr/Met oncoprotein model and generated variant forms of the oncoprotein with ability to bind individually to the PI3-K-p85, PLCg, or to the Grb2 or Shc adapter proteins. They found that variants that recruit the Shc or Grb2 generated transformed fibroblast cells foci, induced anchorage-independent growth,

scattering and also experimental nude mice metastasis; which was not seen in cells expressing the PI3-K variant. This suggests that pathways downstream from Grb2 or Shc are sufficient for cell transformation and metastasis. cDNA microarrays analysis has been used to explore the transcriptional response to HGF of MLP-29 mouse embryo liver cells. The RGD-containing secreted matrix glycoprotein osteopontin (OPN) was identified as a major HGF transcriptional target, mediating HGF-induced invasive growth as an autocrine mediator (Medico et al., 2001).

Under physiological conditions, c-Met expressed on epithelial cells is activated in a paracrine fashion by mesenchymally derived HGF. Yu and Merlino (Yu and Merlino, 2002) have reported in a transgenic transplantation mice model that pulmonary metastasis of c-Met overexpressing tumor cells is stimulated when introduced into transgenic mice overexpressing either HGF or its variant NK2, and that the metastatic potential of the resultant heterotypic c-Met signaling was equivalent to that of the HGF/c-Met autocrine signaling loop. Wanget al. (Wang et al., 2001) have showed that overexpression of c-Met allows activation of the RTK by cell attachment/adherence in a ligandin dependent fashion, with tumorigenic capacity. Transgenic mice overexpressing c-Met in hepatocytes developed hepatocellular carcinoma (HCC). They further showed full regression of the hepatic tumors elicited by transgenic c-Met, with reconsititution of normal tissue architecture, is possible when the transgene was inactivated, even in the case of advanced stages of tumor progression. This study provides strong support for an important role of overexpression of c-Met in sustaining HCC in addition to its pathogenesis. More importantly, it offers convincing evidence that therapeutic inhibition targeting against the oncogene in c-Met overexpressing tumors would have very promising potential.

1.5.7 Angiogenesis

Angiogenesis is defined as the formation of new blood vessels from an existing vascular bed (reviewed by Risau, 1997). It is a key step in physiological processes such as wound healing and the menstrual cycle. In contrast, multiple pathological conditions such as cancer, atherosclerosis, arthritis, diabetic retinopathy, and psoriasis are characterized by overt angiogenesis (reviewed by Griffioen and Molema, 2000). The fine balance between physiological and pathological angiogeneses is mediated by the interplay of multiple endogenous angiogenic and antiangiogenic modulators.

Numerous in vitro studies have shown that c-Met receptors are also expressed by cultured vascular endothelial cells (Bussolino et al., 1992; Ding et al., 2003; Nakamura et al., 1995). SF/HGF is expressed and secreted by vascular smooth muscle cells, pericytes, and fibroblasts (Hayashi et al., 1996; Martin et al., 1999; Rosen et al., 1990) to activate endothelial c-Met receptors in a paracrine fashion. Conditioned media from these cells activate c-Met and lead to functional changes in co-incubated vascular endothelial cells. One report also described SF/HGF expression in vascular endothelial cells, raising the possibility of autocrine stimulation of endothelial c-Met receptors (Nakamura et al., 1995).

Angiogenic property of HGF has been first implicated by Bussolino et al: they showed that HGF induces repairs of a wound in endothelial cell monolayer, stimulates the scatter of endothelial cells grown on three-dimensional collagen gels, inducing an elongated phenotype; in the rabbit cornea, highly purified HGF promotes neovascularization at sub-nanomolar concentrations (Bussolino et al., 1992). Using

two different in vivo assays, Grant et al. showed that physiologic quantities of purified native mouse SF/HGF and recombinant human SF/HGF induce in vivo angiogenesis. The angiogenic activity was blocked by specific anti-SF/HGF antibodies (Grant et al., 1993). Lamszus K et al demonstrated that HGF/SF conferred a growth advantage to human breast cancer xenotransplants, linked with a higher microvessel density (Lamszus et al., 1997). HGF/SF was also shown to be an angiogenic factor in proliferative diabetic retinopathy (Grierson et al., 2000) and in rheumatoid and osteo arthritis (Nagashima et al., 2001). Kuba et al. showed that inhibiting SF/HGF leads to a dramatic decrease in microvessel density in mammary carcinoma xenografts (Kuba et al., 2000).

SF/HGF is a potent motility factor for vascular endothelial cells. Recombinant SF/HGF stimulates the chemotactic migration of neuromicrovascular endothelial cells (Lamszus et al., 1998). Fibroblasts have been shown to induce the migration of human large-vessel endothelial cells in an SF/HGF-dependent manner (Martin et al., 1999). SF/HGF also increases the dissociation and migration of human umbilical vascular endothelial cells (HUVECs). Such action of HGF/SF on HUVECs was achieved by regulation of the endothelial cell-specific cadherin, vascular endothelial (VE)-cadherin (Martin et al., 2001). SF/HGF-induction of endothelial cell migration in endothelial cells derived from the human saphenous vein is mediated by iNOS, a well-described endothelial cell motility factor (Purdie et al., 2002).

SF/HGF strongly induces DNA synthesis and proliferation in vascular endothelial cells of various origins, including neuromicrovascular endothelial cells and human aortic endothelial cells (Hayashi et al., 1996; Lamszus et al., 1998; Nakagami et al.,

2001). Recombinant HGF/SF as well as conditioned media from vascular smooth muscle cells stimulates vascular endothelial cells to grow in an SF/HGF-dependent manner. HGF/SF stimulates cell proliferation through the ERK-STAT3 pathway (Nakagami et al., 2001). In addition to its proliferative effects, SF/HGF also enhances endothelial cell survival and apoptosis resistance. HGF had an anti-apoptotic action through the PI3K-Akt pathway in human aortic endothelial cells (Nakagami et al., 2001). HGF/SF-induced survival of human umbilical endothelial cells is mediated by MAPK/ERK and AKT (Ma H et al., 2002). SF/HGF prevents human aortic endothelial cell death induced by hypoxia in a Bcl-2, but not a Bcl-xL or Bax dependent fashion (Yamamoto et al., 2001). Hepatocyte growth factor prevents endothelial cell death under high D-glucose conditions through inhibition of bax translocation from cytosol to mitochondrial membrane (Nakagami et al., 2002). Protection of hypoxia-induced apoptosis in mouse lung endothelial cells was associated with inhibition of p38 MAPK and Bid/Bax as well as increased expression of Bcl-xL (Wang et al., 2004).

SF/HGF can also affect angiogenesis by regulating the expression levels of other well-known proangiogenic and anti-angiogenic factors such as vascular endothelial growth factor (VEGF) and thrombospondin 1. SF/HGF has been shown to induce VEGF mRNA and protein expression in normal and neoplastic cells (Moriyama et al., 1998; Wojta et al., 1999). SF/HGF was also found to induce the expression of the VEGF receptor flk-1 in an endothelial cell line (Wojta et al., 1999). Induction of VEGF by SF/HGF was shown to be mediated by MAPK, PI3K, PKC-zeta and phosphorylation of Sp1, a regulator of the VEGF promoter (Reisinger et al., 2003; Zhang et al., 2003).

In another human endothelial cell line, VEGF induction by SF/HGF was dependent on the upregulation of essential transcription factor ets-1 (Tomita et al., 2003). Hashiya N et al. demonstrated that ets-1 regulated angiogenesis through the induction of angiogenic growth factors (VEGF and HGF) (Hashiya et al., 2004). The contribution of VEGF to SF/HGF-induced angiogenesis was found to be either additive or synergistic, depending on the cells/tissues examined. For instance, SF/HGF and VEGF had additive effects on HUVEC proliferation and synergistic effects on HUVEC migration (Van et al., 1998). In other studies, SF/HGF was found to act in concert with VEGF to promote human vascular endothelial cell survival and tubulogenesis in 3-D type I collagen gels, a response that did not occur with either growth factor alone. The synergistic effects of combining VEGF and SF/HGF on endothelial survival correlated with the greatly augmented expression of the anti-apoptotic genes Bcl-2 and A1 (Xin et al., 2001). HGF/SF and VEGF have also been shown to promote angiogenesis in a co-culture assay by inducing distinguishable patterns of vascular structures. VEGF increases the length, area and branch point number of induced vessels whereas HGF mediates exclusively vascular area growth resulting in vascular structures of enlarged diameter. Moreover, the combination of both cytokines results in an additive increase of vascular diameter (Beilmann et al., 2004). Consistent with these findings, the genes significantly up- and down-regulated by VEGF versus HGF in endothelial cells exhibit very little overlap, indicating distinct signal transduction (Gerritsen et al., 2003). These data show that the combination of SF/HGF and VEGF results in the cooperative up-regulation of a number of different molecular pathways, leading to a more robust proliferative and angiogenic response. In addition to up-regulating VEGF, SF/HGF was shown to

simultaneously downregulate the expression of thrombospondin 1, a negative regulator of angiogenesis (Zhang et al., 2003). Besides its cooperation with VEGF, HGF/SF can induce angiogenesis independently of VEGF (Sengupta et al., 2003).

1.6 Developmental roles of HGF and c-met

1.6.1 Nervous system development

Possible functions of HGF/SF in the development of the nervous system were first suggested by Claudio Stern and colleagues in 1990, who observed that ectopic application of HGF/SF to the early chick embryo can generate local supernumerary axial structures resembling primitive streak and/or neural plate (Stern et al., 1990). Inductive interactions during development are governed not only by the properties of the inducing cells, but also largely by the responsive capacity, or competence, of the tissue receiving the inducing signals (reviewed by Gurdon, 1987). The epiblast of the chick embryo loses its capacity to respond to neural induction by the organizer (Hensen's node) between stages 4 and 4+. At the primitive streak stage, HGF/SF is expressed specifically in Hensen's node (Streit et al., 1995). After implanting HGF/SF secreting cells, the competence to respond to Hensen's node grafts is retained by checking the glycoprotein L5-220, a marker for competent cells (Streit et al., 1997). Therefore HGF/SF plays a role in maintaining the competence of the epiblast to respond to neural inducing signals during the early steps of neural induction.

Both HGF/SF and c-Met are expressed in the developing nervous system, supporting the view that they function in neuronal development. In accordance with this, various types of glial cells and neurons respond to HGF/SF in vitro. HGF/SF stimulates Schwann cell growth (Krasnoselsky et al., 1994), promotes axon outgrowth of P19 embryonal carcinoma cells (Yang and Park, 1993), enhances neurite outgrowth in neocortical explants (Hamanoue et al., 1996) and promotes the proliferation of

neurospheres and neuronal differentiation of neural stem cells (Kato et al., 2004; Kokuzawa et al., 2003) . The various effects of sensory neurons are only observed in the presence of an additional neural growth factor, NGF, which synergizes with HGF/SF in culture (Maina et al., 1997). The level of Met expression in these neurons (as in sympathetic neurons) is, however, very low; the protein can be detected using anti-Met antibody staining, but the level of Met mRNA is almost undetectable by in situ hybridization. This low level of Met expression might explain why HGF cannot act alone in these cells but can only potentiate the effects of NGF, whereas in other cell types it is able to induce biological responses by itself. The motogenic activity, the stimulation of undirected cell movement away from their original position, of HGF/SF has been proved in neuron system with the evidence that HGF/SF is a key molecular constituent in guiding interneuron migration from the ganglionic eminence to the cerebral cortex (Powell et al., 2001).

Migrating motor axons are guided to their target muscles by both repellent and attractant chemotropic factors. For instance, the mesenchyme and the sclerotome, but not the dermamyotome, induce axonal outgrowth from spinal cord cultures. In a search for diffusible guidance factors for developing spinal motor axons, HGF was found to be a limb-mesenchyme-derived chemoattractant (Ebens et al., 1996). Furthermore, c-met and HGF/SF genes are expressed in patterns that are consistent with a role in axon guidance of motor neurons – that is, HGF/SF in limb bud mesenchyme and c-met in a subpopulation of motor neurons that are more abundant in limb-innervating than in trunk-innervating segments (Ebens et al., 1996; Yamamoto et al., 1997). In addition to its role as a chemoattractant, HGF can also induce the survival of a subpopulation of motor neurons during development. In cultures of purified embryonic rat motor neurons, HGF promotes short-term survival,

with an efficiency comparable to that of other neurotrophic factors such as brain-derived neurotrophic factor (BDNF) and ciliary neurotrophic factor (CNTF) (Ebens et al., 1996; Wong et al., 1997; Yamamoto et al., 1997). Consistent with the pattern of Met expression in vivo, motor neurons from limb-innervating brachial segments show a more potent survival response to HGF than do thoracic motor neurons (Yamamoto et al., 1997). Treatment of embryos with exogenous HGF/SF rescues lumbar but not other somatic motor neurons from cell death (Novak et al., 2000). Thus HGF secreted by limb mesenchyme could selectively support the survival of motor neurons in the limb-innervating segment. HGF and CNTF seem to act in synergy, because a combination of the two factors can rescue neurons that are not rescued by saturating concentrations of either factor alone (Wong et al., 1997). Motor neurons in the spinal cord are grouped into motor pools, each of which innervates a single muscle. Transcription factor PEA3 is a marker of a few such motor pools. Signaling by Met, the HGF receptor, is required for the rostral expansion of the *pea3* domain, while the onset of *pea3* expression is independent of *met* function. *met* expression is observed in pioneer neurons but does not precede that of *pea3* in recruited neurons (Helmbacher et al., 2003).

1.6.2 Muscle and limb development

Another of the interesting developmental functions of c-Met and HGF/SF is a decisive role in the generation of skeletal muscle that derives from long-range migrating precursor cells. Migrating muscle precursor cells emigrate from the dermomyotome, an epithelial structure that develops from somites, and finally generate a subset of the hypaxial muscle groups. These long-range migrating cells are already destined to form skeletal muscle, even though lack of expression of myogenic determination factors such as myogenin or MyoD. These factors are expressed only after the migrating cells reach their final targets. Migrating precursors are generated from the dermomyotome of specific somite only, i.e. occipitally, cervically, and on the levels of the fore and hind limbs. They express the homeobox gene Lbx1, which provides a useful marker for their visualization. In mice, migrating precursor cells give rise to muscles of the extremities, the hypoglossal chord, and the diaphragm.

Prerequisite of the migration of muscle precursor cells into the limb buds is the delamination of cells. It has been shown that de-epithelialization and subsequent migration of dermomyotomal cells can be induced ectopically by grafting of proximal limb bud mesoderm to the flank level (Hayashi and Ozawa, 1995). The underlying molecular mechanism is an interaction between the transmembrane tyrosine kinase receptor c-met expressed by the dermomyotome cells and its ligand scatter factor/hepatocyte growth factor (SF/HGF) that is produced by somatopleural cells of the limb buds. In mice carrying met null mutations myogenic precursor cells fail to migrate, preventing the normal development of limb and body wall muscle, whereas axial muscle is unaffected (Bladt et al., 1995). Migrating myogenic progenitors are

generated from the dermomyotome by an epithelial–mesenchymal transition. The migrating cells cannot be observed in HGF/SF- or c-met-null mutant mouse embryos, conversely, an ectopic application of exogenous SF/HGF leads to de-epithelialization of the dermomyotomal edges even at interlimb level and emigration of dermomyotomal cells (Bladt et al., 1995; Brand-Saberi et al., 1996; Heymann et al., 1996). Thus, HGF/SF and c-met seem to regulate the detachment and emigration of myogenic precursor cells from the dermomyotome in vivo, resembling the cellular response that leads to the identification of HGF/SF as 'scatter factor' in cell culture (Stoker et al., 1987). Since migrating precursors are generated on particular axial levels only, the tight spatio-temporal control of the emigration might be regulated by restricted expression of HGF/SF, although additional signals could participate.

The important role of tightly regulated HGF/SF expression for the ordered development of skeletal muscle also became apparent from the analysis of transgenic mice that over expresses HGF/SF under the control of the metallothionein promoter (Takayama et al., 1996). In these embryos, ectopic expression of HGF/SF in the adjacent neural tube induces inappropriate formation of skeletal muscle in the central neural system (CNS), supporting the notion that in normal development HGF/SF plays an important role in regulating migration of Met-containg myogenic precursor cells. The vertebrate neural crest is another migratory cell population that are able to give rise to a wide variety of derivatives. Interestingly, melanocyte precursors, one neural crest derivative, are also found within such transgenic adult in a number of abnormal ectopic sites, including the CNS. Moreover, melanocytes are produced in excess, indicating that not only migration but also growth and/or survival of the cells are affected (Takayama et al., 1996).

Gene targetting of either HGF or c-met results in the absence of muscle in the limbs. The resulting phenotype of c-met and HGF/SF knockout mice resembles the phenotype of a naturally occurring mutation in the Pax3 gene called *splotch* (Bober et al., 1994; Franz et al., 1993). Pax-3 and c-met show similar expression patterns in the early development of the myogenic compartment – both genes are expressed in migrating myogenic precursor cells and in the ventral dermomyotome, where migratory cells are located prior to emigration (Bladt et al., 1995; Yang et al., 1996). Pax-3 has been shown to regulate the expression of c-met (Daston et al., 1996; Epstein et al., 1996; Tajbakhsh et al., 1997; Yang et al., 1996). Consistent with this, c-met promoter contains a Pax3 binding site, and Pax3 can drive reporter gene expression from the c-met promoter in vitro (Daston et al., 1996; Epstein et al., 1996; Yang et al., 1996). Therefore, it can be concluded that Pax3 controls the release of migrating muscle precursors in vivo by activating c-met. It should be noted, however, that the Pax-3 mutation causes severe additional changes in the dermomyotome, suggesting that Pax-3 also controls other genes important in dermomyotome development (Daston et al., 1996).

Skeletal muscle development involves several waves of myofibre formation. In the mouse, primary fibres form from myoblasts at around embryonic day 13 (E13), secondary fibres start to form on E16 in the same basal lamina, and, in the adult, fibres can be regenerated from stem cells of the adult muscle, the satellite cells. The c-Met receptor might not only function in formation of migratory myogenic precursor cells that generate hypaxial muscle groups but also in subsequent stages of the development of all skeletal muscle. Targeted disruption of either the hg*f* or the *met*

locus in mice confirmed the importance of HGF signaling in development; mice lacking either HGF or its receptor die during embryogenesis, with defects in placenta, liver and muscle (Bladt et al., 1995; Schmidt et al., 1995; Uehara et al., 1995). This early lethality has made it difficult to study the role of HGF in later stages of development. Rescue of the placental defect by aggregation of tetraploid (wild type) and diploid (c-Met-/-) morulae allows development of c-Met mutant animals to term. They lack muscle groups that derive from migratory precursor cells, but display otherwise normal skeletal musculature (Dietrich et al., 1999). Taking the advantage of zebrafish model, loss-of-function experiments reveal that Met and its ligand, hepatocyte growth factor, are required for the correct morphogenesis of the hypaxial muscles in which met is expressed (Haines et al., 2004). In another study, the placental defect was bypassed by replacing the endogenous met gene with a signaling mutant of met, thereby revealing a requirement for Met in late myogenesis for secondary muscle fiber formation (Maina et al., 1996). Finally, satellite cells respond to HGF/SF in cell culture with increased proliferation and delayed differentiation (Allen et al., 1995; Anastasi et al., 1997). Taken together, these results indicate that HGF/SF and c-Met might play independent roles in skeletal muscle development, that is in generation of hypaxial skeletal muscle that derives from migrating precursor cells and in formation of secondary fibres. It is possible that HGF/SF and c-Met also participate in fibre regeneration in the adult organism, but this has not been established in vivo.

1.6.3 Tubulogenesis and angiogenesis

Epithelial tubulogenesis, the organization of epithelial cells into tubular structures, forms the basis for the intricate organization of functional units of parenchymal organs. Tubules can arise in vertebrates through two main mechanisms: the invagination of cells from an epithelial sheet, as occurs in the formation of the neural tube or through the organization of initially unpolarized cells into cord-like structures that invade the surrounding mesenchyme, forming branched hollow tubules lined by polarized cells (reviewed by Hogan and Kolodziej, 2002). The latter mechanism is involved in the formation of organs such as the mammary gland and pancreas and during angiogenesis. HGF/SF plays an important role in the development of tubular organs through this mechanism.

HGF/SF was found to stimulate epithelial cells derived from a variety of different organs to form tubule-like extensions when seeded in three-dimensional matrices (so-called 'branching morphogenesis') (Brinkmann et al., 1995; Montesano et al., 1991; Weidner et al., 1993). During this HGF/SF induced tubulogenesis, cell-cell adhesive contacts are differentially regulated while the polarity and specialization of plasma membrane subdomains reorganize, enabling cells to remain in contact as they rearrange into new structures (Pollack et al., 1998).

In vivo, HGF/SF stimulates tubulogenesis in the adult liver and kidney during organ regeneration after partial hepatectomy or kidney damage, respectively (Bell et al., 1999; Kawaida et al., 1994). Additionally, anti-HGF/SF antibodies perturbed

branching morphogenesis of the ureteric bud in organ cultures (Woolf et al., 1995). In the developing kidney, HGF/SF was expressed in the mesenchyme, while met was expressed in both the ureteric bud and the mesenchyme (Woolf et al., 1995). Interestingly, a renal serine protease HGF/SF activator (HGFA), which cleaves and therefore activates the HGF/SF zymogen, is expressed around the tips of the invading ureteric bud, suggesting a gradient of HGF activity created by HGFA in the developing kidney (van et al., 2001). Inhibition of HGFA activity reduced ureteric bud branching, an effect that can be rescued by active HGF/SF (van et al., 2001).

In the mammary gland, elevated expression of endogenous Met and HGF/SF correlates with stages of active tubulogenesis, expression being high through early pregnancy but virtually absent during late pregnancy and lactation when alveologenesis and gland differentiation take place (Yang et al., 1995). Indeed, overexpression of HGF/SF in reconstituted mouse mammary glands in vivo induces hyperplastic branching morphogenesis (Yant et al., 1998), and specific antisense HGF oligonucleotides prevent branching morphogenesis in whole mammary gland cultures (Yang et al., 1995).

Two phosphorylated tyrosine residues (Y1349 and Y1356) located at the C-terminal end of the Met β chain, together with the surrounding amino acids, constitute a unique multisubstrate docking site which is both necessary and sufficient to mediate Met signal transduction and biological functions, including tubulogenesis (Ponzetto et al., 1994; Sachs et al., 1996). Signaling mediators recruited to Met include enzymes such as Src tyrosine kinase and phosphoinositide 3-kinase (PI3K), as well as several adaptor proteins such as Grb2, Gab1, Shc and c-Cbl. Gab1 associates with Met both

by direct binding to the docking site on Met and through association with Grb2 (Lock et al., 2002; Nguyen et al., 1997). Expression of Gab1 in epithelial cells is sufficient to induce the c-Met-specific activities, including branching morphogenesis (Weidner et al., 1996). Met receptor mutants with impaired ability to bind to Gab1 fail to induce branching morphogenesis, which can be rescued by overexpression of Gab1 (Nguyen et al., 1997; Schaeper et al., 2000). Association of Gab1 with SHP2, but not PI3K, CrkL, or Shc was essential to induce branching morphogenesis (Maroun et al., 2000; Schaeper et al., 2000). SHP2 regulates the kinetics of activation of at least two pathways that are required for branching morphogenesis: the PI3K and MAP kinase pathways. PI3K is critical for c-met-mediated tubulogenesis and cellular motility (Derman et al., 1995; Royal and Park, 1995). Activated PI3K causes branching tubule formation similar to that seen with HGF/SF treatment (Khwaja et al., 1998). The PI3K pathway might also be important for the stimulation of anchorage-independent growth and cytoskeletal reorganization during tubulogenesis (Potempa and Ridley, 1998; Royal and Park, 1995). The duration of Met signaling and of ERK MAP kinase activation has been shown to determine biological outcome: sustained activation of ERK is required for branching morphogenesis (Boccaccio et al., 2002; Maroun et al., 2000). Different from other Gab family members, Gab1 can bind directly to Met through sequences unique to Gab1 (reviewed by Gu and Neel, 2003) which may result in a more stable interaction with Met and thus prolonged Gab1 phosphorylation. This prolonged Gab1 phosphorylation, which correlates with sustained activation of the ERK mitogen-activated protein (MAP) kinase and protein kinase B (PKB)/Akt pathways, is required for HGF-induced branching tubulogenesis but not for cellular motility (Gual et al., 2000). While activation of ERK is necessary and sufficient for the initial stage of tubulogenesis, during which cells depolarize and migrate, ERK

becomes dispensable for the latter stage, during which cells repolarize and differentiate; conversely, the activity of matrix metalloproteases (MMPs) is essential for the late stage but not the initial stage (O'Brien et al., 2004).

During HGF/SF-stimulated branching morphogenesis, cell polarity is transiently lost and subsequently regained and cells move without losing cell–cell contact (Pollack et al., 1998). Similarly HGF can induce certain cell lines to move as coherent cell sheets (Nabeshima et al., 1998). Thus, careful regulation of adherens junction structure is thus required. During HGF/SF-stimulated branching morphogenesis, components of cell-cell junctional complexes undergo profound rearrangements: E-cadherin is randomly distributed around the cell surface, desmoplakins I/II accumulate intracellularly, and the tight junction protein ZO-1 remains localized at sites of cell-cell contact (Pollack et al., 1998). HGF/SF stimulation leads to the selective upregulation of both ECM proteins and integrin molecules (Chiu et al., 2002). Inhibition of integrin α2 function or of fibronectin expression blocks HGF/SF-stimulated branching morphogenesis in MDCK cells (Jiang et al., 2000a; Saelman et al., 1995). A similar requirement for integrin β1 has been reported for both in vivo mammary duct formation and in vitro HGF/SF-stimulated branching morphogenesis of mammary epithelial cells (Klinowska et al., 1999).

1.6.4 Organogenesis

During organogenesis, epithelial-mesenchymal interactions play crucial roles in cell fate determination (or specification), growth, migration, survival, and morphogenesis. Epithelial cells form complex branched tubular structures during development of a variety of organs, including kidney, mammary gland, lung, salivary gland, and liver. In tissue explant experiments, it has been demonstrated that these morphogenic processes depend on mesenchymal factors (Grobstein, 1967; Saxen and Sariola, 1987), and identification of external signaling molecules exchanged between epithelium and mesenchyme hold much interest.

During murine development, the c-Met/HGF receptor gene is expressed in epithelia, while the HGF gene in mesenchymal cells in close vicinity in various organs such as the kidney, lung, pancreas, liver, intestine, stomach, salivary gland, limb bud, tooth, etc (Defrances et al., 1992; Noji et al., 1990; Sonnenberg et al., 1993; Tabata et al., 1996). These expression patterns indicate that HGF is a mesenchymal-derived factor which predominantly acts on neighboring developing epithelia, and in these developing organs, mesenchymal factors are involved in growth and morphogenesis of epithelia. During epithelial development, one particular function of HGF is in duction of epithelial morphogenesis. HGF induces branching tubulogenesis in vitro in several types of cells originating from distinct epithelial tissues, including renal tubules, mammary gland, and hepatic epithelium (Johnson et al., 1993; Montesano et al., 1991; Niranjan et al., 1995; Santos et al., 1994; Soriano et al., 1995; Woolf et al., 1995).

Essential roles of HGF in the organogenesis were defined by targeted distruption of HGF or its receptor c-met (Bladt et al., 1995; Maina et al., 1996; Schmidt et al., 1995; Uehara et al., 1995). These knockout mice are embryonic lethal due to impaired organogensis of the liver and placenta. The embryonic liver is reduced in size and shows extensive loss of hepatocytes, due to apoptotic cell death (Schmidt et al., 1995). In the placenta, the number of labyrinthine trophoblasts is markedly reduced (Schmidt et al., 1995; Uehara et al., 1995). Role of HGF for liver development is highly conserved from amphibian to mammalian species (Aoki et al., 1997). When tyrosine kinase-negative Met mRNA was microinjected into two-cell to eight-cell stages *Xenopus* embryos, liver development was mostly impaired and structures of pronephros and the gut were grossly underdeveloped in the restricted, late stage of development (Aoki et al., 1997)

1.6.5 Hematopoiesis and Lymphopoiesis

Hematopoiesis

Several elements of HGF's biology provide clues to suggest that it may be an important player in the hematopoietic system. First, the receptor for HGF/SF is c-Met, a prototypic receptor tyrosine kinase that is structurally similar to c-kit and FLT3/Flk2, receptor tyrosine kinases with vital roles in hematopoiesis. Second, HGF/SF is produced by marrow stromal cells and some hematopoietic cell lines, and c-Met is expressed by hematopoietic progenitor cells and bone marrow stromal cells (Matsuda-Hashii et al., 2004). Indeed, HGF signaling on marrow stroma has been reported to provide important trophic effects and to induce secretion of IL-11, SDF-1, and SCF (Matsuda-Hashii et al., 2004). Third, HGF/SF is structurally similar to plasminogen, although it has a mutated serine protease domain that prevents it from exerting proteolytic activity. Fourth, functional studies have consistently demonstrated that HGF/SF can induce proliferation of early hematopoietic progenitors (Zarnegar and Michalopoulos, 1995), although its effects are consistently augmented by coculture with other cytokines. For instance, HGF/SF synergizes with IL-3 or GM-CSF for expansion of myeloid cell lines and normal hematopoietic progenitors (Kmiecik et al., 1992; Nishino et al., 1995; Weimar et al., 1998).

The first clue indicating that HGF may be involved in hematopoiesis came from studies on progenitor-enriched murine bone marrow cells and on several murine myeloid progenitor tumor cell lines blocked in the early stages of myeloid differentiation. Such investigations revealed, first, that these cells express c-met, and second, that HGF synergizes with IL-3 or GM-CSF to support the growth of these

cells in culture (Kmiecik et al., 1992; Mizuno et al., 1993). Conflicting results, however, were obtained by these two investigations with regard to whether HGF alone stimulates mitogenesis in myeloid progenitor cell lines. Although HGF synergized with other factors to stimulate growth of progenitor cells, it apparently did not influence the pattern of myeloid differentiation since the ratio of macrophages to granulocytes in resultant colonies remained similar to those obtained with IL-3 or GM-CSF alone (Kmiecik et al., 1992). Later in 1994, Galimi et al. reported that the HGF receptor is present in a small fraction of highly-enriched hematopoietic progenitor cells from human bone marrow and peripheral blood, and further showed that, in the presence of erythropoietin, HGF induces the formation of erythroid lineage colonies when cultured in vitro. However, in the presence of erythropoietin and stem cell factor, it was demonstrated that HGF supported the growth of multipotent colonies (granulocyte-erythroid-megakaryocyte) rather than recruiting erythroid precursors (Galimi et al., 1994). HGF is constitutively produced by BM stromal cells and it enhances hematopoiesis, probably through an autocrine mechanism (Takai et al., 1997).

In Xenopus, strong signals of HGF as well as c-met are detected early in the developing ventral mesoderm, which later gives rise to the ventral blood island (Koibuchi et al., 2004). In all vertebrate development, blood cell formation occurs in two successive waves, which are termed primitive and definitive hematopoiesis, based on the time of initiation, site of development, cell morphology, globin content, and potential to differentiate (Zon, 1995). Primitive hematopoiesis occurs first and gives rise to predominantly erythrocytes (primitive red blood cells). This phenomenon is then followed by definitive hematopoiesis, which leads to the production of all the

blood lineages that are required throughout the life span of a vertebrate. Blocking of HGF signaling pathway in Xenopus embryos resulted in a marked decrease in the number of circulating blood cells and a significant reduction (or absence) of stem cell leukemia (SCL), α-globin, and GATA-1 expression, but not GATA-2 expression, in the ventral blood island (VBI) where primitive red blood cells are exclusively produced. In contrast, no significant difference was observed in the levels of expression of early definitive blood markers, SCL, GATA-2, and GATA-3 in the dorsolateral plate (DLP) where definitive blood cells arise predominantly (Koibuchi et al., 2004). This study demonstrated that HGF is a specific regulator of primitive hematopoiesis rather than definitive hematopoiesis, which is different from mouse mutants. Based on this difference, it is possible that zebrafish hgf may also possess its unique functions.

Lymphopoiesis

HGF has been reported to regulate hematopoiesis in mouse fetal liver and adult bone marrow, where it apparently can substitute for the stem cell factor (SCF) and c-kit system (Nishino et al., 1995; Yu et al., 1998). However, its role in the regulation of lymphopoiesis has not been well characterized. c-met is predominantly expressed on CD38(+)CD77(+) tonsillar B cells while HGF/SF is produced at high levels by tonsillar stromal cells thus providing signals for the regulation of adhesion and migration within the lymphoid microenvironment. Stimulation of c-Met lead to enhanced integrin-mediated adhesion of B cells to both VCAM-1 and fibronectin (van, V et al., 1997). Another study showed that c-Met is expressed in the thymus during early ontogeny, and that c-Met/HGF signals can promote T-cell development (Tamura et al., 1998).

Interleukin-7 (IL-7), originally described as a pre-B cell growth factor, is a nonredundant cytokine that has diverse effects on the hematopoietic and immunologic systems (Komschlies et al., 1995; Namen et al., 1988b; Namen et al., 1988a). In 1998, Lai and coworkers identified an IL-7–associated molecular complex that primed differentiating B cells for subsequent proliferation to IL-7 alone (Lai et al., 1998; McKenna et al., 1998). They named the molecule pre–pro–B cell growth stimulating factor (PPBSF) and reported that it was a self-assembling heterodimer that could be generated by adding IL-7 to stromal cell-conditioned media from IL-$7^{-/-}$ mice. Subsequently, this group discovered that the molecule that partnered with IL-7 in PPBSF was a variant β chain of HGF. Remarkably, this resulted from postsecretion processing, wherein the presence of heparin sulfate-derived oligosaccharides in the microenvironment induced IL-7–HGFβ pairing into a bioactive heterodimer (Lai and Goldschneider, 2001).

Because full characterization of this novel hybrid cytokine could not be performed with the small amounts generated naturally, Lai and colleagues produced a recombinant version of the hybrid cytokine by fusing a signal sequence with IL-7 combined by a linker to HGF β chain (Lai et al., 2006). The resulting single-chain molecule shows potent and unique activity on primitive hematopoietic cells and developing B-cell subsets. Mechanistically, the data suggest that the hybrid cytokine signals through both the high-affinity IL-7R and c-Met and that the pairing of the chains leads to IL-7R and c-Met aggregation and capping on the surface of stimulated cells. This work provides a novel insight into yet another mechanism by which cytokines can mediate specificity in vivo. In this case, postsecretion processing leads

to selective pairing of genetically unrelated molecules, rendering the resultant signal distinct and greater than the sum of its parts.

1.7 Zebrafish as a model organism in developmental biology

One of the most promising experimental models for study of developmental biology emerged in recent years is the zebrafish (*Danio rerio*), a small tropical freshwater teleost fish. A combination of various features makes zebrafish a versatile model organism in vertebrate genetics and developmental biology. The zebrafish offers several distinct advantages for genetic and embryological studies including the external fertilization, rapid development and optical clarity of its embryos.

The versatility of the zebrafish as a model for developmental biology is particularly apparent due to the array of cellular, molecular and genetic techniques available. It is technically easy to introduce DNA into zebrafish embryos using various methods like microinjection, electroporation and microprojectiles. Microinjection, in particular, is the most popular method due to the transparency and easy manipulation of the embryos. Creation of various transgenic lines of the zebrafish carrying the green fluorescent protein (GFP) gene or/and red fluorescent protein (RFP) under the control of various promoters have been extremely helpful in various studies including cell lineage tracing experiments, promoter studies and tissue-specific transgene expression (reviewed by Gong et al., 2001; Wan et al., 2002).

Besides gain-of-function analyses by transgenic approaches, loss-of-function analyses are also important to fully determine the function of a gene *in vivo*. The powerful reverse genetics approach, gene knock-out used in transgenic mice, is lacking in zebrafish. The advent of translation-blocking or splicing-interfering morpholino oligonucleotides has led to a method of sequence specific gene inactivation or

modification in zebrafish (Ekker and Larson, 2001; Nasevicius and Ekker, 2000) thus improving the prospects of a comprehensive large-scale and genome-wide gene analysis in the zebrafish. Morpholinos have been shown to effectively and specifically induce phenotypes similar to that of induced loss-of-function of genes (Nasevicius and Ekker, 2000).

The availability of large repertoire of mutagenesis tools, breeding strategies and screening methods (Malicki et al., 2002) helped to establish the zebrafish as a vertebrate of choice for random, genome-wide, large-scale mutagenesis of genes crucial for development (Driever et al., 1996; Haffter et al., 1996; Malicki et al., 2002; Schulte-Merker, 2000; Talbot and Hopkins, 2000). Today a large number of zebrafish mutants affecting early development and organogenesis, generated by various mutagenesis techniques are available (Chen et al., 2002; Driever et al., 1996; Golling et al., 2002; Haffter et al., 1996; Knapik, 2000; Schulte-Merker, 2000). A variant of a reverse genetic screen, large-scale whole mount *in situ* hybridization screens are feasible in the zebrafish owning to the transparency of the embryos.

The efficient identification of genes disrupted by mutation in zebrafish requires dense maps of the genome. This has been possible because of the availability of large-insert genomic libraries (Amemiya et al., 1999; Zhong et al., 1998) and several genetic linkage maps, which essentially cover the entire zebrafish genome (Gates et al., 1999; Kelly et al., 2000; Postlethwait et al., 1998; Talbot and Hopkins, 2000; Woods et al., 2000). Radiation hybrid (RH) maps with markers, which include simple sequence length polymorphisms (SSLPs), cloned genes and ESTs, have been developed for zebrafish (Geisler et al., 1999; Hukriede et al., 2001; Hukriede et al., 1999; Kwok et

al., 1998). The two zebrafish RH maps, Ekker LN54 and Goodfellow T51, together cover >90% of the zebrafish genome (Talbot and Hopkins, 2000). Efforts were also initiated to obtain the complete sequence of the zebrafish genome, and the draft sequence has been released in mid 2003. To cope with the phenomenal rate of increase of information, Zebrafish Information Network (ZFIN) (http://zfin.org) was established. This is a centralized database for zebrafish researchers, providing links and information about zebrafish genes, mutations, genetic maps etc. (Westerfield et al., 1999a; Westerfield et al., 1999b). In February 2001 the Sanger Institute started sequencing the genome of zebrafish. These assemblies of the genome are accessible in Ensembl (http://www.ensembl.org/Danio_rerio). Besides facilitating the identification of mutants, the genetic maps have been useful in comparative studies between the zebrafish and other vertebrate genomes. In spite of the 450 million years of evolutionary distance between zebrafish and human (Kumar and Hedges, 1998), comparisons of zebrafish and mammalian gene maps have revealed extensive conservation of syntenic relationships among vertebrates (Amores et al., 1998; Barbazuk et al., 2000; Gates et al., 1999; Postlethwait et al., 1998; Postlethwait and Talbot, 1997; Woods et al., 2000; Woods et al., 2005). Identification of conservation of synteny between the zebrafish and human genome has been valuable in defining candidate genes for zebrafish mutants (Karlstrom et al., 1999; Schmid et al., 2000) and in prediction of orthologous gene relationships (Barbazuk et al., 2000). In addition, the human-zebrafish comparative maps can help the understanding of the vertebrate genome. The zebrafish represents a valuable outgroup of vertebrates, distinguishing shared features of mammalian genomes and those derived from ancestral genomes (Gates et al., 1999; Postlethwait et al., 1998; Postlethwait et al., 2000; Woods et al., 2000; Woods et al., 2005).

In addition to the advantages it offers to developmental biologists, zebrafish has a great potential to serve as a model for human disease (reviewed by Barut and Zon, 2000; reviewed by Dooley and Zon, 2000; reviewed by Ward and Lieschke, 2002). For instance, the zebrafish *gridlock* mutant has a defect similar to coarctation of the aorta in humans (Weinstein et al., 1995). In addition, there are zebrafish mutants with cystic kidneys that may represent polycystic kidney disease of humans (Drummond et al., 1998). Comparative analysis of microarray data from zebrafish liver tumors with those from four human tumor types revealed molecular conservation at various levels between fish and human tumors (Lam et al., 2006). Hence, the zebrafish has definitely evolved not only as an ideal model organism for vertebrate developmental biology and genetics but also as a valid animal model for medical research.

1.8 vertebrate liver development

The liver provides many essential functions. It is the largest exocrine gland in the body, producing bile, metabolizing lipids, and is the primary site for detoxification and elimination of body wastes. The liver also performs important endocrine functions by secreting blood proteins such as albumin that maintain homeostasis, as well as regulating blood glucose levels through glycogen storage.

Based on descriptive and experimental embryology in mouse and chicken, liver development can be conceptualized in a series of steps (Zaret, 2002) and from preliminary experiments these appear to be largely conserved in Xenopus (Chalmers and Slack, 2000; Zorn and Mason, 2001). First the endoderm germ layer forms during gastrulation and eventually gives rise in the adult to the liver, pancreas, lung, thyroid and epithelial cells of the gastrointestinal and respiratory systems (Wells and Melton, 1999). The endoderm is then patterned into broad domains along the anterior-posterior axis and anterior endoderm (AE) becomes competent to give rise to foregut derivatives. Around the 4-8 somite stage of development a combination of positive inductive signals from the cardiogenic mesoderm and repressive signals from the trunk mesoderm specifies a group of cells in the ventral foregut endoderm to adopt a hepatic fate (Fukuda-Taira, 1981; Gualdi et al., 1996; Le Douarin et al., 1975). The hepatic endoderm epithelium thickens, delaminates and invades the surrounding mesenchyme to form the liver bud. Continued epithelial/mesenchymal interactions stimulate cell proliferation and morphogenesis as the embryonic organ grows. The

undifferentiated cells in the liver bud, known as hepatoblasts, are bi-potential, giving rise to hepatocytes and biliary epithelium.

Promoter studies examining the transcriptional regulation of liver specific genes in tissue culture, such as transthyretin, α-fetoprotein and albumin have provided extensive molecular information on terminal hepatocyte differentiation (Costa et al., 2003). At the other end of the developmental spectrum, work in Xenopus and zebrafish has begun to elucidate the molecular details of how the endoderm is formed in the first place (Stainier, 2002). Finally genetic analysis in the mouse has identified many of the genes, such as *Hex, Prox1, c-jun, Hlx, HGF, c-Met, Smad2/3 Kras, Sek1, CERB* and *Xbp1* that are required for maintenance, proliferation, morphogenesis and survival of the liver bud once the hepatic lineage is specified (Zaret, 2002).

Classical transplantation experiments in avian embryos and *in vitro* mouse embryos explant cultures, indicate that the cardiogenic mesoderm (CM) induces liver development in the adjacent ventral foregut endoderm between the 4-8 somite stages of development (Fukuda-Taira, 1981; Gualdi et al., 1996; Le Douarin et al., 1975). Only the CM, which includes the precardiac and septum transversum mesenchyme, had this activity and mesoderm from other regions of the embryo could not stimulate hepatic development in foregut endoderm (Fukuda-Taira, 1981; Gualdi et al., 1996; Le Douarin et al., 1975). Furthermore, *in vivo* only the foregut endoderm was competent to initiate hepatogenesis. Zaret and colleagues have shown that FGF and BMP growth factors are good candidates for endogenous liver inducing factors (Zaret, 2002).

In vivo transplantation experiments in chick found that only the foregut endoderm was "competent" to differentiate into liver and CM could not induce hepatic development in posterior endoderm (Fukuda-Taira, 1981; Le Douarin et al., 1975). However, mouse explant studies found that posterior endoderm could express liver markers once isolated from its adjacent dorsal/posterior mesoderm and cultured in vitro. Furthermore, this dorsal mesoderm could repress hepatic induction in foregut co-cultures (Gualdi et al., 1996). This suggests that hepatic potential is normally repressed in the hindgut by dorsal mesodermal signals, while the anterior endoderm is somehow protected. And a model was proposed where Wnt ligands secreted from the trunk mesoderm repress hepatic development in the posterior endoderm, while Wnt-antagonists expressed in the anterior endoderm make the developing foregut refractory to these repressive Wnts and competent to respond to hepatic induction. This model is supported by the fact that Wnt promots biliary differentiation by enhancing stem cell specification, hepatocyte trans-differentiation and promoting biliary survival (Hussain et al., 2004).

In this study, we use zebrafish as the animal model to study liver development. Zebrafish liver development can be divided into two phases: budding and growth. Budding stage (Figure 1.2) can be further divided into three stages based on distinct liver morphology: anterior thickening of intestinal rod between 24 to 28 hours post fertilization (hpf) (Figure 1.2 A, B), leftward bend and a smooth thickening on the outer curvature of the intestinal bulb primordium at 30 hpf (Figure 1.2 C), and a furrow formation between the liver bud and the adjacent oesophagus at 34hpf (Figure 1.2 D). By 50hpf, cells connecting the liver and the intestinal bulb primordium have formed the hepatic duct, which marks the end of budding process. From end of the

budding to 96hpf, the liver is in growth phase. At this phase, the liver is a well-defined strucuture and increases in size and modifies its shape and placement. By 72hpf, the size of the liver has increased moderately but the shape has not changed. By 96hpf, the liver has extends from the left side of the embryo all the way across the midline ventral to the oesophagus, which marks the end of growth phase (Field et al., 2003). In zebrafish model, several genes were identified to be involved in liver development and disease. For instance, *uhrf1* gene, a cell cycle regulator and transcriptional activator of *top2a* expression, is required for hepatic outgrowth and embryonic survival in zebrafish (Sadler et al., 2007). A genetic screen in zebrafish identifies the mutants *vps18, nf2* and *foie gras* as models of liver disease (Sadler et al., 2005).

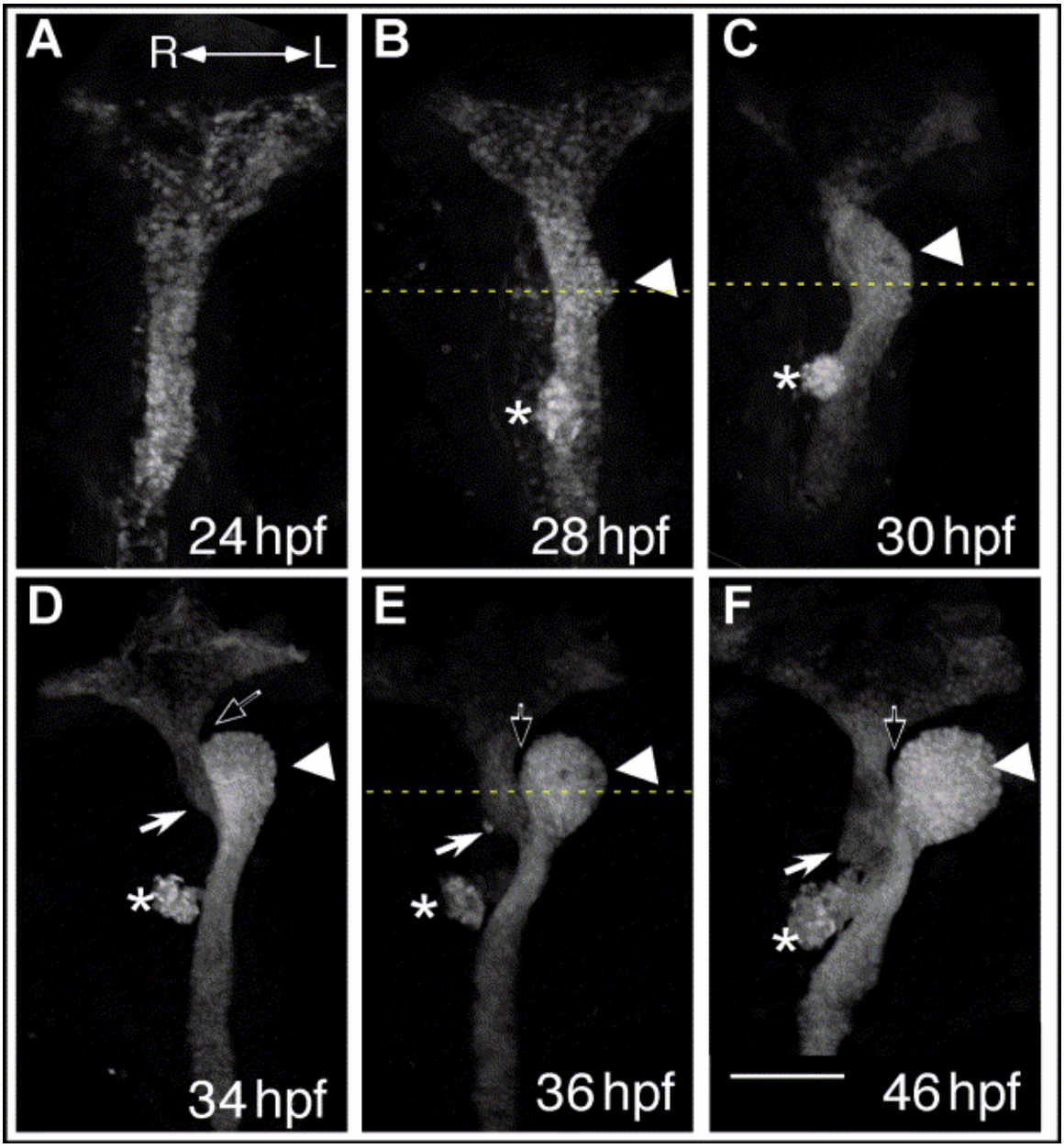

Fig.1.3 Time course of zebrafish liver budding. (A–F) Two-dimensional projections of confocal stacks showing ventral views of the gutGFP line, anterior to the top. Scale bar, 100 μm. Embryos were fixed and imaged at (A) 24, (B) 28, (C) 30, (D) 34, (E) 36, and (F) 46 hpf. (A, B) The liver (arrowhead) starts budding from the intestinal rod between 24 and 28 hpf. (C) At 30 hpf, the liver is a smooth thickening on the outer curvature of the intestinal bulb primordium, which at this time has a clear leftward bend. (D) A furrow (open arrow) begins to form between the medial anterior edge of the liver and the adjacent oesophagus and continues to expand posteriorly (E, F) to separate the liver from the intestinal bulb primordium. The pancreas (asterisk) and endodermal lining of the swim bladder (arrow) can also be seen developing from the intestinal bulb primordium over time. (From Field et al., 2003)

1.9 Somitogenesis and myogenesis

In the vertebrate embryo, the most obviously symmetric embryonic structures are the left and right somitic columns. During somitogenesis, the cells lying on either side of the organizer in the marginal zone mesoderm, will segment into are epithelial spheres of somites that flank the neural tube. The process occurs sequentially from anterior to posterior as the embryo grows posteriorly. The somites subsequently differentiate to give rise to the vertebrate, ribs and skeletal muscles of the body.

Somitogenesis has been shown to be regulated by two mechanisms: 1) the segmentation clock (reviewed by Bessho and Kageyama, 2003) and 2) a continuously regressing posterior-to-anterior gradient of fibroblast growth factor 8 (fgf8) (Dubrulle and Pourquie, 2004) and Wnt signalling in the presomitic mesoderm (PSM) (reviewed by Aulehla and Herrmann, 2004). The clock, a molecular oscillator that involves Notch (Dale et al., 2003; Jiang et al., 2000b) and Wnt signalling (Hofmann et al., 2004) pathways, ensures a regular timing of somite formation by generating cyclic waves of gene expressions along the PSM. The gradient gives rise to a determination front – a concentration threshold below which somite formation can occur (Aulehla et al., 2003; Dubrulle et al., 2001). Both the segmentation clock oscillations and determination front regression occur synchronously on the embryo's left and right sides, resulting in simultaneous, bilateral somitogenesis.

Myogenesis begins during embryonic segmentation and lasts until birth (reviewed by Buckingham et al., 2003). Myogenesis requires the coordination of several processes: the specification of muscle precursors and the control of their proliferation, migration and differentiation (reviewed by Buckingham et al., 2003; reviewed by Parker et al.,

2003). During somitogenesis, the segmentation boundary demarcates a posterior domain, where somite maturation is repressed and an anterior domain, where differentiation begins (reviewed by Iulianella et al., 2003; reviewed by Pourquie, 2003).

Myogenesis is under the influence of numerous signals arising from neighbouring structures, i.e. surface ectoderm, neural tube and notochord. During zebrafish myogenesis, two distinct cell populations give rise to slow and fast muscle fibres (Stickney et al., 2000). The slow muscle derives from the medially located adaxial cells and requires Hedgehog (Hh) signals from the notochord (Barresi et al., 2000; Blagden et al., 1997; Du et al., 1997; Wolff et al., 2003). Slow fibres segregate into two subpopulations: the superficial slow fibres (SSF), which migrate to the lateral somite surface; and the muscle pioneers (MPs) that remain medial. The remaining myotome differentiates into fast muscle fibres (Devoto et al., 1996; Wolff et al., 2003). How the cells of the lateral somites are specified to differentiate into fast muscle is unknown.

The zebrafish has long been recognized as an ideal organism for cellular and histological studies of somite patterning. The overall process of somite development in zebrafish is similar to that in amphibians, birds, and mammals (Kimmel et al., 1995). In zebrafish, gastrulation is first visible when the shield is established on the dorsal side of the embryo. Shield cells are functionally equivalent to the organizer of amphibians and Hensen's node cells in chick (Shih and Fraser, 1996). These cells give rise to the notochord and prechordal plate, and they exert profound patterning influences on surrounding tissues (Mullins, 1999). The paraxial mesoderm develops

from cells around the margin of the early gastrula, which converge toward the dorsal side, forming paraxial mesoderm adjacent to the axial mesoderm that is derived from the shield. This convergence of cells toward the future notochord contributes to the anteroposterior extension of the embryo (Kimmel et al., 1990). During this convergent extension the notochord precursors begin to express signaling molecules such as sonic hedgehog, which exert patterning influences on the paraxial mesoderm. The first somite forms shortly after the end of gastrulation. As somitogenesis continues, the trunk begins to lift off of the yolk and the tail extends. At the end of the first day of development, somite formation is complete and somite patterning nearly so. The most obvious differences between zebrafish and the amniote somite are anatomical: in zebrafish the large myotome is adjacent to the notochord, whereas in chick the large sclerotome is adjacent to the notochord. In addition, myogenesis begins before somite formation in fish whereas in chick it likely begins after somite formation.

1.10 Hypotheses

Since HGF was first discovered as a mitogene for hepatocyte, our study is fisrt focused on the role of HGF in zebrafish liver development. Motogenic and morphogenic outcome of the ligand/receptor would be responsible for Hgf's role in liver budding while apoptotic and proliferative outcome would be responsible for Hgf's role in liver growth. However, from previous literature, we know that HGF has pleotrophic roles in embryonic development, working as mitogene, motogene and morphogene. Due to this, many aspects of Hgf's character would be investigated to reveal its pleotrophic roles in different aspects of zebrafish development. Hgf's role in somitogenesis, hematopoiesis and angiogenesis would reflect HGF as mtiogene, motogene and morphogene.

1.11 Aim of this study

In this study, zebrafish model will be used to study the function of *hgf* and *c-met* and achive the goals as following:

- Molecular cloning of zebrafish *hgf* and *c-met*
- Expression analysis of the zebrafish *hgf* and *c-met*
- Functional analysis of the zebrafish *hgf* and *c-met*

Chapter 2. Materials and methods

2.1 Cloning

2.1.1 DNA isolation

Isolation and purification of plasmid DNA

Small-scale preparation of plasmid DNA was carried out using Qiagen Plasmid Purification kit (Qiagen, USA). The protocol involved alkaline lysis followed by binding of plasmid DNA to a silica-based resin. DNA was eluted in low salt buffer or water. Normally, about 10-20 µg of high copy number plasmid DNA can be isolated from 4 ml of overnight bacterial culture in Luria-Bertani (LB) medium.

Firstly, the bacteria in LB liquid medium with appropriate antibiotics were harvested by centrifugation at 12,000 rpm for 1 minute using the 5415C centrifuge (Eppendorf, Germany). It is recommending to shortly spin the tube again and to use pipet to remove the residue medium. Then the bacterial pellet was resuspended in 200 µl of cell resuspension solution (100 mg/ml RNase A; 10mM EDTA; 25 mM Tris-HCl, pH 7.5). 200 µl of cell lysis solution (0.2 M NaOH; 1% SDS) was added to the bacterial suspension and mixed by gently inverting the tube several times. This mixture was neutralized by adding 200 µl of neutralization buffer (1.32 M KOAc, pH 4.8). After being centrifuged in a microcentrifuge tube at 14,000 rpm for 10 minutes, the supernatant was transferred into a fresh 2-ml tube and 1 ml purification resin was added. The resin/DNA mix was transferred into a Minicolumn and washed with 2 ml of column wash solution (200 mM NaCl; 5 mM EDTA; 20 mM Tris-HCl, pH 7.5;

75% EtOH) using a vacuum manifold. The resin was drained by spinning the minicolumn at 14,000 rpm for 2 minutes. The minicolumn was then transferred to a new microcentrifuge tube and 30 µl of water was added. After 1 minutes incubation at room temperature, plasmid DNA was eluted from the column by centrifugation at 14,000 rpm for 1 minutes.

DNA gel electrophoresis

Typical DNA electrophoresis was performed in 1% agarose gel unless special requirements were presented. The agarose powder was dissolved in 1XTAE (0.04 M Trisacetate; 0.001 M EDTA) by heating. After the solution was cooled to 60°C, ethidium bromide was added to a final concentration of 0.5 µg/ml and mixed thoroughly. Alternatively, a few drops of Ethidium bromide were added to the run buffer to get an approximate concentration of 0.5µg/ml. A voltage of 1-5 V/cm was applied during the electrophoresis.

For long fragment DNA ligation (insertion size above 2kb) and template DNA for in vitro transcription, instead of ethidium bromide, crystal violet is a better choice which can protect the DNA from UV exposure.

Isolation of DNA from agarose gel

QIAquick Gel Extraction Kit (Qiagen, USA) was used to recover DNA fragments of interest ranging from 100 bp to 10 kb from agarose gel according to manufacturer's instructions. Briefly, the gel slide containing the DNA band of interest was cut from the gel and melted at 50°C in Buffer QG for 10 minutes. The volume of the Buffer QG was approximately three times of the gel slice volume. It is recommending to

vortex or rotate the tube containing gel and QG buffer for several times during 50 °C incubation. When the gel is completely melted, add 1 volume of isopropanel and vortex to mix. The column was then centrifuged at 14,000 rpm for 1 minute, washed by adding 0.75 ml of Buffer PE, and spin again. After removing residual Buffer PE by spinning at 14,000 rpm for 1 minute, 20-50 µl of sterile water was added to the top of the column. The column was incubated at room temperature for 1 minute and DNA fragment was eluted into a 1.5-ml centrifuge tube by centrifugation at 14,000 rpm for 1 minute.

Purification of PCR products

Suitable PCR products can be directly purified from the PCR mix. This purified product can be used for various applications including cloning and ligation. QIAquick PCR purification kit was used to purify the PCR product. To begin with, five times volume of Buffer PB was added to one volume of PCR sample. QIAquick spin column was placed in a collection tube. The buffer and PCR sample mix was placed in the spin column and centrifuged for 1 minute. The flow through was discarded. 0.75 ml of Buffer PE was added to the spin column and centrifuge for 1 minute. The flow through was discarded and centrifuged for additional 1 minute. The purified PCR product was then eluted with 20-50 µl of sterile water or TE buffer by incubating for 1 minute and centrifuging for 1 minute. The purified DNA can be stored at –20ºC until further use.

Quantification of DNA

DNA was quantified by optical density reading at 260nm and 280nm using UV-1601 spectrophotometer (Shimadzu, Japan) or directed read by Nano-drop (NanoDrop Technologies, USA). One unit of OD_{260} is equivalent to 50µg/ml of DNA.

2.1.2 Restriction endonuclease digestion of plasmid DNA

Restriction enzyme digestion was employed to screen recombinant clones, isolate specific DNA fragments which is the first step for DNA cloning and mapping, and linearize the plasmid DNA for in vitro transcription. All the restriction enzymes used in the study were purchased from New England Biolabs or Promega (USA). For molecular cloning, digestions were performed at 37°C for 1 to 2 hour; for in-situ probe plasmid linearization, digestions may take overnight to minimize the possibility of un-digested plasmid DNA which may reduce the yield of transcription. Normally 2-4 units of enzyme were used to digest 1µg of plasmid DNA. Digested product can be purified by running agarose gel and gel extraction. If the digested product is only one fragment, QIAquick PCR purification kit can be used to purify the product.

2.1.3 DNA ligation

DNA ligation reaction was carried out typically in 20 µl of volume, containing 2 µl of 10X ligation buffer (0.3 M Tris-HCl, pH 7.8; 0.1 M $MgCl_2$; 0.1 M DTT and 5 mM ATP), insert DNA, vector DNA and 1 unit T4 DNA ligase. The molar ratio of insert to vector DNA was usually between 2:1 to 4:1. Ligation reaction was incubated at room temperature 1 hour for sticky end or 4°C for blunt end ligation overnight.

Subsequently, the ligation reaction was terminated by inactivating the ligase by heating at 80° C for 5 minutes and then transformation was carried out.

2.1.4 Transformation

Preparation of competent cells

Successful cloning relies on high transformation efficiency. Normally $>10^7$ transformed colonies per μg of supercoiled plasmid is good for most cloning applications.

For the preparation of competent bacteria cells, 2 ml of LB broth was incubated with a single fresh colony of *Escherichia coli* (*E.coli*) strain DH5α at 37° C with 250 rpm shaking overnight. In the following morning, 0.5 ml of the culture was re-inoculated into a 250 ml flask containing 50 ml of LB broth and shaken at 250 rpm at 37° C until OD_{600} reached around 0.5. The culture was chilled on ice for 15 minutes after being transferred into 50 ml Falcon 2070 tubes. Cells were pelleted by centrifugation at 1,000 g at 4ºC for 15 minutes. The cell pellets were drained thoroughly and resuspended in RF1 (100 mM RbCl2; 50 mM MnCl2; 30 mM CH3COOK); 10 mM CaCl2 and 15% glycerol) with 1/3 volume of the original bacteria culture. After incubation on ice for 15 minutes, the cells were spun down and resuspended in 1/12.5 of the original volume of RF2 (10 mM MOPS; 10 mM RbCl2; 75 mM CaCl2; 15% glycerol). After another 15 minute-incubation on ice, the competent cells were transferred into 1.5 ml microcentrifuge tubes in aliquot and fast-frozen in liquid nitrogen. These aliquots can be stored at -80° C for several months.

Competent XL-1 Blue cells were prepared by adding 500 µl of overnight culture to about 10-15 ml of fresh LB. The cells were grown by incubation at 37ºC with shaking until the optical cell density reaches an OD600 value of 0.3-0.6. The cells were centrifuged at 6000 rpm for 10 minutes at 4ºC. The pellet was resuspended with 1/10 volume of TSB (LB with 10% Polyethylene glycol (PEG 3350), 5% Dimethyl sulphoxide (DMSO), 10mM $MgCl_2$ and 10mM $MgSO_4$) and incubated on ice for 10 minutes. The cells can be used fresh or stored at –80ºC for about one month.

Transformation

Normally 5-10 µl of ligation reaction was added into 100 µl of *E.coli* DH5 α competent cells. This transformation mixture was then incubated on ice for 30 minutes. The mixture was heated at 42° C for 60 seconds and cooled immediately on ice for 2 minutes. 900 µl of LB or SOC medium was added to the mixture and incubated with shaking (200 rpm) at 37ºC for 1 hr. After incubation, 1/10 and 9/10 of the transformation reaction mixture was spread onto two separate LB plates supplemented with appropriate antibiotics in order to produce proper density of transformant colonies. The plates were incubated at 37° C overnight.

2.1.5 Isolation of RNA

Isolation of total RNA from tissue or embryos

Total RNAs from zebrafish embryos and different tissues were extracted using RNAwiz (Ambion). Briefly, about 200 embryos or 100mg of tissues are homogenized in RNAwiz (use 1 ml of RNAWIZ for every 100 mg of tissue or 10 volumes of reagent per volume of tissue). Samples homogenized in RNAWIZ can be stored at -20 or -80ºC for up to 1 month. Incubate the homogenate at room temperature (RT) for 5

min to dissociate the nucleoproteins from the nucleic acids. Then add 0.2X Starting Volume of chloroform to the homogenate. The chloroform should not contain isoamyl alcohol (IAA) or other additives. Cover the sample, shake vigorously for ~20 seconds, and incubate at RT for 10 minutes. After incubation, mixture is centrifuged at ⩾ 10,000 x g for 15 min at 4ºC. The mixture separates into 3 phases, the colorless upper aqueous phase (containing the RNA), the semi-solid interphase (containing most of the DNA), and the lower organic phase. Without disturbing the interphase, carefully transfer the aqueous phase, into a clean RNase-free tube. Add 0.5X Starting Volume of RNase-free water, 1 Starting Volume of isopropanol, mix well, and incubate at RT for 10 minutes. Centrifuge at ⩾10,000 x g for 15 min at 4ºC to pellet the RNA. After centrifuge, decant the supernatant and wash the pellet with at least 1 Starting Volume of cold 75% ethanol by vortexing. Centrifuge at ⩾10,000 x g for 5 min at 4ºC. Discard the supernatant and air dry the pellet for about 10 min; do not let the RNA dry completely, as this will make it difficult to resuspend. Finally, RNA is resuspended in an appropriate amount of RNase-free water, or in formamide. Briefly vortex or repeatedly pipet to aid in resuspension, and if necessary, heat to ~60ºC. If stored in formamide, the RNA should be precipitated with 4 volumes of ethanol prior to being used in experiments such as RT-PCR.

Measurement of RNA concentration

RNA was quantified by optical density reading at 260nm and 280nm using UV-1601 spectrophotometer (Shimadzu, Japan) or directed read by Nano-drop (NanoDrop Technologies, USA). One unit of OD_{260} is equivalent to 40μg/ml of RNA, OD_{260}:OD_{280} ratios >2.0 indicates good quality of RNA products.

RNA gel electrophoresis

10µg of total RNA was fractionated on 1.2% denaturing agarose gel (1.2% agarose, 1X MOPS, 6% formaldehyde). Each RNA sample contained 50% formamide, 1X MOPS, 7% formaldehyde, 0.1 mg/ml ethidium bromide, and was heated at 65°C for 10 minutes before loading with loading buffer (1X0.4% bromophenol blue, 6% sucrose in water). The gel was run at 80 volts in running buffer containing 1X MOPS and 3% formaldehyde until the dye runs out into the buffer. The gel was then rinsed in distilled water and a picture was taken with a ruler to show the distance among the bands.

2.1.6 Polymerase chain reaction (PCR)

PCR is a powerful tool to amplify DNA fragments by a thermostable DNA polymerase and a pair of primers. It has been extensively used for various purposes like rapid amplification of cDNA ends (RACE) and colony screening.

Standard PCR

Typical PCR was performed in a 50µl reaction using the Perkin Elmer DNA thermal cycler Model 480 and 9600 (Perkin Elmer, USA), Peltier Thermal Cycler PTC200 (MJ Research, USA). Each reaction included 5µl of 10X PCR buffer (0.5M KCl, 0.1M Tris-HCl, pH8.8, 15mM $MgCl_2$, 1% Triton X-100), 1µl of 5mM dNTP, 1µl of 10pmol sense primer, 1µl of 10pmol antisense primer, 0.2µl of 5U/µl Taq polymerase and 1µl template DNA. A typical PCR reaction cycle consists of the following steps: denaturation at 94°C for 5 minutes, followed by 35 cycles of <94°C for 30 seconds, annealing at the required temperature for 1 minute or its variable depending on the product size and 72°C for 1-2 minutes and final extension at 72°C for 10 minutes.

Reverse-transcriptase PCR (RT-PCR)

RT-PCR was performed in either two-step reaction or one-step reaction. In two step reaction, first step involved synthesis of first strand cDNA and the second step involved amplification of fragments of interest from single strand cDNA as template with two gene specific primers. First strand cDNA was synthesized from total RNA. The first strand cDNA synthesis reaction was performed in 50 µl total volume containing 5 µl of 10X first-strand buffer (50 mM Tris-HCl, pH=8.3, 75 mM KCl, 3 mM $MgCl_2$ and 10 mM DTT), 1 µl of 50 mM dNTP, 1 µl of RNAse inhibitor (40 U/µl), 5 µl of oligo dT primer (1 µg/µl), 5µg of total RNA and 1 µl of MMLV reverse transcriptase (50 U/µl). After incubating at 37°C for 1.5 hours, the reaction can be stored at -80°C or used as template for PCR immediately. PCR reaction was carried out using the standard condition described above. The one-step reaction was done using a Qiagen one-step RT-PCR kit (Qiagen, USA). The reaction mix contains all the components including a pair of genespecific primers as recommended by the kit specifications.

Quantitative Reverse-transcriptase PCR (RT-PCR)

qRT-PCR was performed in one-step reaction using QuantiTect SYBR Green RT-PCR Kit (QIAGEN, USA) and Real-Time PCR Thermal Cycler (MJ Research, USA). The reaction was performed in 20µl total volume containing 10µl of 2X QuantiTect SYBR Green RT-PCR Master Mix, 0.2µl of QuantiTect RT Mix, 2 µl of primers (10µM). A typical qRT-PCR reaction cycle consists of the following steps: reverse transcription at 50°C for 30 minutes, denaturation at 95°C for 15 minutes, followed by 35-45 cycles of 95°C for 15 seconds, annealing at the required temperature for 15

seconds and 72° C for 30 seconds. Threshold reading method is modified from Larionov's study (Larionov et al., 2005). Results were analyzed by MJ Research Opticon 2 software (MJ Research, USA).

Rapid amplification of cDNA ends (RACE)

Combination of gene-specific primers and vector primer were applied for RACE. RACE PCR conditions were essentially the same as the standard one as described previously, except that different annealing temperatures were used depending on the melting temperature (Tm) of the gene-specific primers. 25 µl of PCR product was electrophoresized on a 1% agarose gel. The prominent and large bands were recovered by the QIAquick Gel Extraction Kit (Qiagen, USA).

Colony screening PCR

PCR is a simple, fast and sensitive way to detect trace amount of specific DNA molecules. Thus, PCR can be applied to screen for correct recombinant DNA directly using the bacteria colonies, as DNA would be effectively released from bacteria cells under the high temperature conditions during PCR. A pair of vector primers flanking cloned insert will define the size of insert by a PCR. Colony screening by PCR is more sensitive and less time-consuming than restriction enzyme digestion analysis of extracted and purified plasmids.

For PCR screening, colonies to be examined were marked in numerical order. A toothpick was used to touch the colony and the attached bacteria was inoculated in PCR tube preloaded with 20µl pf PCR mixture, containing 0.6U of Taq DNA polymerase, 2µl of 10X PCR buffer, 1µl of 2mM dNTP mix and 0.2µg each of sense

and antisense primers. PCR program includes initial denaturation at 94°C for 5 minutes, followed by 30 cycles of denaturation at 94°C for 30 seconds, annealing at appropriate temperature (for example 55°C) for 45 seconds and elongation at 72°C for 1-2 minutes. PCR product was examined in 1~1.5% agarose gel. Colonies that yielded PCR products with expected size were inoculated for plasmid DNA preparation.

Cloning of PCR products

The recovered PCR products were cloned into the pGEMT easy vector (Promega, USA). The pGEMT easy vector is prepared by cutting vector with EcoRV and adding a 3' terminal thymidine to both ends by the manufacturer. These single 3'-T overhangs at the insertion site greatly improve the efficiency of ligation of PCR products into the plasmid because the Taq DNA polymerase generates a 3' adenine overhang in the PCR products. The ligation reaction was performed as described in section 2.1.3.

2.1.7 Sequencing of double-stranded DNA

Automated sequencing reactions were carried out using the ABI PRISM™ BigDye™ Terminator Cycle Sequencing Ready Reaction Kit (Perkin Elmer). The kit contains a sequencing enzyme AmpliTaq® DNA Polymerase called FS and a set of dye labeled terminators for fluorescent cycle sequencing lager fragments with more accuracy. Each sequencing reaction (20 µl) contains 8 µl of Terminator Ready Reaction Mix, 200-500 ng of double strand DNA, and 1 µl of primer (0.2 µg/µl). PCR was performed on the GeneAmp PCR System 9600 (Perkin Elmer) with 25 cycles of 96°C for 10 seconds, 50°C for 5 seconds and 60°C for 4 minutes, and finally hold at 4°C.

Ethanol precipitation was carried out to purify the extension products. 2 µl of 3 M NaOAc (pH4.6) and 50 µl of 95% ethanol was mixed with the 20-µl reaction mix, and incubated at room temperature for 15 minutes. The tube was spun at 4°C for 20 minutes at 14,000 rpm. The pellet was rinsed with 250 µl of 70% ethanol and air-dried. The DNA pellet was dissolved in 6 µl of loading dye [50 ml contains EDTA (25 mM, pH8.0) 1 ml; 10 ml deionised formamide; 50 mg Dextran blue and 39 ml H_2O] and heated to 92°C for 3 minutes. Samples then were chilled on ice for 2 minutes before being loaded into the sequencing gel (18g urea; 5 ml 10X TBE; 5 ml long range gel solution and26 ml H_2O; 250 µl 10%APS and 35 µl TEMED). The electrophoresis was carried out at 1,690 volts for 5-9 hours. The sequencing ladders were analyzed automatically by an ABI377 sequencer system and software.

2.1.8 Vectors used

pCS2+

pCS2+ is a multipurpose expression vector. Although originally designed for expressing proteins in Xenopus embryos from either injected RNA or DNA, pCS2+ is also useful for high-level transient expression in a wide variety of mammalian and avian cells. It is also functional in zebrafish embryos (as DNA or RNA), and it can be used for in vitro transcription/translation (using, for example, the Promega TnT system). A number of derivatives of CS2 have been constructed that allow fusions to epitope tags and other marker proteins, as well as nuclear localization signals or the gal4 DNA binding and activation domains. In almost all cases, the same reading frames are used for the fusion vectors, to facilitate moving genes between multiple CS2 derivatives.

pCS2+ contains a strong enhancer/promoter (simian CMV IE94) followed by a polylinker and the SV40 late polyadenlyation site. An SP6 promoter is present in the 5' untranslated region of the mRNA from the sCMV promoter, allowing in vitro RNA synthesis of sequences cloned into the polylinker. A T7 promoter in reverse orientation between the polylinker and the SV40 polyA site for probe synthesis, as well as a second polylinker after the SV40 polyA site to provide several possible sites to linearize the vector for SP6 RNA transcription. The vector backbone is from pBluescript II KS+ and includes the amp resistance gene and an f1 origin for producing single stranded DNA. (Fig.2.1)

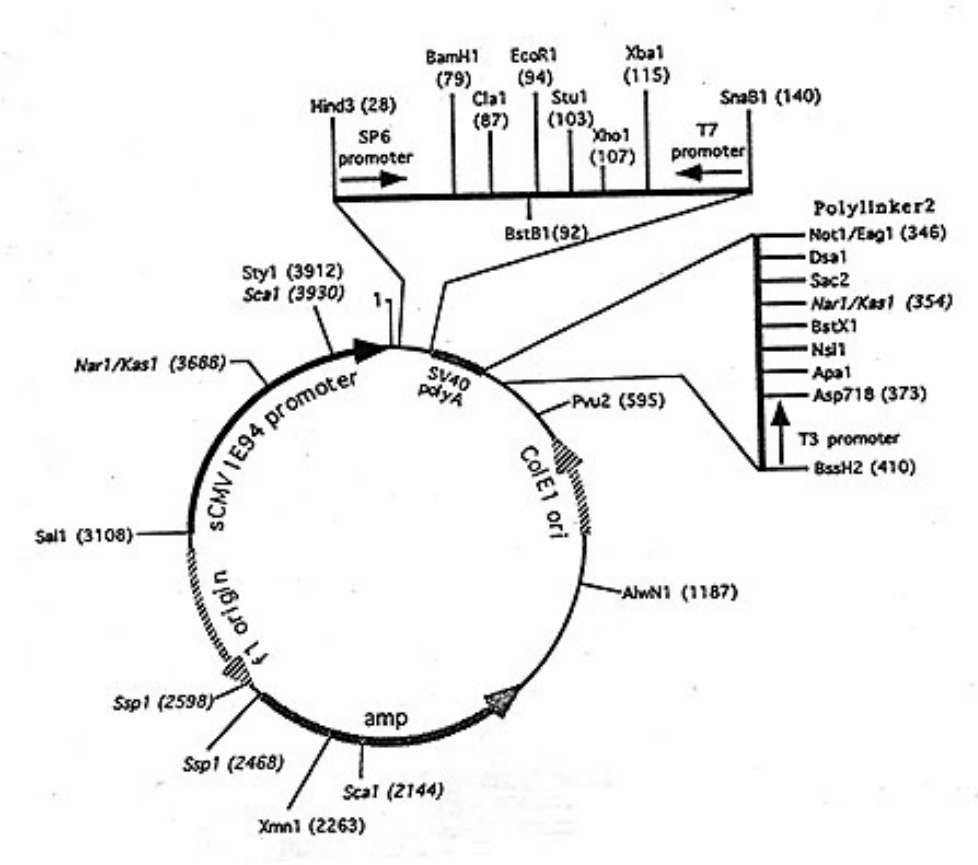

Fig.2.1 pCS2+ vector map. (reproduced from http://faculty.washington.edu)

pGEM®-T easy

The pGEM®-T and pGEM®-T Easy Vector Systems are convenient systems for the cloning of PCR products. The vectors are prepared by cutting Promega's pGEM®-5Zf(+)(b) and pGEM®-T Easy Vectors with EcoR V and adding a 3′ terminal thymidine to both ends. These single 3′-T overhangs at the insertion site greatly improve the efficiency of ligation of a PCR product into the plasmids by preventing recircularization of the vector and providing a compatible overhang for PCR products generated by certain thermostable polymerases (Fig.2.2).

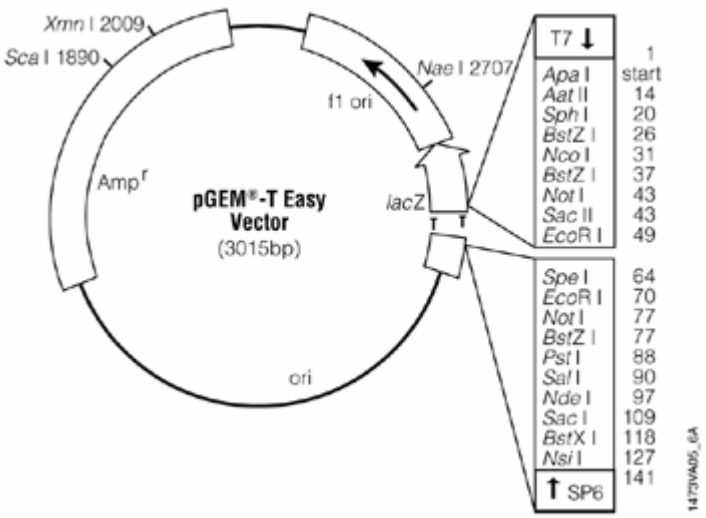

Fig.2.2 pGEM®-T easy vector map. (reproduced from www.promega.com)

2.2 Expression analyses

2.2.1 Zebrafish (Danio rerio) maintenance

A local line of wild-type zebrafish was bought. A Tg(lfabp:RFP; elsA:GFP) fishes line, which has red fluorescent protein (RFP) and green fluorescent protein (GFP) expression in the liver and pancreas respectively (borrowed from Prof. Gong's lab) and a Tg (fli-1:GFP) fish line, which has GFP expression in endothelial cells, was used. The fishes were maintained according to The Zebrafish Book (Westerfield,

1995) and fed with blood worms and/or live brine shrimps thrice a day. Males and females were kept in separate tanks.

Adult wild type zebrafish were bred according to methods described in The Zebrafish Book (Westerfield, 1995). For breeding, two to three pairs of fish were transferred to the breeding tank with RO water (supplemented with 60 mg/ml of sea salt) and left overnight. The males and females were separated using a divider, which was removed the following morning and the fish were allowed to spawn on natural light. Adult transgenic zebrafish were bred in a similar way, except that the breeding tank was set at photo period room (The room which has light automatically on at a pre-set time in the following morning) and no divider was used. As breeding and egg production can cause extensive energy loss to the fish, it is important to ensure that each fish is only used once a week for breeding. Also, the fish must be bred periodically to sustain the productivity of the breeding stocks and the quality and quantity of egg production.

The embryos were collected by pouring all the water through a clean sieve. As the embryos could not pass through the small diameter of the individual hole of the sieve, they were retained on the sieve. The embryos were washed with water and all the debris were removed by siphoning. Embryos were transferred to egg water [1 L Milli Q water supplemented with 1.5 ml stock salts, The Zebrafish Book (Westerfield, 1995)] and placed in an incubator at 28.5^{o} C. Embryos older than 24 hours post fertilization (hpf) were raised in 0.003% 1-phenyl-2-thiourea (PTU, Sigma) in egg water to inhibit the production of pigment. The embryos were constantly monitored under the microscope for staging. Time of development at 28.5oC and morphological features (Kimmel et al., 1995) were used to stage all the embryos in this project.

2.2.2 In situ hybridization

Linearization of plasmid DNA

10µg of plasmid DNA was linearized at the 5' end of the cDNA insert by a proper restriction enzyme at 37°C for 2 hours to overnight. Completion of linearization was confirmed by running the digestion product on 1% agarose gel. After confirming, if there is only one digestion site on the plasmid, digested product can be purified by PCR purification Kit. Otherwise mixed products should be loaded on the gel to separate and be purified by Gel extraction Kit (using crystal violet rather than EB).

Probe incubation and precipitation

1µg of linearized DNA was used to synthesize the DIG/Fluorescein labeled probe. The reaction was performed at 37°C for 2 hours to overnight in a total volume of 20µl containing 2µl of 10X transcription buffer (Roche), 2µl of DIG/Fluorescein-NTP mix [10mM ATP, 10mM CTP, 10mM GTP, 6.5mM UTP and 3.5mM DIG/Fluorescein-UTP (Roche)], 0.5µl of RNase inhibitor (40U/µl) (Roche) and 2µl of T7 or SP6 RNA polymerase (50U/µl) (Roche). Following the reaction, 1 µl of 0.5M EDTA (pH 8.0) was used to stop the restriction digestion. Subsequently, 2.5µl of 4M LiCl and 75µl of cold pure ethanol were added to precipitate the RNA. After washing with 75% ethanol, the RNA probe was resuspended in 50µl of DEPC treated water.

Quantification of labeled probe

The labeled probe was quantified visually by Gel Electrophoresis and quantitated using spectrophotometric analysis at $OD_{260/280}$ nm or Nano-drop.

Preparation of zebrafish embryos

All zebrafish embryos used in this study were staged according to the *Zebrafish Book* (Westerfield, 1989) and indicated as hours post fertilization (hpf) at 28.5°C. Staged embryos were fixed in 4% paraformaldehyde (PFA)/PBS (0.8% NaCl, 0.02% KCl, 0.0144% Na_2HPO_4. 0.024% KH_2PO_4, pH 7.4) for 12 to 24 hours at room temperature or 4ºC. Embryos younger than 16 hpf were fixed before dechorionization and the chorion was removed afterwards. Embryos older than 16 hpf were dechorionated before fixation. Older embryos with tails were hibernated on ice before fixation to prevent the curling of tails. After fixation, the embryos were washed in PBST (0.1% Tween20 in PBS) twice for 1 minute each, followed by four times for 20 minutes each on a nutator (ClAY ADAMS® Brand, Becton Dockinson, USA) at room temperature. After changing PBST to methanol by incubating with 50% and 100% methanol (two times each), the embryos were kept at -20°C for several months. Before they were used for in situ hybridization, the embryos were rehydrated in PBS in two or three times by changing half volume of solution each time.

Proteinase K treatment

This step is especially necessary for embryos older than 14 somites (>16hpf). Embryos were treated with 10 µg/ml of proteinase K in PBST at room temperature. The time of exposure depended upon embryos age and the specific activity of proteinase K, which varied from batch to batch. For most cases, the conditions used are as given.

16-24 hpf 3-4 minutes

24-32 hpf 5-6 minutes

32-50 hpf 10-20 minutes

To stop the reaction, the proteinase K solution was removed completely, and the embryos were fixed again in 4% PFA/PBS for 20 minutes at room temperature. Embryos were first washed in PBST twice for 1 minute and then 4-5 times for 15-20 minutes each.

Prehybridization

Prehybridization was performed by changing half the volume of washing solution with hybridization buffer [50% formamide, 5X SSC, 50 µg/ml Heparine, 500 µg/ml tRNA, 0.1% 0.1% Tween 20, pH6.0 (adjusted bycitric acid)] and incubated at room temperature for 1 hour. This solution was removed and replaced with hybridization buffer; embryos were incubated at 68°C for 5-10 hours.

Hybridization

1-2µl of DIG-labeled probe was diluted in 200µl of hybridization buffer. The probe was denatured by heating at 80°C for 5 minutes followed by 2 minutes of ice bath. Embryos of different stages or treatments were selected and placed in one tube or separate tubes depending on the experimental conditions. The original buffer was replaced with the denatured probe dissolved in hybridization buffer. Hybridization was performed at 68°C in a circulating water bath overnight with shaking.

Post-Hybridization washes

The next day, the probe was removed and replaced with prewarmed 100% hybridization wash solution (hybridization buffer without tRNA and heparine) for 15

minutes. The embryos were then washed in the following order of wash solutions 75% hybridization wash solution: 25% 2X SSCT (SSC with 0.1% Tween 20), 50% hybridization wash solution:50% 2X SSCT, 25% hybridization wash solution:75% 2X SSCT for 15-20 minutes each. This was followed by 2X SSCT wash twice for 30-45 minutes each and 0.2X SSCT wash twice for 30-45 minutes each. Subsequently, the embryos were washed twice with PBST (PBS with 0.1% Tween 20) at room temperature for 5 minutes each.

Preparation of preabsorbed DIG

Commercial DIG-AP antibodies (Boehringer) should be preincubated with biological tissues, preferably of the same origin as the sample used for hybridization, in order to decrease the staining background and increase signal-to-noise ratio. Anti-DIG and Fluorescein-AP was diluted to 1:500 and 1:50 in Maleic Acid buffer (0.15M Maleic acid, 0.1M Nacl; pH 7.5)/10% FCS (Fetal calf serum, Gibco BRL) respectively and incubated with 50 zebrafish embryos of any stages on a nutator at 4°C overnight. After that, the antibodies solution was transferred to a new tube and diluted to 1:5000 and 1:500 with Maleic Acid buffer/10% FCS. 10µl of 0.5M EDTA (pH8.0) and 5µl of 10% sodium azide were added to prevent bacterial growth. The preabsorbed antibody was stored at 4°C and can be used for many times.

Incubation with preabsorbed antibodies

The embryos after hybridization and post hybridization washes were incubated in Maleic Acid buffer/10% FCS for 2 hours at room temperature to block non-specific binding sites for antibody. After removing the blocking solution, the embryos were incubated with preabsorbed anti-DIG-AP antibody at 4°C overnight.

Color development

Embryos were washed in PBST twice for 1 minute each, and 4 times for 15-20 minutes each on a nutator at room temperature followed by washing in buffer 9.5 (0.1M Tris-HCl, pH9.5, 50mM $MgCl_2$, 10mM NaCl and 0.1% Tween 20) once for 30 seconds and twice for 10 minutes each. 4.5µl of NBT (Nitroblue tetrazolium, Boehringer Mannheim, 50mg/ml in 70% dimethyl formamide) and 3.5µl of BCIP (5-bromo, 4-chloro, 3-indodyl phosphate salt, Boehringer Mannheim, Germany; 50mg/ml in H_2O) was added into 1ml of buffer 9.5 with embryos and mixed thoroughly. Embryos were kept in dark at room temperature for few minutes to several hours, and the progress of staining was monitored from time to time under a Leica MZ12 microscope (Leica, Germany). To stop the reaction, staining solution was removed and the embryos were washed in 1X PBST twice for 10 minutes each. Embryos can be preserved in 4% PFA/PBS at 4^{o}C.

Mounting and photography

Selected embryos were washed with PBST twice for 10 minutes each and transferred to 50% glycerol/PBS, equilibrated at room temperature for several hours. For whole mounts, a single chamber was made by placing stacks of 3-5 small cover glasses on both side of a 25.4X76.2 mm microscope slide. Small cover glasses in the stacks will be perfectly solid 1 hour after placing a drop of Permount between them. Selected embryo was transferred to the chamber in a small drop of 50% glycerol/PBS and oriented by a needle. A 22X44 mm cover glass with a small drop of the same buffer was superimposed onto the embryo. The orientation of the embryo can be adjusted by gently moving the cover glass. For flat specimen, the yolk of selected embryo was

removed completely by needles. The embryo without yolk was then placed onto a slide with a small drop of 50% glycerol/PBS and adjusted to a proper orientation by removing excess of liquid and with the help of needles. A small fragment of cover glass (a bit larger than the specimen) was covered onto the embryo. Care was taken to avoid bubbles and a drop of 50% glycerol/PBS was added to fill the space under the cover glass. This specimen was sealed with nail polish along the edge of the cover glass to prevent it from drying. Photographs were taken using a camera mounted to an Olympus AX-70 microscope (Olympus, Japan). The films used were Kodak Gold 200 and 400 ASA.

2.2.3 Cryosectioning embryos

Preparation of slides and blocks

The fixed and stained embryos were first transferred into molten 1.5% bactoagar, equilibrated with 30% sucrose (at 48ºC) in a detached cap of eppendorf tube. The samples were adjusted to the required orientation with needles before the agar solidified. After the agar block solidified, a small block was cut with razor or blade in such a way that a flat base and a slanting top edge was created for proper positioning and sectioning of the sample. The block was then transferred to 30% sucrose solution and incubated at 4ºC overnight for equilibration.

Sectioning, mounting and photography

Subsequently, the block was placed on the frozen surface of a layer of tissue freezing medium cryostat (Reichert-Jung, Germany) on the prechilled tissue holder. The block was then coated with a drop of cryostat freezing medium and frozen in liquid nitrogen until the block had solidified completely. The frozen block was placed in the cryostat

chamber (Reichert-Jung, Germany) for 30 minutes to 1 hour to equilibrate with chamber temperature of –25ºC. Normally, 10µm thick sections were cut and placed on superfrost plus slides (Fisher, USA). The slides were dried on a 42ºC hot plate for about 30 minutes to 1 hour. The sections were then fixed briefly with 4% PFA-PBS for 10 minutes and washed gently with PBS for 3 times, 10 minutes each and cryosectioned (10-20 µm). These sections was either embedded in several drops of glycerol and covered with glass cover-slip for photography or used for section *in situ* hybridization or immunohistochemistry

2.3 Functional analyses

2.3.1 Microinjection into embryos

The samples for injection were prepared to different concentrations in respective buffers. Morpholino antisense oligos were prepared in 1X Danieau solution (58 mM NaCl; 0.7 mM KCl; 0.4 mM $MgSO_4$; 0.6 mM $Ca(NO_3)_2$; 5.0 mM pH 7.6 HEPES). The needles used for the microinjection were prepared using optimized conditions of heat and pull time for different purposes using the Sutter Micropipette puller P-97 (Sutter Instruments Co, USA). The conditions for normal injections into 1-2 cell embryos used were Pressure-500, heat-500/550, pull-150/150, velocity-100/100 and time-150/150. Antisense oligos were injected into the cytoplasm of 1-2 cell stage zebrafish embryos using Picoinjector PLI-100 (Medical Systems Corp, Greenvale, NY, USA) by placing the embryos under a dissection microscope (Olympus SZX12). Each embryo received the specific volume of the samples depending on the concentration of the sample. The injected embryos were reared in egg water (1ml of

egg water contains 10% NaCl, 0.3% KCl, 0.4% CaCl2, 1.63% MgSO4.7H2O, 0.01% methylene blue, and 95 ml ddH2O).

2.3.2 Design of morpholino anti-sense nucleotide oligo (MO)

MO has become an attractive method to specifically block gene function (Nasevicius and Ekker, 2000; Summerton and Weller, 1997). Design of an efficient antisense Morpholino required the careful consideration of certain criterias. For translation blocking MO, the target sequence, approximately 25 bp for MO should be located in the post-spliced mRNA in the region from the 5'cap to about 30 bp 3' to the AUG translational start site. For splicing interfering MO, the target sequence, approximately 25 bp for MO should be located in the pre-mRNA intron and exon junction. Different from translation blocking MO, splicing interfering MO modifies the mRNA splicing and alters the nucleotide sequence structure of mRNA. Hence, the knockdown effect by splicing interfering MO can be easily detected by RT-PCR. It is especially useful when antibody is not available. Using the criterias MOs were designed and ordered from http://www.gene-tools.com.

2.4 List of primers and morpholino oligos.

Primers

HGFpf	5’TGGGACTCGCAGAAACCTCAT3’
HGFpr	5’AGGGAATTTCAGAGCCATCAGG3’
HGF3ex	5'TGCGGAGTGTATGAATGGATGTGAGGAG3'
HGF3in	5'GCTGGTCACCTCCACTTCCACATCG3'
HGF5ex	5'CAGATAGCGATGTGGAAGTGGAGGTGAC3'
HGF5in	5'AGAGGGCTACAGGGGTACAGTCAACGTG3'
HGFf	5'TGCGGTTTGATCCTGTTCATCCTTCACA3'
HGFr	5'ACCAAAGCAAACTTTAGCCTCCAAAATG3'
HGFb3ex	5'ATGACGTGTAACGGAGAAAGTTATCGTG3'
HGFb5ex	5'GTTTGACTCCACAGCGAGGGATGTTGGT3'

HGFb3in	5'GCTGGGACCTTGAGGAACCACATAAACA3'
HGFb5in	5'TAGGCACAGTGGGATCAGTAGTGAAGCA3'
HGFbfex	5'CACTGTCCACAAGAGCCACTGCA3'
HGFbrex	5'ACAGATTCTGGCTGCTCGTCTGC3'
HGFbfin	5'AGGAAACGCCAAGATTCCTCACA3'
HGFbrin	5'CTCGTCTGCACTTCGGTCCAGTA3'
c-met3ex	5'GTCGTTTGGTGTTTTGCTGTGGGAACTG3'
c-met3in	5'GAAGCTGCCTGTCAAATGGATGGCG3'
c-met5ex1	5'CTCTGGTTGTAACAGTCTCCGGCCTTGC3'
c-met5in1	5'CAGTTCCCACAGCAAAACACCAAACGAC3'
c-met5ex2	5’TCGTTCCAGCAACCACGTCTATCAG3’
c-met5in2	5’TGACCTCTGAGTGGAGCGGAGGAAGGAG3’
c-metf	5'GAGGGAGGAAGAGCGGACAACTTTTGAG3'
c-metr	5'TTTTAGGTGTCTCAGGTGCAGCAGTCGC3'
ASpliceSense	5'GTGTTTGTTTAATCTCCTCGTC3'
ASpliceAnti-sense	5'CAAAGTAGAATGCCCTGCAG3'
ARTSense	5'GTTTGTTTAATCTCCTCGTCT3'
ARTAnti-sense	5'AGTGAGTTCAGTGAAGCACC3'.
BSpliceSense	5'TGCCATCTGTCATGCAACAT3'
BSpliceAnti-sense	5'TTTTCTGATCAAAGCTGAAT3'
CSpliceSense	5'ATGTTTAACTTCTCCATGTG3'
CSpliceAnti-sense	5'AAAGCGGGAAACCACCACCT3'.

Morpholino Oligos

HGFa-ATG	5'CATAATGTCCGATCTCATGTTTCTC3'
HGFa-ATG5mis	5'CATAATCTCGGATGTCATCTTTGTC3'
HGFb-ATG	5'AAATTTTGTAAATCCACATGTCGCT3'
HGFb-ATG5mis	5'AAAGTTTCTAAATGCACATCTCCCT3'
c-met-ATG	5'CAGCTTCAGAATAGTGAATTGTCAT3'
c-met-ATG5mis	5'CACCTTGAGAATACTGAATTATGAT3'
HGFa-ex1	5'GTATGCTGGTCACTTACCCACATTC3'
HGFb-ex1	5'GAAAATCAAACTTACCTGAGTAAAC3'
c-met-ex1	5'TTAGCTGAAAGCTCTTACCTGGTTG3'
HGFb-ex2	5'AAACTTTGAAGCCCTTTGTACCTGC3'
HGFb-ex3	5'AATAAAACACTCTTGCTTACCTTTC3'

Chapter 3. Results

3.1 Cloning of Zebrafish *hgfa*, *hgfb* and *c-met*

3.1.1 Isolation of *hgfa, hgfb and c-met* full-length cDNA

3.1.1.1 Isolation of *hgf* full-length cDNA

Degenerate PCR was first used to isolate the full-length cDNA and several attempts had proven this approach to be unsuccessful, which may be due to the low homology of HGF between zebrafish and other species. By blasting *Xenopus hgf* cDNA sequence against the Ensembl zebrafish genome database, a predicted cDNA sequence of 1650bp with the annotation of *hgf* was found. Based on that predicted zebrafish *hgf* fragment, a pair of primers (HGFpf and HGFpr) near 3' prime end was designed to isolate the partial sequence from zebrafish. Because this cDNA sequence is assembled from the genome DNA sequence according to the predicted intron-exon junction, attention was paid to avoid primers crossing the predicted different exons and from the first or last exon. This precaution was later proven to be useful since there were some mismatch between the predicted cDNA sequence and the isolated cDNA sequence by RT-PCR, and the last exon in the predicted cDNA sequence can not be found in the isolated full-length cDNA sequence, which was due to the mis-prediction of intron-exon junction by the genome database.

Based on this isolated *hgf* fragment of 379bp, we designed primers for Rapid Amplification of cDNA Ends (RACE) to obtain the full-length cDNA by nested PCR. 3' RACE with nested PCR (HGF3ex and HGF3in) resulted in isolation of an 800bp

fragment that reaches to the 3' end of the gene. 5' RACE with nested PCR (HGF5ex and HGF5in) resulted in isolation of a 3000bp fragment that reaches to the 5' end of the gene. These two fragments were cloned into pGEM®-T Easy vector (Promega, USA) and sequenced. Full-length cDNA was then amplified by RT-PCR from 24 hour post fertilization (hpf) zebrafish total RNA using a pair of primers (HGFf and HGFr) which flank the complete open reading frame (ORF) of 2339bp. Schematic representation of this cloning process is shown in Fig.3.1. The nucleotide sequence of the zebrafish *hgf* and its deduced amino acid sequence are shown in Fig.3.2. This *hgf* was later renamed *hgfa* after a second copy of *hgf* gene was found from the zebrafish genome.

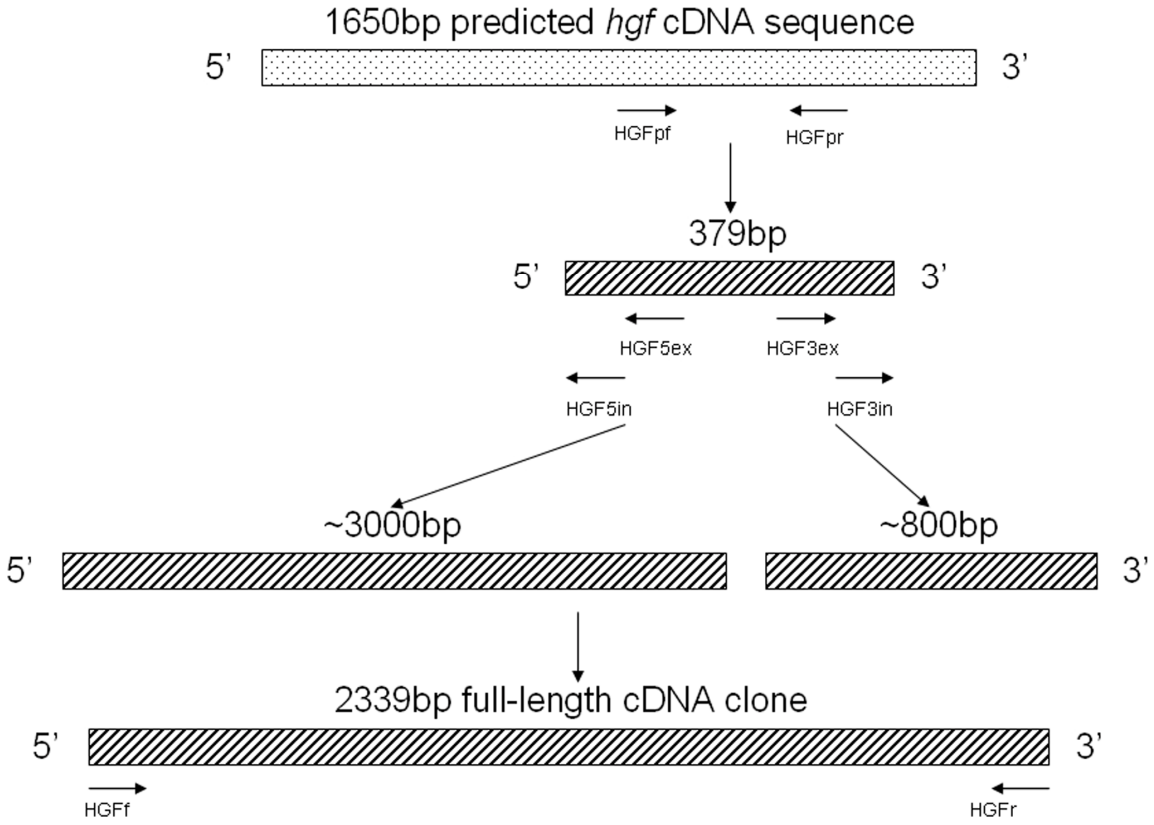

Fig.3.1 Schematic representation of the procedure of isolation and cloning of full-length zebrafish *hgfa* cDNA clone by RACE-PCR.

```
1          TTGAGAAAGAGAGAGAGAGTGAGAGAGCAGTCGCTGCGGTTTGATCCTGTTCATCCTTCA
61         CACCAGCAGCAGCAGCAGCATCAACTCGGACTTTATAGACTCTCCACCCCACAGCCTGGA
121        ATATCAAACCGAGAAACATGAGATCGGACATTATGTGGATGTATCAAGCTCTTCTCTTTG
1                                  M  R  S  D  I  M  W  M  Y  Q  A  L  L  F
181        TCGTACTGACCGTGAATGTGGATTGCAGAAAACAGACATTGCAGAGGTATCAGAAAAGTG
15         V  V  L  T  V  N  V  D  C  R  K  Q  T  L  Q  R  Y  Q  K  S
241        AAAACAGCCGACTGCTTTGTACAGACTGTCCAGAATCCCCTCGAATTAGGAACCTGTCGC
35         E  N  S  R  L  L  C  T  D  C  P  E  S  P  R  I  R  N  L  S
301        TGGAGGAATGCGCACGCAAATGTAGCAAGAGCAAGAAGTCCTGCAGGGCATTCTACTTTG
55         L  E  E  C  A  R  K  C  S  K  S  K  K  S  C  R  A  F  Y  F
361        ACCACATAAACAGGAAATGTCACTTTCTTCCTTTTGACCGTTTCTCCGAAGGCGCGAAGA
75         D  H  I  N  R  K  C  H  F  L  P  F  D  R  F  S  E  G  A  K
421        GAGAGCGAAAACCCAGTTGTGACCTTTACGAGAAGAAAGACTATGTGAGGGAGTGCATCA
95         R  E  R  K  P  S  C  D  L  Y  E  K  K  D  Y  V  R  E  C  I
481        TTGGGTCAGGTGTCAACTACAAGGGGAGAAGGTCATTCACAAAGACTGGAATTACGTGCC
115        I  G  S  G  V  N  Y  K  G  R  R  S  F  T  K  T  G  I  T  C
541        AATCCTGGAATATGTCCGTCCCACATGAGCACAATTTTAAGCCTACCAGACACAAAAAGT
135        Q  S  W  N  M  S  V  P  H  E  H  N  F  K  P  T  R  H  K  K
601        CTGACCTACGTCAGAACTTTTGCCGAAATCCAGACAATGATCCAAATGGGCCCTGGTGCT
155        S  D  L  R  Q  N  F  C  R  N  P  D  N  D  P  N  G  P  W  C
661        TCACTGAACTCACTGAGACCCGGCACCAGGATTGTGGACTGCCTCAGTGTTCAGATGTGG
175        F  T  E  L  T  E  T  R  H  Q  D  C  G  L  P  Q  C  S  D  V
721        AGTGTATGAAATGTAATGGGGAAACCTACAGAGGGCCCATGGATCATACAGAGAGTGGGA
195        E  C  M  K  C  N  G  E  T  Y  R  G  P  M  D  H  T  E  S  G
781        AAGAGTGCCAGAGATGGGACTCGCAGAAACCTCATAAACACACCTACCAGCCTCACAGGC
215        K  E  C  Q  R  W  D  S  Q  K  P  H  K  H  T  Y  Q  P  H  R
841        ATGTAGGTAAAGGTCTGGATGACAACTTCTGCCGCAATCCCAATAATGATGTTCGTCCGT
235        H  V  G  K  G  L  D  D  N  F  C  R  N  P  N  N  D  V  R  P
901        GGTGTTACACGATGGACAAAAACACCCCTTGGGAGTACTGTAACATCAGTGTGTGTGACT
255        W  C  Y  T  M  D  K  N  T  P  W  E  Y  C  N  I  S  V  C  D
961        CAGATAGCGATGTGGAAGTGGAGGTGACCAGCTCTTGTTTTCGGGGTCAAGGAGAGGGCT
275        S  D  S  D  V  E  V  E  V  T  S  S  C  F  R  G  Q  G  E  G
1021       ACAGGGGTACAGTCAACGTGACCCCTGCAGGTGTGACCTGTCAACGCTGGGACGCTCTCT
295        Y  R  G  T  V  N  V  T  P  A  G  V  T  C  Q  R  W  D  A  L
1081       CTCCTCACATCCATTCATACACTCCGCACAACTATAAATGCAAGGATCTGAGGGAGAACT
315        S  P  H  I  H  S  Y  T  P  H  N  Y  K  C  K  D  L  R  E  N
1141       ATTGCAGAAATCCTGATGGCTCTGAAATTCCCTGGTGTTTCACCACAGACGCAAAAGTGC
335        Y  C  R  N  P  D  G  S  E  I  P  W  C  F  T  T  D  A  K  V
1201       GCAAAGCTTTCTGTACCAACATTCCCAGATGCGAATCAGAGAGCTCTGACAGCACAGAAT
355        R  K  A  F  C  T  N  I  P  R  C  E  S  E  S  S  D  S  T  E
1261       GTTATGAAGACAACGGAGAGAGTTATCGTGGCAATTTGTCGAAAACGAGATCTGGTATTC
375        C  Y  E  D  N  G  E  S  Y  R  G  N  L  S  K  T  R  S  G  I
1321       CTTGCGGACTCTGGTCTGACCACACATTCAGGAGAGACACCCGGTCAGCGAAGGCCAGCG
395        P  C  G  L  W  S  D  H  T  F  R  R  D  T  R  S  A  K  A  S
1381       CGGGTTTAGAGTTGAACTTGTGCAGGAATCCAGACAGAGATAAGCACGGGCCGTGGTGCT
415        A  G  L  E  L  N  L  C  R  N  P  D  R  D  K  H  G  P  W  C
1441       ACACGTCCAACTCCTCCATTCCCTGGGACTACTGCGGACTGGAGCGCTGTAAATCAATGT
435        Y  T  S  N  S  S  I  P  W  D  Y  C  G  L  E  R  C  K  S  M
1501       CATCGGATGACCATCAAATGAGTGGAGGACCAAAACCATCTTGCTTTATACATAAAACCA
455        S  S  D  D  H  Q  M  S  G  G  P  K  P  S  C  F  I  H  K  T
1561       CACGGATTGTTGGGGGAATGCGAGTGCAGCGGGCAGAGGATGGAAGTTGGGTGGTCAGCA
475        T  R  I  V  G  G  M  R  V  Q  R  A  E  D  G  S  W  V  V  S
1621       TTCAGAAAGGGAACAGACACTGGTGCGGTGGCTCTCTCATCAGAGAAGAATGGGTTCTCA
495        I  Q  K  G  N  R  H  W  C  G  G  S  L  I  R  E  E  W  V  L
1681       CTGATCAACAGTGCTTCCCCACCTGCGTTCCTGACCTCTCCGAGTACACCGTGCAGGTGG
515        T  D  Q  Q  C  F  P  T  C  V  P  D  L  S  E  Y  T  V  Q  V
1741       GGCTTCTTCATCTCAATGCATCCGCCGGCACGCAGGCTCTCCGAATCGCACATGTGGTCT
```

```
535       G  L  L  H  L  N  A  S  A  G  T  Q  A  L  R  I  A  H  V  V
1801      GCGGGCCCGAGGGATCCAACTTGGCCCTGCTCAAACTCACAACGCCTGCCCCTCTCTCTG
555       C  G  P  E  G  S  N  L  A  L  L  K  L  T  T  P  A  P  L  S
1861      AGCATGTGCGAACTGTTCAGCTTCCGGTCGCTGGCTGTGCTGTTGCAGAAGGCACTCTGT
575       E  H  V  R  T  V  Q  L  P  V  A  G  C  A  V  A  E  G  T  L
1921      GTCTCATGTATGGATGGGGAGACACTAAAGGCACAGGACACGAGGGCAGTCTGAAGATGG
595       C  L  M  Y  G  W  G  D  T  K  G  T  G  H  E  G  S  L  K  M
1981      TGGGACTTCCAATTGTCAGCAACAAGAGGTGTTCACAAAGCCACAATGGCATCCTGCCCA
615       V  G  L  P  I  V  S  N  K  R  C  S  Q  S  H  N  G  I  L  P
2041      TCACCGAGACCAAAATCTGTGCTGGAGGCAAGAGAGATCAGGGCGTTTGTGAGAAAGACT
635       I  T  E  T  K  I  C  A  G  G  K  R  D  Q  G  V  C  E  K  D
2101      ACGGTGGCCCTTTGGTGTGCCAGGAAGGAGAGAGCAAAGTGATAGTTGGCGTCAGCATCA
655       Y  G  G  P  L  V  C  Q  E  G  E  S  K  V  I  V  G  V  S  I
2161      ACGGCCGTGGTTGTGCAGTAGCGAGACGTCCTGCTGTCTTCGTCAACGTGGCCTTCTACT
675       N  G  R  G  C  A  V  A  R  R  P  A  V  F  V  N  V  A  F  Y
2221      CTGAATGGATCCGCAAGGTCTTCAAGTACTATTCAGACATGGAAATAAGTTACTAGATCT
695       S  E  W  I  R  K  V  F  K  Y  Y  S  D  M  E  I  S  Y
2281      CCATATGTGGTAAATAAGACTAAATGGTTTAGCATCTACATCGTGAAGGACGATTAGCAT
2341      TCAAACATTTTGGAGGCTAAAGTTTGCTTTGGTGTATAGATGTTGCATAATAACCACTGG
2401      TACAGAAAAGGTGCAAGATTATCGATGTGTTTGTGAACAAATGAAGGAAATGACAACATC
2461      GGAACTTTTTTTAGGAGATTGTTGTGGCTGGTGAGAAATCAAGGACAGATGATGAATGAA
2521      CTGTGGCGTTCATCCATGTGAAAGCAGATGTTGTTCTTAATGTCATTCCCTGGAATTACT
2581      TGAAGACGACATTTTCGGTTTTTGTTTTTTGCAGCTTGCTGAATTTTACAGTGCTTTTAA
2641      GGACTAGATTCAGTATTACTGTTTCCAAAACACCTTTTTTAACATTGGTTACTAAAGAAA
2701      TCAGATTGCAAACCGCAATATGCGCTGCCGTTGGTTTATAAACGCCTATCTGGGGCATTA
2761      TCAGACACTTCCAGAATGTTTCGGTGATGGTCTAACGTTTCGCACCTTGCCTTACTCCAG
2821      TTTGGAGAGATTTTGTGGCTCCTTTGGGGCTGTTTTCTTTTTTTATGTACTGCACTCTAA
2881      AGAGTGTGCTAAAATGTCACTCTGTAGGTCTTATAGATCTGAAATTACAAACATTTGGAG
2941      GTCTTTTCTTTCACATGGTGTAATTTATATATATATCTGTCGAAATTTTATACGCGGTAT
3001      TTATTTATACCTTTTATAGATGGACCCGAGCCGTGGCATTTCATCCTCCAGTAGTGTTTA
3061      TTGTGTTTAATCTGGCGTGCAGATTTGAATCATAACATTTGTAAACAAAACAAACGGATG
3121      ATATGTCTTTGAAGGAAAATATTGGGTCATAACAGAGCGCTTCGACTCAAAGACGACTCC
3181      CTGAAGGTTTAAAAGCCACACATGCGGAGGGTCTTTTAAGAACAAGTTTAGCCATGAGTG
3241      CAAAGATACTTCATCAAACTGCAGTACTGAATAGAGTAACGCACAGGCAGGGTTTTTACA
3301      AGGTTTTTACAAGTACAAGAATGTATTTTGATTTAAATGTTGTGTTCGCTGTGTGTATAC
3361      AGAAAAGTGCCTGTTTTTGTGGCGTTTTATTGATTTTCGCAGTTAATGTAATTCCTCTTT
3421      GCGCTGCTGCCCTCATTGGTCGTTTTATTGAATATCTAGGCTGCTGTTATTTTTGACATT
3481      ATTTTTAGGACTGTTTTGTATTTTCAACTTTTAAAAATGTATGTAAATACATCTGTGACA
3541      TTTTGTTTTTTTTTTTATTTGTAAATAATTAAATCGTTAAAAATAAAAAAAAAAAAAAAA
3601      AAAAAAAAAAAAAAAAAAA
```

Fig.3.2 The nucleotide sequence of the zebrafish *hgfa* and deduced amino acid sequence. The position of nucleotides and amino acid residues are indicated on left side. Start codon in red.

When the isolated full-length cDNA sequence of zebrafish *hgf* was blasted against the zebrafish genome database, another *hgf* homologue was found. So we termed the first gene as *hgfa* and the latter one as *hgfb*. The predicted zebrafish *hgfb* cDNA ORF was 1149bp in length. Based on this predicted sequence, a set of nested primers (HGFb3ex, HGFb5ex, HGFb3in and HGFb5in) was designed to isolate a 389bp partial sequence of zebrafish HGFb by RT-PCR. Similar to *hgfa*, some mismatches were found between the predicted *hgfb* cDNA sequence and the isolated *hgfb* cDNA sequence due to mis-prediction of intron-exon junction.

The set of nested primers which were used for isolation of partial sequence of zebrafish *hgfb*, was used for RACE to obtain the full-length cDNA by nested PCR. 3' RACE with nested PCR (HGFb3ex and HGFb3in) resulted in isolation of a 1200bp fragment that reached to the 3' end of the gene. 5' RACE with nested PCR (HGF5ex and HGFb5in) resulted in isolation of a 4000bp fragment that reach to the 5' end of the gene. These two fragments were cloned into pGEM®-T Easy vector (Promega, USA) and sequenced. Full-length cDNA was then amplified by RT PCR from 24 hpf zebrafish total RNA using a set of nested primers (HGFbfex, HGFbrex, HGFbfin and HGFbrin) which flank the complete ORF of 2535bp. Schematic representation of this cloning process is shown in Fig.3.3. The nucleotide sequence of the zebrafish *hgfb* and deduced amino acid sequence are shown in Fig.3.4.

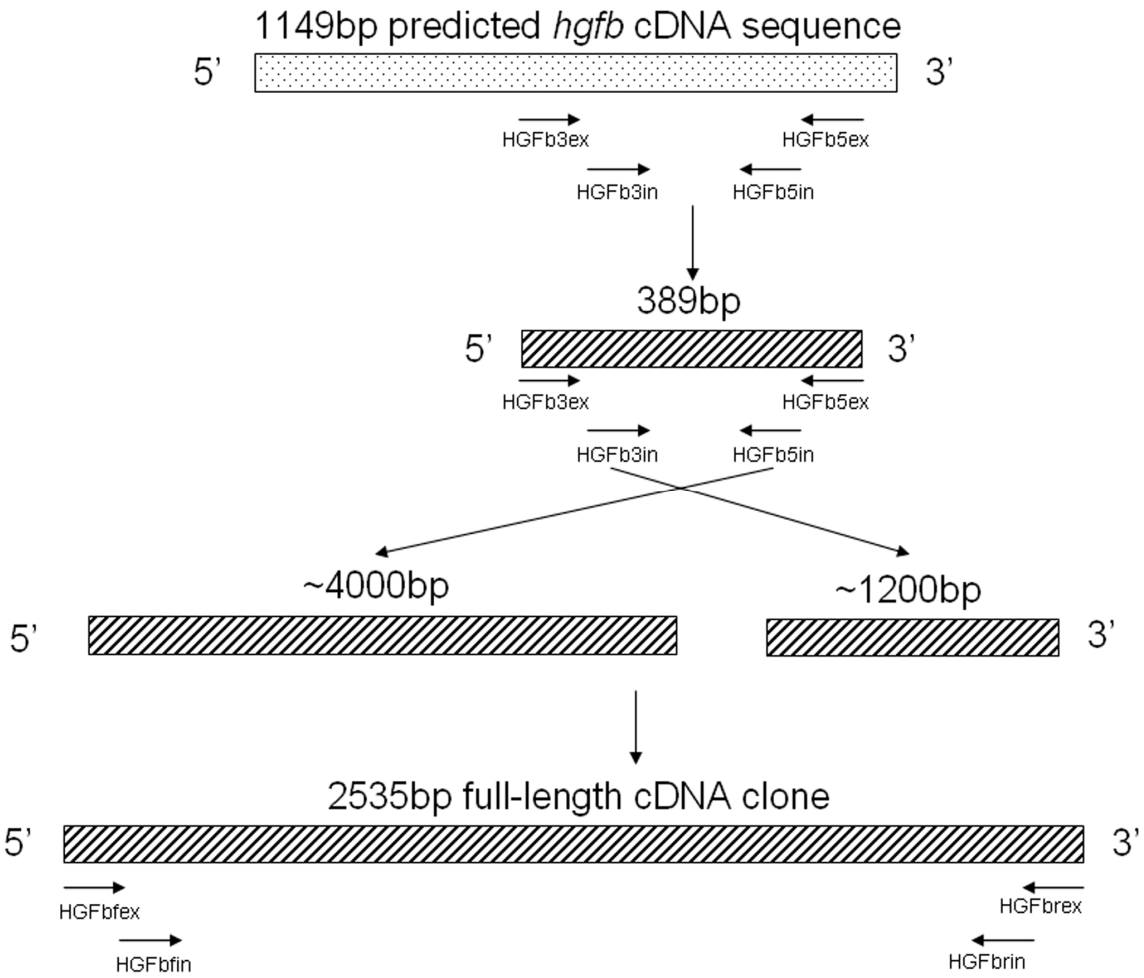

Fig.3.3 Schematic representation of the procedure of isolation and cloning of full-length zebrafish *hgfb* cDNA clone by RACE-PCR.

```
1          AGGAAACGCCAAGATTCCTCACATATCTTTTGTATTTTTGTTTTTGGGTCACATTAAACT
61         CTTTAAAGCGACATGTGGATTTACAAAATTTTGCTCTGTGTGGCCGTTTTGGTTTACTCA
1                       M  W  I  Y  K  I  L  L  C  V  A  V  L  V  Y  S
121        GAAACGAAGAGACATGCTCTGCAAGACTACCAGAAGACTGATGCCGTGCGCTTGGTCACT
17          E  T  K  R  H  A  L  Q  D  Y  Q  K  T  D  A  V  R  L  V  T
181        CCATCTGATGCATCCTACATGACCAAAGGCCGCAAGATGAGCATAGGAAAGTGTGCACGA
37          P  S  D  A  S  Y  M  T  K  G  R  K  M  S  I  G  K  C  A  R
241        CGCTGTAGCCGCAACAGGAAGCTCCAGTTCACCTGCAGAGCATTCAGCTTTGATCAGAAA
57          R  C  S  R  N  R  K  L  Q  F  T  C  R  A  F  S  F  D  Q  K
301        AGTACCAAATGTCATCTACTCTCCTATGACAGCCTCACCTTTGGTGTCCGCATGGAGAAT
77          S  T  K  C  H  L  L  S  Y  D  S  L  T  F  G  V  R  M  E  N
361        GACTTCAACTTCGATCTATATGAGAAGAAAGACTTCATGAGAGAATGCATCATTGGTAAT
97          D  F  N  F  D  L  Y  E  K  K  D  F  M  R  E  C  I  I  G  N
421        GGACTCAACTACAAAGGGAAAAGATCGGTGACTAAAAGTGGAGTCCAGTGCCAACTCTGG
117         G  L  N  Y  K  G  K  R  S  V  T  K  S  G  V  Q  C  Q  L  W
481        AATTCCAAAATGCCGCACGAGCACAATTTCTTACCCCAGAGGCACAAGCATCGAGATCTA
137         N  S  K  M  P  H  E  H  N  F  L  P  Q  R  H  K  H  R  D  L
541        CGGGATAATTTATGTCGTAATCCGGACAACACCACAACGGGTCCTTGGTGTTTTACCACA
157         R  D  N  L  C  R  N  P  D  N  T  T  T  G  P  W  C  F  T  T
601        GACCCCAAACTACGTCACCAGGACTGCAGCATCCCACAATGCTCGGAGGTGGAATGTATG
177         D  P  K  L  R  H  Q  D  C  S  I  P  Q  C  S  E  V  E  C  M
661        ACGTGTAACGGAGAAAGTTATCGTGGACCCTTGGACCACACGGAGAGTGGTCGGGAATGC
197         T  C  N  G  E  S  Y  R  G  P  L  D  H  T  E  S  G  R  E  C
721        CAGCGCTGGGACCTTGAGGAACCACATAAACACATTTTCCACCCTAAAAGGTACCCCGAT
217         Q  R  W  D  L  E  E  P  H  K  H  I  F  H  P  K  R  Y  P  D
781        AAAGGTCTAAAGGACAACTACTGCAGGAACCCAGACGGGCGCCAGAGACCCTGGTGTTTC
237         K  G  L  K  D  N  Y  C  R  N  P  D  G  R  Q  R  P  W  C  F
841        ACCACCGATCCCAGCACTCCATGGGAGTACTGTAACATCAAACAGTGCGATTCAGACAAC
257         T  T  D  P  S  T  P  W  E  Y  C  N  I  K  Q  C  D  S  D  N
901        AGTGGTGACGTTGAAAACACAACAACGTGTTTCCGTGGACGCGGAGAGGGGTATCGCGGG
277         S  G  D  V  E  N  T  T  T  C  F  R  G  R  G  E  G  Y  R  G
961        ACGGTTGGCATCACACCTGATGGAGTGACTTGTCAGCGATGGGATGCCCAGTTTCCCCAT
297         T  V  G  I  T  P  D  G  V  T  C  Q  R  W  D  A  Q  F  P  H
1021       CGACACTCGTATACGCCACAGAATTACCATTGCAAGGATCTGCGGGAGAACTACTGTAGA
317         R  H  S  Y  T  P  Q  N  Y  H  C  K  D  L  R  E  N  Y  C  R
1081       AATCCTGATGGTCGTCATCTTCCATGGTGCTTCACTACTGATCCCACTGTTCCTATAGCT
337         N  P  D  G  R  H  L  P  W  C  F  T  T  D  P  T  V  P  I  A
1141       TTCTGCACCAACATCCCTCGCTGTGGACTCAAACCTCCTGAACCTGAAGAGTGTTATAAG
357         F  C  T  N  I  P  R  C  G  L  K  P  P  E  P  E  E  C  Y  K
1201       GGCATTGGAGACATGTACAATGGCCACCGGTCAAAGACTCGCTCAGGCATTCCCTGTGCC
377         G  I  G  D  M  Y  N  G  H  R  S  K  T  R  S  G  I  P  C  A
1261       CCATGGAAAGACCACAGTGAAAGTAACGAAAGAGATGTGAACTTGCTGACGGCTGAACAG
397         P  W  K  D  H  S  E  S  N  E  R  D  V  N  L  L  T  A  E  Q
1321       GCAGGGAACTTCTGCAGAAATCCAGACAAGGACAAACACGGCCCGTGGTGTTACACCAAC
417         A  G  N  F  C  R  N  P  D  K  D  K  H  G  P  W  C  Y  T  N
1381       AGCTCATCCATCCCCTGGGATTACTGCTCTCTCAAACCCTGTGAGCCTTCACATAACAAT
437         S  S  S  I  P  W  D  Y  C  S  L  K  P  C  E  P  S  H  N  N
1441       CTGCCACAAAAAAGATGAGGTTACAAAGAGCTCGTGTTTTGTTCATAAGCAGGTGAGAATC
457         L  P  Q  K  D  E  V  T  K  S  S  C  F  V  H  K  Q  V  R  I
1501       GTCGGTGGCGGGCCTGTCCCAATTAAAGAGGGCAGCTGGATGGTCAGCATACAGAAAGGG
477         V  G  G  G  P  V  P  I  K  E  G  S  W  M  V  S  I  Q  K  G
1561       AGCAGTCACTGGTGTGGAGGCGCTCTGGTCAGGGAGGAGTGGGTGCTGACAGACAAAGAC
497         S  S  H  W  C  G  G  A  L  V  R  E  E  W  V  L  T  D  K  D
1621       TGCTTCTCCTCATGTGTGCCTGACCTATCAGAGTACAGAGTTTGGCTCGGTATTACCCAT
517         C  F  S  S  C  V  P  D  L  S  E  Y  R  V  W  L  G  I  T  H
1681       CTGAACGAATCAGGTGAGAATGACTTCCACAGACAGGAGAGGAGAATCTCGCATGTCATC
537         L  N  E  S  G  E  N  D  F  H  R  Q  E  R  R  I  S  H  V  I
```

```
1741      TGTGGCCCAGAAGACTCTAGTCTCGCCCTTCTCCGCCTTTCCCAACCTGCACTCCCGAGT
557        C  G  P  E  D  S  S  L  A  L  L  R  L  S  Q  P  A  L  P  S
1801      GAGCGTGTCCGAGTTATTCAGCTGCCCGTAGCAGACTGCAGCATTCAGGAGGACACCATC
577        E  R  V  R  V  I  Q  L  P  V  A  D  C  S  I  Q  E  D  T  I
1861      TGCTCTGTGTACGGCTGGGGGGAAACCAAAGGCACTGGACATGAGGGAACGCTGAAAAGA
597        C  S  V  Y  G  W  G  E  T  K  G  T  G  H  E  G  T  L  K  R
1921      GTTCATCTGCCCATAGTGAGCAATGAACGATGCCAGCAGCTTCACAGAGGGACTCTTCCC
617        V  H  L  P  I  V  S  N  E  R  C  Q  Q  L  H  R  G  T  L  P
1981      ATCACTAGTTCTAAACTGTGTGCCGGTGGCAGAAGAGATGAAGGAGTTTGTGAGAAAGAC
637        I  T  S  S  K  L  C  A  G  G  R  R  D  E  G  V  C  E  K  D
2041      TACGGGGGCCCTCTAGTATGTCAAGAGAGTAACAGTAAAGTCATTGTTGGTGTGAGCATA
657        Y  G  G  P  L  V  C  Q  E  S  N  S  K  V  I  V  G  V  S  I
2101      AATGGCAGAGGATGTGCCAGGCATAACCGACCAGCCATTTTTGTGAACGTGGCCTTCTAC
677        N  G  R  G  C  A  R  H  N  R  P  A  I  F  V  N  V  A  F  Y
2161      GCTGGATGGATTCATAAAGTTTACAGAAATTATCCAAACTCAGAACTGAACAATTGATCA
697        A  G  W  I  H  K  V  Y  R  N  Y  P  N  S  E  L  N  N
2221      CGAGAGCAGGATTGAAAATCCGATCTGTGATATAAGAACAAAATATCTCCACAAATCCAA
2281      CAGCTCCTTTCTTGATTTATTTTGTTCATCAACAACAAAACAAGTATTATTGGAAGCTTT
2341      CCCAGCGTGGCCATGAAGCATATATTCCAAAACTACTAAAAGTGCTTTAAACTGATGCTC
2401      TAAATTCAAGCAGTTTGTACACCTAATAATGCCAGAACCGCAGAGCAAGGCACTGGGAGA
2461      CAAGAGTCTCAACAGGCTATATTCGCAACTAGCCATACGGAAAGATAAAGACTACTGGAC
2521      CGAAGTGCAGACGAG
```

Fig.3.4 The nucleotide sequence of the zebrafish *hgfb* and deduced amino acid sequence. The position of nucleotides and amino acid residues are indicated on left side. Start codon in red.

3.1.1.2 Isolation of c-met full-length cDNA

A 177bp partial cDNA clone of zebrafish c-met corresponding to the tyrosine kinase domain was obtained from previous study in Dr. Ge's lab using degenerate PCR cloning. By blasting this sequence against NCBI database, a longer fragment of zebrafish c-met was obtained, which has 436bp nucleotides.

Based on this 436 bp fragment, we design primers for RACE to obtain the full-length cDNA of *c-met* by nested PCR. 3' RACE with nested PCR (c-met3ex and c-met3in) resulted in isolation of a 400bp fragment that reach to the 3' end of the gene. First round 5' RACE with nested PCR (c-met5ex1 and c-met5in1) resulted in isolation of a 2000 bp fragment that did not reach the 5' end of the gene. Therefore, a second round of 5' RACE with nested PCR (c-met5ex2 and c-met5in2) against the 5'end of the 2000 bp fragment was performed. This identified other two fragments of 900bp and 2000 bp respectively, and the 2000 bp fragment contained the 5' end of the gene. These four fragments were cloned into pGEM®-T Easy vector (Promega, USA) and sequenced. Full-length cDNA was amplified by RT PCR from 24hpf zebrafish total RNA using a pair of primers (c-metf and c-metr) which flank the complete ORF (4316bp). Schematic representation of this cloning process is shown in Fig.3.5. The nucleotide sequence of the zebrafish *c-met* and deduced amino acid sequence is shown in Fig.3.6.

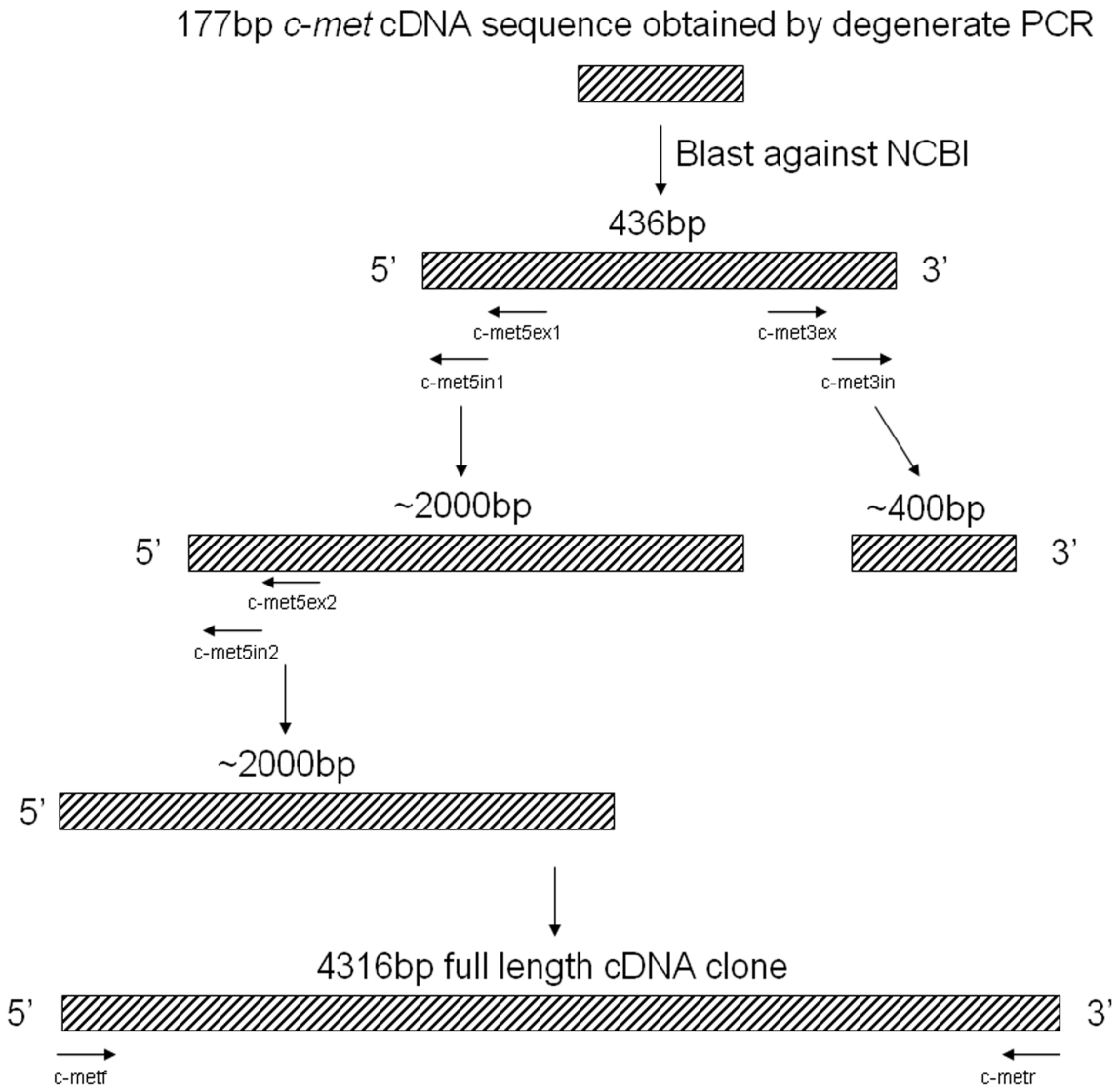

Fig.3.5 Schematic representation of the procedure of isolation and cloning of full-length zebrafish *c-met* cDNA clone by RACE-PCR.

```
1          CGACCCGCAGCGTTTGCGGAGAGAACGACAACAAACCCTTTAAACTGCTGTGACCCATTC
61         AGAGCCTGAGTCACCCTAGCACACATTCCCTGAGTGAATACGAGGTTCCGGAGAGAGAGG
121        GAGGAAGAGCGGACAACTTTTGAGAGAAAGCGCGCAGAGATTCACCGTCGCATCCCATCC
181        CGAGACTGTTGGCATCCGAGAGAAACTGCGCGCGCCTTGAGTAACAAGGACCGTTAAAAG
241        ATGTGATTATTTCCTTTTTCTGTCTCCGACAGGTGTCTTTATTTTACAGAGGAACAAAGA
301        TGACAATTCACTATTCTGAAGCTGCTTCCATCCTAATCATCCTTCAGTCGCTGTGGTGGG
1          M  T  I  H  Y  S  E  A  A  S  I  L  I  I  L  Q  S  L  W  W
361        GCTTGAATTGTCAATGTGAGGAACCAATAGAAAGCTCCAAACTCGACCTCTCAGTGACCT
21         G  L  N  C  Q  C  E  E  P  I  E  S  S  K  L  D  L  S  V  T
421        ATGACCTCCCTTACTTTGTGTCTGACACCCCCATTCAGAAGCTGTTGGAAATCAATGGAA
41         Y  D  L  P  Y  F  V  S  D  T  P  I  Q  K  L  L  E  I  N  G
481        CAGTGTATGTCGGTGCCGTCAATAGACTTTACGCTCTGTCGAAAGACCTGAAGAAGAAAC
61         T  V  Y  V  G  A  V  N  R  L  Y  A  L  S  K  D  L  K  K  K
541        ATGAGTATAAGACTGGACCGGTCCATGAGGGTCCAGACTGCAAGACCCCAACAGATCGAT
81         H  E  Y  K  T  G  P  V  H  E  G  P  D  C  K  T  P  T  D  R
601        GCAGTGGTTGTGAAAACAAGCCCCGCAACATAAACAACACCAATATGGCCCTGTTAATGG
101        C  S  G  C  E  N  K  P  R  N  I  N  N  T  N  M  A  L  L  M
661        AGACGTTCTATGACCTGGAACTTTTCAGCTGTGGCTCAGCCGGGAATGGCGTCTGCAGTC
121        E  T  F  Y  D  L  E  L  F  S  C  G  S  A  G  N  G  V  C  S
721        GTCATGTGTTAGAGGATGGGCCTCTGGGTGCGGAAGTAACTTGCATGTACACCAAAAAGA
141        R  H  V  L  E  D  G  P  L  G  A  E  V  T  C  M  Y  T  K  K
781        ATGAAGGCAGCAGCCATGGATGCCCAGACTGCCTGGCTGGACCTGCGGGCACTCAGATCC
161        N  E  G  S  S  H  G  C  P  D  C  L  A  G  P  A  G  T  Q  I
841        TCAACATAATGAGCGGTCGTGTTGTGAGGTTCTTCGTCGCGAACTCTGAACCTCTTGAGT
181        L  N  I  M  S  G  R  V  V  R  F  F  V  A  N  S  E  P  L  E
901        CAAACGGTCCACGTCTCCACCACACTATTTCCATTAGGAAGATGCGTGAAACTCAAGATG
201        S  N  G  P  R  L  H  H  T  I  S  I  R  K  M  R  E  T  Q  D
961        GCTTTGAGTTCTTTTCCGATCAGTCCTACATGGATTTGGCCCCTTCACTGCGGGGGAACT
221        G  F  E  F  F  S  D  Q  S  Y  M  D  L  A  P  S  L  R  G  N
1021       ATCCACTACATTATGTCTACTCTTTCCAGAGTGGTCCTTATGTATATTTTCTCACCGTCC
241        Y  P  L  H  Y  V  Y  S  F  Q  S  G  P  Y  V  Y  F  L  T  V
1081       AACGCGAAGGTGGCAACTCGAAAGCTTTCCACACGAGAATCGTACGCATGTGTTCTTCAG
261        Q  R  E  G  G  N  S  K  A  F  H  T  R  I  V  R  M  C  S  S
1141       ATTCTGAGATCCTGCGTTATGTAAAAATGCCCTTTGAGTGCATTTACTCTGAGCGAAGGA
281        D  S  E  I  L  R  Y  V  K  M  P  F  E  C  I  Y  S  E  R  R
1201       GAAAAAGGCGTTCGGCTCAAGTGGCTTTCAACGTTCTCCAGGCTGCTCATGTGGCCAAAG
301        R  K  R  R  S  A  Q  V  A  F  N  V  L  Q  A  A  H  V  A  K
1261       TTGGCTATGACTTTCAGCAGGAGATGGGCTTGAAAGAAGGAGAGGACGTGCTGTTTGCTG
321        V  G  Y  D  F  Q  Q  E  M  G  L  K  E  G  E  D  V  L  F  A
1321       CCTTTGCCCGGAGCAAACCGGACTCACCAGAGCCCACCGCCAGCTCCGCCGTTTGCCTTA
341        A  F  A  R  S  K  P  D  S  P  E  P  T  A  S  S  A  V  C  L
1381       TCTCCATCACGGACATCAATGAATTCTTCAAGGTTTTCATTCAGAAGGGTTACACAAGGA
361        I  S  I  T  D  I  N  E  F  F  K  V  F  I  Q  K  G  Y  T  R
1441       AACTCCATCACTTTCCAGGATCTGAAGAGAAAACCTTCAACCAGACGTTTGTAGGAGATT
381        K  L  H  H  F  P  G  S  E  E  K  T  F  N  Q  T  F  V  G  D
1501       CCTTCAGCTGTGAGAAACATGAAAGAGGCTATCGGCTAGAAGTTACAAGCACCAACCCGC
401        S  F  S  C  E  K  H  E  R  G  Y  R  L  E  V  T  S  T  N  P
1561       GCCGGGACTATTTTCATGGCCGCTTCCGGAATGTTCTTCTCACTTCCATAGCTGTGGTGC
421        R  R  D  Y  F  H  G  R  F  R  N  V  L  L  T  S  I  A  V  V
1621       CGATCCAAAACCACACTGTGGCCAGCCTTGGCACAGCTGAAGGCCGCGTCATCCAGGTGG
441        P  I  Q  N  H  T  V  A  S  L  G  T  A  E  G  R  V  I  Q  V
1681       TGGTTTCCCGCTTTGGCAAGACAGAGCCACATGTGGACTTCCGCTTGGACACGCTCCCTG
461        V  V  S  R  F  G  K  T  E  P  H  V  D  F  R  L  D  T  L  P
1741       TGTCTTCAGAAATGGCCCTGCTGTCTCCACAGCATCACAACGGCTCCTTATTGTTGATAA
481        V  S  S  E  M  A  L  L  S  P  Q  H  H  N  G  S  L  L  L  I
1801       CAGGAAACAAGGTCTCAAAGCTTCCTGTGATCGGGCCTGGATGTGAGCAGTTGTGGACTT
501        T  G  N  K  V  S  K  L  P  V  I  G  P  G  C  E  Q  L  W  T
```

```
1861      GTAGCTCGTGTCTTCTTGCTCCGGGCTTCATGGGCTGTGGATGGTGCAGGACCAGCAACC
521       C  S  S  C  L  L  A  P  G  F  M  G  C  G  W  C  R  T  S  N
1921      TGTGCACCAGGGCCCCTCGATGCCCCCAGTCCCAATGGATCCAGGACTCCTGCCCCCTCC
541       L  C  T  R  A  P  R  C  P  Q  S  Q  W  I  Q  D  S  C  P  L
1981      TCATCACCTCGATCTCTCCTTCCTCCGCTCCACTCAGAGGTCAAACCAACATCACAATCT
561       L  I  T  S  I  S  P  S  S  A  P  L  R  G  Q  T  N  I  T  I
2041      GTGGCAAAAACTTTGGCTTTAACAAAAAAGACAGATTTGATACCAAACTGATAGACGTGG
581       C  G  K  N  F  G  F  N  K  K  D  R  F  D  T  K  L  I  D  V
2101      TGGTTGCTGGAACGAAGTGTAAATTGGAAAGGAAGGACAGTAACAATAATCGGTTGGTCT
601       V  V  A  G  T  K  C  K  L  E  R  K  D  S  N  N  N  R  L  V
2161      GTGGACTGGACCATGTGAACTGGTCCAGCGTGGACTCTGTGGTCACAGTGCGCAGTGGCA
621       C  G  L  D  H  V  N  W  S  S  V  D  S  V  V  T  V  R  S  G
2221      AGGAACAGGCCCAGAAAGATGGCTTCTCATTTGTGAATCCAGTTATCATAGAGATCTTCC
641       K  E  Q  A  Q  K  D  G  F  S  F  V  N  P  V  I  I  E  I  F
2281      CAGAGTTTGGACCTCAGTCTGGTGGGACAATGCTCACTATCAGCGGTTCATTCTTGGACA
661       P  E  F  G  P  Q  S  G  G  T  M  L  T  I  S  G  S  F  L  D
2341      GTGGAAATGTGCAAACAGTCACAGTGGGGAACGCTACCTGTGTGCTGCAGAGTGTTTCAG
681       S  G  N  V  Q  T  V  T  V  G  N  A  T  C  V  L  Q  S  V  S
2401      CCACAATGTTAACATGTCGTACACCACCTCAGCCCTCGCCATCCCAACACAAGGTACAGC
701       A  T  M  L  T  C  R  T  P  P  Q  P  S  P  S  Q  H  K  V  Q
2461      TGCACATTGATGGAGTAATATTTGAAGCGCCTGTCAGCTACACCTACAACAAGAACCCAC
721       L  H  I  D  G  V  I  F  E  A  P  V  S  Y  T  Y  N  K  N  P
2521      ACATCTCCAGCGTCCAGCCCAAACATTCTTTCATCAGTGGAGGAAGCACGGTGACAGTGA
741       H  I  S  S  V  Q  P  K  H  S  F  I  S  G  G  S  T  V  T  V
2581      ATGGCTTCTACCTGCACTCAGCTCTTCAGCCTCAGATGGTTCTCACTGCTGCCACTGAGG
761       N  G  F  Y  L  H  S  A  L  Q  P  Q  M  V  L  T  A  A  T  E
2641      GCAAACTCTTCCAAGTGACCTGCAGTCATGATGAGGATAAGAGAAATATCCTTTGCATCA
781       G  K  L  F  Q  V  T  C  S  H  D  E  D  K  R  N  I  L  C  I
2701      CGCCCTCCCTGAAAGGCCTCAGCGTTCAGCCTCCGGTCGCCACTAAAATGACCTTCGTCC
801       T  P  S  L  K  G  L  S  V  Q  P  P  V  A  T  K  M  T  F  V
2761      TGGATGGTTTTTCCACTGATCAGTACGACCTGCTGTACGTGGAAGATCCCAAATTTGAGG
821       L  D  G  F  S  T  D  Q  Y  D  L  L  Y  V  E  D  P  K  F  E
2821      AGTTTCAGAAGCCCACTGTCACACCAAGGGGCAAAAAGAACATTCTGGAGATTAAGGTCC
841       E  F  Q  K  P  T  V  T  P  R  G  K  K  N  I  L  E  I  K  V
2881      CCCCTGTGAATCAAGAGGCGGTGAAAAACGGTGAGGTGCTGAGAGTTTCAAATCGGACCT
861       P  P  V  N  Q  E  A  V  K  N  G  E  V  L  R  V  S  N  R  T
2941      GCGAGAGCGTCACTTTGGTGGGCAACACGCTCGAATGCACCGTACCCATGGAGCTCCAGA
881       C  E  S  V  T  L  V  G  N  T  L  E  C  T  V  P  M  E  L  Q
3001      CCGCCGCCAAAGAGCTGGAGGTGGAGTGGAAGCAGGCCACATCATCTGTGATCTTGGGCC
901       T  A  A  K  E  L  E  V  E  W  K  Q  A  T  S  S  V  I  L  G
3061      GTGTGATTTTGGCTCAAGACCAGGATTACAGGATACTGATCACTGGAGGAGTGTGTGTGT
921       R  V  I  L  A  Q  D  Q  D  Y  R  I  L  I  T  G  G  V  C  V
3121      CCATCCTCCTCCTGCTCCTGATCGCTGTGTTTGTTTGGATCAAGAGAAAGAAGCACATTA
941       S  I  L  L  L  L  L  I  A  V  F  V  W  I  K  R  K  K  H  I
3181      ATGATTTAGCTAAGACTATGGTTTGGTATGACGGCCGGGCTCACATTCCGCACTTGGACA
961       N  D  L  A  K  T  M  V  W  Y  D  G  R  A  H  I  P  H  L  D
3241      TGTTGGCAAACGCGAGGAGTGTCAGTCCCACTAATGAAATGGTCTCTCACGAGTCGGTGG
981       M  L  A  N  A  R  S  V  S  P  T  N  E  M  V  S  H  E  S  V
3301      ACTATAGAACCACTTTGCTTGAGGACCAAAACTTGCCTCTGTCTCAGACAGAGTCCTGCC
1001      D  Y  R  T  T  L  L  E  D  Q  N  L  P  L  S  Q  T  E  S  C
3361      GGCCTCATCTCTACGCTCATTCCCATGTGGATCTGTCCCCAATGCTCGGGCCAATGGAAG
1021      R  P  H  L  Y  A  H  S  H  V  D  L  S  P  M  L  G  P  M  E
3421      GGGACCTGGCGTCTCCGCTGCTGCCCTCTACAGCGCCTATAGATCTAGGCAGCCTCCATC
1041      G  D  L  A  S  P  L  L  P  S  T  A  P  I  D  L  G  S  L  H
3481      CTGAGCTGCTGAAGGAGGTCCAGCATGTGGTCATCGCAAGAGAAGATCTGCTCTTACATG
1061      P  E  L  L  K  E  V  Q  H  V  V  I  A  R  E  D  L  L  L  H
3541      TCAATGAGATCATCGGGAGAGGGCACTTCGGCTGCGTGTTTCATGGAACCCTCCTCGAGC
```

```
1081      V  N  E  I  I  G  R  G  H  F  G  C  V  F  H  G  T  L  L  E
3601      CAGATGGCCAGAAGCAGCACTACGCCATCAAGTCCTTAAACCGAATCACAGATATCGAGG
1101      P  D  G  Q  K  Q  H  Y  A  I  K  S  L  N  R  I  T  D  I  E
3661      AGGTGTCTCAGTTTCTGAAGGAGGGCATCATCATGAAGGATTTCAGCCATCCCAATGTGC
1121      E  V  S  Q  F  L  K  E  G  I  I  M  K  D  F  S  H  P  N  V
3721      TTTCTCTGCTGGGAATCTGCCTGCCCAGCGAGGGTTCGCCTCTCGTCGTGTTGCCTTACA
1141      L  S  L  L  G  I  C  L  P  S  E  G  S  P  L  V  V  L  P  Y
3781      TGAAGCACGGAGATCTGCGCAACTTTATCAGAGATGAAAGTCATAACCCCACAGTGAAGG
1161      M  K  H  G  D  L  R  N  F  I  R  D  E  S  H  N  P  T  V  K
3841      ACCTGATGGGTTTCGGGCTGCAGGTGGCTAAAGGAATGGAGTATCTCGCCAGCAAGAAAT
1181      D  L  M  G  F  G  L  Q  V  A  K  G  M  E  Y  L  A  S  K  K
3901      TTGTTCACCGAGACCTCGCGGCCAGAAACTGCATGCTGGATGAGAGCTACACAGTGAAGG
1201      F  V  H  R  D  L  A  A  R  N  C  M  L  D  E  S  Y  T  V  K
3961      TGGCAGATTTTGGCCTGGCCAGAGACGTGTATGATAAAGAATACTACAGCGTACACAACA
1221      V  A  D  F  G  L  A  R  D  V  Y  D  K  E  Y  Y  S  V  H  N
4021      AGCACGGAGTGAAGCTGCCTGTCAAATGGATGGCGTTAGAAAGCCTGCAGACACACAAGT
1241      K  H  G  V  K  L  P  V  K  W  M  A  L  E  S  L  Q  T  H  K
4081      TCACAACCAAATCGGATGTGTGGTCGTTTGGTGTTTTGCTGTGGGAACTGATGACCCGAG
1261      F  T  T  K  S  D  V  W  S  F  G  V  L  L  W  E  L  M  T  R
4141      GCGCTCCGCCATACTCTGATGTGAACTCCTTCGACATTACAGTGTTTCTTCTGCAAGGCC
1281      G  A  P  P  Y  S  D  V  N  S  F  D  I  T  V  F  L  L  Q  G
4201      GGAGACTGTTACAACCAGAGTTCTGCCCTGATGCACTCTATAATGTCATGATTGAGTGCT
1301      R  R  L  L  Q  P  E  F  C  P  D  A  L  Y  N  V  M  I  E  C
4261      GGCACCCCAAACCCGAGCGTCGACCAACTTTCTCAGAACTAGTGTCTCGCATCTCCGCCA
1321      W  H  P  K  P  E  R  R  P  T  F  S  E  L  V  S  R  I  S  A
4321      TCTTCTCAAGCTTCAGCGGAGAGCACTACATCCTCCTGAACACCACCTACGTCAACATCG
1341      I  F  S  S  F  S  G  E  H  Y  I  L  L  N  T  T  Y  V  N  I
4381      ACAAAATGACACCCTACCCCTCTCTCATATCATCTCAGAGCAACCTCGACCGCGACTGCT
1361      D  K  M  T  P  Y  P  S  L  I  S  S  Q  S  N  L  D  R  D  C
4441      GCACCTGAGACACCTAAAAAAAAAAAAAAAAAAAAAAAAA
1381      C  T
```

Fig.3.6 The nucleotide sequence of the zebrafish c-met and deduced amino acid sequence. The position of nucleotides and amino acid residues are indicated on left side. Start codon in red.

3.1.2 Sequence analyses of zebrafish Hgfa, Hgfb and c-Met

HGF amino acid sequences of different species are aligned (Fig.3.8) and the protein domains of zebrafish Hgfa and Hgfb are predicted by SMART (http://smart.embl-heidelberg.de/) and signal peptide is predicted by SignalP 3.0 Server (http://www.cbs.dtu.dk/services/SignalP/), and compared with human HGF (Fig.3.9).

Amino acid identity between zebrafish Hgfa and Hgfb is 60% while the nucleotide identity between zebrafish *hgfa* and *hgfb* is only 50%. Amino acid identities between zebrafish Hgfa with other vertebrate species including Human, Mice, Rat, Cat, Dog, Chicken and Xenopus HGF are 44% to 46% while identities between zebrafish Hgfb with other vertebrate species HGF are 46% to 49%. Amino acid identities of PAN_AP domain (divergent subfamily of APPLE domains) between zebrafish Hgfa with other verterbrate species' HGF are 24% to 34% while amino acid identities of PAN_AP domain between zebrafish Hgfb with other verterbrate species' HGF are 31% to 43%. Amino acid identities of kringle domain between zebrafish Hgfa with other verterbrate species' HGF are 53% to 57% while amino acid identities of kringle domain between zebrafish Hgfb with other verterbrate species' HGF are 56% to 59%. Amino acid identities of trypsin-like serine protease domain between zebrafish Hgfa with other verterbrate species' HGF are 40% to 42% while amino acid identities of trypsin-like serine protease domain between zebrafish Hgfb with other verterbrate species' HGF are 43% to 47%. Compared to other domains in HGF, kringle domain is the most conserved domain in HGF.

Results show that zebrafish Hgfa, Hgfb and human HGF share the same domains and structural organization (Fig.3.7). From the N terminal to C terminal, the domains are: a signal peptide which lead HGF to secretion; a PAN_AP domain which is a divergent subfamily of APPLE domains and possess protein- and/or carbohydrate-binding functions; four kringle domains which possess affinity for free lysine and lysine-containing peptides; a trypsin-like serine protease domain which is most likely not catalytically active due to some of the required catalytic sites were not detected in this domain and catalytic residue H is replaced with Q(518) in Hgfa and S(520) in Hgfb, D is replace with N(561) in Hgfa and S(563) in Hgfb, S is replace with Y(595) in Hgfa Y(597) in Hgfb (Fig.3.8) (Kitadokoro et al., 1994).

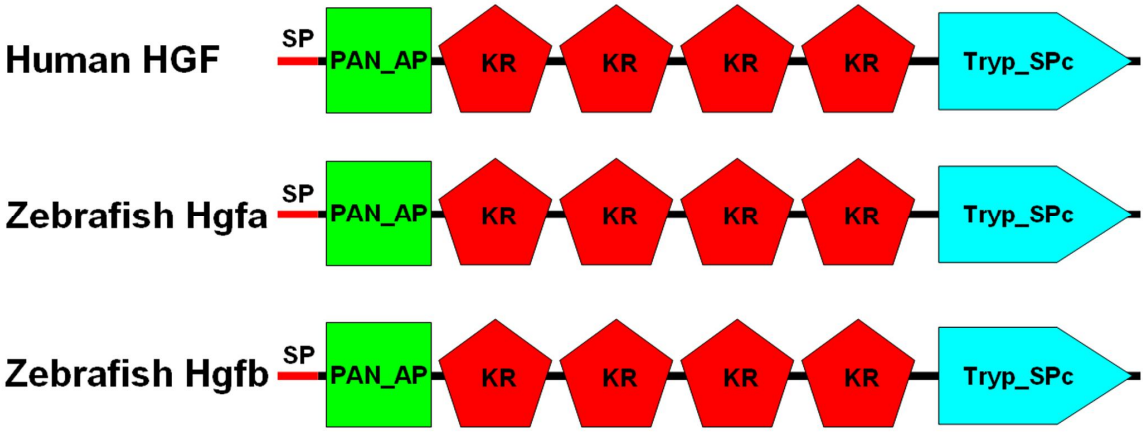

Fig.3.7 Comparison of the predicted domain and signal peptide of zebrafish Hgfa and Hgfb with human HGF. Domains are predicted by SMART (`http://smart.embl-heidelberg.de/`) and signal peptide is predicted by SignalP 3.0 Server (http://www.cbs.dtu.dk/services/SignalP/). SP, singnal peptide; PAN_AP, divergent subfamily of APPLE domains; KR, Kringle domain; Tryp_SPc, Trypsin-like serine protease domain.

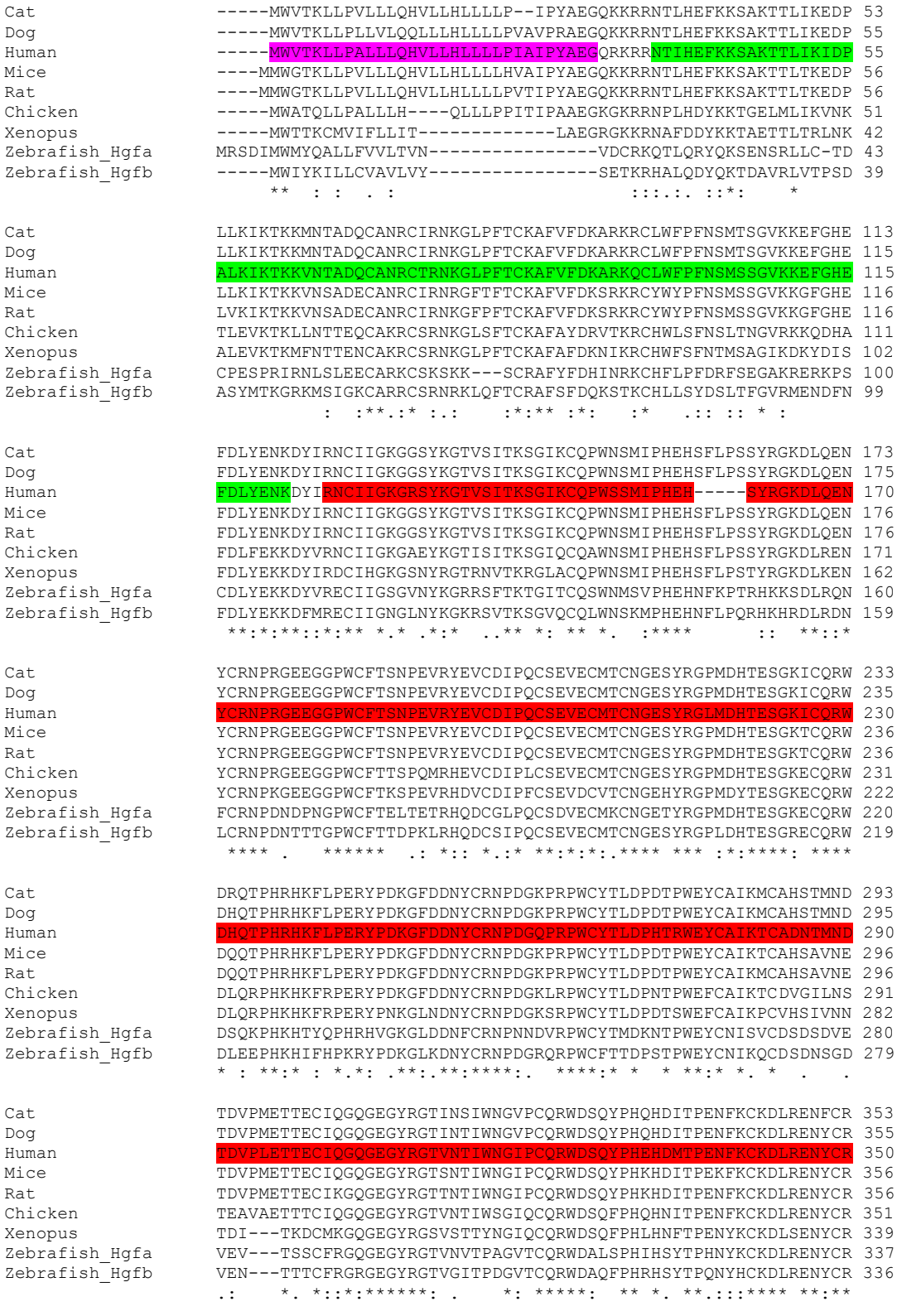
Cat -----MWVTKLLPVLLLQHVLLHLLLLP--IPYAEGQKKRRNTLHEFKKSAKTTLIKEDP 53
Dog -----MWVTKLLPLLVLQQLLLHLLLLPVAVPRAEGQKKRRNTLHEFKKSAKTTLIKEDP 55
Human -----MWVTKLLPALLLQHVLLHLLLLPIAIPYAEGQRKRRNTIHEFKKSAKTTLIKIDP 55
Mice ----MMWGTKLLPVLLLQHVLLHLLLLHVAIPYAEGQKKRRNTLHEFKKSAKTTLTKEDP 56
Rat ----MMWGTKLLPVLLLQHVLLHLLLLPVTIPYAEGQKKRRNTLHEFKKSAKTTLTKEDP 56
Chicken -----MWATQLLPALLLH----QLLLPPITIPAAEGKGKRRNPLHDYKKTGELMLIKVNK 51
Xenopus -----MWTTKCMVIFLLIT-------------LAEGRGKKRNAFDDYKKTAETTLTRLNK 42
Zebrafish_Hgfa MRSDIMWMYQALLFVVLTVN----------------VDCRKQTLQRYQKSENSRLLC-TD 43
Zebrafish_Hgfb -----MWIYKILLCVAVLVY----------------SETKRHALQDYQKTDAVRLVTPSD 39
** : : . : :::.:. ::*: *
Cat LLKIKTKKMNTADQCANRCIRNKGLPFTCKAFVFDKARKRCLWFPFNSMTSGVKKEFGHE 113
Dog LLKIKTKKMNTADQCANRCIRNKGLPFTCKAFVFDKARKRCLWFPFNSMTSGVKKEFGHE 115
Human ALKIKTKKVNTADQCANRCTRNKGLPFTCKAFVFDKARKQCLWFPFNSMSSGVKKEFGHE 115
Mice LLKIKTKKVNSADECANRCIRNRGFTFTCKAFVFDKSRKRCYWYPFNSMSSGVKKGFGHE 116
Rat LVKIKTKKVNSADECANRCIRNKGFPFTCKAFVFDKSRKRCYWYPFNSMSSGVKKGFGHE 116
Chicken TLEVKTKLLNTTEQCAKRCSRNKGLSFTCKAFAYDRVTKRCHWLSFNSLTNGVRKKQDHA 111
Xenopus ALEVKTKMFNTTENCAKRCSRNKGLPFTCKAFAFDKNIKRCHWFSFNTMSAGIKDKYDIS 102
Zebrafish_Hgfa CPESPRIRNLSLEECARKCSKSKK---SCRAFYFDHINRKCHFLPFDRFSEGAKRERKPS 100
Zebrafish_Hgfb ASYMTKGRKMSIGKCARRCSRNRKLQFTCRAFSFDQKSTKCHLLSYDSLTFGVRMENDFN 99
: :**.:* :.: :*:** :*: :* .:: :: * :
Cat FDLYENKDYIRNCIIGKGGSYKGTVSITKSGIKCQPWNSMIPHEHSFLPSSYRGKDLQEN 173
Dog FDLYENKDYIRNCIIGKGGSYKGTVSITKSGIKCQPWNSMIPHEHSFLPSSYRGKDLQEN 175
Human FDLYENKDYIRNCIIGKGRSYKGTVSITKSGIKCQPWSSMIPHEH-----SYRGKDLQEN 170
Mice FDLYENKDYIRNCIIGKGGSYKGTVSITKSGIKCQPWNSMIPHEHSFLPSSYRGKDLQEN 176
Rat FDLYENKDYIRNCIIGKGGSYKGTVSITKSGIKCQPWNSMIPHEHSFLPSSYRGKDLQEN 176
Chicken FDLFEKKDYVRNCIIGKGAEYKGTISITKSGIQCQAWNSMIPHEHSFLPSSYRGKDLREN 171
Xenopus FDLYEKKDYIRDCIHGKGSNYRGTRNVTKRGLACQPWNSMIPHEHSFLPSTYRGKDLKEN 162
Zebrafish_Hgfa CDLYEKKDYVRECIIGSGVNYKGRRSFTKTGITCQSWNMSVPHEHNFKPTRHKKSDLRQN 160
Zebrafish_Hgfb FDLYEKKDFMRECIIGNGLNYKGKRSVTKSGVQCQLWNSKMPHEHNFLPQRHKHRDLRDN 159
:*:::*:** *.* .*:* ..** *: ** *. :**** :: **::*
Cat YCRNPRGEEGGPWCFTSNPEVRYEVCDIPQCSEVECMTCNGESYRGPMDHTESGKICQRW 233
Dog YCRNPRGEEGGPWCFTSNPEVRYEVCDIPQCSEVECMTCNGESYRGPMDHTESGKICQRW 235
Human YCRNPRGEEGGPWCFTSNPEVRYEVCDIPQCSEVECMTCNGESYRGLMDHTESGKICQRW 230
Mice YCRNPRGEEGGPWCFTSNPEVRYEVCDIPQCSEVECMTCNGESYRGPMDHTESGKTCQRW 236
Rat YCRNPRGEEGGPWCFTSNPEVRYEVCDIPQCSEVECMTCNGESYRGPMDHTESGKTCQRW 236
Chicken YCRNPRGEEGGPWCFTTSPQMRHEVCDIPLCSEVECMTCNGESYRGPMDHTESGKECQRW 231
Xenopus YCRNPKGEEGGPWCFTKSPEVRHDVCDIPFCSEVDCVTCNGEHYRGPMDYTESGKECQRW 222
Zebrafish_Hgfa FCRNPDNDPNGPWCFTELTETRHQDCGLPQCSDVECMKCNGETYRGPMDHTESGKECQRW 220
Zebrafish_Hgfb LCRNPDNTTTGPWCFTTDPKLRHQDCSIPQCSEVECMTCNGESYRGPLDHTESGRECQRW 219
**** . ****** .: *:: *.:* **:*:*:.**** *** :*:****: ****
Cat DRQTPHRHKFLPERYPDKGFDDNYCRNPDGKPRPWCYTLDPDTPWEYCAIKMCAHSTMND 293
Dog DHQTPHRHKFLPERYPDKGFDDNYCRNPDGKPRPWCYTLDPDTPWEYCAIKMCAHSTMND 295
Human DHQTPHRHKFLPERYPDKGFDDNYCRNPDGQPRPWCYTLDPHTRWEYCAIKTCADNTMND 290
Mice DQQTPHRHKFLPERYPDKGFDDNYCRNPDGKPRPWCYTLDPDTPWEYCAIKTCAHSAVNE 296
Rat DQQTPHRHKFLPERYPDKGFDDNYCRNPDGKPRPWCYTLDPDTPWEYCAIKMCAHSAVNE 296
Chicken DLQRPHKHKFRPERYPDKGFDDNYCRNPDGKLRPWCYTLDPNTPWEFCAIKTCDVGILNS 291
Xenopus DLQRPHKHKFRPERYPNKGLNDNYCRNPDGKSRPWCYTLDPDTSWEFCAIKPCVHSIVNN 282
Zebrafish_Hgfa DSQKPHKHTYQPHRHVGKGLDDNFCRNPNNDVRPWCYTMDKNTPWEYCNISVCDSDSDVE 280
Zebrafish_Hgfb DLEEPHKHIFHPKRYPDKGLKDNYCRNPDGRQRPWCFTTDPSTPWEYCNIKQCDSDNSGD 279
* : **:* : *.*: .**:.**:****:. ****:* * * **:* *. * . .
Cat TDVPMETTECIQGQGEGYRGTINSIWNGVPCQRWDSQYPHQHDITPENFKCKDLRENFCR 353
Dog TDVPMETTECIQGQGEGYRGTINTIWNGVPCQRWDSQYPHQHDITPENFKCKDLRENYCR 355
Human TDVPLETTECIQGQGEGYRGTVNTIWNGIPCQRWDSQYPHEHDMTPENFKCKDLRENYCR 350
Mice TDVPMETTECIQGQGEGYRGTSNTIWNGIPCQRWDSQYPHKHDITPEKFKCKDLRENYCR 356
Rat TDVPMETTECIKGQGEGYRGTTNTIWNGIPCQRWDSQYPHKHDITPENFKCKDLRENYCR 356
Chicken TEAVAETTTCIQGQGEGYRGTVNTIWSGIQCQRWDSQFPHQHNITPENFKCKDLRENYCR 351
Xenopus TDI---TKDCMKGQGEGYRGSVSTTYNGIQCQRWDSQFPHLHNFTPENYKCKDLSENYCR 339
Zebrafish_Hgfa VEV---TSSCFRGQGEGYRGTVNVTPAGVTCQRWDALSPHIHSYTPHNYKCKDLRENYCR 337
Zebrafish_Hgfb VEN---TTTCFRGRGEGYRGTVGITPDGVTCQRWDAQFPHRHSYTPQNYHCKDLRENYCR 336
.: *. *::*:******: . *: *****: ** *. **.:::**** **:**

```
Cat                 NPDGAESPWCFTTDPNIRVGYCSQIPKCDVSSGQ--DCYRGNGKNYMGNLSKTRSGLTCS 411
Dog                 NPDGAESPWCFTTDPNIRVGYCSQIPKCDVSSGQ--DCYRGNGKNYMGNLSKTRSGLTCS 413
Human               NPDGSESPWCFTTDPNIRVGYCSQIPNCDMSHGQ--DCYRGNGKNYMGNLSQTRSGLTCS 408
Mice                NPDGAESPWCFTTDPNIRVGYCSQIPKCDVSSGQ--DCYRGNGKNYMGNLSKTRSGLTCS 414
Rat                 NPDGAESPWCFTTDPNIRVGYCSQIPKCDVSSGQ--DCYRGNGKNYMGNLSKTRSGLTCS 414
Chicken             NPDGSESPWCFTTDPNIRIGYCSQIPKCDVSNEQ--DCYRGNGKSYMGNLSNTRIGLTCS 409
Xenopus             NPDGSESPWCFTTDPNIRIGHCSQIKKCQASNQQ--ECYYGNGSTYKGTLSRTRFRLPCS 397
Zebrafish_Hgfa      NPDGSEIPWCFTTDAKVRKAFCTNIPRCESESSDSTECYEDNGESYRGNLSKTRSGIPCG 397
Zebrafish_Hgfb      NPDGRHLPWCFTTDPTVPIAFCTNIPRCGLKPPEPEECYKGIGDMYNGHRSKTRSGIPCA 396
                    **** . *******..:  ..*::* .*  .  :  :** . *. * *  *.**  :.*.

Cat                 MWEKNMEDLHRH--IFWEPDASKLNKNYCRNPDDDAHGPWCYTGNPLIPWDYCPISRCEG 469
Dog                 MWEKNMEDLHRH--IFWEPDASKLNKNYCRNPDDDAHGPWCYTGNPLIPWDYCPIFRCEG 471
Human               MWDKNMEDLHRH--IFWEPDASKLNENYCRNPDDDAHGPWCYTGNPLIPWDYCPISRCEG 466
Mice                MWDKNMEDLHRH--IFWEPDASKLNKNYCRNPDDDAHGPWCYTGNPLIPWDYCPISRCEG 472
Rat                 MWDKNMEDLHRH--IFWEPDASKLTKNYCRNPDDDAHGPWCYTGNPLVPWDYCPISRCEG 472
Chicken             TWDKNIEDLRRHIQIFREPDVSKLKKNYCRNPDDDFHGPWCYTDDPLIPWDYCPISRCTG 469
Xenopus             MWEKNLQDLKRH--TFNEPDVSILQKNYCRNPDNDAHGPWCYTDDPFVPWDYCPISRCEG 455
Zebrafish_Hgfa      LWSDHTFRRDTR----SAKASAGLELNLCRNPDRDKHGPWCYTSNSSIPWDYCGLERCKS 453
Zebrafish_Hgfb      PWKDHSESNERD----VNLLTAEQAGNFCRNPDKDKHGPWCYTNSSSIPWDYCSLKPCEP 452
                     *..:               :    * ***** * *******... :***** :  *

Cat                 DTTPTIVNLDHPVISCAKTKQLRVVNG--IPTRTNVGWMVSLKYRNKHICGGSLIKESWI 527
Dog                 DTTPTIVNLDHPVISCAKTKQLRVVNG--IPTRTNVGWMVSLKYRNKHICGGSLIKESWI 529
Human               DTTPTIVNLDHPVISCAKTKQLRVVNG--IPTRTNIGWMVSLRYRNKHICGGSLIKESWV 524
Mice                DTTPTILNLDHPVISCAKTKQLRVVNG--IPTQTTVGWMVSLKYRNKHICGGSLIKESWV 530
Rat                 DTTPTIVNLDHPVISCAKTKQLRVVNG--IPTQTTVGWMVSLKYRNKHICGGSLIKESWV 530
Chicken             DTTPTTTSLDDTVIPCASTKHLRVVNG--IPTQTNEGWVVSLTYRNKHICGGTLVKEEWV 527
Xenopus             DTAKIMANIDSP-ITCSSSKQLRVVNG--IPAQTRKVWMVSVRYRNAHKCGGTLIKENWV 512
Zebrafish_Hgfa      MSSDDHQMSGGPKPSCFIHKTTRIVGGMRVQRAEDGSWVVSIQKGNRHWCGGSLIREEWV 513
Zebrafish_Hgfb      SHNNLPQKDEVTKSSCFVHKQVRIVGGGPVPIKE-GSWMVSIQKGSSHWCGGALVREEWV 511
                              .  .*   *  *:*.*  :       *:**:   . * ***:*::*.*:

Cat                 LTARQCFPSRNKDLKDYEAWLGIHDVHGRGDEKR-KQVLNVSQLVYGPEGSDLVLLKLAR 586
Dog                 LTARQCFPSRNRDLKDYEAWLGIHDVHGKGDEKR-KQVLNVSQLVYGPEGSDLVLLKLAR 588
Human               LTARQCFPSR--DLKDYEAWLGIHDVHGRGDEKC-KQVLNVSQLVYGPEGSDLVLMKLAR 581
Mice                LTARQCFPARNKDLKDYEAWLGIHDVHERGEEKR-KQILNISQLVYGPEGSDLVLLKLAR 589
Rat                 LTARQCFPARNKDLKDYEAWLGIHDVHERGEEKR-KQILNISQLVYGPEGSDLVLLKLAR 589
Chicken             LTARQCFPSRYKDLKDYKAWLGVHNIKGKGEEKH-RQVRNISQLIYGPAGSDLVLLKLSR 586
Xenopus             LTARQCFLSGDIDLKYYEAWLGVHNIYST-TEKH-KQILNISQLVHGPKGSNLVLLKLSR 570
Zebrafish_Hgfa      LTDQQCFPTCVPDLSEYTVQVGLLHLNASAG----TQALRIAHVVCGPEGSNLALLKLTT 569
Zebrafish_Hgfb      LTDKDCFSSCVPDLSEYRVWLGITHLNESGENDFHRQERRISHVICGPEDSSLALLRLSQ 571
                    ** ::** :   **. * . :*: .:          *  .::::: ** .*.*.*::*:

Cat                 PAVLDDFVSTIDLPNYGCTIPEKTTCSVYGWGYTGSINSDGLLRVAHLYIMGNEKCSQYH 646
Dog                 PAILDDFVSTIDLPNYGCTIPEKTTCSVYGWGYTGSINFDGLLRVAHLYIMGNEKCSQYH 648
Human               PAVLDDFVSTIDLPNYGCTIPEKTSCSVYGWGYTGLINYDGLLRVAHLYIMGNEKCSQHH 641
Mice                PAILDNFVSTIDLPSYGCTIPEKTTCSIYGWGYTGLINADGLLRVAHLYIMGNEKCSQHH 649
Rat                 PAILDNFVSTIDLPSYGCTIPEKTTCSIYGWGYTGLINADGLLRVAHLYIMGNEKCSQHH 649
Chicken             PAILTNFVEIIRLPISGCTIPEKTSCSVFGWGYTGLPNYDGLLRVANLFILGNEKCNQYL 646
Xenopus             PATLNAYVDRIKLPNYGCTIPEKTTCSVYGWGHTGTNDYDGQLQEGTLHIVGNEKCNENH 630
Zebrafish_Hgfa      PAPLSEHVRTVQLPVAGCAVAEGTLCLMYGWGDTKGTGHEGSLKMVGLPIVSNKRCSQSH 629
Zebrafish_Hgfb      PALPSERVRVIQLPVADCSIQEDTICSVYGWGETKGTGHEGTLKRVHLPIVSNERCQQLH 631
                    **     *  : **  .*:: * * * ::*** *   . :* *:   * *:.*::*.:

Cat                 QGKVTLNESEICAGAENIVSGPCEGDYGGPLVCEQHKMRMVLGVIVPGRGCAIPNRPGIF 706
Dog                 QGKVTLNESEICAGAENIVSGPCEGDYGGPLVCEQHKMRMVLGVIVPGRGCAIPNRPGIF 708
Human               RGKVTLNESEICAGAEKIGSGPCEGDYGGPLVCEQHKMRMVLGVIVPGRGCAIPNRPGIF 701
Mice                QGKVTLNESELCAGAEKIGSGPCEGDYGGPLICEQHKMRMVLGVIVPGRGCAIPNRPGIF 709
Rat                 QGKVTLNESELCAGAEKIGSGPCEGDYGGPLICEQHKMRMVLGVIVPGRGCAIPNRPGIF 709
Chicken             KGKITVNESEICAVAETIGAGPCERDYGGPLVCEQNRLKIVVGVIVPGRGCAIRNRPGIF 706
Xenopus             KGKITVNESEICAIGETANIGPCERDYGGPLICEENRTHLVQGVIIPGRGCAIQKRPVIF 690
Zebrafish_Hgfa      NGILPITETKICAGGKRD-QGVCEKDYGGPLVCQEGESKVIVGVSINGRGCAVARRPAVF 688
Zebrafish_Hgfb      RGTLPITSSKLCAGGRRD-EGVCEKDYGGPLVCQESNSKVIVGVSINGRGCARHNRPAIF 690
                    .* :.:..:::** ..    * ** ******:*:: . ::: ** : *****  .** :*
```

```
Cat                 VRVAYYAKWIHKIILTYKIPQS-- 728
Dog                 VRVAYYAKWIHKIILTYKIQQS-- 730
Human               VRVAYYAKWIHKIILTYKVPQS-- 723
Mice                VRVAYYAKWIHKVILTYKL----- 728
Rat                 VRVAYYAKWIHKVILTYKL----- 728
Chicken             VRVSYYSRWIHKIMMTYRKP---- 726
Xenopus             VRVAYYAKWIHKIMLTYKAP---- 710
Zebrafish_Hgfa      VNVAFYSEWIRKVFKYYSDMEISY 712
Zebrafish_Hgfb      VNVAFYAGWIHKVYRNYPNSELNN 714
                    *.*::*: **:*:   *
```

Fig.3.8 Amino acid sequence alignment of HGFs from Cat, Chicken, Dog, Human, Mice, Rat, *Xenopus* and Zebrafish. The identical residues are indicated by asterisk. Required catalytic sites for trypsin-like serine protease domain are not detected and catalytic residues are replaced with amino acids are highlighted in yellow. Human HGF's domains are highlighted in different colors: singnal peptide in pink; PAN_AP domain (divergent subfamily of APPLE domains) in green; Kringle domain in red; Trypsin-like serine protease domain in turquoise.

c-Met amino acid sequences of different species are also aligned (Fig.3.10) and the protein domains of zebrafish c-Met is predicted by SMART (http://smart.embl-heidelberg.de/) and signal peptide is predicted by SignalP 3.0 Server (http://www.cbs.dtu.dk/services/SignalP/), and compared to human c-MET (Fig. 3.9). Amino acid identities between zebrafish c-Met with other vertebrate species including Human, Mice, Rat, Cat, Dog, Chicken and Xenopus c-MET are 51% to 53% while identity between zebrafish c-Met with fugu Met is 59%. Amino acid identities of semaphorin domain between zebrafish c-Met with other verterbrate species' c-MET are 43% to 47%. Amino acid identities of PSI domain (domain found in Plexins, Semaphorins and Integrins) between zebrafish c-Met with other verterbrate species' c-MET are 41% to 50%. Amino acid identities of IPT domain (Ig-like, plexins, transcription factors) between zebrafish c-Met with other verterbrate species' c-MET are 38% to 52%. Amino acid identities of tyrosine kinase catalytic domain between zebrafish c-Met with other verterbrate species' c-MET are 81% to 90%. Compared to other domains in c-MET, tyrosine kinase catalytic domain is the most conserved domain in c-MET.

Results show that zebrafish c-Met and human c-MET share the same domains and structural organization (Fig.3.9). From the N terminal to C terminal, the domains are: a signal peptide which lead c-Met to form transmembrane protein; a semaphorin domain; a PSI domain which is found in Plexins, Semaphorins and Integrins; four IPT domains which has an immunoglobulin like fold; a tyrosine kinase domain which is highly conseverd and have 80% to 90% identities with other vertebrate species' c-MET tyrosine kinase domain and tyrosine residues within this domain are highly conserved (Fig.3.10).

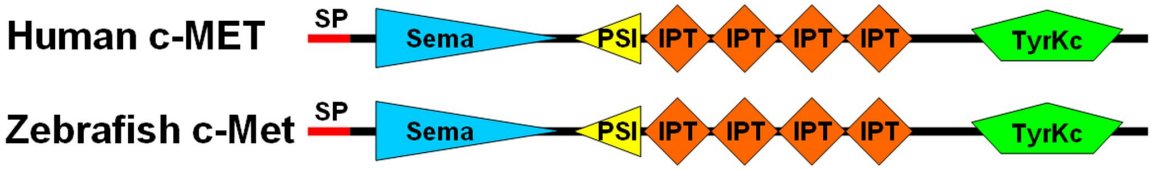

Fig.3.9 Comparison of the predicted domain and signal peptide of zebrafish c-Met with human c-MET. Domains are predicted by SMART (http://smart.embl-heidelberg.de/) and signal peptide is predicted by SignalP 3.0 Server (http://www.cbs.dtu.de/services/SignalP/). SP, singnal peptide; Sema, semaphorin domain; PSI, domain found in Plexins, Semaphorins and Integrins; IPT, Ig-like, plexins, transcription factors; TyrKc, Tyrosine kinase catalytic domain.

```
Cat             MKAPAVLAPGILVLLFTLVQKSYGECREALVKSEMNVNMKYQLPNFTAETPIQNVVLHKH 60
Dog             MKAPAVLAPGILVLLFTLVQKSYGECKEALVKSEMNVNMKYQLPNFTAETPIQNVVLHKH 60
Human           MKAPAVLAPGILVLLFTLVQRSNGECKEALAKSEMNVNMKYQLPNFTAETPIQNVILHEH 60
Mice            MKAPTVLAPGILVLLLSLVQRSHGECKEALVKSEMNVNMKYQLPNFTAETPIQNVVLHGH 60
Rat             MKAPTALAPGILLLLLTLAQRSHGECKEALVKSEMNVNMKYQLPNFTAETPIQNVVLHGH 60
Chicken         MKPVTAYPSGIILFLFALLQRSHGQCKEAAKKSEMNLNVKYDLPNFITETPIQNVVLYKH 60
Xenopus         ----MLVAVPVALLFLSLLPQCMGQCEEAAKMAEMDLNLKLNLQNFTTDTPIQSIIMFKG 56
Fugu            --MNLCSFPAAVLLLWALSASAEGHCQKSPEPNKLNLSVSYELPTFTAEFPIQNVVTLDG 58
Zebrafish       MTIHYSEAASILIILQSLWWGLNCQCEEPIESSKLDLSVTYDLPYFVSDTPIQKLLEING 60
                            ::: :*      .*.:.    ::::.:. :*  * :: ***.::

Cat             HIYLGAVNYIYVLNDKDLQKVAEYKTGPVLEHPDCFPCQDCSHKANLSGGVWKDNIN--- 117
Dog             HIYLGAVNYIYVLNDKDLQKVAEYKTGPVLEHPDCSPCQDCSHKANLSGGVWEDNIN--- 117
Human           HIFLGATNYIYVLNEEDLQKVAEYKTGPVLEHPDCFPCQDCSSKANLSGGVWKDNIN--- 117
Mice            HIYLGATNYIYVLNDKDLQKVSEFKTGPVLEHPDCLPCRDCSSKANSSGGVWKDNIN--- 117
Rat             HIYLGATNYIYVLNDKDLQKVSEFKTGPVVEHPDCFPCQDCSSKANVSGGVWKDNVN--- 117
Chicken         HVYIGAVNKIYVLN-ETLQNISVYKTGPILESPGCAPCEDCKDKANLSNSVWKDNVN--- 116
Xenopus         YVYVGAVNKIYVLN-ENLTKISEYKTGPLLKHSDCLPCKNCTDNLLSPNGTWKDSVN--- 112
Fugu            IIYVGATNRIYALA-PSLTKLSEYRTGPLLANQTCGQKVANAS----SGGGRKDNLN--- 110
Zebrafish       TVYVGAVNRLYALS-KDLKKKHEYKTGPVHEGPDCKTPTDRCS----GCENKPRNINNTN 115
                 :::**.* :*.*    * :   ::***:     *                   .:*

Cat             MALLIDTYYDDQLISCGSVHRGTCQRHVLPPSNTAD-------ILSKVHCMYSPQADEES 170
Dog             MALLVDTYYDDQLISCGSVHRGTCQRHILPPSNIAD-------IQSEVHCMYSSQADEEP 170
Human           MALVVDTYYDDQLISCGSVNRGTCQRHVFPHNHTAD-------IQSEVHCIFSPQIEE-P 169
Mice            MALLVDTYYDDQLISCGSVNRGTCQRHVLPPDNSAD-------IQSEVHCMFSP--EEES 168
Rat             MALLVDTYYDDQLISCGSVNRGTCQRHVLPPDNAAD-------IQSEVHCMFSPLAEEES 170
Chicken         MALLLETYYDDQLISCGSVSGGVCHRHIIPPDNPAD-------IESEVHCMYSPQVDGEA 169
Xenopus         MALFVQDFYDDQLISCGNIRKGECQRHTLHSDKPWD-------IASDVHCLYSSQMVEDK 165
Fugu            VALVVENIYDKGLFSCGSADNGVCRRHVLEDDVSLDEEGRQKSVDELVYCFTDLKQDKGQ 170
Zebrafish       MALLMETFYDLELFSCGSAGNGVCSRHVLEDGP----------LGAEVTCMYTKKNEGSS 165
                :**.::  **  *:***.   * * ** :  .           :   * *:

Cat             SHCPDCVVSALGTKVLISEKGRFINFFVGNTINSSY----LTDHSLHSISVRRLKETQDG 226
Dog             SQCPDCVVSALGTKVLISEKDRFINFFVGNTINSSD----HPDHSLHSISVRRLKETQDG 226
Human           SQCPDCVVSALGAKVLSSVKDRFINFFVGNTINSSY----FPDHPLHSISVRRLKETKDG 225
Mice            GQCPDCVVSALGAKVLLSEKDRFINFFVGNTINSSY----PPGYSLHSISVRRLKETQDG 224
Rat             GQCPDCVVSALGAKVLLSEKDRFINFFVGNTINSSY----PPDYSLHSISVRRLKETQDG 226
Chicken         DNCPDCVVSTLGTKVLVTEKDRFVNFFVGNTMTSAF----QPPHVLHSISVRRLKETQDG 225
Xenopus         DSCPDCIVSTAGSKILVTVGDRFVKFFVGSTLTGQ-------PSTIHSVSVRRLKETQDG 218
Fugu            PRDSDVVVSPSGSQVLNVESN-MIMFFVGNSEIPGSGNVTGPTARPHTMSLRKMKTSQNG 229
Zebrafish       HGCPDCLAGPAGTQILNIMSGRVVRFFVANSEPLES---NGPRLH-HTISIRKMRETQDG 221
                   .* :... *:::*    . .: ***..:              *::*:*::: :::*

Cat             FKFLTDQSYIDVLPEFRDSYPIKYIHAFESNRFIYFLTVQRETLDAQTFHTRIIRFCSVD 286
Dog             FKFLTDQSYIDVLPEFRDSYPIKYVHAFESNHFIYFLTVQRETLDAQTFHTRIIRFCSVD 286
Human           FMFLTDQSYIDVLPEFRDSYPIKYVHAFESNNFIYFLTVQRETLDAQTFHTRIIRFCSIN 285
Mice            FKFLTDQSYIDVLPEFQDSYPIKYIHAFESNHFIYFLTVQKETLDAQTFHTRIIRFCSVD 284
Rat             FKFLTDQSYIDVLGEFRDSYPIKYIHAFESNHFIYFLTVQKETLDAQTFHTRIIRFCSVD 286
Chicken         FEFLTDQSYIDILPQFRDSYPIKYVHAFEHDHFVYFLTVQRESLDSQTFHTRIIRFCTLD 285
Xenopus         FEYLTDQSYIDVLPHLRDIYPIRYIYTFESNNFVYFLTVQRESLDSQAYHTRIVRICSSD 278
Fugu            FTFFSNRSYMDLIPPLRGSYYLRYVYSFHSGPFTYFLTVQQVSKDSQTYHTRIVRMCSSD 289
Zebrafish       FEFFSDQSYMDLAPSLRGNYPLHYVYSFQSGPYVYFLTVQREGGNSKAFHTRIVRMCSSD 281
                * :::::**:*:   ::. * ::*:::*. . : ******:   ::::::***:*:*: :
```

```
Cat             SGLHSYMEMPLECILTEKRRKRS-TREEVFNILQAAYVSKPG--AHLAKQIGANLNDDIL 343
Dog             SGLHSYMEMPLECILTEKRRKRS-TREEVFNILQAAYVSKPG--AHLAKQIGANLNDDIL 343
Human           SGLHSYMEMPLECILTEKRKKRS-TKKEVFNILQAAYVSKPG--AQLARQIGASLNDDIL 342
Mice            SGLHSYMEMPLECILTEKRRKRS-TREEVFNILQAAYVSKPG--ANLAKQIGASPSDDIL 341
Rat             SGLHSYMEMPLECILTEKRRKRS-TREEVFNILQAAYVSKPG--ANLAKQIGASPYDDIL 343
Chicken         SEMRSYMEMPLECIFTEKRRKRS-IRKEVFNILQAAYVSKPG--AALAHEMGLGLIDDIL 342
Xenopus         SELRSYIEMPLECIFTEKRRKRS-TASAVFNIVQAAYLGRAG--EDLAEEMGVKPDDDIL 335
Fugu            HDIRRYVEMPLECISTDKRRRRSMEDVKVFNILQAATVTKVGSDVELQRQLRLEEGDDVL 349
Zebrafish       SEILRYVKMPFECIYSERRRKRRSAQV-AFNVLQAAHVAKVG--YDFQQEMGLKEGEDVL 338
                  :  *::**:*** :::*::*      .**::*** : : *    : .::     :*:*

Cat             YGVFAQSKPDSAEPMNRSAVCAFPIKYVNEFFNKIVNKNNVRCLQHFYGPNHEHCFN--- 400
Dog             YGVFAQSKPDSAEPMNRSAVCAFPIKYVNEFFNKIVNKNNVRCLQHFYGPNHEHCFN--- 400
Human           FGVFAQSKPDSAEPMDRSAMCAFPIKYVNDFFNKIVNKNNVRCLQHFYGPNHEHCFN--- 399
Mice            FGVFAQSKPDSAEPVNRSAVCAFPIKYVNDFFNKIVNKNNVRCLQHFYGPNHEHCFN--- 398
Rat             YGVFAQSKPDSAEPMNRSAVCAFPIKYVNDFFNKIVNKNNVRCLQHFYGPNHEHCFN--- 400
Chicken         YGVFAQTNQIPQEPTNRSAVCAVSVRTINEFFNKIVDKQNMKCLQHFYGKDSKYCLN--- 399
Xenopus         YGVFAQSKPDSPEPNNRSAVCAVSVKTINEFFNSAADKQNTKCLEHFYGKDNRLCINN-- 393
Fugu            FAAFARGKPNSTEATPNSAICVMSLKLINSMFKMYMQKCNTVDLYHFTGSDKKSCYNVSS 409
Zebrafish       FAAFARSKPDSPEPTASSAVCLISITDINEFFKVFIQKGYTRKLHHFPGSEEKTFNQTFV 398
                :..**: :  . *.   **:* ..:  :*.:*:   :*     * ** * : .   :

Cat             -RTLLRNSSGCEVRSDEYRTEFTTALQRVDLFMGQFNQVLLTSISTFIKGDLTIANLGTS 459
Dog             -RTLLRNSSGCEARNDEYRTEFTTALQRVDLFMGQFNQVLLTSISTFIKGDLTIANLGTS 459
Human           -RTLLRNSSGCEARRDEYRTEFTTALQRVDLFMGQFSEVLLTSISTFIKGDLTIANLGTS 458
Mice            -RTLLRNSSGCEARSDEYRTEFTTALQRVDLFMGRLNQVLLTSISTFIKGDLTIANLGTS 457
Rat             -RTLLRNSSGCEVRSDEYRTEFTTALQAVDLFMGRLNHVLLTSISTFIKGDLTIANLGTS 459
Chicken         -RAFSRNASYCRAQDDEYRLEVTTPLQRVDLFMGQFNNILLTSISVFTKGNLTIANLGTS 458
Xenopus         -KRFLRNASHCSTPIDEYRVEVTTVLRRLDLFMDQFRNVLLTSISVFTQGRLTIANLGTS 452
Fugu            SDDCDPHEGIHEGKEGKYRLQVTQFVQRLEYWQKVLTNTLVTSITVVTVHGRAVGYLGTA 469
Zebrafish       GDSFS-----CEKHERGYRLEVTSTNPRRDYFHGRFRNVLLTSIAVVPIQNHTVASLGTA 453
                          ** :.*      : :   : . *:***:..     ::. ***:

Cat             EGRFMQVVVSRSGSSTPHVNFRLDSHPVSSEAIVEHPLNQNGYTLVVTGKKITKIPLNGL 519
Dog             EGRFMQVVVSRSGLSTPHVNFRLDSHPVSPEAIVEHPLNQNGYTLVVTGKKITRIPLNGL 519
Human           EGRFMQVVVSRSGPSTPHVNFLLDSHPVSPEVIVEHTLNQNGYTLVITGKKITKIPLNGL 518
Mice            EGRFMQVVLSRTAHLTPHVNFLLDSHPVSPEVIVEHPSNQNGYTLVVTGKKITKIPLNGL 517
Rat             EGRFMQVVLSRTAHFTPHVNFLLDSHPVSPEVIVEHPSNQNGYTLVVTGKKITKIPLNGL 519
Chicken         EGRFMQIVVSRSEPTAPHVSFQLDSHAVSPQVVVEQSAAADGYTLVVTGKKITKVPLNGP 518
Xenopus         EGRFMQVIISRTGQPKPHVNFLLEARPISPEIVINTASEESGYTLVNTGMQIIKVPLVVL 512
Fugu            DGRHIQVVFSRFAS--PHVNIRLDSRPVSGSVVLPGQDPSEGALLLTTGNKITKVPLIGP 527
Zebrafish       EGRVIQVVVSRFGKTEPHVDFRLDTLPVSSEMALLSPQHHNGSLLLITGNKVSKLPVIGP 513
                :** :*::.**     ***.: *:: .:* .  :      .*  *: ** :: ::*:

Cat             GCEHFQSCSQCLSAPPFVQCGWCHDK--CVQLEECPSGTWTQEICLPTIYEVFPTSAPLE 577
Dog             GCEHFQSCSQCLSAPPFVQCGWCHDR--CVHLEECPTGAWTQEVCLPAIYEVFPTSAPLE 577
Human           GCRHFQSCSQCLSAPPFVQCGWCHDK--CVRSEECLSGTWTQQICLPAIYKVFPNSAPLE 576
Mice            GCGHFQSCSQCLSAPYFIQCGWCHNQ--CVRFDECPSGTWTQEICLPAVYKVFPTSAPLE 575
Rat             GCGHFQSCSQCLSAPYFIQCGWCHNR--CVHSNECPSGTWTQEICLPAVYKVFPTSAPLE 577
Chicken         GCHHFQSCSQCLLAPAFMRCGWCGQQ--CLRAPECNGGTWTQETCLPRVYEILPSSAPLE 576
Xenopus         TCGHLKSCSHCLSSPS-VNCGWSKNH--CSTKQECLNEEWIQETCPPAVYEVFPSSAPLE 569
Fugu            GCDHLTTCTSCLVSSRVTECGWCEGR--CTRANQCPPSVWTQEYCTPVVTKVFPTSGPIR 585
Zebrafish       GCEQLWTCSSCLLAPGFMGCGWCRTSNLCTRAPRCPQSQWIQDSCPLLITSISPSSAPLR 573
                 * :: :*: ** :.    ***.     *    .*    * *: *   : .: *.*.*:.

Cat             GGTMLTVCGWDFGFRRNNKFDLKKTRVFLGNESCTLTLSESTT--NMLKCT-VGPAVNEH 634
Dog             GGTVLTVCGWDFGFRRNNKFDLKKTKVFLGNESCTLTLSESTT--NMLKCT-VGPAVNEH 634
Human           GGTRLTICGWDFGFRRNNKFDLKKTRVLLGNESCTLTLSESTM--NTLKCT-VGPAMNKH 633
Mice            GGTVLTICGWDFGFRKNNKFDLRKTKVLLGNESCTLTLSESTT--NTLKCT-VGPAMSEH 632
Rat             GGTMLTICGWDFGFKKNNKFDLRKTKVLLGNESCTLTLSESTT--NTLKCT-VGPAMSEH 634
Chicken         GGTKLTLCGWDFGFSKNNRFELRNTVVHIGGQICALEAKSSNK--NKLECT-APAAKNAS 633
Xenopus         GGTQLTICGSDFVLSKNNNFDLKNTVVIIGKKRCKIEGKFSNQ--NKLVCR-TDSSVSSV 626
Fugu            GSTTVTMCGRNFGFDKTESFKASLVTVEVAGVPCKLSRQDYASRWTEIQCSPMFSGNFTP 645
Zebrafish       GQTNITICGKNFGFNKKDRFDTKLIDVVVAGTKCKLERKDSNN--NRLVCG-LDHVNWSS 630
                * * :*:** :* : :.: *.     * :.   * :  .      . : *

Cat             FNISIIISNGRGTAQYSTFSYVDPVITSIFPSYGPKTGGTLLTLTGKYLNSGNSRHISIG 694
Dog             FNISIIISNGRGTAQYSTFSYVDPIITSISPSYGPKNGGTLLTLTGKYLNSGNSRHISMG 694
Human           FNMSIIISNGHGTTQYSTFSYVDPVITSISPKYGPMAGGTLLTLTGNYLNSGNSRHISIG 693
Mice            FNVSVIISNSRETTQYSAFSYVDPVITSISPRYGPQAGGTLLTLTGKYLNSGNSRHISIG 692
Rat             FNVSVIVSNSRETTQYSAFSYVDPVITSISPRYGPHAGGTLLTLTGKYLNSGNSRHISIG 694
Chicken         FNISSSVSVGHGKTLFNTFSYVNPIITSISPTYGPKSGGTLLTIAGKYLNSGKSRRIFVG 693
Xenopus         FNMSSSVSNGKQVVNFTTFSYVNPIITSIRPSYGPRAGRTLLTIKGHYLDSGKDRKVYIG 686
Fugu            SGHTVKVTSGHKIATIEGFTFVDPVVSEIFPTFGPKSGNTMLTIRGAFLDTGNKREVTVG 705
Zebrafish       VDSVVTVRSGKEQAQKDGFSFVNPVIIEIFPEFGPQSGGTMLTISGSFLDSGNVQTVTVG 690
                 .    :  .:  .    *::*:*:: .* * :**  * *:**: * :*::*: : : :*
```

```
Cat             GKTCTLKSVSDSILECYTPAQTIPTEFPIKLKIDLANREMN-SFSYQEDPIVYAIHPTKS 753
Dog             GKTCTLKSVSDSILECYTPAQATATEFPIKLKIDLANREMN-SFSYQEDPIVYAIHPTKS 753
Human           GKTCTLKSVSNSILECYTPAQTISTEFAVKLKIDLANRETS-IFSYREDPIVYEIHPTKS 752
Mice            GKTCTLKSVSDSILECYTPAQTTSDEFPVKLKIDLANRETS-SFSYREDPVVYEIHPTKS 751
Rat             GKTCTLKSVSDSILECYTPGHTVSAEFPVKLKIDLADRVTS-SFSYGEDPFVSEIHPTKS 753
Chicken         EKPCSLKSTSESSVECYTPAQRIPQEYRVRVGIDGAIRDAKGYFTYREDPVVLKIHPAKS 753
Xenopus         KEMCNIKSVSSAAIVCLTPGQGTTGTYLVALKIDNANRESSTRFTYMEDPSVSSIKPVKS 746
Fugu            KAACKIQSLSATMLTCKTPPHAVPSKQPVRLTVDSVARDAPVLYTYHQDPIISSIQPSRS 765
Zebrafish       NATCVLQSVSATMLTCRTPPQPSPSQHKVQLHIDGVIFEAPVSYTYNKNPHISSVQPKHS 750
                   * ::* * : : * ** :  .    : : :* .       ::* ::* :  ::* :*

Cat             FISGGSTITAVGKNLNSVSVLRMVISVHETRRNFTVACHHRSNSEIICCTTPSLQQLNLQ 813
Dog             FISGGSTITAVGKNLNSVSVLRMVIDVHETRRNFTVACQHRSNSEIICCTTPSLQQLNLQ 813
Human           FISGGSTITGVGKNLNSVSVPRMVINVHEAGRNFTVACQHRSNSEIICCTTPSLQQLNLQ 812
Mice            FISGGSTITGIGKTLNSVSLPKLVIDVHEVGVNYTVACQHRSNSEIICCTTPSLKQLGLQ 811
Rat             FISGGSTITGIGKNLNSVSTPKLVIEVHDVGVNYTVACQHRSSSEIICCTTPSLQQLDLQ 813
Chicken         FLSGGSTITAQGINLNSVCFPRMVITVPKLGMNFSVACSHRSSSEIICCTTPSLKAFNLQ 813
Xenopus         FLSGGSSITAYGKNLNAVASPLMVIHLSKLEVSYNMSCIHRSTSELIWCSTPSLKELNLE 806
Fugu            FVSGGCTVAAHGLFLQSGLQPQMVLTTGQDAEVFHVSCVYGENRTSIQCTTPSLAKLALQ 825
Zebrafish       FISGGSTVTVNGFYLHSALQPQMVLTAATEGKLFQVTCSHDEDKRNILCITPSLKGLSVQ 810
                *:***.:::  *  *::     :*:        : ::* : .    * * ****  : ::

Cat             LPLKTKAFFMLDGIHSKYFDLIYVHNPVFKPFEKPVMISIGNENVLEIKGNDIDPEAVK- 872
Dog             LPLKTKAFFMLDGIHSKYFDLIYVHNPVFKPFEKPVMISIGNENVLEIKGNDIDPEAVK- 872
Human           LPLKTKAFFMLDGILSKYFDLIYVHNPVFKPFEKPVMISMGNENVLEIKGNDIDPEAVK- 871
Mice            LPLKTKAFFLLDGILSKHFDLTYVHNPVFEPFEKPVMISIGNENVVEIKGNNIDPEAVK- 870
Rat             LPLKTKAFFLLDGILSKHFDLTYVHDPMFKPFEKPVMISMGNENVVEIKGDDIDPEAVK- 872
Chicken         PPFVTKVFFIFDGVSSLYFDFDYVNNPVFKHFEKPVLISRSNPNVLEIKGNHIDSEAVK- 872
Xenopus         PPITTRVFFILDGVISNNFELSYVNNPIFETFGKPVVFPIGNKNILEIKGDHIDSEAVR- 865
Fugu            PPVVTKVAFVLDGYMTEQWDLIYVEDP---LFQDPKLTSKDNKSIVELKGDRMDREAMK- 881
Zebrafish       PPVATKMTFVLDGFSTDQYDLLYVEDPKFEEFQKPTVTPRGKKNILEIKVPPVNQEAVKN 870
                 *. *:  *::**  :  ::: **.:*    * .* : . .: .::*:*   :: **::

Cat             GEVLKVGNKSCETIYSDSEAVLCKVPNDLLKLN-NELNIEWKQAVSSTILGKVIVQPDQN 931
Dog             GEVLKVGNKSCETIYSDSKAVLCKVPNDLLKLN-NELNIEWKQAVSSTVLGKVIVQPDQN 931
Human           GEVLKVGNKSCENIHLHSEAVLCTVPNDLLKLN-SELNIEWKQAISSTVLGKVIVQPDQN 930
Mice            GEVLKVGNQSCESLHWHSGAVLCTVPSDLLKLN-SELNIEWKQAVSSTVLGKVIVQPDQN 929
Rat             GEVLKVGNKSCENLHWHSEALLCTVPSDLLKLNGGELNIEWKQAVSSTVLGKVIVQPDQN 932
Chicken         GEVLKVGNKSCENLLLQSETILCTVPSDLLKSN-SELNIEWKQEVLSTVIGKVLIRQDQN 931
Xenopus         GEVLKVGNKSCEIVQSKSDSVSCSVPTDLFKSN-SELKIEFVQEVPSIIIGKVMVTQDQN 924
Fugu            CQVLTVSNHSCESLTLVGNTLECTVPTELQTTTSKELQVEWRQADSIRHLGKVTLAQEQD 941
Zebrafish       GEVLRVSNRTCESVTLVGNTLECTVPMELQT-AAKELEVEWKQATSSVILGRVILAQDQD 929
                 :** *.*::** :   . :: *.** :* .    **::*: *      :*:* :  :*:

Cat             FTGLIVGVISISIILLLLLGVFLWLKKRKQIKDLGSELVRYDARVHTPHLDRLVSARSVS 991
Dog             FTGLIAGVISISTIVLLLLGLFLWLKRKKQIKDLGSELVRYDARVHTPHLDRLVSARSVS 991
Human           FTGLIAGVVSISTALLLLLGFFLWLKKRKQIKDLGSELVRYDARVHTPHLDRLVSARSVS 990
Mice            FAGLIIGAVSISVVVLLLSGLFLWMRKRK-HKDLGSELVRYDARVHTPHLDRLVSARSVS 988
Rat             FAGLIIGAVSISVVVLLVSGLFLWLRKRK-HKDLGSELVRYDARVHTPHLDRLVSARSVS 991
Chicken         FTGLIAGVVSTSVLIYIFLVFFLWRRKKKQIKDLGSDLVRYDGRVHTPHLDRLVSARSVS 991
Xenopus         FTGIITGVVSCVVLLLLMFGILIWMKKRKQLKDLGGDMVLYDGRVHTPHLDRLVSARSIS 984
Fugu            YTGLIVGCMCVSLLLLLLGTLLLWKK-NKHIDDLS--EVWYDGRGHIQHLDRLANARSVS 998
Zebrafish       YRILITGGVCVSILLLLLIAVFVWIKRKKHINDLAKTMVWYDGRAHIPHLDMLANARSVS 989
                :  :* * :.    : :.  .::* : .*  .**.   * **.* *  *** *..***:*

Cat             PTTEMVSNESVDYRATFPEDQFPNSSQNGSCRQVQYPLT--DLSP---MLNSG-----DS 1041
Dog             PTTEMVSNESVDYRATFPEDQFPNSSQNGSCRQVQYPLT--DLSP---MLTSG-----DS 1041
Human           PTTEMVSNESVDYRATFPEDQFPNSSQNGSCRQVQYPLT--DMSP---ILTSG-----DS 1040
Mice            PTTEMVSNESVDYRATFPEDQFPNSSQNGACRQVQYPLT--DLSP---ILTSG-----DS 1038
Rat             PTTEMVSNESVDYRATFPEDQFPNSSQNGACRQVQYPLT--DLSP---ILTSG-----DS 1041
Chicken         PTTEMVSSESVDYRSTFLEDQFPSMSQNGSCRPAQYPHS--DLSP---ILSSG-----DS 1041
Xenopus         PTTEMVSSESVDYRSTVQEDPFPNSSQNGSCRPAQYAHR--DLSP---ILSSG-----DS 1034
Fugu            PTNEMVSHESVDYRTNLLEDQGSDRPETCRAGPPIYGGNGELLSPRLVALGSGLGLGMEG 1058
Zebrafish       PTNEMVSHESVDYRTTLLEDQNLPLSQTESCRPHLYAHSHVDLSP---MLGP-----MEG 1041
                **.**** ******:.. **     .:.  .    *      :**    * .      :.

Cat             DISSPLLQNTVHIDLSALNPELVQAVQHVVIGPSSLIVHFNEVIGRGHFGCVYHGTLLDS 1101
Dog             DISSPLLQNTVHIDLSALNPELVQAVQHVVIGPSSLIVHFNEVIGRGHFGCVYHGTLLDN 1101
Human           DISSPLLQNTVHIDLSALNPELVQAVQHVVIGPSSLIVHFNEVIGRGHFGCVYHGTLLDN 1100
Mice            DISSPLLQNTVHIDLSALNPELVQAVQHVVIGPSSLIVHFNEVIGRGHFGCVYHGTLLDN 1098
Rat             DISSPLLQNTVHIDLSALNPELVQAVQHVVIGPSSLIVHFNEVIGRGHFGCVYHGTLLDS 1101
Chicken         DLASPLLQTNVHIDISALNPDLVKEVQHVVIGADSLMVHFSEVIGRGHFGCVSHGTLLDN 1101
Xenopus         DIASPLLHSYVHIDISALSTDLMKEIEHMVIRVDRLIVHFNRVIGRGLSGCVSHGTLHDT 1094
Fugu            ELVSPLLMAPVHIDPSCLHPDLLTEVQHVVIAREQLLLHLNQVIGRGHFGCVFHGTLLEP 1118
Zebrafish       DLASPLLPSTAPIDLGSLHPELLKEVQHVVIAREDLLLHVNEIIGRGHFGCVFHGTLLEP 1101
                :: ****   . ** ..* .:*:  ::*:**  . *::*...:****  *** **** :
```

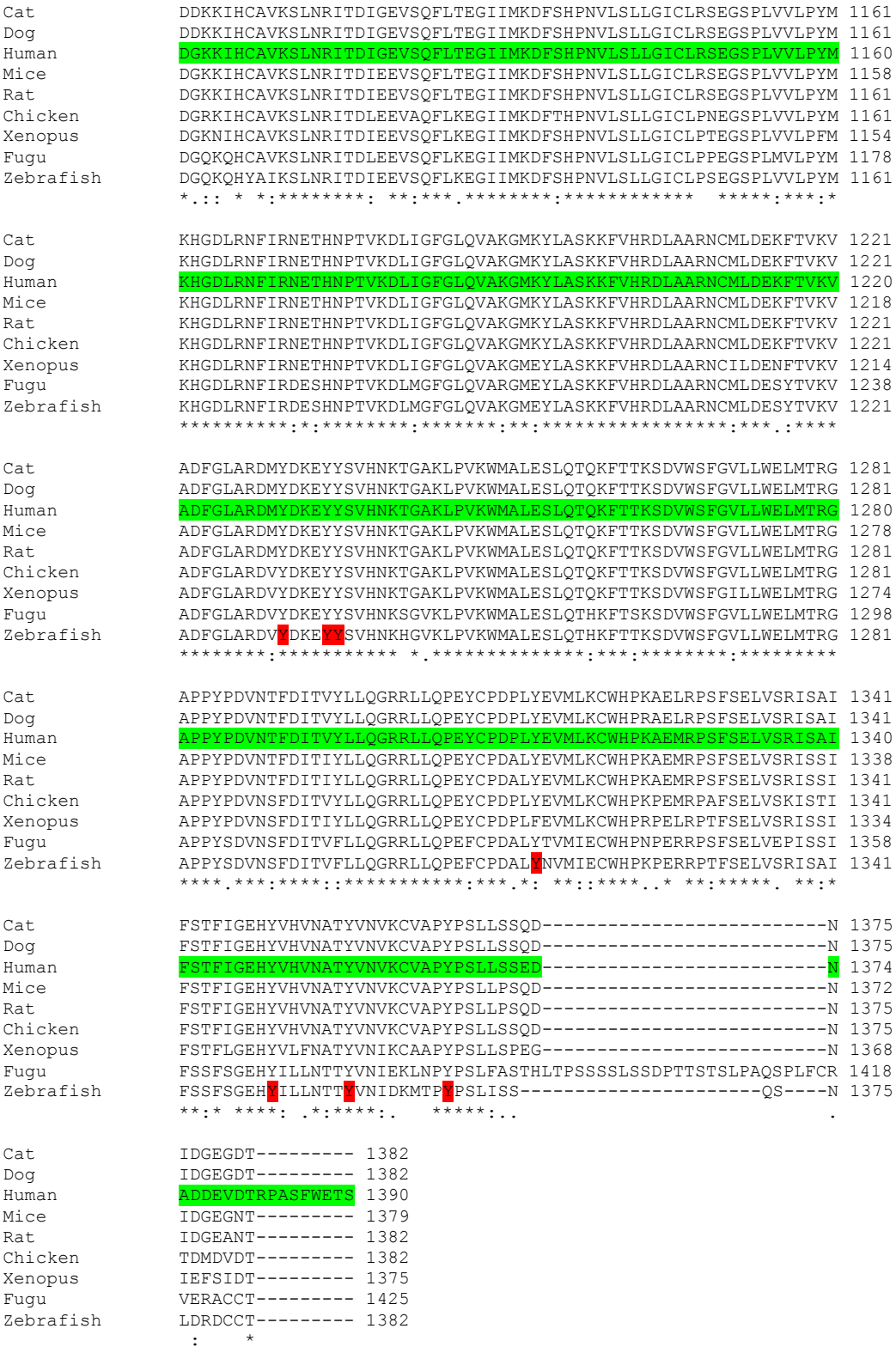

Fig.3.10 Amino acid sequence alignment of Cat, Dog, Human, Mice, Rat, Chicken, Xenopus, Fugu and Zebrafish c-Met. The identical residues are indicated by asterisk. Conserved tyrosine residues in zebrafish c-Met tyrosine kinase catalytic domain are highlighted in red. Human c-MET's domains are highlighted in different colors: singnal peptide in pink; semaphorin domain in turquoise; PSI domain (domain found in Plexins, Semaphorins and Integrins) in yellow; IPT domains (Ig-like, plexins,

transcription factors) in grey; transmembrane domain in blue; Tyrosine kinase catalytic domain in green.

3.1.3 Phylogenetic analyses of zebrafish Hgfa, Hgfb and c-Met

Phylogenetic analyses were performed to explore the relationship between HGF or c-MET from different vertebrate species by ClustalW in http://www.trex.uqam.ca. Parameters for data anlysis and results output are used as default setting, expect for data analysis using slow mode and results output in radial style. As shown in Fig.3.11, zebrafish Hgfa and Hgfb were most closely related to the *Xenopus* hgf. And in Fig.3.12, although zebrafish c-Met was most closely related to predicted *Fugu* c-met, the closest c-met homologue are *Xenopus* c-met.

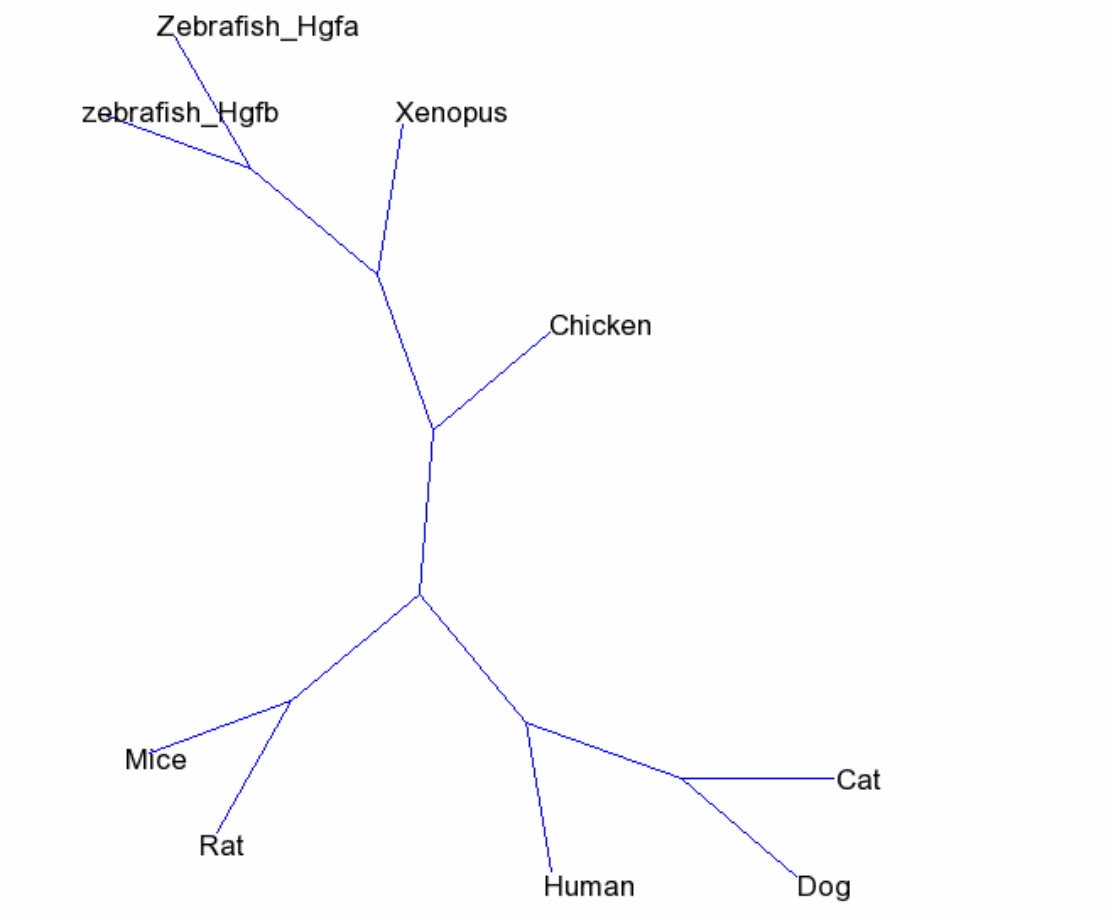

Fig.3.11 Phylogenetic tree of Cat, Chicken, Dog, Human, Mice, Rat, Xenopus, and Zebrafish Hgf. Phylogenetic tree are generated by amino acid sequence.

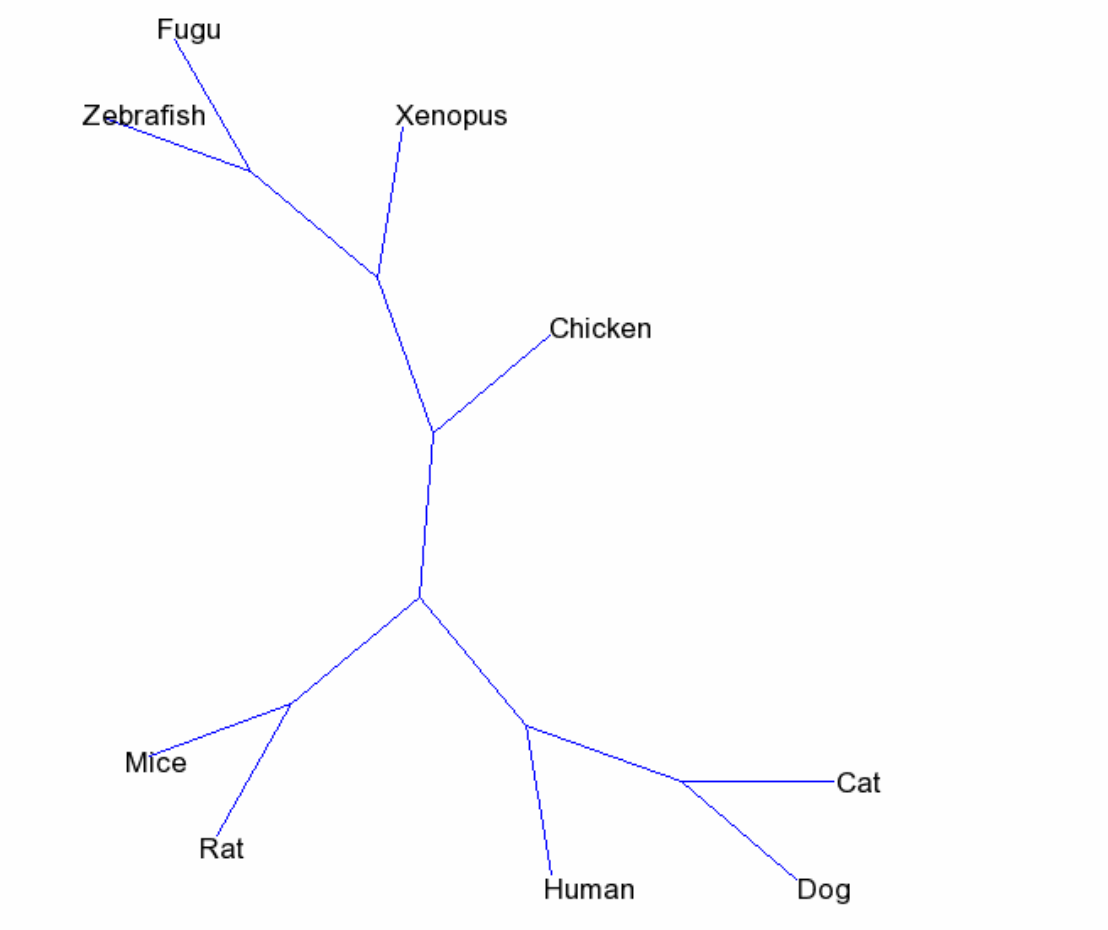

Fig.3.12 Phylogenetic tree of Cat, Chicken, Dog, Fugu, Human, Mice, Rat, Xenopus, and Zebrafish c-Met. Phylogenetic tree are generated by amino acid sequence.

3.1.4 Genomic localization and synteny analyses of zebrafish *hgf*a, *hgfb* and *c-met*

3.1.4.1 Genomic localization and synteny analyses of zebrafish *hgfa*

Genomic localization of zebrafish *hgfa* was analyzed through Ensembl zebrafish genome database (version: Ensembl release 45 - Jun 2007). Zebrafish *hgfa* was found to locate at Chromosome 4 from 21682362 to 21713937. Similar to human *HGF*, zebrafish *hgfa* also contains 18 exons.

To determine the syntenic relationship, genes adjacent to zebrafish *hgfa* were examined. In zebrafish, four genes and *hgfa* are found to be arranged in the following sequence from 5' to 3': *snd1* (Staphylococcal nuclease domain-containing protein 1), *hgfa*, *si:ch211-251k4.1* (encoding a protein similar to CACNA2D1 (calcium channel, voltage-dependent, alpha 2/delta subunit 1)), *atp6v1f* (ATPase, H+ transporting, lysosomal 14kDa, V1 subunit F) and *si:dkey-159a18.7* (a putative orthologue of *NP_001008396.1*). In human, these four genes are also found to be adjacent to *HGF*, however, in a different arrangement as in the following sequence from 5' to 3': *ATP6V1F, HGF*, *CACNA2D1, NP_001008396.1*and *SND1* (Fig.3.13). Although these five genes are adjacent to each other in zebrafish and human, their arrangements are different. Hence, syntenic relationship is not strongly indicated.

A

Zebrafish Chr4	*snd1*	*hgfa*	*si:ch211-251k4.1*	*atp6v1f*	*si:dkey-159a18.7*
Human Chr7	*SND1*	*HGF*	*CACNA2D1*	*ATP6V1F*	*NP_001008396.1*

B

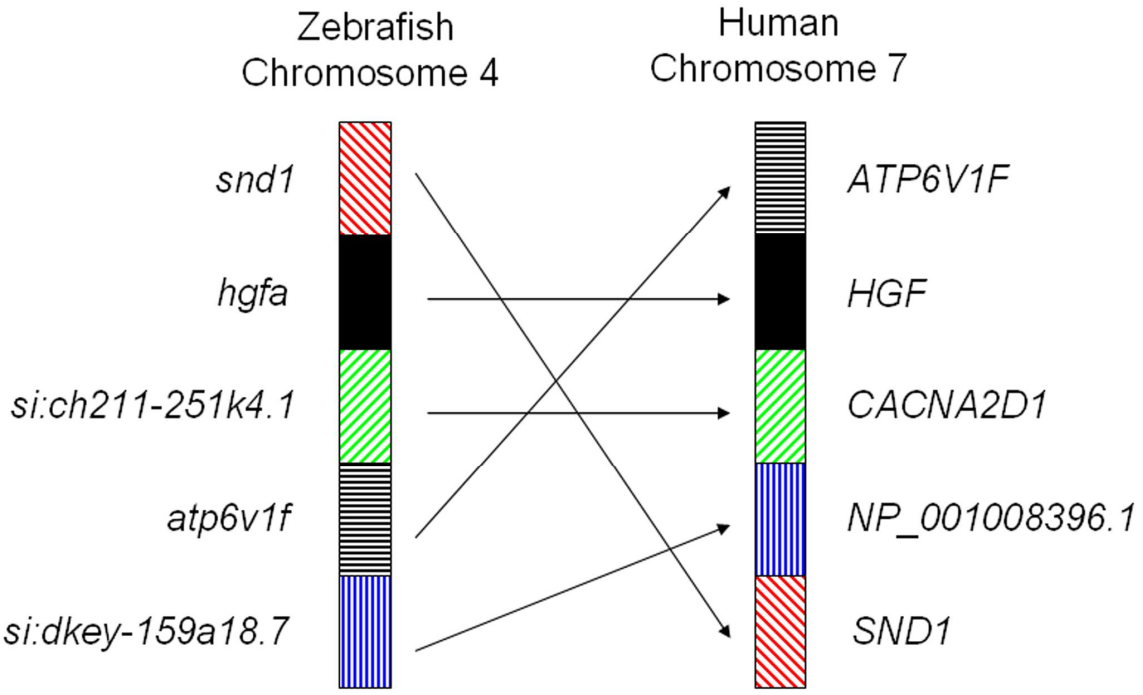

Fig.3.13 Genomic localization of zebrafish *hgfa*. (A). Orthologues of zebrafish and human genes in *hgfa* chromosome region. (B). Syntenic relationship between zebrafish chromosome 4 and human chromosome 7 showing chromosomal shuffling. The genes adjacent to HGFa on chromosome 4 are conserved on chromosome 7 of human.

3.1.4.2 Genomic localization of zebrafish *hgfb*

Genomic localization of zebrafish *hgfb* was also analyzed similarly through Ensembl zebrafish genome database (version: Ensembl release 45 - Jun 2007). Zebrafish *hgfb*'s first 9 exons are located in scaffold Zv6_NA2108 from 84183 to 124854 and last 8 exons of *hgfb* are in scaffold Zv6_NA946 from 243369 to 257447. There is a gap of 96bp between the 9th exon and the 11th exon which can not be located in the zebrafish genome database. Both of the scaffolds haven't been mapped yet. Seventeen exons of zebrafish *hgfb* have been found, which is one exon (exon 10 missing) less than the human *HGF*. It is possible that there are still gaps in the zebrafish genome sequence and the *hgfb* gene region.

To determine the syntenic relationship, genes adjacent to zebrafish *hgfb* were examined. In scaffold Zv6_NA946, no adjacent gene can be found. In scaffold Zv6_NA2108, the only gene adjacent to *hgfb*, *LOC558257*, encoding a protein similar to CACNA2D1, is found at 5' of *hgfb*, while *CACNA2D1* is located adjacent to *HGF* and 3'. Thus, the region containing *hgfb* on zebrafish scaffold Zv6_NA2108 might be syntenic to the chromosomal region containing *HGF* in human chromosome 7 (Fig.3.14).

A

Zebrafish scaffold Zv6_NA2108	*LOC558257*	*hgfb*
Human Chr7	*CACNA2D1*	*HGF*

B

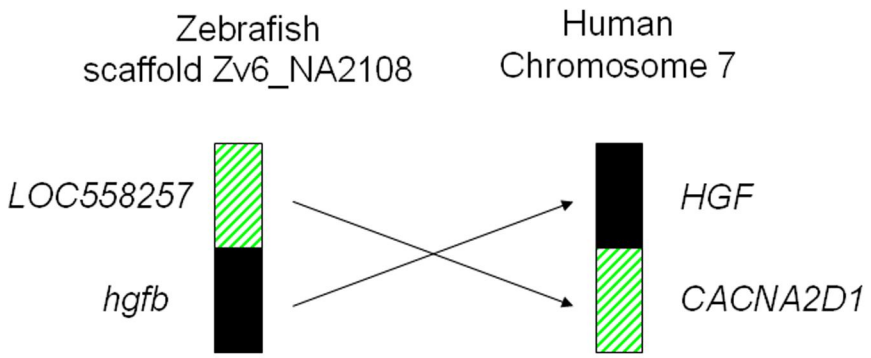

Fig.3.14 Genome localization of *hgfb*. (A) Ortholoues of zebrafish and human genes in *hgfb* chromosome region. The orthologs are aligned in the same column. (B). The gene adjacent to *hgfb* on scaffold Zv6_NA2108 is conserved on chromosome 7 of human.

3.1.4.3 Genomic localization and synteny analyses of zebrafish *c-met*

Zebrafish *c-met* was found to locate at Chromosome 25 from 10668539 to 12040365 (version: Ensembel release 45 – Jun 2007). In previous version of zebrafish genome data v19.3a.2 (3 Mar 2004), zebrafish *c-met* can be found at three scaffolds: NA13458, ctg 15876 and ctg 11348. Combining the blast results from these two versions of zebrafish genome database, 21 exons can be located which is identical to the human c-met exon number.

Based on genomic localzation of zebrafish *c-met* and synteny analysis, the region containing *c-met* on zebrafish Chromosome 25 might be syntenic to the chromosomal region containing *c-MET* in human chromosome 7. Presence of *cav1* (caveolin 1) and *cav2* (caveolin 2) close to the map position of *c-met* on zebrafish Chromosome 25 corresponds to their conserved presence on human chromosome 7 in close vicinity of map positions of c-met in human. Some chromosomal rearrangement might have occurred during evolution on the site near *c-met* in zebrafish chromosomal 25 since several genes locate on zebrafish chromosomal 25 close to *c-met*, namely, *eif3s1* and *557889*, while their orthologues in human are found on chromosome 15 and 2, respectively (Fig. 3.15).

A

Zebrafish Chr25	*met*	*cav1*	*cav2*
Human Chr7	*MET*	*CAV1*	*CAV2*

B

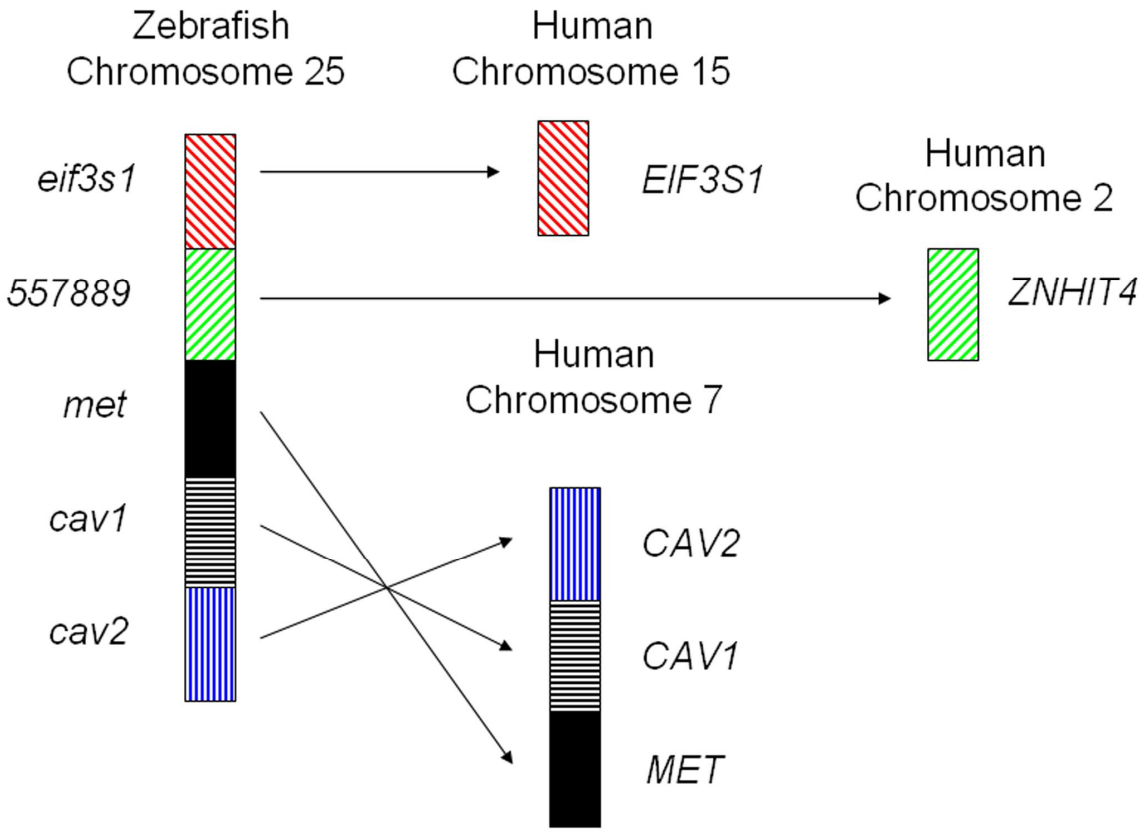

Fig.3.15 Genome localization of *c-met*. (A). Ortholoues of zebrafish and human genes in *c-met* chromosome region. The orthologs are aligned in the same column. (B). Syntenic relationship between zebrafish chromosome 25 and human chromosome 7 showing chromosomal rearrangement. The genes adjacent to c-met on one side of chromosome 25 are conserved on chromosome 7 of human in the same orientation and order.

3.2 Expression analysis of *hgfa*, *hgfb* and *c-met* during zebrafish embryonic development

3.2.1 Expression analysis by real-time RT-PCR

In order to understand the functions of *hgfa*, *hgfb* and its receptor *c-met* during development, it is important to determine its temporal expression profile. Embryos at different developmental stages were collected and RNA was extracted. Expression level of *hgfa*, *hgfb* and *c-met* were then determined by SYBR green real-time RT-PCR using β actin as the internal reference.

All three genes can be detected at 0 hpf stage, but the expression level is very low (Fig.3.16), indicating possible low level maternal mRNA. *hgfa* zygotic expression profile has one peak around 24hpf (Fig.3.16.A), a stage of active somitogenesis and neurogenesis occurs. *hgfb* zygotic expression profile has two peaks, one is around 24 hpf and another is around 3 day post fertilization (dpf) to 4dpf, (Fig.3.16.B). *c-met* zygotic expression profile has one peak at 12hpf and decrease sharply at 24hpf, then increase gradually and the second peak around 3-4dpf (Fig.3.16.C). The peak expression of *hgfb* and *c-met* around 3-4dpf correspond to the stage of liver growth. Although all three genes can be detected at 1 cell stage (0 hpf) by qRT-PCR, which indicated their maternal expression, their expression pattern at 1cell stage can not be detected by whole mount in-situ hybridization. Importantly, all three genes are expressed at all stages analyzed, suggesting important and multiple roles of this ligand-receptor signaling pathway in zebrafish embryonic development.

A

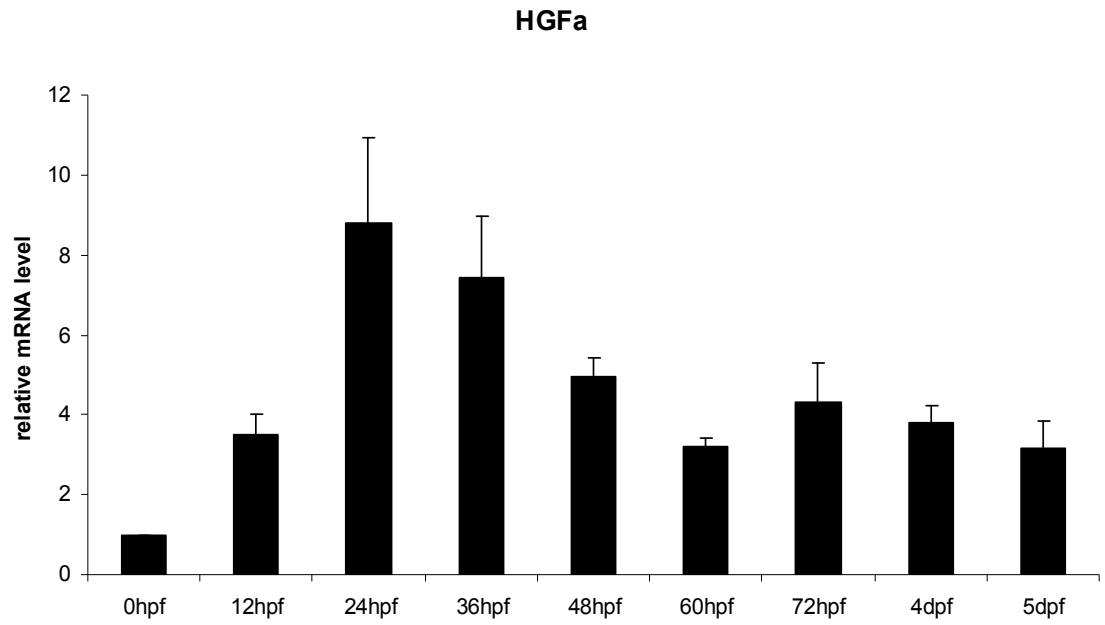
HGFa
relative mRNA level
12
10
8
6
4
2
0
0hpf
12hpf
24hpf
36hpf
48hpf
60hpf
72hpf
4dpf
5dpf

B

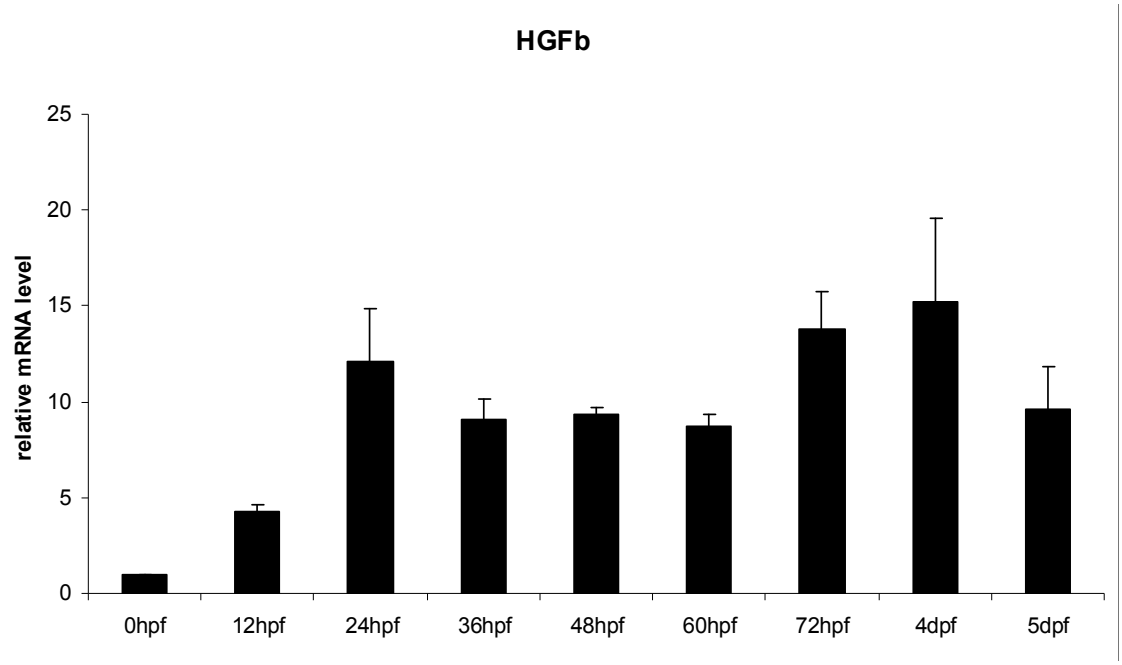
HGFb
relative mRNA level
25
20
15
10
5
0
0hpf
12hpf
24hpf
36hpf
48hpf
60hpf
72hpf
4dpf
5dpf

C

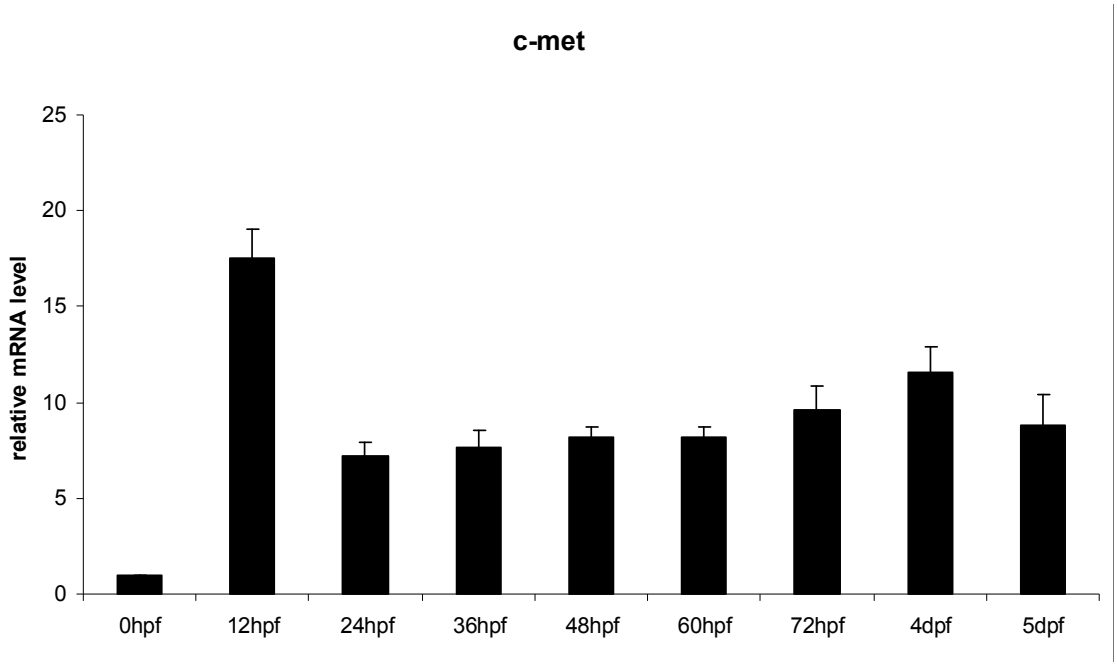

Fig.3.16 Relative mRNA levels of zebrafish *hgfa*, *hgfb* and *c-met* in WT embryos. (A) *hgfa*. (B) *hgfb*. (C) *c-met*. Relative mRNA levels are compared to 0hpf stage.

3.2.2 Expression analysis by whole mount in situ hybridization (WISH)

In order to understand the functions of *hgfa*, *hgfb* and its receptor *c-met* during development, it is important to determine their spatial and temporal expression profile. Embryos at different developmental stages were collected and the spatial distribution of transcripts of *hgfa*, *hgfb* and *c-met* were analyzed by WISH.

3.2.2.1 Expression analysis of *hgfa*

To study the spatial and temporal expression of *hgfa* during zebraifhs embryonic development, WISH was carried out using digoxigenin labeled RNA probe. Embryos from 0hpf stage to 6dpf were examined. The signal of *hgfa* was discernable starting from 7 somites stage in the somites, and this expression persisted up to 30hpf (Fig.3.17 A-E). *hgfa*'s expression in pectoral fin and ear is evident 30hpf to 48hpf (Fig.3.17 E-H). Although HGF mRNA was found in liver in other vertebrates, zebrafish *hgfa* can not be detected in liver (data not shown).

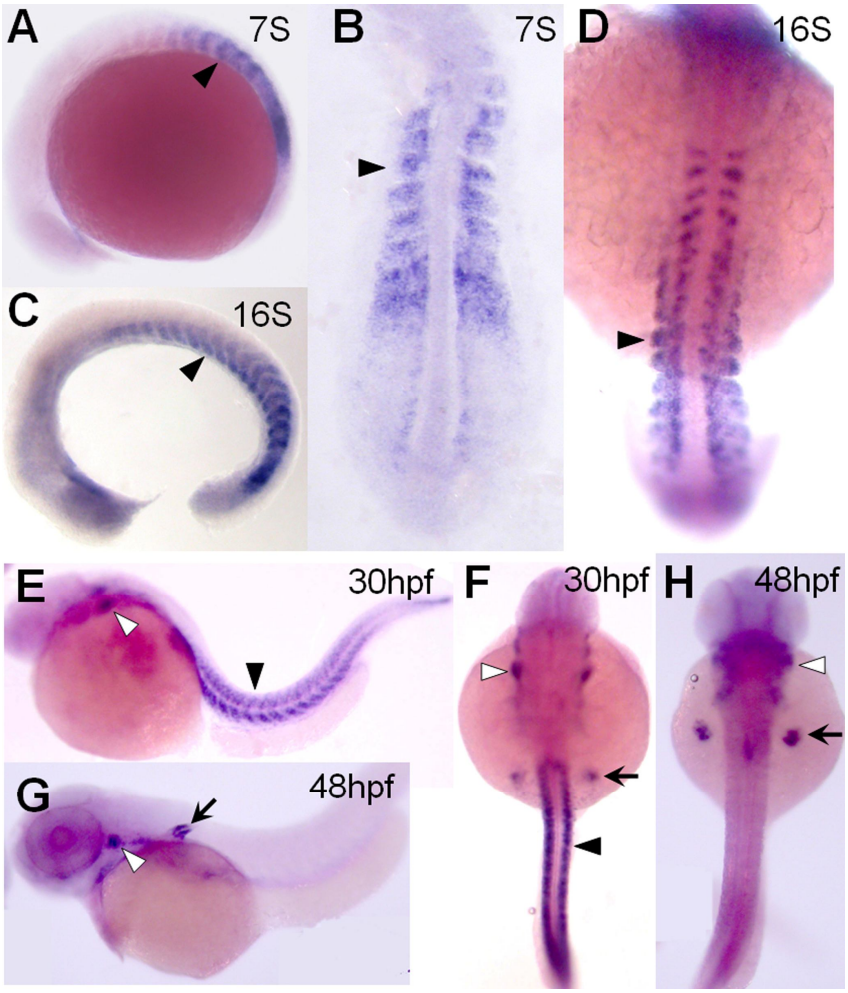

Fig.3.17 Expression pattern of zebrafish *hgfa* detected by WISH. Embryos are anterior to the left and dorsal to the top, except in B, D, G, and H, which are dorsal views with anterior to the top. (A) The 7-somites stage. (B) The 7-somites stage (flat mount dorsal view). (C) The 16-somites stage. (D) The 16-somites stage (dorsal view). (E) The 30-hpf stage. (F) The 30-hpf stage (dorsal view). (G) 48-hpf stage. (H) 48-hpf stage (dorsal view). The black arrowhead points to the somites. The white arrowhead points to the otic vesicle (G) or ear (H). The black arrow points to the fin bud.

3.2.2.2 Expression analysis of *hgfb*

To study the spatial and temporal expression of *hgfb* during zebraifhs embryonic development, WISH was carried out using digoxigenin labeled RNA probe. Embryos from 0hpf stage to 6dpf were examined. At 6dpf stage, digoxigenin labeled RNA probe of *hgfb* and fluorescein labeled RNA probe of *ceruloplasmin* (*Cp*) were used in the expression analysis of *hgfb* in liver by two-color WISH. The signals of *hgfb* were discernable starting from 1-somite stage in dorsolateral placode on both sides of the midline which later become restricted into several patches in the neural system, and this expression persists up to 36hpf (Fig.3.18 A-N). *hgfb* expression in nephric duct opening was detectable as early as 12-somite stage and last till 4dpf (Fig.3.18 F-S). *hgfb* expression in swimbladder was also seen from 36hpf to 4dpf (Fig.3.18 N-R) and at 24hpf *hgfb* could be detected in the primordium of swimbladder (Fig.3.18 K-L). Expression of *hgfb* in liver was first detected at 4dpf in a scattered manner and this expression pattern persisted at least till 6dpf (Fig.3.18 R). Two-color WISH of *hgfb* and *Cp* as well as tissue section revealed *hgfb* expression in liver mesenchymal cells at 6dpf but not in hepatocytes (Fig. T-V). This expression pattern of *hgfb* is completely different from the Hanies' *hgfs'* where they did not detect any differences in expression pattern between the two hgf genes (Haines et al., 2004).

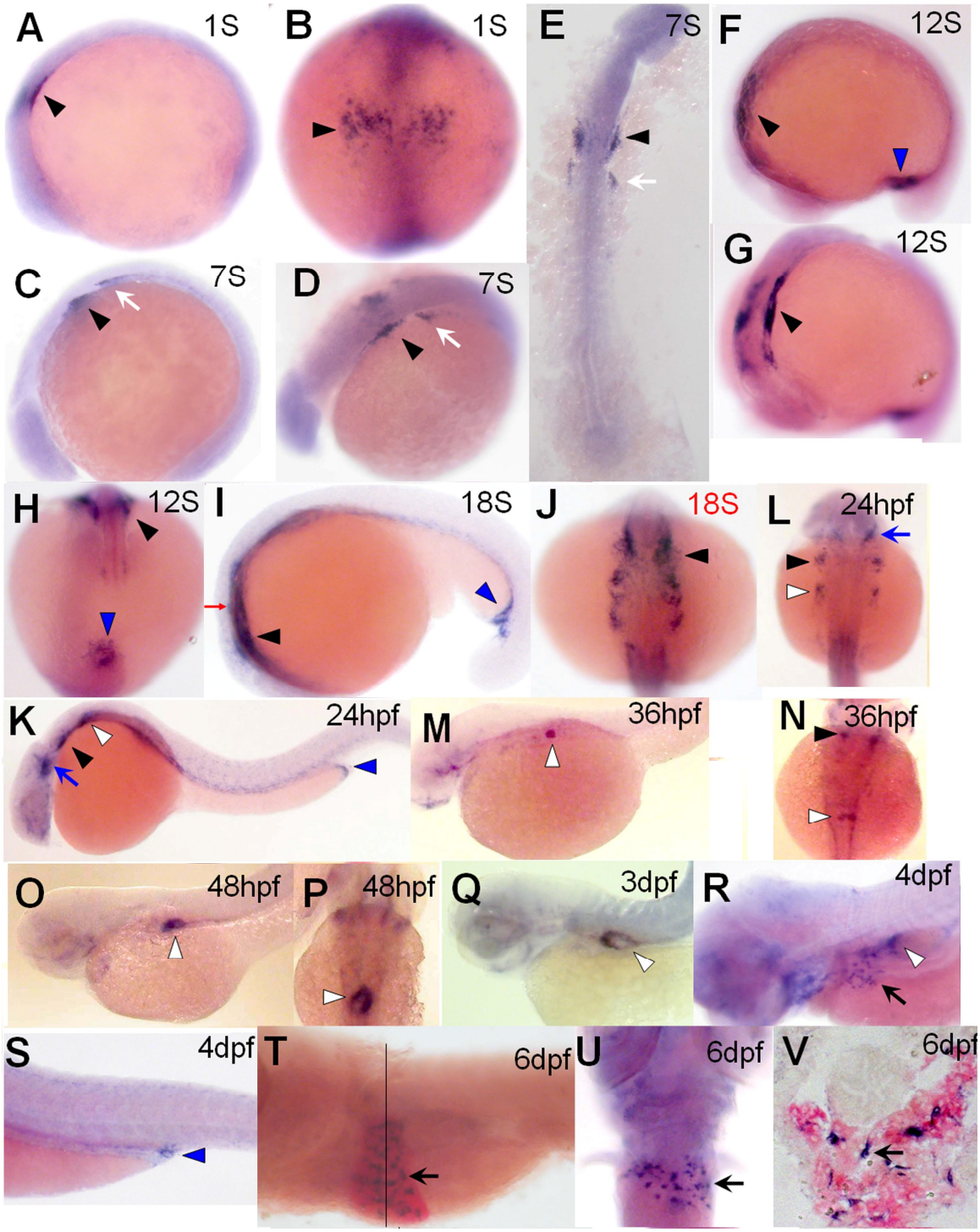

Fig.3.18 Expression pattern of zebrafish *hgfb* detected by WISH. Embryos are anterior to the left and dorsal to the top, except in B, E, J, L, N and P, which are dorsal views with anterior to the top, in H and T, which are ventral views with anterior to the top. (A) The 1-somites stage. (B) The 1-somites stage (dorsal view). (C) The 7-somites stage. (D) The 7-somites stage (dorsal lateral view). (E) The 7-somites stage (flat mount dorsal view). (F) The 12-somites stage. (G) The 12-somites stage (dorsal lateral view). (I) The 18-somites stage. (J) The 18-soimtes stage (dorsal view, direction indicated in I as red arrow). (K) The 24hpf stage. (L) The 24 hpf stage (dorsal view). (N) The 36hpf stage (dorsal view). (O) The 48hpf stage. (P) The 48hpf

stage (dorsal view). (Q) The 3dpf stage. (R) The 4dpf stage. (S) The 4dpf stage. (T) The 6dpf stage (Two probes staining: Ceruloplasmin stained with red color; HGFb stained with blue color). (U) The 6dpf stage (ventral view). (V) The 6dpf stage. Shown is a transverse section through the plate in S. The black arrowhead points to the dorsolateral placode. The white arrow points to the anterior primordium of nephric duct. The blue arrowhead points to the pronephric duct opening (I, K and S) or the primordium of pronephric duct opening (F and H). The blue arrow points to the trigeminal placode. The white arrowhead points to the swimbladder (M to R) and the primordium of swimbladder (K and L). The black arrow points to the liver.

3.2.2.3 Expression analysis of *c-met*

The signals of *c-met* were first discernable starting at 1somite stage in the presumptive forebrain and midbrain, and this expression persists up to 12somitestage (Fig.3.19 A-F). *c-met*'s expression in the pronephric mesoderm or the pronephric duct is detectable from 1somite stage to 24hpf (Fig.3.19 B-N). *c-met*'s expression in migrating lateral line primordial is detectable from 18hpf to 24hpf (Fig.3.19 J-M), which was also revealed in Haines' study (Haines et al., 2004). Tussue section revealed *c-met* expression in motor neurons from 18hpf to 24hpf (Fig.3.19 J-N). *c-met* expression is also detected in the pectoral fin and gut from 48hpf to 3dpf (Fig.3.19 O-Q). The expression of *c-met* in pancreas is only detectable at 4pdf (Fig.3.19 T and V). *c-met* is expressed in liver from 48hpf to 6dpf (Fig.3.19 P-U). At 3dpf, it is expressed in hepatocytes as revealed by the two probes WISH and tissue section (Fig.3.19 R).

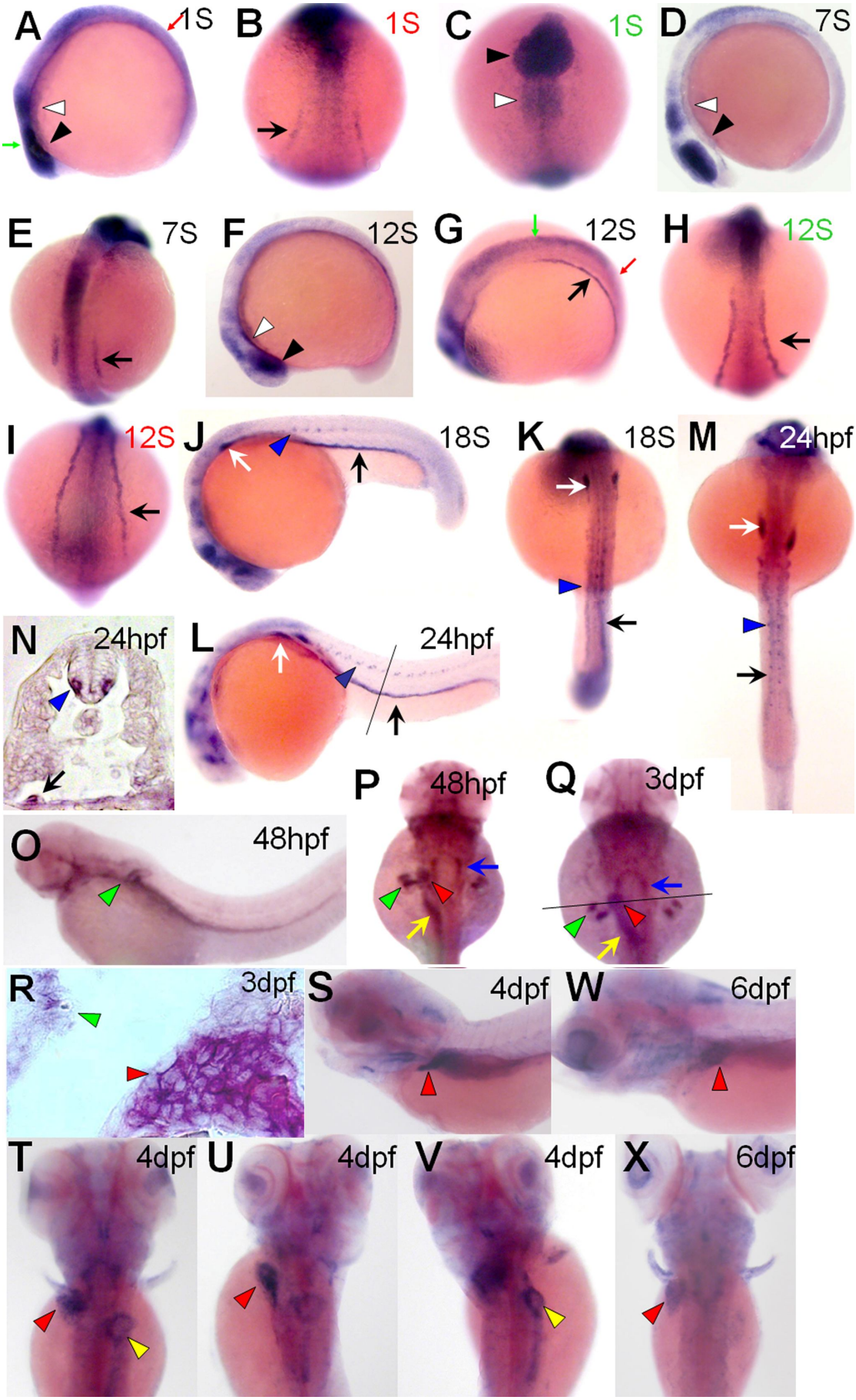
A
1S
B
1S
C
1S
D
7S
E
7S
F
12S
G
12S
H
12S
I
12S
J
18S
K
18S
M
24hpf
N
24hpf
L
24hpf
P
48hpf
Q
3dpf
O
48hpf
R
3dpf
S
4dpf
W
6dpf
T
4dpf
U
4dpf
V
4dpf
X
6dpf

Fig.3.19 Expression pattern of zebrafish *c-met* detected by WISH. Embryos are anterior to the left and dorsal to the top, except in B, C, E, H, I, K, M, P, Q, T, U, V and X, which are dorsal views with anterior to the top. (A) The 1-somites stage. (B) The 1-somites stage (dorsal view, direction indicted in A as red arrow). (C) The 1-somites stage (dorsal view, direction indicted in A as green arrow). (D) The 7-somites stage. (E) The 7-somites stage (dorsal lateral view). (F) The 12-somites stage. (G) The 12-somites stage (dorsal lateral view). (H) The 12-somites stage (dorsal view, direction indicted in G as green arrow). (I) The 12-somites stage (dorsal view, direction indicted in G as red arrow). (J) The 18-soimtes stage. (K) The 18-somites stage (dorsal view). (L) The 24hpf stage. (M) The 24hpf stage (dorsal view). (N) The 24hpf stage. Shown is a transverse section through the plate in L. (O) The 48hpf stage. (P) The 48hpf stage (dorsal view). (Q) The 3dpf stage (dorsal view). (R) The 3dpf stage (Two probes staining: Ceruloplasmin stained with red color; c-met stained with blue color). Shown is a transverse section through the plate in Q. (S) The 4dpf stage. (T) The 4dpf stage (dorsal view). (U) The 4dpf stage (dorsal lateral view from left side). (V) The 4dpf stage (dorsal lateral view from right side). (W) The 6dpf stage. (X) The 6dpf stage (dorsal view). The black arrowhead points to the presumptive forebrain. The white arrowhead points to the presumptive midbrain. The black arrow points to the pronephric mesoderm (B and E) or the pronephric duct (G to M). The white arrow points to the migrating lateral line primordia. The blue arrowhead points to the motor neuron. The green arrowhead points to the pectoral fin. The yellow arrow points to the gut. The red arrowhead points to the liver. The blue arrow points to the caudal hindbrain. The yellow arrowhead points to the pancreas.

3.3 Functional study of *hgfa*, *hgfb* and *c-met* in zebrafish embryonic development

To study the function of *hgfa*, *hgfb* and its receptor *c-met*, gene knockdown by microinjecting morpholino modified antisense oligonucleotides targeting at each gene into 1-2 cell stage fertilized embryos were carried out. Morpholino modified antisense oligonucleotides have been shown to effectively and specifically suppress gene expression in zebrafish embryos (Corey and Abrams, 2001; Draper et al., 2001; Nasevicius and Ekker, 2000).

3.3.1 Role of *hgfa* in zebrafish embryonic development

3.3.1.1 Knockdown of *hgfa* induces curved trunk

Two types of antisense morpholino oligonucleotides (MO) were used in this analysis. One targets at the start codon region to inhibit translation, named as HGFa-ATG MO. A 5bp mismatch control MO was designed and named as HGFa-ATG5mis MO. Another MO HGFa-ex1 is designed against the splice-donor sites of exon 1 to interfere with mRNA splicing. Both MOs induced a curved trunk phenotype (Fig.3.20 and Fig.3.21) and the percentage of the embryos showing this phenotype did not vary much during different developmental stage from 2dpf to 5dpf (Fig.3.21 and Fig.3.22). To verify the knockdown effect, different approaches were applied for these two types of MO. For HGFa-ATG MO, different doses of MO were injected and a dosage-dependent induction of the curved-tail phenotype was observed. At the 1ng per embryo injection dose, no curved trunk phenotype was observed in the pool of embryos injected with HGFa-ATG5mis MO, but persisted in the HGFa-ATG pool at

40% (Fig.3.22). In contrast, *hgfb* morphants showed relative low percentage of embryos with curved trunk (7% at 10ng per embryo injection, 15% at 1ng per embryo injection) compared to the *hgfa* morphants (53% at 10ng per embryo injection, 40% at 1ng per embryo injection) (Fig.3.22). For MO blocking mRNA splicing, embryos were separated into different pools based on the phenotype. *hgfa* mRNA level of each pool was examined by qRT-PCR and the result showed that *hgfa* mRNA level is lower in the pool with curved trunk phenotype than the pool without phenotype (Fig.3.23).

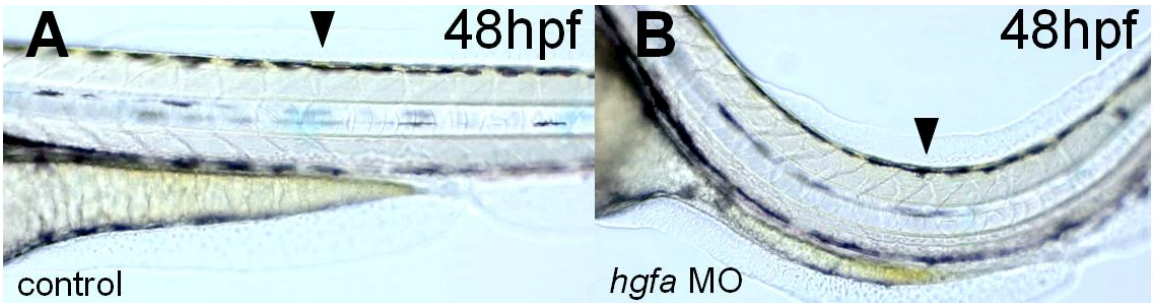

Fig.3.20 Zebrafish *hgfa* knockdown induces curved trunk. Embryos are dorsal view with anterior to the top. (A) control-injected embryo at 48hpf stage. The black arrowhead points to the normal trunk. (B) *hgfa* knockdown morphant at 48hpf stage. The black arrowhead points to the curved trunk.

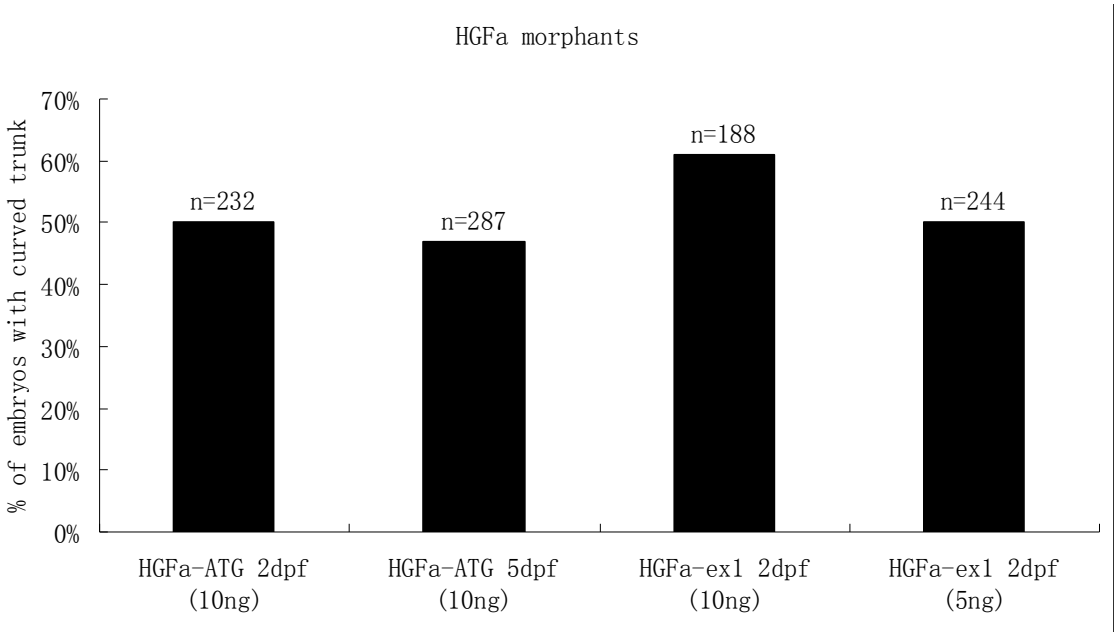

Fig.3.21 Curved trunk observed in *hgfa* morphants.

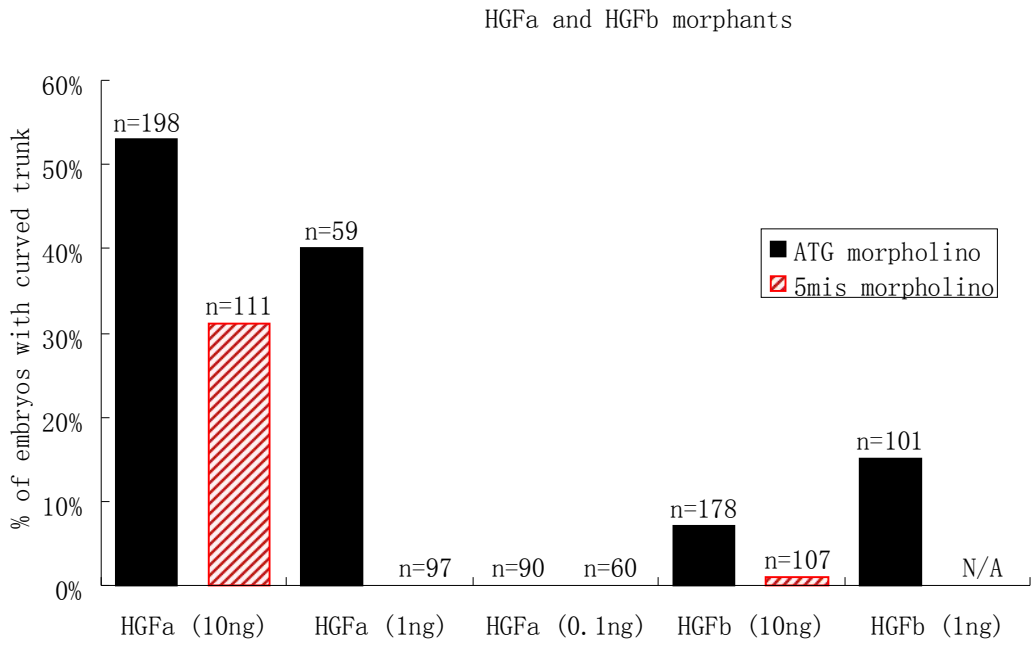

Fig.3.22 Curved trunk observed in *hgfa* and *hgfb* morphants.

Confirmation of knockdown effect of HGFa MO

HGFa-ex1 MO is against the first exon and first intron junction, which will lead to the first intron inclusion into the splicing interfered product, and the first intron inclusion will introduce a premature stop codon. *hgfa* splicing interfered product is verified by RT-PCR using the forward primer from first intron and the reverse primer from the third or fourth exon which can avoid amplify the genome DNA and sequencing results showed that the splicing products is just as predicted (data not show). And the endogenous *hgfa* mRNA level is verified by qRT-PCR using the forward primer from first exon and the reverse primer from the second exon, which can avoid amplify the hgfa splicing interfered product due to the large 5000bp first intron size. Results showed that endogenous *hgfa* mRNA level was lower in morphants with curved trunk, ISV growth delay compared to morphants without phenotype. However this lower level of *hgf*a mRNA can not been determined for the morphants with liver shifting phenotype (Fig.3.23). And the knockdown product can be detected (Fig.3.24). However, in WT (24hpf and 36hpf) this knockdown product can still be detected (Fig.3.24).

A

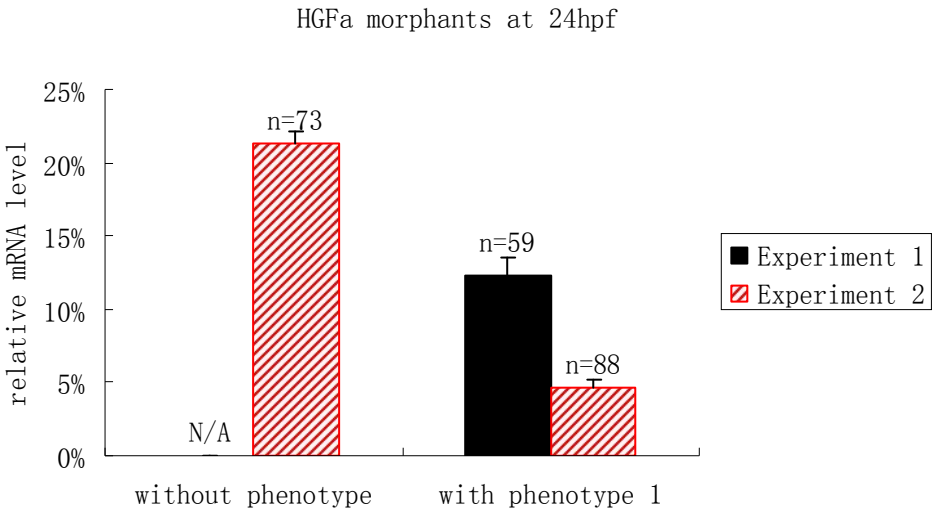
HGFa morphants at 24hpf
relative mRNA level
25%
20%
15%
10%
5%
0%
n=73
n=59
n=88
N/A
without phenotype
with phenotype 1
Experiment 1
Experiment 2

B

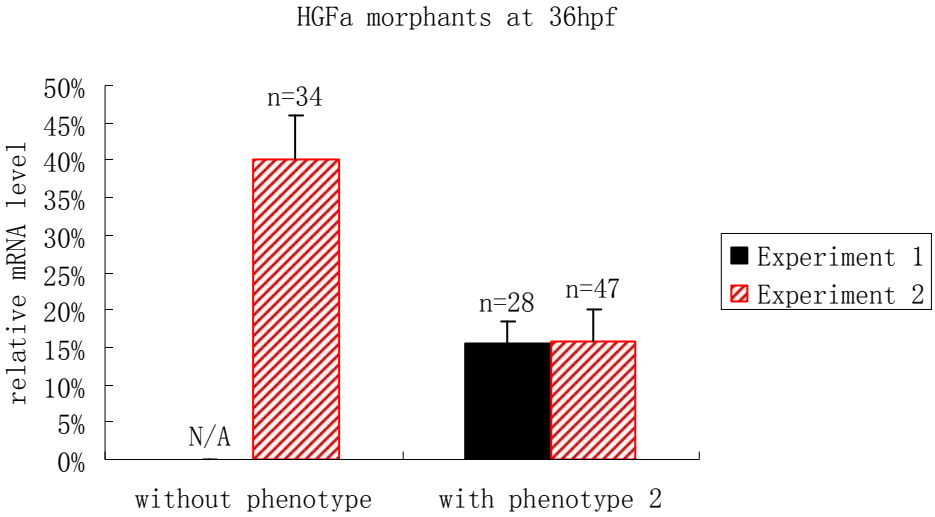
HGFa morphants at 36hpf
relative mRNA level
50%
45%
40%
35%
30%
25%
20%
15%
10%
5%
0%
n=34
n=28
n=47
N/A
without phenotype
with phenotype 2
Experiment 1
Experiment 2

C

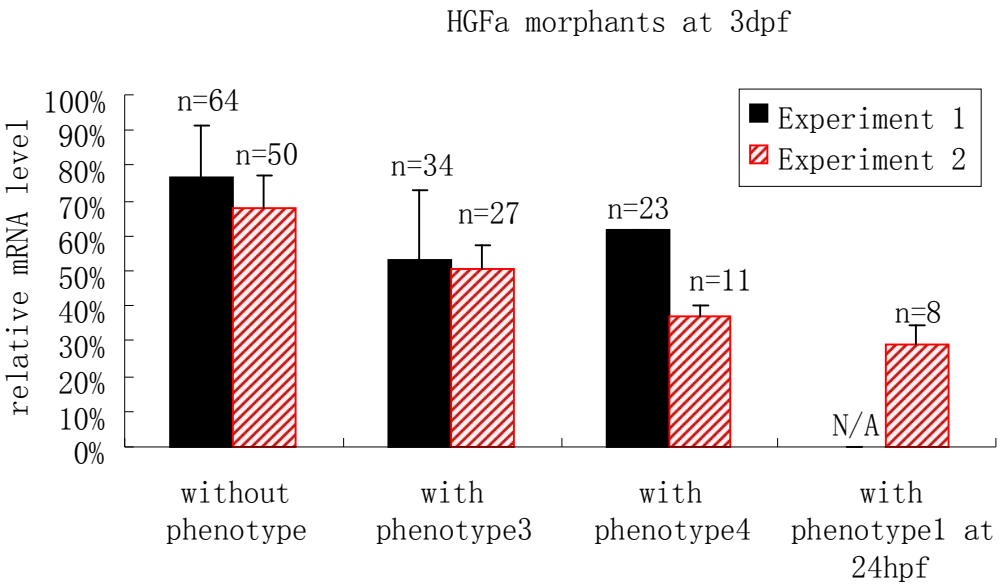

Phenotype 1: curved trunk
Phenotype 2: ISV growth delay
Phenotype 3: curved trunk with liver on left side
Phenotype 4: curved trunk with liver on right side

Fig.3.23 Relative mRNA levels of zebrafish *hgfa* in *hgfa* morphants compared to WT embryo. A, B and C are knockdown level in *hgfa* morphants at 24hpf, 36hpf and 3dpf respectively.

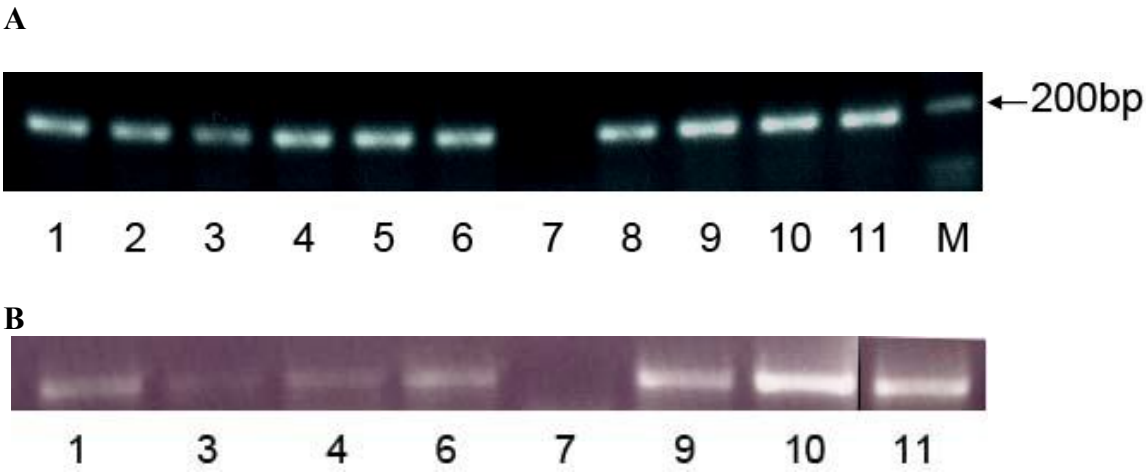

Fig.3.24 Detection of knockdown product of HGFa-ex1 MO in *hgfa* morphants and WT embryos. RNA template for each lane are: 1. 24hpf wt; 2. 24hpf *hgfa* morphants without phenotype; 3. 24hpf *hgfa* morphants with curved trunk; 4. 36hpf wt; 5. 36hpf *hgfa* morphants without phenotype; 6. 36hpf *hgfa* morphants showing ISV growth delay; 7. 3dpf wt; 8. 3dpf *hgfa* morphants showing curved trunk at 24hpf; 9. 3dpf *hgfa* morphants without phenotype; 10. 3dpf *hgfa* morphants showing curved trunk with liver on left side; 11. 3dpf *hgfa* morphants showing curved trunk with liver on right side; M: Marker. (A): Primers are A Splice Sense and A Splice Antisense. (B): Primers are A RT Sense and A RT Antisense.

3.3.1.2 *hgfa* is required for zebrafish somitogenesis

hgfa expression in somites and the curved trunk phenotype in *hgfa* morphants indicate that *hgfa* might play a role in somitogenesis. Expression of *myoD*, a marker for myocytes which represents the terminal differentiation of somites, was analyzed in the *hgfa* morphants at the 9-somite stage.

Wild-type (WT) embryos expressed *myoD* in the adaxial cells and in the posterior halves of the somites (Fig. 3.20.A). Analysis of *hgfa* morphants revealed four phenotypes that were not observed in the control WT embryos. The four phenotypes were

1) Reduced *myoD* expression in the somites (Fig.3.25.B);

2) *myoD* expression in the somites on the left side only (Fig.3.25.C);

3) *myoD* expression in the somites on the right side only (Fig.3.25.D); and

4) No expression of *myoD* in the somites (Fig.3.25.E).

The most significant observation was the reduction in *myoD* expression in the somites, as it accounted for 38% of the *hgfa* morphants (Fig.3.26).

By testing HGFa-ATG MO at two injection concentrations (10ng and 1ng per embryo), HGFa-ATG Morphant's phenotype is dosage dependent (Fig.3.26). However, HGFa-ATG5mis Morphant (10ng per embryo) as control can still generate the similar phenotype as HGFa-ATG Morphant, at a lower percentage compared to HGFa-ATG Morphants (10ng or 1ng per embryo). The possibility is that the HGFa-ATG5mis MO can still bind to *hgfa* mRNA start codon region with a lower affinity compared to HGFa-ATG MO, and can generate moderate knockdown effect. Further

diluted injection of HGFa-ATG5mis should be tested.

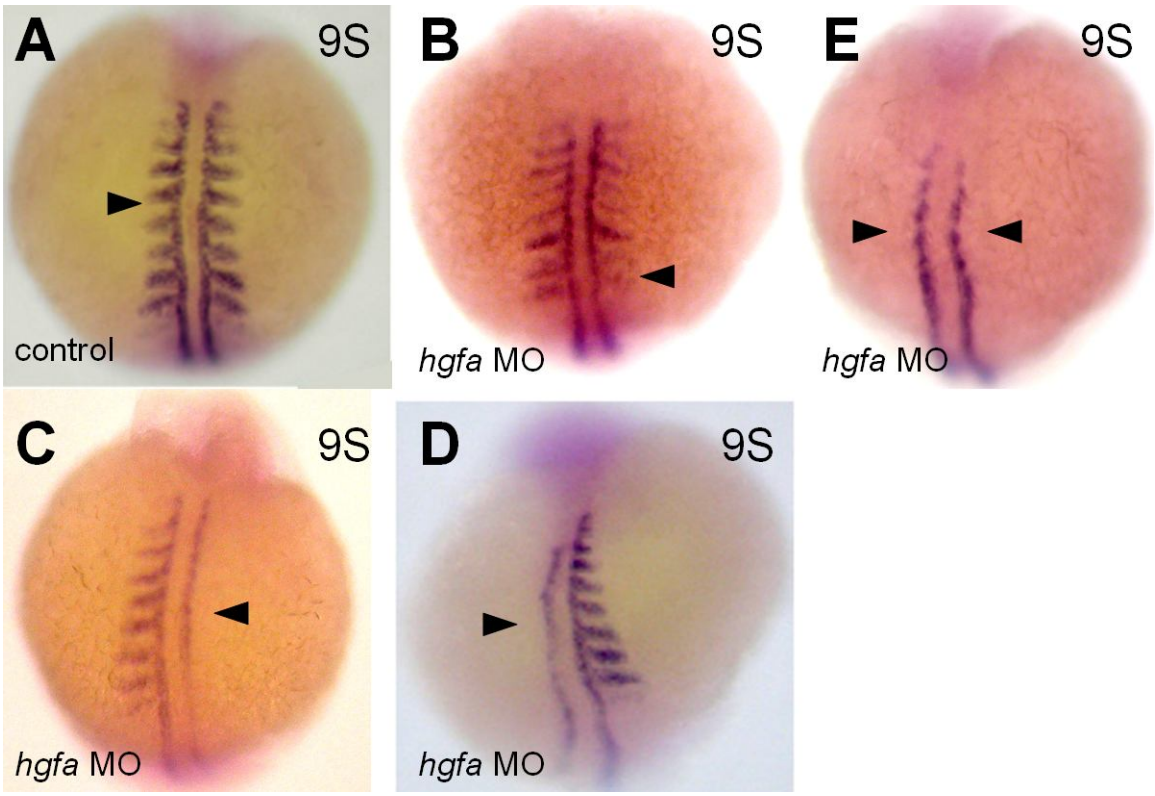

Fig.3.25 Zebrafish *hgfa* knockdown disrupts *myoD* expression pattern. Embryos are dorsal view with anterior to the top. (A) control-injected embryo at 9 somites stage. The black arrowhead points to the normal myoD staining in somites. (B) *hgfa* knockdown morphant at 9 somites stage. The black arrowhead points to the reduced MyoD expression in somites. (C) *hgfa* knockdown morphant at 9 somites stage. The black arrowhead points to the ablation of MyoD expression in the right side somites. (D) *hgfa* knockdown morphant at 9 somites stage. The black arrowhead points to the ablation of MyoD expression in the left side somites. (E) *hgfa* knockdown morphant at 9 somites stage. The black arrowhead points to the ablation of MyoD expression in somites on both sides.

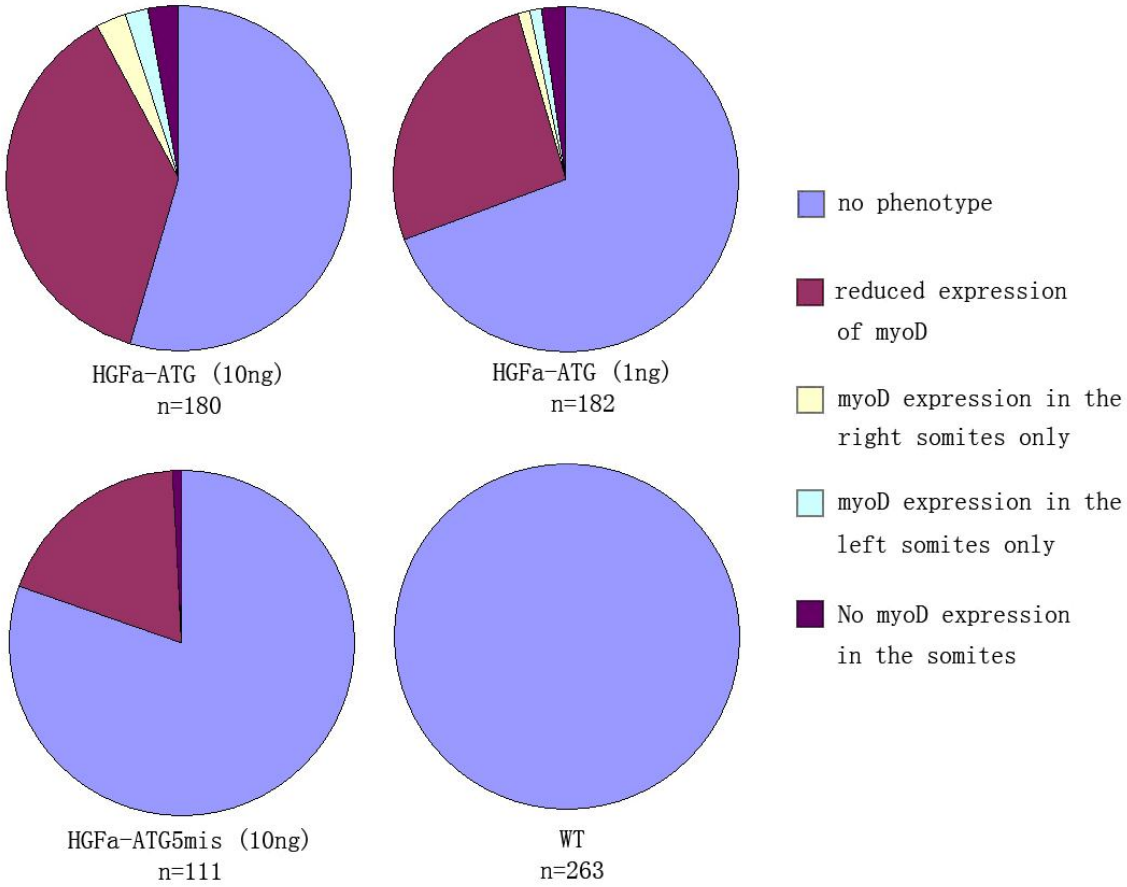

Fig.3.26 Phenotypes observed in *hgfa* morphants at 9-somite stage, with *myoD* as marker.

Since *myoD* expression is disrupted in *hgfa* morphants and *fgf8* signalling is required for *myoD* expression in the somites (Groves et al., 2005), *fgf8* expression was analyzed in *hgfa* morphants to investigate the possibility that knocking down *hgfa* might affect the *myoD* expression through *fgf8*. Therefore, fgf8 expression was analyzed in *hgfa* morphants (HGFa-ATG MO). At the 8-somite stage, WT embryos expressed *fgf8* in each of the newly formed somite and presomitic mesoderm (PSM) (Fig.3.27.A). Two abnormal phenotypes were detected in the *hgfa* morphants:

1) Asymmetrical *fgf8* expression in the somites (Fig.3.27.B and C); and

2) Reduced *fgf8* expression in somites and reduced numbers of somites (Fig.3.27.D).

Thus, the knockdown of *hgfa* significantly reduced the expression of *fgf8*, with 45% of the *hgfa* morphants showing a reduction in *fgf8* expression and/or number of somites (Fig.3.28).

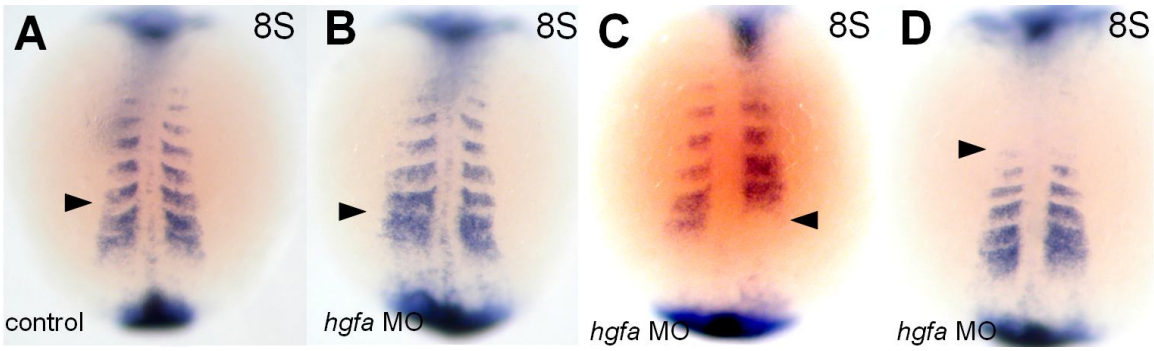

Fig.3.27 Zebrafish *hgfa* knockdown disrupts *fgf8* expression pattern. Embryos are dorsal view with anterior to the top. (A) control-injected embryo at 8 somites stage. The black arrowhead points to the normal *fgf8* staining in somites. (B) *hgfa* morphant at 8 somites stage. The black arrowhead points to the asymmetry *fgf8* expression in somites, the expression region of *fgf8* is wider on the left side of embryo. (C) *hgfa* morphant at 8 somites stage. The black arrowhead points to the asymmetry *fgf8* expression in somites, the expression region of *fgf8* is different at the axial level between left and right side of embryo. (D) *hgfa* morphant at 8 somites stage. The black arrowhead points to the reduced expression of *fgf8* expression in the somites.

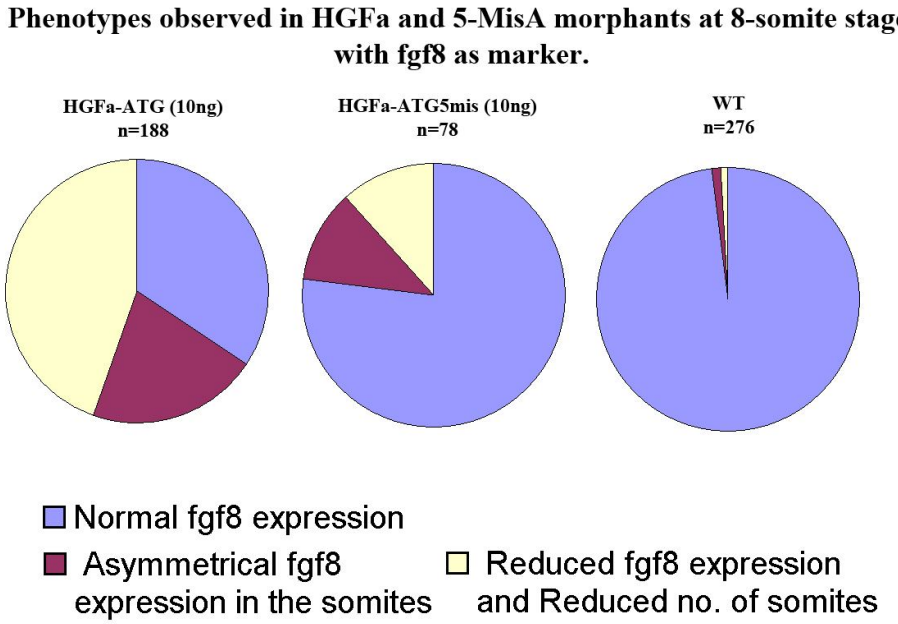

Fig.3.28 Phenotypes observed in HGFa-ATG and HGFa-ATG5mis morphants at 8-somite stage, with *fgf8* as marker.

Since *fgf8* and *myoD* expression pattern is disrupted in *hgfa* morphants, and the expression of *fgf8* and *myoD* in the somites and/or presomitic mesoderm (PSM) are regulated by RA (retinoic acid) (Hamade et al., 2006), the expression of a key enzyme in RA synthesis- *aldehyde dehydrogenase 1 A2* (*aldh1a2*, previous name: *raldh2*) was analyzed in *hgfa* morphants.

At the 12-somite stage, WT embryos expressed *aldh1a2* in each somite and the presomitic mesoderm (PSM) (Fig.3.29.A). Two phenotypes that were not observed in the WT embryos were detected in the *hgfa* morphants and the appearance of these phenotypes is dose-dependent (Fig.3.30). The two phenotypes were:

1) Reduced expression of *aldh1a2* in somites (Fig.3.29.C); and

2) Asymmetry expression of *aldh1a2* in somites (Fig.3.29.D and E).

Thus, the knockdown of *hgfa* disrupted the expression of *aldh1a2*, with 18% of the *hgfa* morphants showing a reduction in *aldh1a2* expression and/or number of somites and 20% of the *hgfa* morphants showing asymmetry expression of *aldh1a2* (Fig.3.30).

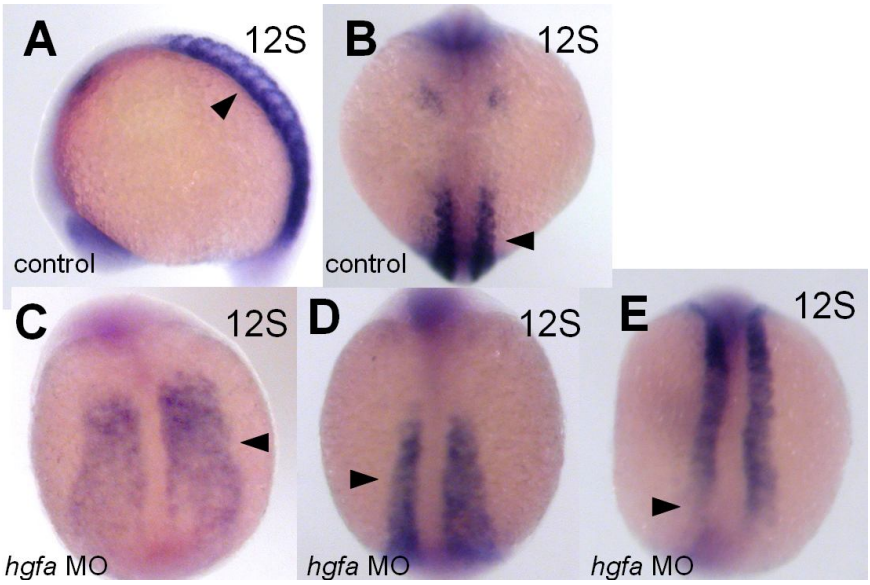

Fig.3.29 Zebrafish *hgfa* knockdown disrupts *aldh1a2* expression pattern. Embryos are dorsal view with anterior to the top, except in A, which is lateral view with anterior to the left. (A) control-injected embryo at 12 somites stage (lateral view). The black arrowhead points to the normal aldh staining in somites. (B) control-injected embryo at 12 somites stage. The black arrowhead points to the normal aldh1a2 staining in somites. (c) *hgfa* morphant at 12 somites stage. The black arrowhead points to the widened aldh1a2 expression in somites with reduced expression level. (D) *hgfa* morphant at 12 somites stage. The black arrowhead points to the asymmetry *aldh1a2* expression in somites, the expression region of aldh1a2 is wider on the right side of embryo. (E) *hgfa* morphant at 12 somites stage. The black arrowhead points to the asymmetry *aldh1a2* expression in somites, the expression region of aldh1a2 is different at the axial level between left and right side of embryo.

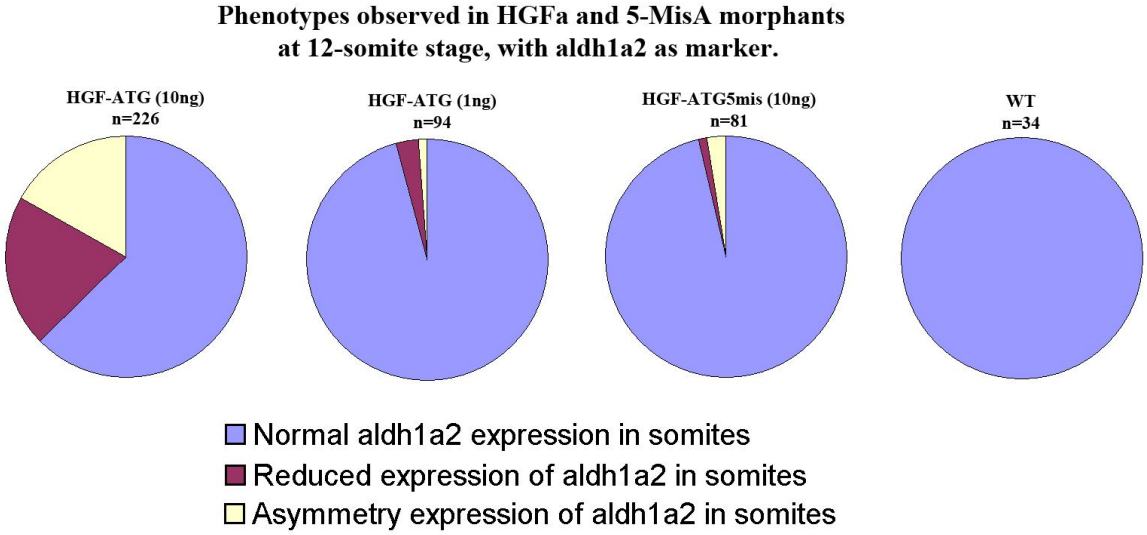

Fig.3.30 Phenotypes observed in HGFa-ATG and HGFa-ATG5mis morphants at 12-somite stage, with *aldh1a2* as marker.

3.3.1.3 *hgfa* is involved in blood vessel development

Angiogenic property of HGF has been evidenced by many studies in vivo (Grant et al., 1993;Kuba et al., 2000;Lamszus et al., 1997;Nagashima et al., 2001). However, HGF's impact on embryonic angiogenesis is not clear yet. Here, we take the advantage of *Tg(fli1:GFP)*, which illuminate the blood vessel with green fluorescence, to study if *hgfa* or *hgfb* has any roles in blood vessel development. In this transgenic line, GFP expression was under the control of the endothelial cell specific fli-1 gene promoter (Lawson and Weinstein, 2002). Two types of MO were used in this analysis. One targets at the start codon region to inhibit translation, named as HGFa-ATG MO. Another MO is designed against the splice-donor sites of exon 1 to interfere with mRNA splicing which is named as HGFa-ex1 MO. Both HGFa-ATG and HGFa-ex1 MO can cause delay in intersegmental vessel (ISV) and dorsal longitudinal anastomotic vessel (DLAV) growth (Fig.3.31). In HGFa-ex1 morphants, 58% (n=81) shows ISV and DLAV growth delay and embryos were separated into different pools based on the blood vessel phenotype. *hgfa* mRNA level of each pool was examined by qRT-PCR and the result showed that *hgfa* mRNA knockdown is more effective in the pool with delayed ISV growth (Fig 3.23).

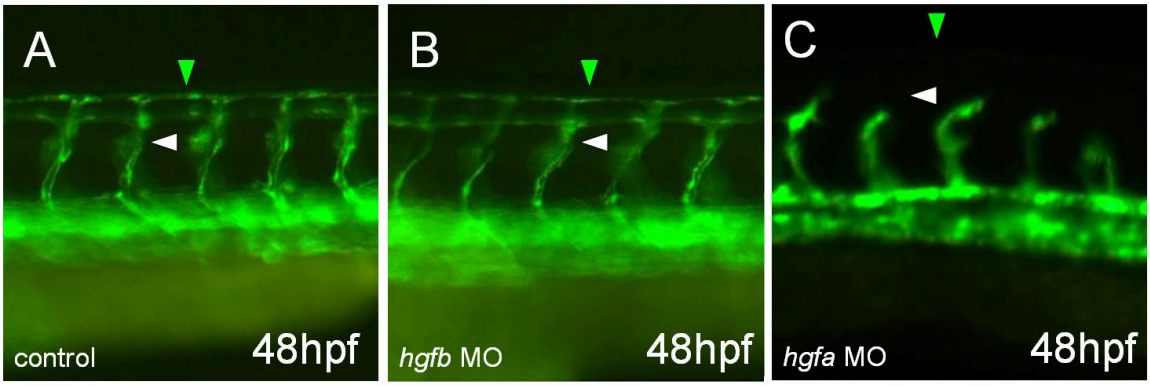

Fig.3.31 Zebrafish *hgfa* knockdown causes growth delay of ISV and DLAV. Embryos are lateral view with anterior to the left. (A) control-injected embryo at 48dpf. The white arrowhead points to the normal ISV. The green arrowhead points to the normal DLAV. (B) *HGFb* knockdown morphant at 48hpf. The green arrowhead points to the normal DLAV. (C) *hgfa* knockdown morphant at 48hpf. The white arrowhead points to the ISV which stops sprouting at midway for more than 10 hours. The green arrowhead points to the missing DLAV.

3.3.1.4 *hgfa* is involved in the asymmetric positioning of liver during zebrafish development

Since HGF is a known mitogen for hepatocytes in mammals, we investigated if *hgfa* play a role in zebrafish liver formation. Two types of MO were used in this analysis. One targets at the start codon region to inhibit translation, named as HGFa-ATG MO. Another MO is designed against the splice-donor sites of exon 1 to interfere with mRNA splicing which is named as HGFa-ex1 MO. Both HGFa-ATG and HGFa-ex1 MO lead to the shift of liver from left side to right side of the embryo (Fig.3.32). For HGFa-ATG MO, this phenotype is dosage dependent (Fig.3.33). For HGFa-ex1 MO, embryos were separated into different pools based on the phenotype. *hgfa* mRNA level of each pool was examined by qRT-PCR. There is no relationship between the knockdown level and this phenotype (Fig.3.39). However, there is a correlation of the curved trunk phenotype with the liver position switching phenotype which proves the specificity of the MO knockdown effect. Otherwise, the specificity of the MO knockdown would be doubted with the question that why one MO can generate two phenotypes are not correlated. More embryos in the curved-trunk pool (45%) which have this phenotype compared to the non-curved trunk pool (10%) (Fig.3.34). *hgfb* is much less effective in this function. At 1ng per embryo MO dose, only *hgfa* MO generated a shift in liver position. These results indicate a role of *hgfa*, but not *hgfb* in determining the asymmetric positioning of liver to the left side of the embryo in zebrafish.

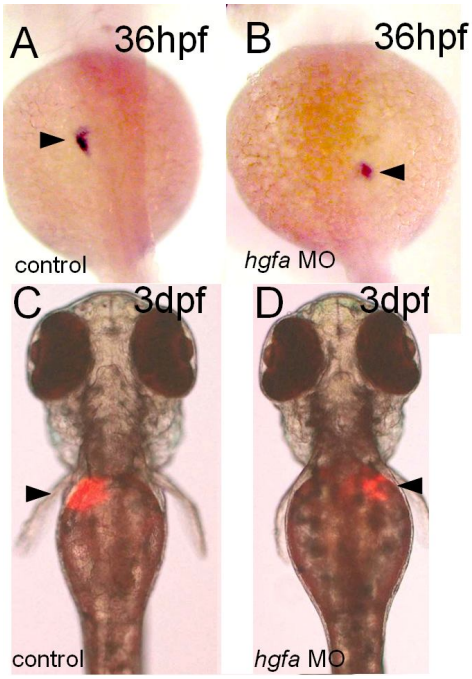

Fig.3.32 Zebrafish *hgfa* knockdown causes liver shifting from left side to right side. A and B are embryos stained with ceruloplasmin, a liver maker. In A and B, pictures are taken by stereo microscope and embryos are dorsal view with anterior to the top. C and D are *lfabp:RFP* embryos, which show liver with red florescence. In C and D, pictures are taken by inverted microscope and embryos are ventral view with anterior to the top. (A) control-injected embryo at 36hpf. The black arrowhead points to the normal liver position which is on the left side of the embryo. (B) *hgfa* knockdown morphant at 36hpf. The black arrowhead points to the shifted liver position which is on the right side of the embryo. (C) control-injected embryo at 3dpf. The black arrowhead points to the normal liver position which is on the left side of the embryo. (D) *hgfa* knockdown morphant at 3dpf. The black arrowhead points to the shifted liver position which is on the right side of the embryo.

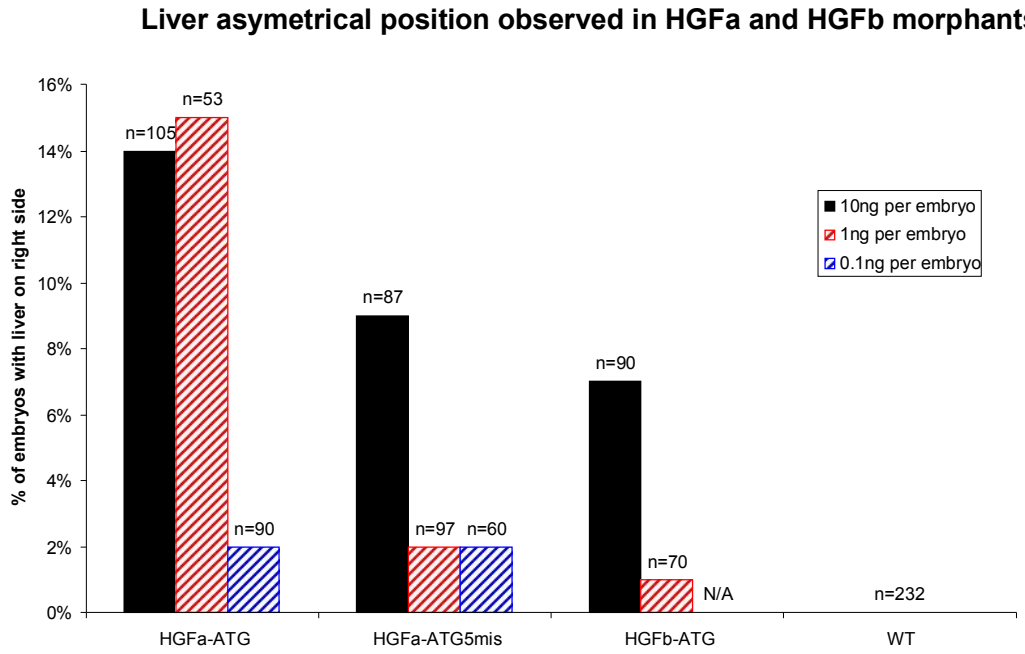

Fig.3.33 Liver asymmetrical position observed in *hgfa* and *hgfb* morphants. With HGFb-ATG and HGFa-ATG5mis MO as control and the different dose of injection, this effect is proved to be dose-dependent and specific.

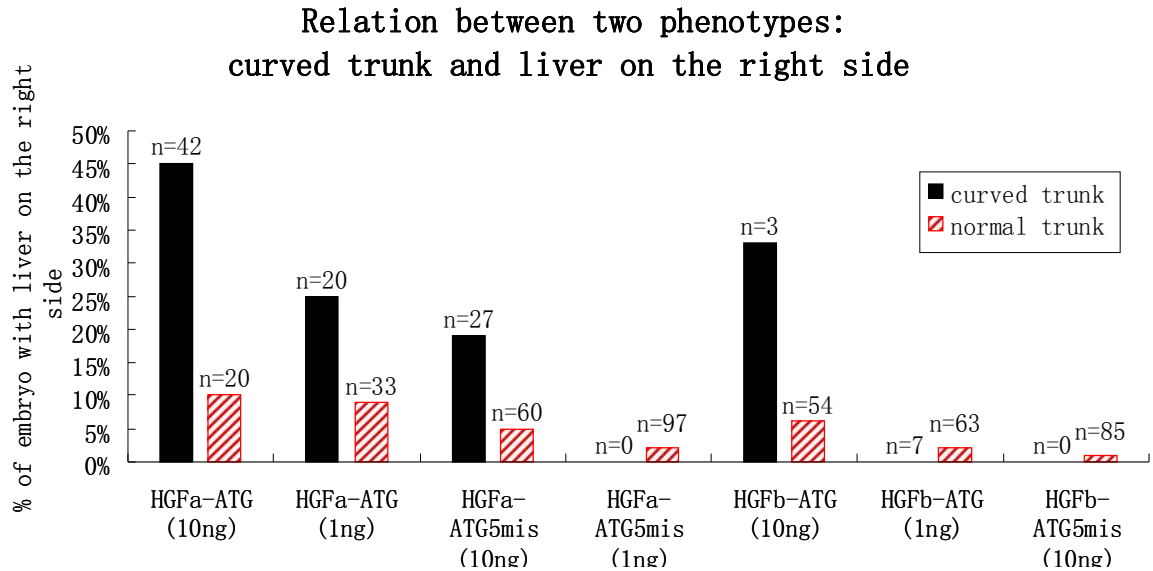

Fig.3.34 Relation between two phenotypes in *hgfa* or *hgfb* morphants: curved trunk and liver on the right side.

3.3.1.5 Pancreas position is shifted from right side to left side in *hgfa* morphants

Pancreas and liver share a same pool of progenitor cells (Ward et al., 2007), and pancreas is located on the right side which is opposite to liver's position. Since liver position was shown to be shifted from left side to right side in *hgfa* morphants, pancreas was examined in *hgfa* morphants. HGFa-ATG MO was used in this analysis and the result showed pancreas position is shifted from right side to left side in *hgfa* morphants in a dose-dependent manner (Fig.3.35 and Fig.3.36). The position of both endocrine pancreas and exocrine pancreas are shifted to the left in *hgfa* morphants as shown by the expression of insulin and elastase B (*elaB*) respectively (Fig. 3.35 and 3.36).

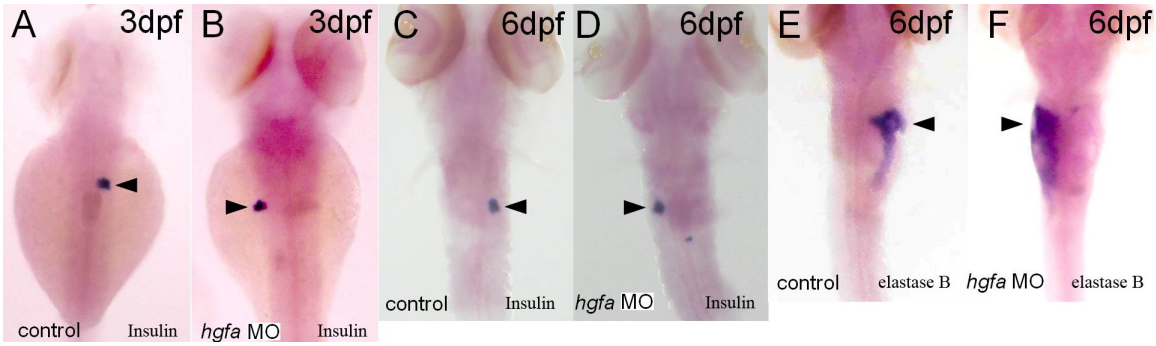

.

Fig.3.35 Zebrafish *hgfa* knockdown causes pancreas shifting from right side to left side. Embryos are dorsal view with anterior to the top. A-D are embryos stained with insulin, an endocrine pancreas maker. E and F are embryos stained with elastase B, an exocrine pancreas marker. (A) control-injected embryo at 3dpf. The black arrowhead points to the normal endocrine pancreas position which is on the right side of the embryo. (B) *hgfa* morphant at 3dpf. The black arrowhead points to the shifted endocrine pancreas position which is on the left side of the embryo. (C) control-injected embryo at 6dpf. The black arrowhead points to the normal endocrine pancreas position which is on the right side of the embryo. (D) *hgfa* morphant at 6dpf. The black arrowhead points to the shifted endocrine pancreas position which is on the left side of the embryo. (E) control-injected embryo at 6dpf. The black arrowhead points to the normal exocrine pancreas position which is on the right side of the

embryo. (F) *hgfa* morphant at 6dpf. The black arrowhead points to the shifted exocrine pancreas position which is on the left side of the embryo.

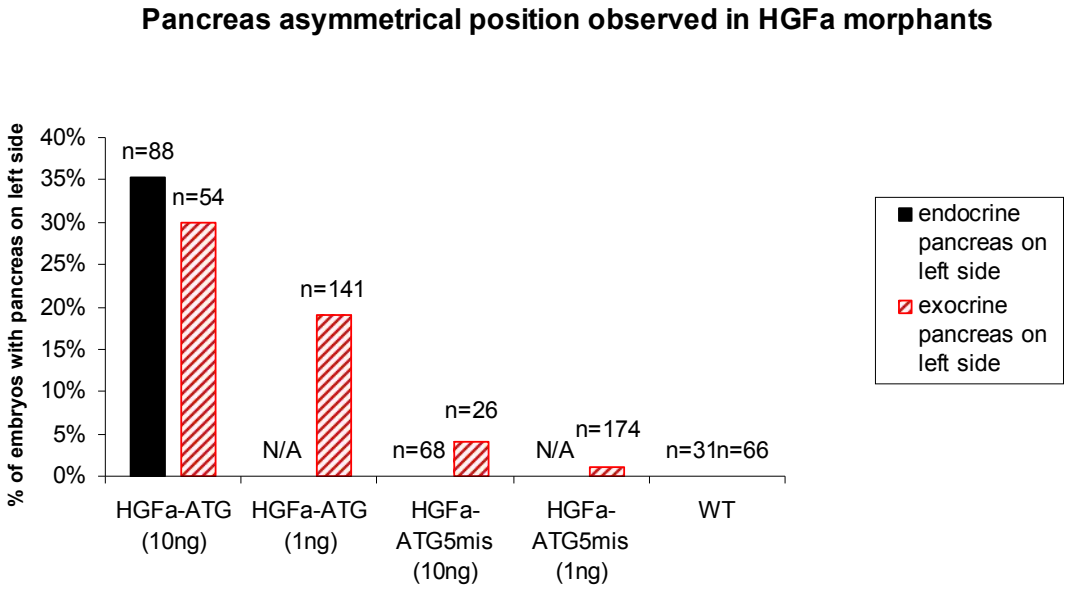

Fig.3.36 Pancreas shifting observed in *hgfa* morphants, with *insulin* or *elastaseB* as marker.

3.3.1.6 Simultaneous position shift of liver and pancreas in *hgfa* morphants

To determine if liver and pancreas were shifted simultaneous in *hgfa* morphants, double in-situ hybridization of liver marker *Cp* and exocrine pancreas marker *elaB* were carried out. Result showed that in the *hgfa* morphants, liver and pancreas were shifted simultaneously to the opposite side of the embryo (Fig.3.37). All together, the above results indicate that *hgfa* is involved in the asymmetrical positioning of liver and pancreas in zebrafish embryo.

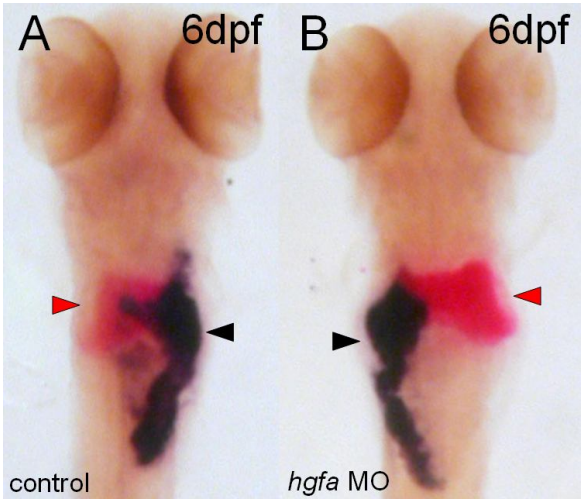

Fig.3.37 Zebrafish *hgfa* knockdown causes liver and pancreas shifting simultaneously within single embryo. Embryos are dorsal view with anterior to the top and stained with elastase B in black, ceruloplasmin in red. (A) control-injected embryo at 6dpf. The black arrowhead points to the normal exocrine pancreas position which is on the right side of the embryo. The red arrowhead points to the normal liver position which is dominantly on the left side of the embryo. (B) *hgfa* morphant at 6dpf. The black arrowhead points to the shifted exocrine pancreas position which is on the left side of the embryo. The red arrowhead points to the shifted liver position which is dominantly on the right side of the embryo.

3.3.2 Liver development is disrupted in *hgfb* morphants

Based on the expression of *hgfb* in liver, its role in liver development was predicted. Loss of function study by MO knockdown was carried out, and *Tg(lfabp:RFP)* was used as an indicator for liver development. At 3dpf, liver formed normally in control and the *hgfb* morphants (Fig.3.38.A and B). However, obvious differences between control embryos and the *hgfb* morphants were discernable subsequently with liver in a much smaller size from 4dpf to 6dpf (Fig.3.38 D, G and J). Some of the morphants with the smaller liver phenotype was accompanied with a heart edema (Fig.3.38.E, H and K). In HGFb-ex2, HGFb-ex3 or HGFb-ex2+HGFb-ex3 morphants, the smaller liver phenotype is dose-dependent (Fig.39). It seems that *hgfb* is required for the growth phase of liver development, possibly by promoting hepatocyte proliferation.

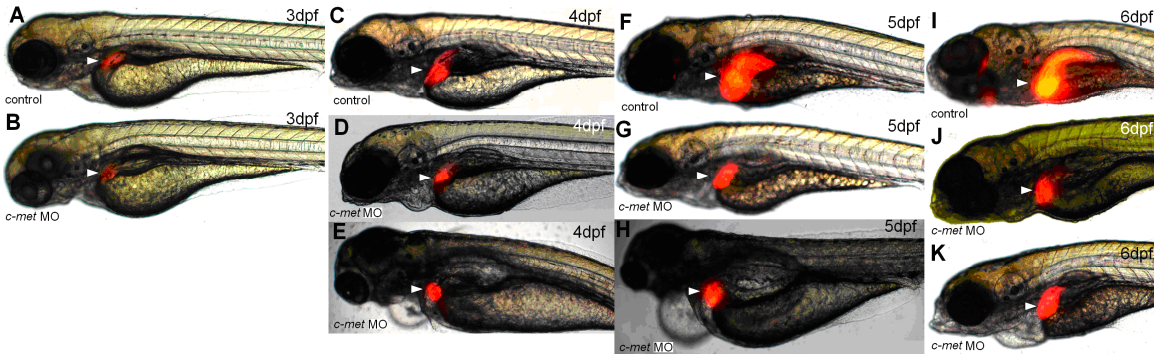

Fig.3.38 Zebrafish *hgfb* knockdown causes liver growth defect. Embryos are lateral view with anterior to the left. White arrowhead in all the figures points to liver. (A) control-injected embryo at 3dpf. (B) *hgfb* morphant at 3hpf. (C) control-injected embryo at 4dpf. (D) *hgfb* morphant at 4hpf. (E) *hgfb* morphant at 4hpf with heart edema. (F) control-injected embryo at 5dpf. (G) *hgfb* morphant at 5hpf. (H) *hgfb* at 5hpf with heart edema. (I) control-injected embryo at 6dpf. (J) *hgfb* morphant at 6hpf. (K) *hgfb* morphant at 6hpf with heart edema.

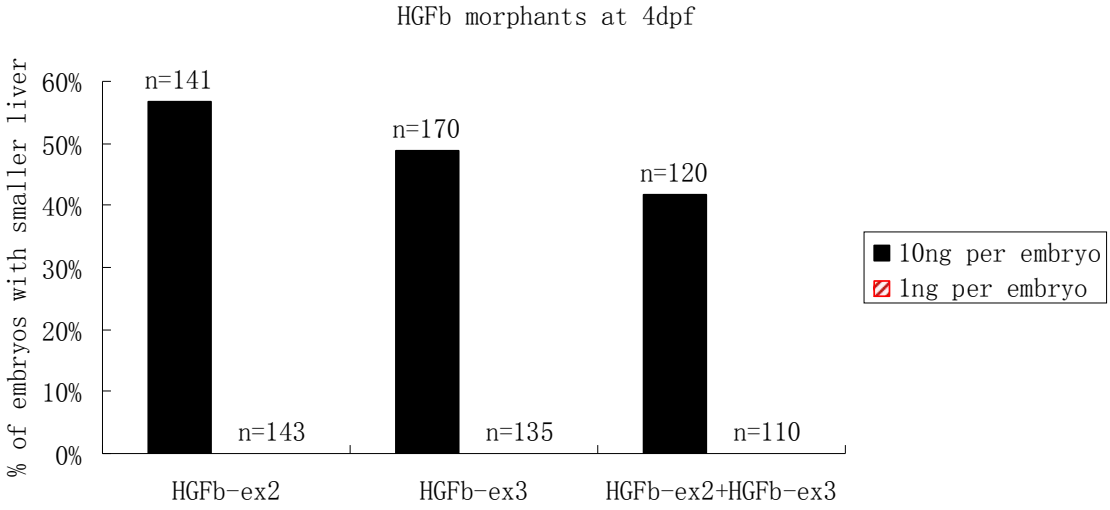

Fig.3.39 Smaller liver size in *hgfb* morphants was revealed by *Tg(lfabp: RFP)* transgenic zebrafish.

Confirmation of knockdown effect of HGFb MO

HGFb-ex1 MO is against the first exon and first intron junction, which will lead to the first intron inclusion into the splicing interfered product, and the first intron inclusion will introduce a premature stop codon. *hgfb* splicing interfered product is verified by RT-PCR using the forward primer from first intron and the reverse primer from the third exon, which can avoid amplify the *hgfb* splicing interfered product due to that the first intron size is above 5000bp. And the endogenous *hgfb* mRNA level is verified by qRT-PCR using the forward primer from first exon and the reverse primer from the second exon.

For the endogenous *hgfb* mRNA, an unexpected increase was detected in the HGFb-ex1 morphants (Fig.3.40) though the splicing interfered product is detectable (Fig.3.41). Hence, another set of MOs blocking pre-mRNA splicing, HGFb-ex2 and HGF-ex3, was designed. HGFb-ex2, which is against the second exon and second intron junction, will lead to the second exon deletion; HGFb-ex3, which is against the third exon and third intron junction, will lead to third exon deletion. And co-injection of these two MOs would lead to the exon2 and exon3 deletion. Splicing interfered products of HGFb-ex2 and/or HGFb-ex3 are verified by RT-PCR using the primers flanking the exon2 and exon3. And the endogenous *hgfb* mRNA level in HGFb-ex2 morphant is verified by qRT-PCR using the forward primer from the second exon and the reverse primer from the fourth exon; the endogenous *hgfb* mRNA level in HGFb-ex3 morphant is verified by qRT-PCR using the forward primer from the third exon and the reverse primer from the fourth exon; the endogenous *hgfb* mRNA level in HGF-ex2 and HGF-ex3 co-injected morphant is verified by qRT-PCR using forward primer from second exon and third exon junction and the reverse primer from the

fourth exon. Results showed that endogenous *hgfb* mRNA level is lower in the pools with phenotype and this difference is more distinguishable in the HGFb-ex2 and HGFb-ex3 co-injected morphants (Fig.3.42).

In the detection of knockdown product of HGFb-ex2 and/or HGFb-ex3, totally six different bands are detected according to size (Fig.3.43). After sequencing, band 1 is matching the WT *hgfb* sequence; band 3 and band 4 are matching the *hgfb* exon2 or exon3 deletion sequence respectively; band 6 is matching the *hgfb* exon2 and exon3 deletion sequence; band 2 is matching the *hgfb* exon2 partial deletion sequence which is due to a cryptic splicing site (AGGA) within exon2; band 5 is matching the *hgfb* exon2 partial deletion and exon3 deletion sequence.

Splicing interfered products of band 2, band 3 and band 4 will cause the reading frame shifting and introduce a premature stop codon. Splicing interfered products of band 5 and band 6 will cause the deletion of hairpin loop domain which is an essential site for heparin binding and biological activity of HGF (Mizuno et al., 1994).

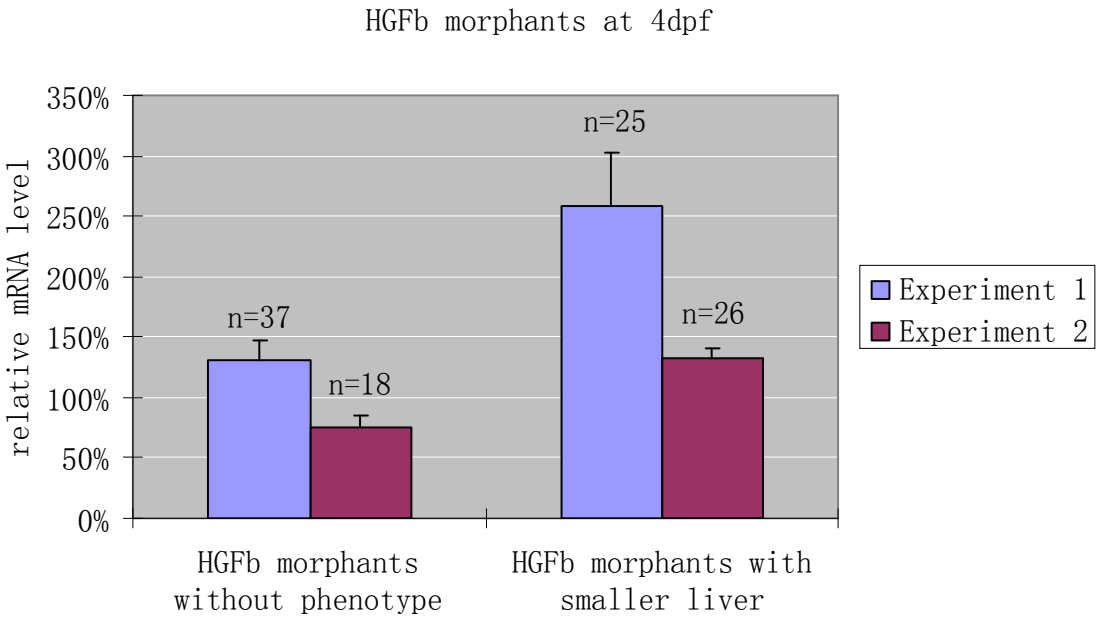

Fig.3.40 Relative mRNA levels of zebrafish *hgfb* in HGFb-ex1 morphants compared to WT embryo.

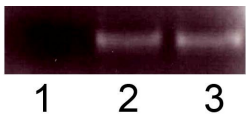

Fig.3.41 Detection of knockdown product of HGFb-ex1 in *hgfb* morphants and WT embryos. RNA template for each lane are: 1. 4dpf wt; 2. 4dpf HGFb-ex1 morphants without phenotype; 3. 4dpf HGFb-ex1 morphants with smaller liver. Primers are B Splice Sense and B Splice Antisense.

A

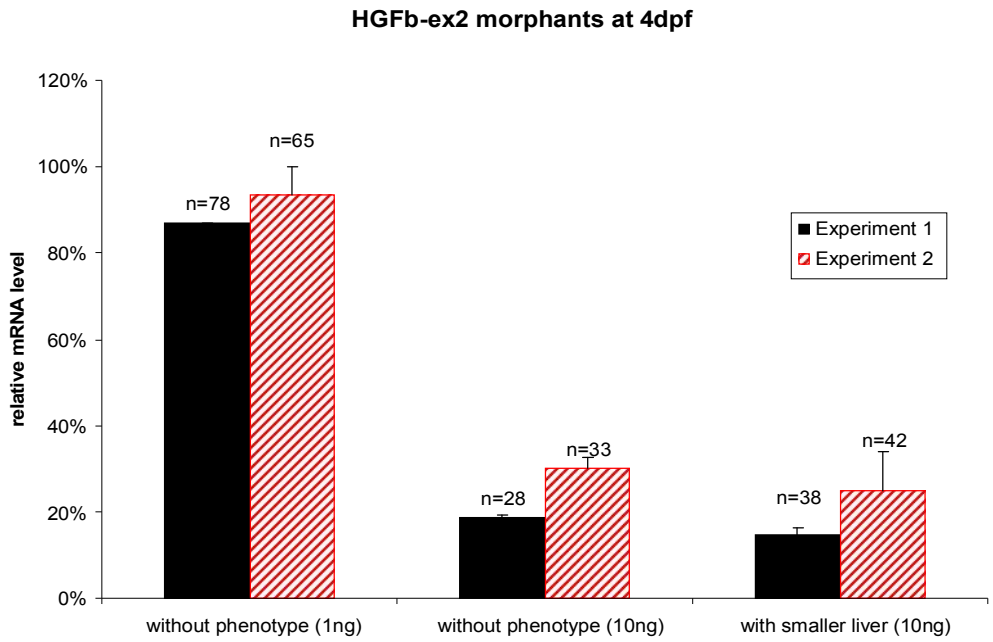
HGFb-ex2 morphants at 4dpf
relative mRNA level
120%
100%
80%
60%
40%
20%
0%
n=78
n=65
n=28
n=33
n=38
n=42
Experiment 1
Experiment 2
without phenotype (1ng)
without phenotype (10ng)
with smaller liver (10ng)

B

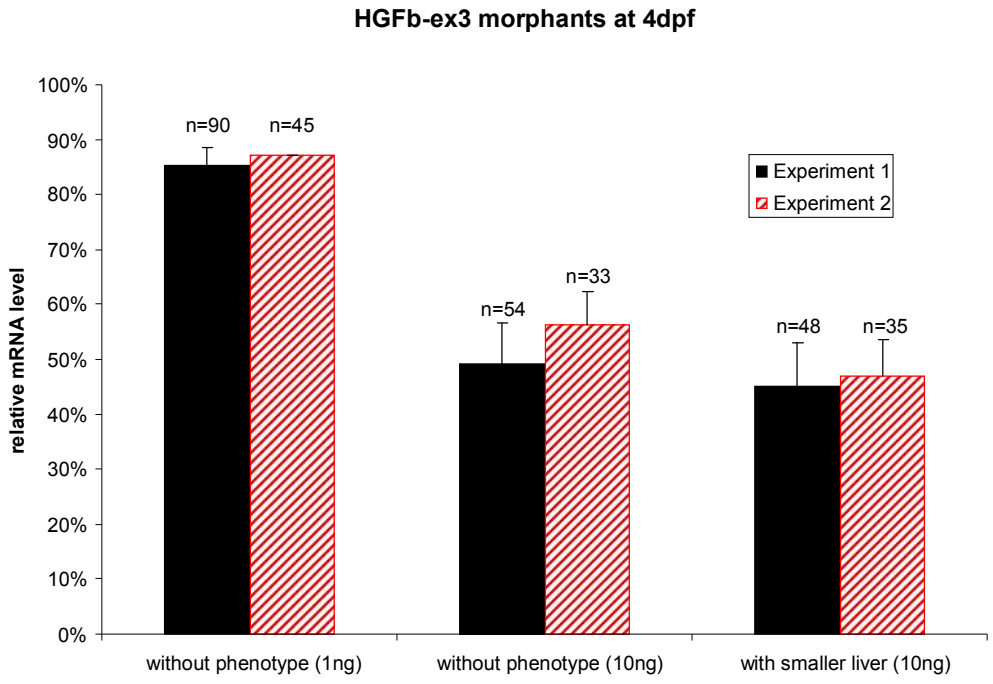
HGFb-ex3 morphants at 4dpf
relative mRNA level
100%
90%
80%
70%
60%
50%
40%
30%
20%
10%
0%
n=90
n=45
n=54
n=33
n=48
n=35
Experiment 1
Experiment 2
without phenotype (1ng)
without phenotype (10ng)
with smaller liver (10ng)

C

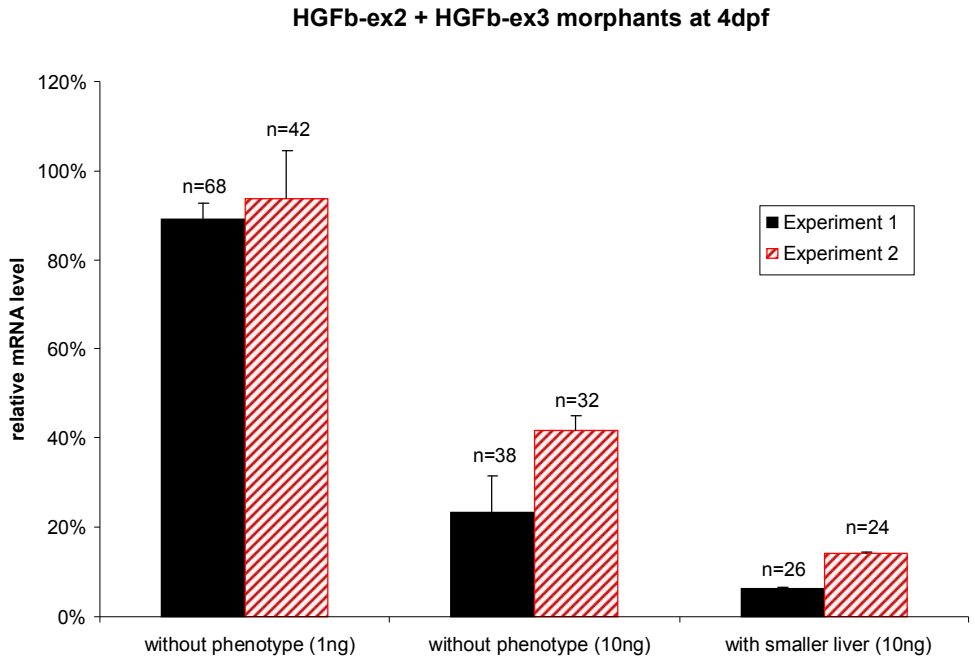

Fig.3.42 Relative mRNA levels of zebrafish *hgfb* in HGFb-ex2 and/or HGFb-ex3 morphants compared to WT embryo. A is the HGFb-ex2 morphants, B is the HGFb-ex3 morphant and C is the HGFb-ex2 and HGFb-ex3 co-injected morphant. Amount of injection and the phenotype of the pools are indicated under the column.

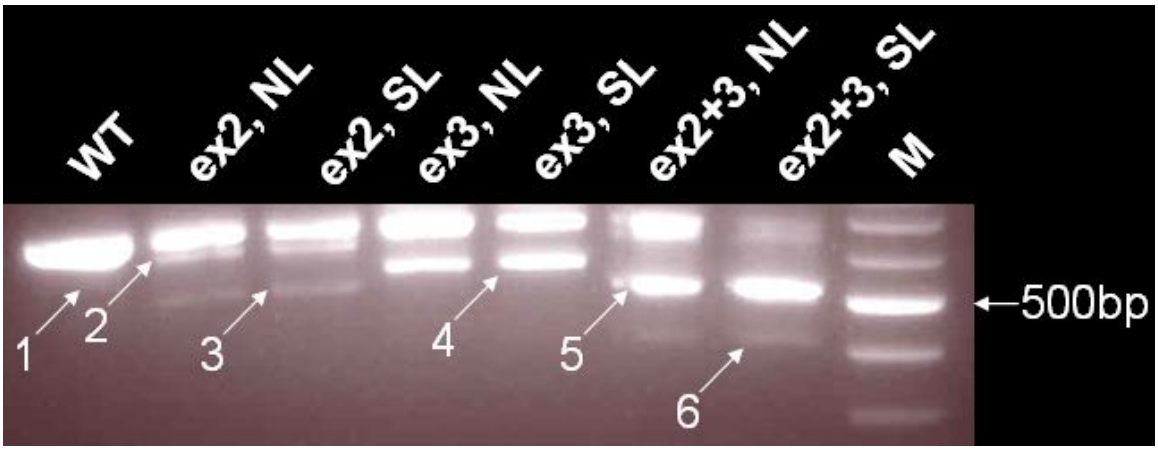

Fig.3.43 Detection of knockdown product of HGFb-ex2 and/or HGFb-ex3 MO in *hgfb* morphants and WT embryos. ex2, HGFb-ex2; ex3, HGFb-ex3; ex2+3, HGFb-ex2 and HGFb-ex3; NL, normal liver; SL, smaller liver; M, marker. 1, WT *hgfb*; 2, *hgfb* exon2 partial deletion; 3, *hgfb* exon2 deletion; 4, *hgfb* exon3 deletion; 5, *hgfb* exon2 partial deletion and exon3 deletion; 6, *hgfb* exon2 and exon3 deletion.

3.3.3. Liver development is disrupted in *c-met* morphants

Based on the expression of *c-met* in liver, its role in liver development was predicted. Loss of function study by MO knockdown was carried out in *Tg(lfabp:RFP)* line. At 3dpf, liver in control and *c-met* morphants formed normally (Fig.3.44.A and B). However, obvious differences between control and *c-met* morphants were discernable subsequently with liver in a much smaller size from 4dpf to 6dpf (Fig.3.44 D, G and J). Some of the morphants with the smaller liver phenotype was accompanied with a heart edema (Fig.3.44.E, H and K). At the dose of 10ng per embryo MO injection, 61% (n=194) of embryos showed smaller liver phenotype at 4dpf, and at a lower dose of 1ng per embryo MO injection, 0% (n=123) of embryos showed smaller liver phenotype at 4dpf. These results indicate a requirement of *c-met* in liver growth. Very likely, *hgfb* functions through *c-met* to promote liver growth.

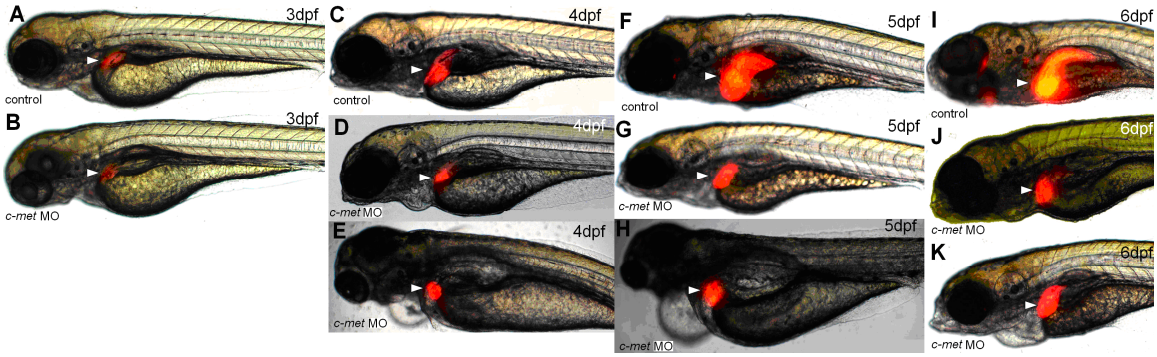

Fig.3.44 Zebrafish *c-met* knockdown causes liver growth defect. Embryos are lateral view with anterior to the left. White arrowhead in all the figures points to liver. (A) control-injected embryo at 3dpf. (B) *c-met* morphant at 3hpf. (C) control-injected embryo at 4dpf. (D) *c-met* morphant at 4hpf. (E) *c-met* morphant at 4hpf with heart edema. (F) control-injected embryo at 5dpf. (G) *c-met* morphant at 5hpf. (H) *c-met* morphant at 5hpf with heart edema. (I) control-injected embryo at 6dpf. (J) *c-met* morphant at 6hpf. (K) *c-met* morphant at 6hpf with heart edema.

Confirmation of knockdown effect of c-Met MO

c-met-ex1 MO is against the first exon and first intron junction, which will lead to the first intron inclusion into the splicing interfered product, and the first intron inclusion will introduce a start codon and a premature stop codon. *c-met* splicing interfered product is verified by RT PCR using the forward primer from first intron and the reverse primer from the third exon and sequencing results showed that the splicing products is just as predicted (data not show). And the endogenous *c-met* mRNA level is verified by qRT-PCR using the forward primer from first exon and the reverse primer from the second exon, which can avoid amplify the *c-met* splicing interfered product due to that the first intron size is above 5000bp. Results showed that endogenous *c-met* mRNA level is lower in the pools with phenotype (Fig.3.45). And the knockdown product can be detected (Fig.3.46).

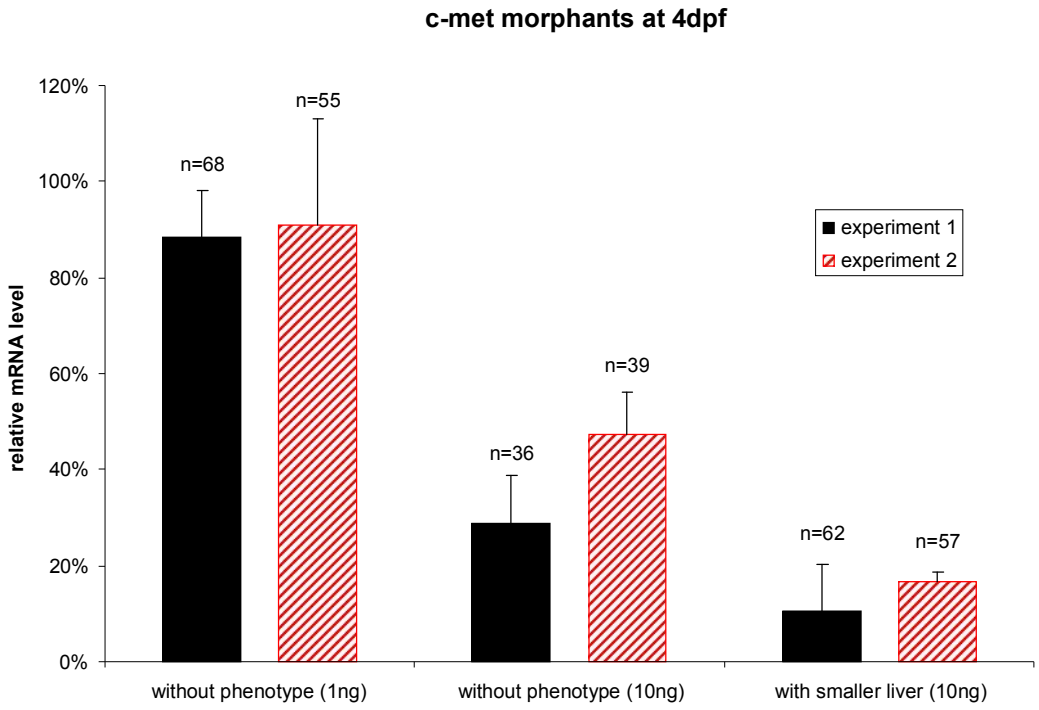

Fig.3.45 Relative mRNA levels of zebrafish *c-met* in c-met-ex1 morphants compared to WT embryo.

Fig.3.46 Detection of knockdown product of c-met-ex1 MO in *c-met* morphants and WT embryos. RNA template for each lane are: 1. 4dpf wt; 2. 4dpf c-met-ex1 morphants without phenotype; 3. 4dpf c-met-ex1 morphants with smaller liver. Primers are C Splice Sense and C Splice Antisense.

Chapter 4. Disscussion

4.1 Zebrafish is a complementary model to study the function of HGF and its receptor in vertebrate development

During the past decades, numerous efforts have been put into the study of HGF and its receptor c-met. The early embryonic lethality of HGF or c-met knock-out mice made the functional study of this ligand/receptor pair in later embryonic and fetal development as well as adult difficult. Use of zebrafish model with the morpholino antisense oligonucleotide knock-down approach makes the study of HGF and c-met at late development stages possible. Additionally, in contrast to other vertebrates, liver is not a site of hematopoiesis in fish embryos, allowing the investigation of hepatic development independently of defects due to anemia. With the small body size, zebrafish embryos receive sufficient amounts of oxygen by simple diffusion allowing the embryo developing relatively normally (Stainier, 2001). To study *hgf* and *c-met* in zebrafish model, full length cDNA of two *hgfs* (*hgfa* and *hgfb*) and one *c-met* were isolated and cloned. Their expression and function during zebrafish embryonic development were analyzed by various experimental tools. Since *hgfa* is expressed in the somites of zebrafish embryo, *hgfa* is hypothesized to have a role in the development of the somites. Hence, the distinctive role of *hgfa* during zebrafish development, in particular, *hgfa*'s function in somitogenesis, was investigated by using MO knockdown method and subsequently visualization of the somites by whole mount in situ hybridization for *myoD*, *fgf8* and *aldh1a2*. Although *hgfa* can not be detected in liver, knocking down of *hgfa* can affect the positioning of liver as well as pancreas. Expression patterns of *hgfb* and *c-met* in liver implied their roles in

zebrafish liver development. Functional analysis using MO knockdown method revealed that knockdown of either *hgfb* or its receptor *c-met* caused reduction in liver size.

4.2 Zebrafish *hgfa* and *hgfb* and *c-met* genes

Most of the zebrafish genome contains duplicated segments that probably result from an genome-wide duplication about 400 million years ago. This duplication occurred in the ray fin fish lineage after it diverged from the lobe fin lineage (that includes avian or mammalian species). For this reason, zebrafish often have two copies of a gene that is present as a single copy in mammals (Postlethwait et al., 2000). In this work, we isolated two zebrafish *hgf* genes, named as *hgfa* and *hgfb*. However, only one *c-met* was found. It is possibly that there is another *c-met* which has not been discovered. Alternatively, the two *hgfs* could share one common receptor and carry out distinct functions in different organs or developmental stages.

Our results support both the hypothesis. From the expression pattern, *hgfa* and *c-met* are co-expressed in fin, *hgfb* and *c-met* are co-expressed in liver. These co-expression of *hgfs* and *c-met* support the hypothesis that the two *hgfs* could share one receptor. HGF and c-met mRNA transcripts was found to co-localize in somite in mice and chicken (Andermarcher et al., 1996; Daston et al., 1996; Thery et al., 1995; Yang et al., 1996). However, only *hgfa* was detected in somite and no *c-met* somitic expression is detected. Haines et al. (Haines et al., 2004) showed earlier that *c-met* expression in somitic is specifically restricted to the ventral lateral margin of anterior somites. However, *c-met*'s expression in nephric duct (Fig.3.19) is not detect in Haines's study. Initially I speculated that Haines's *c-met* expression in somite and this study's *c-met* expression in nephric duct, which are both located at the ventral lateral region of the trunk, may be spatially in vicinity and difficult to differentiate. However, after comparing the sections (Fig.3.19 N) (Haines et al., 2004), Haines's *c-met* ventral

lateral expression is within the somite and my *c-met* ventral lateral expression is not within the somite but within the nephric duct. The possible reason is that the two sections are not at the same axial level. Hence, it is possible that in the anterior part (maybe first two or three somites according to Hanies's results), *c-met* is expressed in the ventral lateral part of somites. However, in the posterior part, c-met is expressed in the nephric duct. This means *c-met* is not expressed in most of the somites, which is in contrast with *c-met*'s expression in other vertebrates (Andermarcher et al., 1996; Daston et al., 1996; Thery et al., 1995; Yang et al., 1996). And this disaccord supports the hypothesis that there might be one additional zebrafish *c-met* to co-express with *hgfa* in somites. Functionally, knockdown *hgfb* or *c-met* both induce smaller liver, and knockdown *hgfa* alone induce curved trunk. This result also suggested that this *c-met* is probably the recptor of hgfb, but not *hgfa* and maybe one more zebrafish *c-met* exists to support *hgfa* function in somites.

To investigate the possibilities raised above, the following experiment can be designed. Human cell line's *c-MET* excelluar domain can be replaced by zebrafish c-met extracelluar domain. And the signaling pathway activated by zebrafish *hgfa* or *hgfb* in this cell line can be measured. If both *hgfs* can activate the *c-MET* signaling pathway, then it will support the hypothesis that the two *hgfs* could share one receptor. Otherwise, there is possibly one additional *c-met* in zebrafish. If both *hgfs* can bind to this hybrid *c-MET* and activate the signaling pathway, in vitro study can be done to investigate if the two *hgfs* have any difference at the biological level (eg. Scatter activity, morphogenetic activity, anti-apoptosis activity, etc.) to further support the idea that the two *hgfs* might bind to the same receptor to carry out distinct functions in different organs or developmental stages

4.3 Distinct expression pattern of *hgfa* and *hgfb*

Two partial cDNA sequences of zebrafish *hgf* have been reported earlier (Haines et al., 2004). The two different *hgfs*, named as *hgf1* (NCBI accession NO.: NM_001013274) and *hgf2* (NCBI accession NO.: AY690481) exhibited identical expression profiles during development (Haines et al., 2004). However, in this study, the expression pattern of *hgfa* (corresponding to *hgf1* by sequence comparison) and *hgfb* (corresponding to *hgf2* by sequence comparison) are distinct both temporally as well as spatially. The possible reason of this discrepancy could be the probes they used which are based on partial sequences and short cDNA fragmants. In contrast, the probes used in this study are generated from the full length cDNA sequences including UTR. Although the updated *hgf1* sequence in NCBI (updated by zebrafish genome database at 03-JAN-2007) covers the whole ORF, Haines et al. only isolated the fragment of *hgfs* for probe synthesis. And the updated *hgf1* sequence is missing 39bp of *hgfa* in ORF region, which may be due to the mis-prediction of the intron-exon junction. *hgf2* isolated by Haines et al. is only 205bp in length and located at the 3 prime end (Fig.4.1). By alignment of *hgf1* and *hgf2*'s nucleotide sequences at the corresponding region, they share 65% of identity, indicating this region of *hgfs* share higher homology than the full ORF sequence of two *hgfs*, which is 50% based on our sequence comparison. And using this higher homology region for probe synthesis may be difficult to differentiate the *hgf1* and *hgf2*'s expression pattern.

```
hgfb            CTTCCCATCACTAGTTCTAAACTGTGTGCCGGTGGCAGAAGAGATGAAGGAGTTTGTGAG 1962
hgf2            ------------------------------------------------------CAG 3
hgfa            CTGCCCATCACCGAGACCAAAATCTGTGCTGGAGGCAAGAGAGATCAGGGCGTTTGTGAG 1956
hgf1            CTGCCCATCACCGAGACCAAAATCTGTGCTGGAGGCAAGAGAGATCAGGGCGTTTGTGAG 1917
                                                                        **

hgfb            AAAGACTACGGGGGCCCTCTAGTATGTCAAGAGAGTAACAGTAAAGTCATTGTTGGTGTG 2022
hgf2            AAAGACTACGGGGGCCCTCTAGTATGTCAAGAGAGTAACAGTAAAGTCATTGTTGGTGTG 63
hgfa            AAAGACTACGGTGGCCCTTTGGTGTGCCAGGAAGGAGAGAGCAAAGTGATAGTTGGCGTC 2016
hgf1            AAAGACTACGGTGGCCCTTTGGTGTGCCAGGAAGGAGAGAGCAAAGTGATAGTTGGCGTC 1977
                *********** ****** * ** ** ** **  *  * ** ***** ** ***** **

hgfb            AGCATAAATGGCAGAGGATGTGCCAGGCATAACCGACCAGCCATTTTTGTGAACGTGGCC 2082
hgf2            AGCATAAATGGCAGAGGATGTGCCAGGCATAACCGACCAGCCATTTTTGTGAACGTGGCC 123
hgfa            AGCATCAACGGCCGTGGTTGTGCAGTAGCGAGACGTCCTGCTGTCTTCGTCAACGTGGCC 2076
hgf1            AGCATCAACGGCCGTGGTTGTGCAGTAGCGAGACGTCCTGCTGTCTTCGTCAACGTGGCC 2037
                ***** ** *** * ** *****       *  ** ** **  * ** ** *********

hgfb            TTCTACGCTGGATGGATTCATAAAGTTTACAGAAATTATCCAAACTCAGAACTGAACAAT 2142
hgf2            TTCTACGCTGGATGGATTCATAAAGTTTACAGAAATTATCCAAACTCAGAACTGAACAAT 183
hgfa            TTCTACTCTGAATGGATCCGCAAGGTCTTCAAGTACTATTCAGACATGGAAATAAGTTAC 2136
hgf1            TTCTACTCTGAATGGATCCGCAAGGTCTTCAAGTACTATTCAGACATGGAAATAAGTTAC 2097
                ****** *** ****** *  ** ** * **   * *** ** **   *** * *   *

hgfb            T-GATCACGAGAGCAGGATTGAAAATCCGATCTGTGATATAAGAACAAAATATCTCCACA 2201
hgf2            T-GATCACGAGAGCAGGATTGAA----------------------------------- 205
hgfa            TAGATCTCCATATGTGGTAAATAAGACTAAATGGTTTAGCATCTACATCGTGAAGGACGA 2196
hgf1            TAG---------------------------------------------------------- 2100
                * *
```

Fig.4.1 Comparison of *hgf1, hgf2, hgfa* and *hgfb*. Numbers indicate nucleotides position from start codon (*hgf1, hgfa* and *hgfb*) or from the first nucleotide revealed (*hgf2*).

Comparing *hgfa* and *hgfb*'s expression pattern in this study with *hgfs* expression pattern in Haines' study, common expression pattern can be found between *hgfa* in this study and *hgfs* in Haines' study (Haines et al., 2004). In Hanies' study, *hgfs* transcripts can be detected throughout the fin bud mesenchyme with increased expression in the fin at 36 and 48hpf (Haines et al., 2004). In my study, *hgfa*'s expression in fin can be detected at 30 and 48hpf (Fig.3.17), however, not throughout the whole fin bud mesenchyme, but in the dorsaventral dorsal and ventral muscle mass within the fin (Fig.3.17 G). This result parallels the result obtained on *Hgf* expression in the mouse (Ebens et al., 1996), in which *Hgf* is expressed in the dorsal and ventral muscle mass within forelimb. The possibility for this difference between

Haine's *hgfs* and *hgfa*'s expression in fin might be due to the different length of cDNA sequence used for probe synthesis.

Haines found *hgfs* initiates expression broadly and at low level within somites at all axial levels at 22hpf, with stronger expression evident at somite boundaries (Haines et al., 2004). However, I found *hgfa* initiates expression broadly within somite at all axial levels from 7somites stage, not at the somite boundaries, and at 48hpf, *hgfa* transcripts can no longer be detected within the somite (Fig 3.17). For *hgfs* expression in notochord and neueral tube (Haines et al., 2004), I failed to detect the same expression pattern in my study for either *hgfa* or *hgfb*. Some additional expression pattern of *hgfa* was found in the developing ear (Fig 3.17), which has no parallel in other species.

hgfb's expression pattern is quite different from the *hgfa*'s expression pattern and the published *hgfs* expression pattern (Haines et al., 2004). There are many tissues or organs expressing *hgfb*. *hgfb*'s expression in liver was detectable from 4dpf in a salt and pepper pattern, and the section of two probes WISH of *hgfb* and *Cp* at 6dpf revealed that *hgfb* is expressed in stromal cells in liver, not hepatocyte (Fig.3.18). *hgfb*'s expression at the pronephric duct opening was evident from 12somites stage to 4dpf (Fig.3.18), which has no parallel in other species. Interestingly, in the swim bladder, an organ unique to fish, *hgfb* is expressed from 36hpf to 4dpf (Fig.3.18).

qRT-PCR of *hgfa* and *hgfb* during different developmental stages revealed their different expression profile at the temporal level (Fig 3.16). For *hgfa*, there is a peak at 24hpf to 36hpf stage, corresponding to the stage of somitogensis and fin budding.

For *hgfb*, there are two peaks, one at 24hpf and another at 3dpf to 4dpf. The 3dpf to 4dpf expression peak of *hgfb* is corresponding to the stage of liver growth, together with the expression pattern of *hgfb* in liver, indicating *hgfb* may be required for liver growth.

4.4 *c-met* express in various tissues and organs

In Haines' study (Haines et al., 2004), c-met expression is detected in fin and PHM (posterior hypaxial muscle) muscle precursors, as well as the PLLP (posterior lateral line primordial). In this study, *c-met* expression in fin and PLLP is very distinguishable and the expression of *c-met* in PLLP is not necessary at the same axial level when migrating caudally (Fig.3.19). *c-met*'s expression in fin is only restricted to dorsoventral muscle masses of the fin (Fig.3.19 Q), which was also found in Hanies's study (Haines et al., 2004). With *hgfa*'s expression in dorsaventral muscle masses (Fig.3.17 G), it is highly likely that *hgfa/c-met* signaling pathway might play role in fin development. Two probes WISH of *hgfa* and *c-met* and section cross the fin would help to investigate if it is a paracrine or autocrine signaling in fin development. Several new expression profiles of *c-met* were revealed in this study. *c-met* expression in head is evident from 1-somite stage to 12-somites stage (Fig.3.19), corresponding to the peak expression level of *c-met* at 12somite stages in qRT-PCR analysis (Fig.3.16). *c-met* was found to be expressed in the developing pronephric duct (Fig.3.19). This expression pattern can also be found in Xenopus (Koibuchi et al., 2004). The expression of *hgfb* in the posterior opening of the pronephric duct suggests the involvement of *hgfb* and *c-met* paracrine signaling in pronephric duct development.

c-met expression in motor neuron is evident at 18somites stages to 24hpf (Fig 3.19). In mouse or rat, *c-Met* was also found in motor neuron and *Hgf* act as an axonal chemoattractant, a neurotrophic factor and a survival factor for motor neuron (Ebens et al., 1996; Yamamoto et al., 1997). However, zebrafish *c-met* expression in motor neuron is not revealed in Haines' study (Haines et al., 2004).

Expression of *c-met* in liver was distinguishable from 48hpf, section of two probes WISH of *c-met* and *ceruloplasmin* at 3dpf revealed that *c-met* might be expressed in hepatocyte (Fig 3.19). With the expression of *hgfb* in the liver mesenchyme cells, this expression of *c-met* in hepatocyte may indicate paracrine signaling of *hgfb* and *c-met* in liver growth. And this co-expression of *HGF* and *c-met* in liver was also revealed in rat or mice (Hu et al., 1993; Yang and Park, 1995), in which *HGF* was localized in the nonparanchymal cells and *c-met* in the hepatocyte.

c-met expression in exocrine pancreas is only detectable at 4dpf in this study (Fig 3.19). Although *c-met* was reported to be expressed or play roles in the adult pancreas, regenerating pancreas or pancreatic cancer cells (Otonkoski et al., 1996; Otte et al., 2000), there is no published evidence up to now showing its expression in the developing pancreas.

4.5 *hgfa* plays a role in somitogenesis and myogenesis

From the above results, different phenotypes of *hgfa* morphants were observed at different somite stages. Curved trunk is morphological evident in *hgfa* morphants (Fig.3.20) and together with the expression of *hgfa*'s expression in somite, indicating *hgfa*'s role in somitogenesis. To initially test the possibility that *hgfa* plays a role during somitogenesis, the expression of *myoD*, a marker for terminal differentiation of somites, was analyzed for the *hgfa* morphants at the 9-somite stage. At the 9-somite stage, although *myoD* expression in either the left or right somites only were revealed, the main phenotypes observed were the reduction in *myoD* expression and *myoD* expression in the adaxial cells was not affected (Fig.3.25). Hence, *hgfa* is required for normal *myoD* expression in the somites, indicating *hgfa*'s role in somitogenesis.

Meanwhile, although some of the phenotypes of the *hgfa* morphants were also seen in the HGFa-ATG5mis MO injected embryos, this could be due to the close similarity between the MO sequences. Both of these MOs are 25 bases in length, with only 5 random bases being different between them. Moreover, the HGFa-ATG MO functions as a steric hindrance that prevents the translation of the specific mRNA which it binds to. Hence, it is possible that the HGFa-ATG5mis MO could also bind the same mRNA, but with lowered affinity (due to the 5 mismatched bases). As seen in Fig.4.2, MO less than 20-mer still have inhibition effects. Also, compared to the HGFa-ATG morphants (which were microinjected with 10ng of HGFa-ATG MO per embryo), the number of HGFa-ATG5mis MO injected embryos (which were microinjected with

10ng of HGFa-ATG5mis morpholino) showing the phenotypes were smaller (Fig.3.26, Fig.3.28 and Fig.3.30).

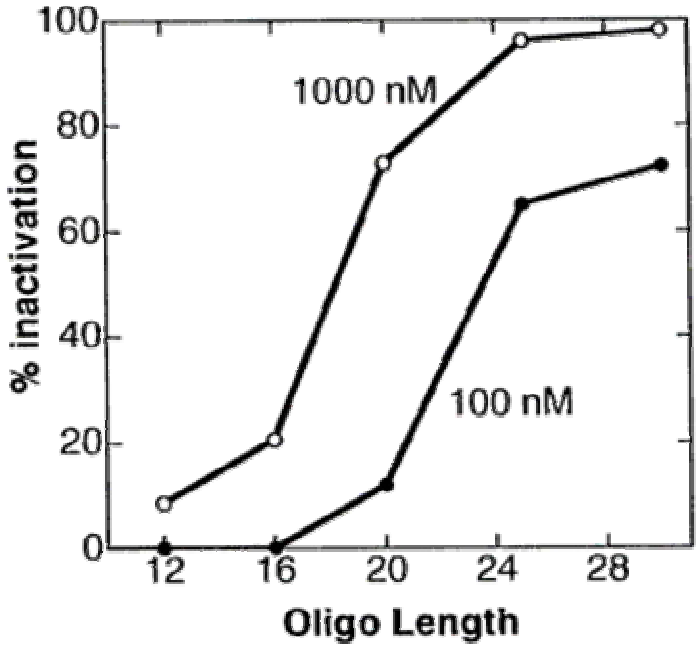

Fig.4.2 In a cell-free translation system the great gains in efficacy with increasing length of Morpholino Oligos. (from www.gene-tools.com)

When the HGFa-ATG MO was microinjected at 1ng per embryo, smaller percentages of the phenotypes were observed in the HGFa-ATG morphants comparing with those microinjected at 10ng per embryo. Thus, the phenotypes observed in the HGFa-ATG morphants are MO dose-dependent. This suggests that the HGFa-ATG MO inhibition of the translation of *hgfa* mRNA may be dose-dependent.

Since *myoD* expression is disrupted in *hgfa* morphants and *fgf8* signalling is required for *myoD* expression in the somites (Groves et al., 2005), *fgf8* expression was analyzed in *hgfa* morphants. At the 8-somite stage, the main phenotype observed was the reduction in *fgf8* expression, together with a reduction in the number of somites (Fig.3.27). Thus, *hgfa* is required for normal *fgf8* expression in the somites.

Since the continuously regressing posterior-to-anterior gradient of *fgf8* plays a critical role in positioning the determination front for somites formation (Dubrulle et al., 2001; Dubrulle and Pourquie, 2004), and the knockdown of *hgfa* has shown to affect the expressions of *myoD*, *fgf8* in this study, *hgfa* might plays a role in somitogenesis.

However, it is puzzling that the *hgfa* morphants were able to continue survival, in spite of the severe developmental defects. There are a few possible reasons to explain this. One, there are other myogenic regulatory transcription factors (MRFs), such as *myf5* and *myogenin*, involved in somitogenesis and myogenesis. These factors might be upregulated to compensate for the reduction and loss of *myoD* in the *hgfa* morphants. Two, other *fgfs* might also be involved in somitogenesis and could be co-expressed with *fgf8*, especially the close homologues *fgf17* and *fgf17b*. These *fgfs* could be upregulated to compensate for the loss of *fgf8* in the *hgfa* morphants. In addition, some recovery of somitogenesis and myogenesis could be driven by later-acting *fgfs*. Last but not least, it has been shown that a lack of *fgf* signalling does not lead to death of lateral somite cells, but rather, cause them to remain in a less differentiated state, i.e., similar to an immature somite (Groves et al., 2005). Hence, it is possible that other later-acting genes can induce these cells to undergo terminal differentiation.

Since the knockdown of *hgfa* causes a reduction in both *myoD* and *fgf8* expressions, and that *fgf8* is expressed in the somites approximately 1 hour before the somatic expression of *myoD* (Reifers et al., 1998), it is possible that *hgfa* affects *myoD* expression through its effect on *fgf8*. This hypothesis is further supported by the study carried out by Groves (Groves et al., 2005). They have found that the lateral cells in

the posterior somite require *fgf8* signalling to initiate the expression of *myoD* and consequently, to undergo terminal differentiation into fast muscle fibres. Furthermore, *fgf8* expression within the somite is sufficient for *myoD* expression in the lateral somite. By exposing the embryos to SU5402, a drug that blocks the phosphorylation of *fgf* receptors and thus, prevents downstream signalling, *myoD* expression in the lateral somites is abolished (Groves et al., 2005). Hence, they have showed that *fgf8* signalling is required for *myoD* expression in the somites and further terminal differentiation. Thus, *fgf8* drives lateral fast myogenesis in zebrafish.

In another recent study done by Hamade et al. (Hamade et al., 2006), *fgf8* is found to be a major relay factor in retinoic acid (RA)-mediated activation of myogenesis. The expression of *fgf8* and *myoD* in the somites and/or PSM are regulated by RA. Localized synthesis of RA by *aldh1a2* in the anterior PSM and in somites, activates *fgf8* expression, which in turn, induces the expression of myogenic genes and fast muscle differentiation. Inhibition of RA signaling decreases both *myoD* expression and muscle differentiation. Therefore, RA and *fgf8* are indicated as key regulators of myogenesis in zebrafish (Fig. 4.3). Hence, the RA synthesis by *aldh1a2* was *checked* in *hgfa* morphants. And at the 12-somite stage, the phenotype observed was the reduction or asymmetry expression of *aldh1a2* (Fig.3.29). Thus, *hgfa* is required for normal *aldh1a2* expression in somites. Since knockdown of *hgfa* has been shown to affect the expressions of *fgf8* and *aldh1a2* in this study, it is hypothesized that *hgfa* has an effect on RA and *fgf8* signaling, and might plays a role in myogenesis.

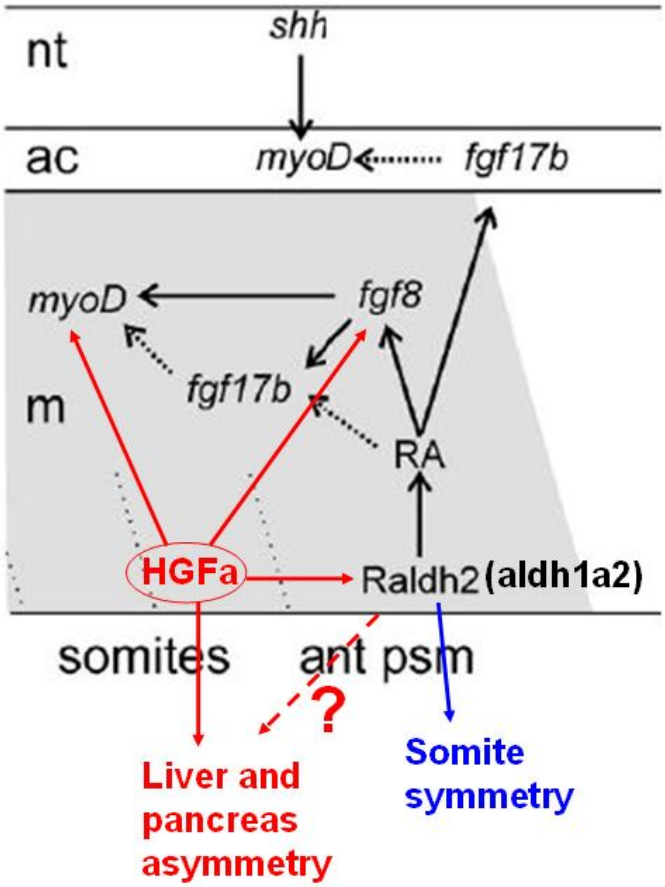

Fig.4.3 Model of *myoD* regulation by RA and *fgf8* signalling pathways and *hgfa*'s role during embryonic development. Schematic drawing of the posterior somites and the PSM of a 10-somite stage embryo. Arrows indicate relationships identified; dotted arrows represent possible relationships. Anterior presomitic mesoderm and somites are indicated by grey shading. *aldh1a2* expressed in somites and anterior PSM synthesises RA, which in turn controls expression of *fgf8* and possibly *fgf17b* in somites and anterior PSM. *fgf8* and possibly *fgf17b* activate expression of *myoD* in somites. RA also activates *fgf17b* expression in adaxial cells, which in turn may control expression of *myoD* in these cells together with *Shh*. ac, adaxial cells; ant psm, anterior presomitic mesoderm; m, mesoderm; nt, neural tube. (Hamade et al., 2006).

4.6 *hgfa* influence angiogenesis in zebrafish embryos

Using the *Tg(fli:GFP)*, ISV and DLAV sprouting delay about 10 to 24 hours can be observed in *hgfa* morphant at dorsal part (Fig.3.31) and this delay is dependent on the level of *hgfa* knockdown (Fig.3.23). It is noted that the ISV sprouting route is different at the dorsal part and ventral part (Childs et al., 2002). At the ventral part, ISV sprouts between the somite bondary, while the dorsal part, ISV does not follow the somite boundary, where it runs directly to the DLAV by penetrating the somites (Fig.4.4). It is also speculated that during the ventral-to-dorsal migration, angioblasts encounter distinct signals, or different levels of a signal arrayed in a morphogenetic gradient that dictates the fate of the individual cell and the shape of the vessel (Childs et al., 2002). This is supported by our finding that in *hgfa* morphant, ISV sprouting is only affected at the dorsal part, not the ventral part. Based on *hgfa*'s expression in somites and role in somitogenesis or myogenesis, and the penetration of ISV through somites during the dorsal part sprouting, ISV and DLAV sprouting delay at dorsal part in *hgfa* morphant might be the consequence of somitogenesis or myogenesis disruption in *hgfa* morphant.

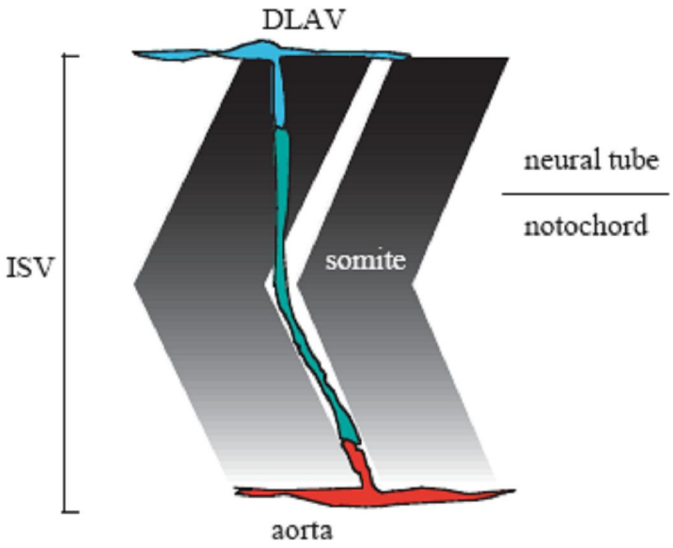

Fig.4.4 Model of the construction of a zebrafish ISV. An intersegmental vessel (ISV) is composed of three types of endothelial cells, distinguished by their morphologies. The dorsal connection to the DLAV is a T-shaped cell (blue); the ventral connection to the aorta is an inverted 'T' (red). The connecting cell (green) courses between the somites ventral to the notochord-neural tube interface, and appears not to follow the somite boundary dorsally, where it runs directly to the DLAV.(Childs et al., 2002)

4.7 *hgfa* plays a role in the left-right positioning of liver and pancreas

Although *hgfa*'s expression in liver is not detectable in this study, the asymmetric position of liver was found to be shifted from left side to right side in *hgfa* morphants (Fig.3.32). Another asymmetrically positioned organ, pancreas, was later found to be shifted from right side to the left side in *hgfa* morphants (Fig 3.35). And the position of liver and pancreas can shift within a single *hgfa* morphant simultaneously (Fig 3.37).

Since *hgfa* expression is symmetrical and this knockdown effect is asymmetrical, it is very interesting to study how interfering symmetrical signal can induce asymmetrical effects. Recent studies about RA showed that the symmetry arrangement of the somitogenesis is not the default mode, but protected by the RA from the asymmetrical clues (Hornstein and Tabin, 2005; Kawakami et al., 2005; Vermot et al., 2005; Vermot and Pourquie, 2005).

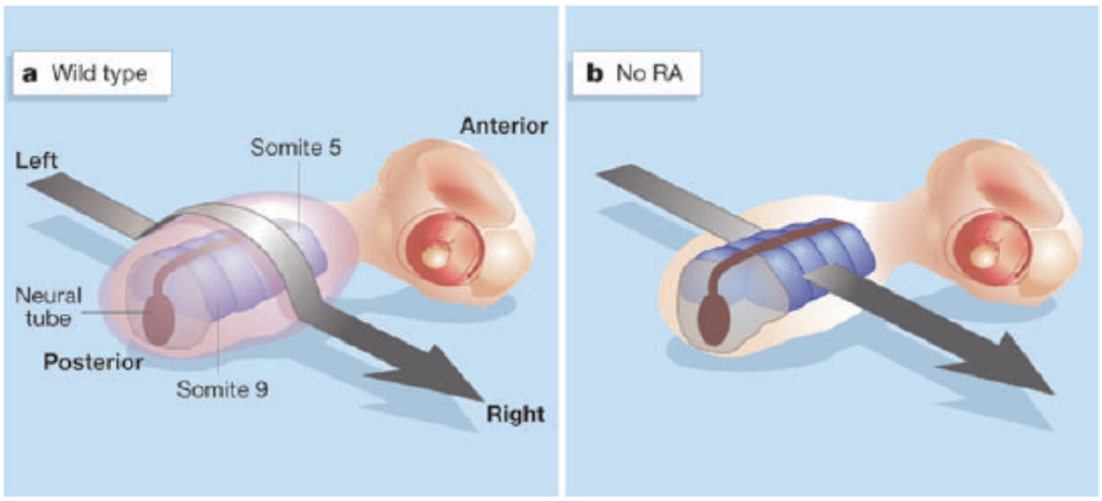

Fig.4.5 Maintaining symmetrical somitogenesis. A vertebrate embryo is shown from the back. a, The new papers1–3 show that, in wild-type embryos, a protective effect of retinoic acid (RA; pink field) masks the flow of left–right information (black

arrow) to enable the symmetrical bilateral formation of new somites (blue). b, Blocking RA production exposes somites to left–right signals and takes their generation out of synchrony.

When separate the embryo into different pools basing on the curving trunk phenotype, the liver shifting ratio is higher in the curving trunk pool (45%) than the non-curving trunk pool (10%) (Fig.3.34). Together with the expression pattern of *hgfa* (not in liver or pancreas), shifting of those asymmetrical arranged organs may be the consequence of the disrupted somitogenesis. In this study, *aldh1a2*, which acts as a key enzyme in RA synthesis and converts retinal to retinoic acid, is disrupted in the *hgfa* morphants. RA has been proven to protect the symmetrical somitogenesis from the asymmetrical signals (Fig.4.5). It is speculated that RA may not only protect the symmetrical somitogenesis but also protect the asymmetrical organ which is beneath the somites (Fig.4.4). However, until now no reports has mentioned if RA will affect the asymmetrical organogenesis.

Almost no study showed that how somitogenesis affect asymmetrical arranged organs, the mechanism remains unclear. Previous studies have shown that RA can protect the symmetry of somitogenesis through *fgf8* (Hamade et al., 2006), however, didn't mention about this protection form RA can also shield other asymmetrically positioned organs. This is a gap from the *hgfa* affecting the RA and symmetry of somitogenesis to *hgfa* affecting the liver and pancreas asymmetrical postion. And this study may give the first indication that RA protection may shield asymmetrically positioned organs. To confirm this, studies were taken to determine whether the asymmetrically organs' position are shifted in the RA deprived mutant using the DEAB. However, the results were not constant (data not included).

Another possible explanation is the MO delivery method. When using qRT-PCR analysis to check the gene knockdown level, within single batch of injected embryos, different pools have different knockdown level. This variation is probably due to that current MO delivery method may cause inconstant distribution of MO. I use microinjection to deliver MO into the embryo. The injection position is roughly at the york below the cell. The injection position may vary, which may lead to different take up of MO for the cell. Especially when injected at two cell stage, variation of injection position may cause the two cells within one single embryo taking different amount of morpholino, which may explain the one side *myoD* expression phenotype in *hgfa* morphant (Fig.3.25 C and D). So the limitation of morpholino delivery method may lead to that the knockdown level are not uniform at the spatial level, which might affect the asymmetrical clues. To verify the knock down effect at spatial level, MO targeting the first intron and first exon junction, which cause intron inclusion, can be used. The spatial distribution of intron inclusion knockdown products can be revealed by the probe targeting to the intron.

The lack of *hgfa* expression in the liver and pancreas suggests that the liver and pancreas phenotypes observed in the *hgfa* morphants could be caused by a non-cell autonomous effect. Cell transplantation experiment will be helpful to investigate this possbilibty.

4.8 *hgfb* and its receptor *c-met* are essential for zebrafish liver development

WISH of *hgfb* and its receptor *c-met* revealed their expressions at different locations at different developmental stages, which was consistent with previous studies showing that HGF and c-met signaling played a pivotal role in the regulation of growth and development (Birchmeier and Gherardi, 1998). As most importantly for the current study, *hgfb* and *c-met* were shown to be expressed in liver, with *hgfb* expressed at liver from 4dpf to 6dpf and *c-met* from 36hpf to 6dpf. In previous studies on HGF and its receptor c-met, the presence of HGF in day 19 rat liver (Defrances et al., 1992), the expression of HGF mRNA during human and rat fetal liver development (Selden et al., 1990), and the expression of HGF's receptor c-met during mouse and rat embryogenesis (Chan et al., 1988) all suggested the HGF helped to regulate fetal liver development. Therefore, *hgfb* and *c-met* expression in zebrafish liver found in this work also implied their role in zebrafish liver development.

Primary hepatocytes are epithelial cells. Exchange of signals between the mesenchymal and epithelial cell compartments has long been recognized as a major driving force in epithelial growth, morphogenesis and differentiation (Birchmeier and Gherardi, 1998). Previous studies have already shown in mouse that c-met was expressed in epithelial cells in many organs, and HGF transcripts were produced by adjacent mesenchymal cells during development, and they interacted in a paracrine manner (Sonnenberg et al., 1993). In this study, *hgfb*'s expression in the liver

mesenchyme (Fig.3.18 V) and *c-met*'s expression in hepatocytes (Fig.3.19 R) also revealed their paracrine singling in liver development.

From 4dpf onwards, smaller liver phenotype could be observed in *hgfb* morphants, *c-met* morphants and double-knockdown morphants in a significantly higher percentage compared with controls. Together with the knockdown effect revealed by qRT-PCR and detection of the splicing interfered products by RT-PCR, the smaller liver phenotype was at first thought to be the direct and single effect of *hgfb* and *c-met* knockdown.

Having observed the small liver phenotype in *hgfb* and *c-met* morphants, it was hypothesized that the reduction in liver size might be due to increased apoptosis rate or decreased proliferation rate of liver cells. Using BrdU as a proliferation marker, it was found that the proliferation rates in liver cells for both morphants and controls were similar, which were around 10% (Xiaorui Wang, NUS honors student 2006/2007). This was an indication that *hgfb* and *c-met* knockdown had no effect on liver cell proliferation. However, this result was relatively preliminary and the extent of liver apoptosis has not been determined. Hence, no solid conclusion can be drawn up to now for the mechanism of reduced size of liver in *hgfb/c-met* morphants. In mouse HGF knockout mutants, the embryonic liver is reduced in size and shows extensive loss of hepatocytes, due to apoptotic cell death (Schmidt et al., 1995). Therefore, in the future work, it is necessary to check if the reduced size of liver in *hgfb* or *c-met* morphants is due to increased apoptosis of liver cells.

4.9. Comparison of HGF/c-Met functions in vertebrates

The expressions and functions of HGF and c-Met are highly consevered among different species. HGF and c-Met are co-expressed and playing roles in many organs and tisuues, such as nervous system, muscle, liver etc. However, there are some differences of HGF and c-Met roles between different species. One example is the HGF and c-met's role in hematopoiesis. In *Xenopus*, strong signals of HGF as well as c-met were detected early in the developing ventral mesoderm, which later gives rise to the ventral blood island (Koibuchi et al., 2004). In all vertebrate development, blood cell formation occurs in two successive waves, which are termed primitive and definitive hematopoiesis, based on the time of initiation, site of development, cell morphology, globin content, and potential to differentiate (Zon, 1995). Primitive hematopoiesis occurs first and gives rise to predominantly erythrocytes (primitive red blood cells). This phenomenon is then followed by definitive hematopoiesis, which leads to the production of all the blood lineages that are required throughout the life span of a vertebrate. Blocking of HGF signaling pathway in Xenopus embryos resulted in a marked decrease in the number of circulating blood cells and a significant reduction (or absence) of stem cell leukemia (SCL), α-globin, and GATA-1 expression, but not GATA-2 expression, in the ventral blood island (VBI) where primitive red blood cells are exclusively produced. In contrast, no significant difference was observed in the levels of expression of early definitive blood markers, SCL,GATA-2, and GATA-3 in the dorsolateral plate (DLP) where definitive blood cells arise predominantly (Koibuchi et al., 2004). Koibuchi's study (Koibuchi et al., 2004) demonstrated that HGF is a specific regulator of primitive hematopoiesis rather than definitive hematopoiesis in *Xenopus*, which is different from mouse mutants. Another unique expression of HGF is the zebrafish *hgfb*'s expression in swimblader

which was first revealed in this study. This unique expression of HGF may shed light to the understanding of development of swimbladder, a unique organ in fish.

Chapter 5. Conclusions

In this work, the roles of HGF and its receptor c-Met in zebrafish embryonic development were investigated. Full-length cDNAs of two zebrafish *hgfs* and its receptor *c-met* were cloned. The zebrafish *hgfs* were named as *hgfa* and *hgfb*. Expression analysis revealed distinctive expression pattern between *hgfa* and *hgfb*. *hgfa* is mainly expressed in somite from 7-somite stage to 30 hpf, pectoral fin from 30 hpf to 48 hpf and ear from 30 hpf to 48 hpf, while *hgfb* is expressed in liver from 4 dpf to 6 dpf, pronephric duct opening from 12-somite stage to 4 dpf and swim bladder from 36 hpf to 4 dpf. Their receptor c-met is detected in liver from 48 hpf to 6 dpf, pectoral fin from 48 hpf to 3 dpf, pronephric duct from 1-somite stage to 24 hpf, head from 1-somite stage to 12-somite stage, pancreas at 4 dpf and motor neuron from 18 hpf to 24 hpf. The co-expression of *hgfa* and *c-met* in pectoral fin at 48 hpf, *hgfb* and *c-met* in liver from 4 dpf to 6 dpf, *hgfb* in the pronephric duct opening and *c-met* in proneprhic duct 12-somite stage to 24 hpf, indicate their paracrine signaling in zebrafish embryonic development.

The functional analysis of *hgfa* by morpholino antisense oligonucleotide knockdown demonstrates its role in somitogensis and myogenesis, consistent with HGF's role in muscle and limb development in other verterates. Although *hgfa* is not expressed in liver, suppression of hgfa expression lead to the shift of liver position from left to right side of the body. Two phenotypes in *hgfa* morphants, curving trunk and liver position shifting, are proven to be correlated. RA (retinoic acid) has been proven to protect the symmetric somitogenesis from the asymmetrical clues. In this study, *aldh1a2* (RA synthesis enzyme) is disrupted in *hgfa* morphants. This gives the thought that RA might protect not only the symmetric somitognesis but also the asymmetric

organogenesis. However, deprivation of RA by DEAB can not generate the stable liver shifting phenotype. Given the one side missing of *myoD* expression, another possibility was coming into mind that the shifting of liver in *hgfa* morphants may not only require the knock down of *hgfa* but also the different knock down level at the spatial level which may be due to the limitation of the morpholino delivery method. When microinjecting into embryos older than one-cell stage, the uniform distribution of morpholino in each cell is not guaranteed. This would also explain why the liver shifting phenotype is not *hgfa* knockdown level dependent. The splicing morpholino make it possible to verify the different knock down level at the spatial level. This future work might be important to reveal the mechanism for liver shifting in *hgfa* morphant. Angiogenesis is also disrupted when *hgfa* was knocked-down as evidenced by the interruption of dorsal intersegmental vessel sprouting in *hgfa* morphants. Whether this is a direct effect on vessel formation or a secondary effect of somitogenesis disruption in *hgfa* morphants is unclear at this moment.

The functional analysis of *hgfb* and *c-met* in liver development demonstrate their specific roles in liver growth, but not liver budding. The smaller liver phenotype in *hgfb* and *c-met* morphants is depedent on the extent of gene expression knockdown. There are two possible mechanisms for this smaller liver phenotype: one is the reduced cell proliferation, another is the accelerated cell apoptosis. Preliminary results showed that cell proliferation is not affected in *hgfb* and *c-met* morphants. Further confirmation of the proliferation results as well as analysis of the liver cell apoptosis could reveal the mechanism for small liver phenotype in *hgfb* and *c-met* morphants.

References List

Allen,R.E., Sheehan,S.M., Taylor,R.G., Kendall,T.L., and Rice,G.M. (1995). Hepatocyte growth factor activates quiescent skeletal muscle satellite cells in vitro. *J. Cell Physiol* **165,** 307-312.

Amemiya,C.T., Zhong,T.P., Silverman,G.A., Fishman,M.C., and Zon,L.I. (1999). Zebrafish YAC, BAC, and PAC genomic libraries. *Methods Cell Biol.* **60,** 235-258.

Amores,A., Force,A., Yan,Y.L., Joly,L., Amemiya,C., Fritz,A., Ho,R.K., Langeland,J., Prince,V., Wang,Y.L. et al. (1998). Zebrafish hox clusters and vertebrate genome evolution. *Science* **282,** 1711-1714.

Anastasi,S., Giordano,S., Sthandier,O., Gambarotta,G., Maione,R., Comoglio,P., and Amati,P. (1997). A natural hepatocyte growth factor/scatter factor autocrine loop in myoblast cells and the effect of the constitutive Met kinase activation on myogenic differentiation. *J. Cell Biol.* **137,** 1057-1068.

Andermarcher,E., Surani,M.A., and Gherardi,E. (1996). Co-expression of the HGF/SF and c-met genes during early mouse embryogenesis precedes reciprocal expression in adjacent tissues during organogenesis. *Dev. Genet.* **18,** 254-266.

Aoki,M., Ogihara,T., and Morishita,R. (2001). [HGF as a key molecule in cardiovascular diseases]. *Nippon Rinsho* **59,** 2460-2469.

Aoki,S., Takahashi,K., Matsumoto,K., and Nakamura,T. (1997). Activation of Met tyrosine kinase by hepatocyte growth factor is essential for internal organogenesis in Xenopus embryo. *Biochem. Biophys. Res. Commun.* **234,** 8-14.

Asami,O., Ihara,I., Shimidzu,N., Shimizu,S., Tomita,Y., Ichihara,A., and Nakamura,T. (1991). Purification and characterization of hepatocyte growth factor from injured liver of carbon tetrachloride-treated rats. *J. Biochem. (Tokyo)* **109,** 8-13.

Aulehla,A. and Herrmann,B.G. (2004). Segmentation in vertebrates: clock and gradient finally joined. *Genes Dev.* **18,** 2060-2067.

Aulehla,A., Wehrle,C., Brand-Saberi,B., Kemler,R., Gossler,A., Kanzler,B., and Herrmann,B.G. (2003). Wnt3a plays a major role in the segmentation clock controlling somitogenesis. *Dev. Cell* **4,** 395-406.

Barbazuk,W.B., Korf,I., Kadavi,C., Heyen,J., Tate,S., Wun,E., Bedell,J.A., McPherson,J.D., and Johnson,S.L. (2000). The syntenic relationship of the zebrafish and human genomes. *Genome Res.* **10,** 1351-1358.

Bardelli,A., Basile,M.L., Audero,E., Giordano,S., Wennstrom,S., Menard,S., Comoglio,P.M., and Ponzetto,C. (1999). Concomitant activation of pathways downstream of Grb2 and PI 3-kinase is required for MET-mediated metastasis. *Oncogene* **18,** 1139-1146.

Barresi,M.J., Stickney,H.L., and Devoto,S.H. (2000). The zebrafish slow-muscle-omitted gene product is required for Hedgehog signal transduction and the development of slow muscle identity. *Development* **127,** 2189-2199.

Barut,B.A. and Zon,L.I. (2000). Realizing the potential of zebrafish as a model for human disease. *Physiol Genomics* **2,** 49-51.

Beilmann,M., Birk,G., and Lenter,M.C. (2004). Human primary co-culture angiogenesis assay reveals additive stimulation and different angiogenic properties of VEGF and HGF. *Cytokine* **26,** 178-185.

Bell,A., Chen,Q., DeFrances,M.C., Michalopoulos,G.K., and Zarnegar,R. (1999). The five amino acid-deleted isoform of hepatocyte growth factor promotes carcinogenesis in transgenic mice. *Oncogene* **18,** 887-895.

Besser,D., Bardelli,A., Didichenko,S., Thelen,M., Comoglio,P.M., Ponzetto,C., and Nagamine,Y. (1997). Regulation of the urokinase-type plasminogen activator gene by the oncogene Tpr-Met involves GRB2. *Oncogene* **14,** 705-711.

Bessho,Y. and Kageyama,R. (2003). Oscillations, clocks and segmentation. *Curr. Opin. Genet. Dev.* **13,** 379-384.

Birchmeier,C., Birchmeier,W., Gherardi,E., and Vande Woude,G.F. (2003). Met, metastasis, motility and more. *Nat. Rev. Mol. Cell Biol.* **4,** 915-925.

Birchmeier,C. and Gherardi,E. (1998). Developmental roles of HGF/SF and its receptor, the c-Met tyrosine kinase. *Trends Cell Biol.* **8,** 404-410.

Bladt,F., Riethmacher,D., Isenmann,S., Aguzzi,A., and Birchmeier,C. (1995). Essential role for the c-met receptor in the migration of myogenic precursor cells into the limb bud. *Nature* **376,** 768-771.

Blagden,C.S., Currie,P.D., Ingham,P.W., and Hughes,S.M. (1997). Notochord induction of zebrafish slow muscle mediated by Sonic hedgehog. *Genes Dev.* **11,** 2163-2175.

Bober,E., Brand-Saberi,B., Ebensperger,C., Wilting,J., Balling,R., Paterson,B.M., Arnold,H.H., and Christ,B. (1994). Initial steps of myogenesis in somites are independent of influence from axial structures. *Development* **120,** 3073-3082.

Boccaccio,C., Ando',M., and Comoglio,P.M. (2002). A differentiation switch for genetically modified hepatocytes. *FASEB J.* **16,** 120-122.

Bottaro,D.P., Rubin,J.S., Faletto,D.L., Chan,A.M., Kmiecik,T.E., Vande Woude,G.F., and Aaronson,S.A. (1991). Identification of the hepatocyte growth factor receptor as the c-met proto-oncogene product. *Science* **251,** 802-804.

Brand-Saberi,B., Muller,T.S., Wilting,J., Christ,B., and Birchmeier,C. (1996). Scatter factor/hepatocyte growth factor (SF/HGF) induces emigration of myogenic cells at interlimb level in vivo. *Dev. Biol.* **179,** 303-308.

Brinkmann,V., Foroutan,H., Sachs,M., Weidner,K.M., and Birchmeier,W. (1995). Hepatocyte growth factor/scatter factor induces a variety of tissue-specific morphogenic programs in epithelial cells. *J. Cell Biol.* **131,** 1573-1586.

Buckingham,M., Bajard,L., Chang,T., Daubas,P., Hadchouel,J., Meilhac,S., Montarras,D., Rocancourt,D., and Relaix,F. (2003). The formation of skeletal muscle: from somite to limb. *J. Anat.* **202,** 59-68.

Bussolino,F., Di Renzo,M.F., Ziche,M., Bocchietto,E., Olivero,M., Naldini,L., Gaudino,G., Tamagnone,L., Coffer,A., and Comoglio,P.M. (1992). Hepatocyte growth factor is a potent angiogenic factor which stimulates endothelial cell motility and growth. *J. Cell Biol.* **119,** 629-641.

Chalmers,A.D. and Slack,J.M. (2000). The Xenopus tadpole gut: fate maps and morphogenetic movements. *Development* **127,** 381-392.

Chan,A.M., King,H.W., Deakin,E.A., Tempest,P.R., Hilkens,J., Kroezen,V., Edwards,D.R., Wills,A.J., Brookes,P., and Cooper,C.S. (1988). Characterization of the mouse met proto-oncogene. *Oncogene* **2,** 593-599.

Chan,P.C., Liang,C.C., Yu,K.C., Chang,M.C., Ho,W.L., Chen,B.H., and Chen,H.C. (2002). Synergistic effect of focal adhesion kinase overexpression and hepatocyte growth factor stimulation on cell transformation. *J. Biol. Chem.* **277,** 50373-50379.

Chen,W., Burgess,S., Golling,G., Amsterdam,A., and Hopkins,N. (2002). High-throughput selection of retrovirus producer cell lines leads to markedly improved efficiency of germ line-transmissible insertions in zebra fish. *J. Virol.* **76,** 2192-2198.

Childs,S., Chen,J.N., Garrity,D.M., and Fishman,M.C. (2002). Patterning of angiogenesis in the zebrafish embryo. *Development* **129,** 973-982.

Chiu,S.J., Jiang,S.T., Wang,Y.K., and Tang,M.J. (2002). Hepatocyte growth factor upregulates alpha2beta1 integrin in Madin-Darby canine kidney cells: implications in tubulogenesis. *J. Biomed. Sci.* **9,** 261-272.

Comoglio,P.M. (1993). Structure, biosynthesis and biochemical properties of the HGF receptor in normal and malignant cells. *EXS* **65,** 131-165.

Comoglio,P.M. and Boccaccio,C. (2001). Scatter factors and invasive growth. *Semin. Cancer Biol.* **11,** 153-165.

Cooper,C.S., Park,M., Blair,D.G., Tainsky,M.A., Huebner,K., Croce,C.M., and Vande Woude,G.F. (1984). Molecular cloning of a new transforming gene from a chemically transformed human cell line. *Nature* **311,** 29-33.

Corey,D.R. and Abrams,J.M. (2001). Morpholino antisense oligonucleotides: tools for investigating vertebrate development. *Genome Biol.* **2,** REVIEWS1015.

Costa,R.H., Kalinichenko,V.V., Holterman,A.X., and Wang,X. (2003). Transcription factors in liver development, differentiation, and regeneration. *Hepatology* **38,** 1331-1347.

Dale,J.K., Maroto,M., Dequeant,M.L., Malapert,P., McGrew,M., and Pourquie,O. (2003). Periodic notch inhibition by lunatic fringe underlies the chick segmentation clock. *Nature* **421,** 275-278.

Daston,G., Lamar,E., Olivier,M., and Goulding,M. (1996). Pax-3 is necessary for migration but not differentiation of limb muscle precursors in the mouse. *Development* **122,** 1017-1027.

Defrances,M.C., Wolf,H.K., Michalopoulos,G.K., and Zarnegar,R. (1992). The presence of hepatocyte growth factor in the developing rat. *Development* **116,** 387-395.

Delaria,K.A., Muller,D.K., Marlor,C.W., Brown,J.E., Das,R.C., Roczniak,S.O., and Tamburini,P.P. (1997). Characterization of placental bikunin, a novel human serine protease inhibitor. *J. Biol. Chem.* **272,** 12209-12214.

Delehedde,M., Sergeant,N., Lyon,M., Rudland,P.S., and Fernig,D.G. (2001). Hepatocyte growth factor/scatter factor stimulates migration of rat mammary fibroblasts through both mitogen-activated protein kinase and phosphatidylinositol 3-kinase/Akt pathways. *Eur. J. Biochem.* **268,** 4423-4429.

Denda,K., Shimomura,T., Kawaguchi,T., Miyazawa,K., and Kitamura,N. (2002). Functional characterization of Kunitz domains in hepatocyte growth factor activator inhibitor type 1. *J. Biol. Chem.* **277,** 14053-14059.

Derman,M.P., Chen,J.Y., Spokes,K.C., Songyang,Z., and Cantley,L.G. (1996). An 11-amino acid sequence from c-met initiates epithelial chemotaxis via phosphatidylinositol 3-kinase and phospholipase C. *J. Biol. Chem.* **271,** 4251-4255.

Derman,M.P., Cunha,M.J., Barros,E.J., Nigam,S.K., and Cantley,L.G. (1995). HGF-mediated chemotaxis and tubulogenesis require activation of the phosphatidylinositol 3-kinase. *Am. J. Physiol* **268,** F1211-F1217.

Devoto,S.H., Melancon,E., Eisen,J.S., and Westerfield,M. (1996). Identification of separate slow and fast muscle precursor cells in vivo, prior to somite formation. *Development* **122,** 3371-3380.

Di Renzo,M.F., Olivero,M., Martone,T., Maffe,A., Maggiora,P., Stefani,A.D., Valente,G., Giordano,S., Cortesina,G., and Comoglio,P.M. (2000). Somatic mutations of the MET oncogene are selected during metastatic spread of human HNSC carcinomas. *Oncogene* **19,** 1547-1555.

Dietrich,S., bou-Rebyeh,F., Brohmann,H., Bladt,F., Sonnenberg-Riethmacher,E., Yamaai,T., Lumsden,A., Brand-Saberi,B., and Birchmeier,C. (1999). The role of SF/HGF and c-Met in the development of skeletal muscle. *Development* **126,** 1621-1629.

Ding,S., Merkulova-Rainon,T., Han,Z.C., and Tobelem,G. (2003). HGF receptor up-regulation contributes to the angiogenic phenotype of human endothelial cells and promotes angiogenesis in vitro. *Blood* **101,** 4816-4822.

Dong,G., Loukinova,E., Chen,Z., Gangi,L., Chanturita,T.I., Liu,E.T., and Van,W.C. (2001). Molecular profiling of transformed and metastatic murine squamous carcinoma cells by differential display and cDNA microarray reveals altered expression of multiple genes related to growth, apoptosis, angiogenesis, and the NF-kappaB signal pathway. *Cancer Res.* **61,** 4797-4808.

Dooley,K. and Zon,L.I. (2000). Zebrafish: a model system for the study of human disease. *Curr. Opin. Genet. Dev.* **10,** 252-256.

Draper,B.W., Morcos,P.A., and Kimmel,C.B. (2001). Inhibition of zebrafish fgf8 pre-mRNA splicing with morpholino oligos: a quantifiable method for gene knockdown. *Genesis.* **30,** 154-156.

Driever,W., Solnica-Krezel,L., Schier,A.F., Neuhauss,S.C., Malicki,J., Stemple,D.L., Stainier,D.Y., Zwartkruis,F., Abdelilah,S., Rangini,Z. et al. (1996). A genetic screen for mutations affecting embryogenesis in zebrafish. *Development* **123,** 37-46.

Drummond,I.A., Majumdar,A., Hentschel,H., Elger,M., Solnica-Krezel,L., Schier,A.F., Neuhauss,S.C., Stemple,D.L., Zwartkruis,F., Rangini,Z. et al. (1998). Early development of the zebrafish pronephros and analysis of mutations affecting pronephric function. *Development* **125,** 4655-4667.

Du,S.J., Devoto,S.H., Westerfield,M., and Moon,R.T. (1997). Positive and negative regulation of muscle cell identity by members of the hedgehog and TGF-beta gene families. *J. Cell Biol.* **139,** 145-156.

Dubrulle,J., McGrew,M.J., and Pourquie,O. (2001). FGF signaling controls somite boundary position and regulates segmentation clock control of spatiotemporal Hox gene activation. *Cell* **106,** 219-232.

Dubrulle,J. and Pourquie,O. (2004). fgf8 mRNA decay establishes a gradient that couples axial elongation to patterning in the vertebrate embryo. *Nature* **427,** 419-422.

Duh,F.M., Scherer,S.W., Tsui,L.C., Lerman,M.I., Zbar,B., and Schmidt,L. (1997). Gene structure of the human MET proto-oncogene. *Oncogene* **15,** 1583-1586.

Dunsmore,S.E., Rubin,J.S., Kovacs,S.O., Chedid,M., Parks,W.C., and Welgus,H.G. (1996). Mechanisms of hepatocyte growth factor stimulation of keratinocyte metalloproteinase production. *J. Biol. Chem.* **271,** 24576-24582.

Ebens,A., Brose,K., Leonardo,E.D., Hanson,M.G., Jr., Bladt,F., Birchmeier,C., Barres,B.A., and Tessier-Lavigne,M. (1996). Hepatocyte growth factor/scatter factor is an axonal chemoattractant and a neurotrophic factor for spinal motor neurons. *Neuron* **17,** 1157-1172.

Ekker,S.C. and Larson,J.D. (2001). Morphant technology in model developmental systems. *Genesis.* **30,** 89-93.

Epstein,J.A., Shapiro,D.N., Cheng,J., Lam,P.Y., and Maas,R.L. (1996). Pax3 modulates expression of the c-Met receptor during limb muscle development. *Proc. Natl. Acad. Sci. U. S. A* **93,** 4213-4218.

Fan,S., Ma,Y.X., Gao,M., Yuan,R.Q., Meng,Q., Goldberg,I.D., and Rosen,E.M. (2001). The multisubstrate adapter Gab1 regulates hepatocyte growth factor (scatter factor)-c-Met signaling for cell survival and DNA repair. *Mol. Cell Biol.* **21,** 4968-4984.

Fernandez-Valle,C., Tang,Y., Ricard,J., Rodenas-Ruano,A., Taylor,A., Hackler,E., Biggerstaff,J., and Iacovelli,J. (2002). Paxillin binds schwannomin and regulates its density-dependent localization and effect on cell morphology. *Nat. Genet.* **31,** 354-362.

Ferracini,R., Di Renzo,M.F., Scotlandi,K., Baldini,N., Olivero,M., Lollini,P., Cremona,O., Campanacci,M., and Comoglio,P.M. (1995). The Met/HGF receptor is over-expressed in human osteosarcomas and is activated by either a paracrine or an autocrine circuit. *Oncogene* **10,** 739-749.

Field,H.A., Ober,E.A., Roeser,T., and Stainier,D.Y. (2003). Formation of the digestive system in zebrafish. I. Liver morphogenesis. *Dev. Biol.* **253,** 279-290.

Franz,T., Kothary,R., Surani,M.A., Halata,Z., and Grim,M. (1993). The Splotch mutation interferes with muscle development in the limbs. *Anat. Embryol. (Berl)* **187,** 153-160.

Fukuda-Taira,S. (1981). Hepatic induction in the avian embryo: specificity of reactive endoderm and inductive mesoderm. *J. Embryol. Exp. Morphol.* **63,** 111-125.

Furge,K.A., Zhang,Y.W., and Vande Woude,G.F. (2000). Met receptor tyrosine kinase: enhanced signaling through adapter proteins. *Oncogene* **19,** 5582-5589.

Furlong,R.A., Takehara,T., Taylor,W.G., Nakamura,T., and Rubin,J.S. (1991). Comparison of biological and immunochemical properties indicates that scatter factor and hepatocyte growth factor are indistinguishable. *J. Cell Sci.* **100 (Pt 1),** 173-177.

Galimi,F., Bagnara,G.P., Bonsi,L., Cottone,E., Follenzi,A., Simeone,A., and Comoglio,P.M. (1994). Hepatocyte growth factor induces proliferation and differentiation of multipotent and erythroid hemopoietic progenitors. *J. Cell Biol.* **127,** 1743-1754.

Gao,C.F. and Vande Woude,G.F. (2005). HGF/SF-Met signaling in tumor progression. *Cell Res.* **15,** 49-51.

Gates,M.A., Kim,L., Egan,E.S., Cardozo,T., Sirotkin,H.I., Dougan,S.T., Lashkari,D., Abagyan,R., Schier,A.F., and Talbot,W.S. (1999). A genetic linkage map for zebrafish: comparative analysis and localization of genes and expressed sequences. *Genome Res.* **9,** 334-347.

Geisler,R., Rauch,G.J., Baier,H., van,B.F., Bross,L., Dekens,M.P., Finger,K., Fricke,C., Gates,M.A., Geiger,H. et al. (1999). A radiation hybrid map of the zebrafish genome. *Nat. Genet.* **23,** 86-89.

Gerritsen,M.E., Tomlinson,J.E., Zlot,C., Ziman,M., and Hwang,S. (2003). Using gene expression profiling to identify the molecular basis of the synergistic actions of

hepatocyte growth factor and vascular endothelial growth factor in human endothelial cells. *Br. J. Pharmacol.* **140,** 595-610.

Gherardi,E., Gray,J., Stoker,M., Perryman,M., and Furlong,R. (1989). Purification of scatter factor, a fibroblast-derived basic protein that modulates epithelial interactions and movement. *Proc. Natl. Acad. Sci. U. S. A* **86,** 5844-5848.

Gherardi,E. and Stoker,M. (1990). Hepatocytes and scatter factor. *Nature* **346,** 228.

Gilmore,A.P. and Burridge,K. (1996). Regulation of vinculin binding to talin and actin by phosphatidyl-inositol-4-5-bisphosphate. *Nature* **381,** 531-535.

Giordano,S., Bardelli,A., Zhen,Z., Menard,S., Ponzetto,C., and Comoglio,P.M. (1997). A point mutation in the MET oncogene abrogates metastasis without affecting transformation. *Proc. Natl. Acad. Sci. U. S. A* **94,** 13868-13872.

Gohda,E., Tsubouchi,H., Nakayama,H., Hirono,S., Sakiyama,O., Takahashi,K., Miyazaki,H., Hashimoto,S., and Daikuhara,Y. (1988). Purification and partial characterization of hepatocyte growth factor from plasma of a patient with fulminant hepatic failure. *J. Clin. Invest* **81,** 414-419.

Golling,G., Amsterdam,A., Sun,Z., Antonelli,M., Maldonado,E., Chen,W., Burgess,S., Haldi,M., Artzt,K., Farrington,S. et al. (2002). Insertional mutagenesis in zebrafish rapidly identifies genes essential for early vertebrate development. *Nat. Genet.* **31,** 135-140.

Gong,Z., Ju,B., and Wan,H. (2001). Green fluorescent protein (GFP) transgenic fish and their applications. *Genetica* **111,** 213-225.

Grant,D.S., Kleinman,H.K., Goldberg,I.D., Bhargava,M.M., Nickoloff,B.J., Kinsella,J.L., Polverini,P., and Rosen,E.M. (1993). Scatter factor induces blood vessel formation in vivo. *Proc. Natl. Acad. Sci. U. S. A* **90,** 1937-1941.

Grierson,I., Heathcote,L., Hiscott,P., Hogg,P., Briggs,M., and Hagan,S. (2000). Hepatocyte growth factor/scatter factor in the eye. *Prog. Retin. Eye Res.* **19,** 779-802.

Griffioen,A.W. and Molema,G. (2000). Angiogenesis: potentials for pharmacologic intervention in the treatment of cancer, cardiovascular diseases, and chronic inflammation. *Pharmacol. Rev.* **52,** 237-268.

Grobstein,C. (1967). Mechanisms of organogenetic tissue interaction. *Natl. Cancer Inst. Monogr* **26,** 279-299.

Groves,J.A., Hammond,C.L., and Hughes,S.M. (2005). Fgf8 drives myogenic progression of a novel lateral fast muscle fibre population in zebrafish. *Development* **132,** 4211-4222.

Gu,H. and Neel,B.G. (2003). The "Gab" in signal transduction. *Trends Cell Biol.* **13,** 122-130.

Gual,P., Giordano,S., Williams,T.A., Rocchi,S., Van,O.E., and Comoglio,P.M. (2000). Sustained recruitment of phospholipase C-gamma to Gab1 is required for HGF-induced branching tubulogenesis. *Oncogene* **19,** 1509-1518.

Gualdi,R., Bossard,P., Zheng,M., Hamada,Y., Coleman,J.R., and Zaret,K.S. (1996). Hepatic specification of the gut endoderm in vitro: cell signaling and transcriptional control. *Genes Dev.* **10,** 1670-1682.

Gurdon,J.B. (1987). Embryonic induction--molecular prospects. *Development* **99,** 285-306.

Haffter,P., Granato,M., Brand,M., Mullins,M.C., Hammerschmidt,M., Kane,D.A., Odenthal,J., van Eeden,F.J., Jiang,Y.J., Heisenberg,C.P. et al. (1996). The identification of genes with unique and essential functions in the development of the zebrafish, Danio rerio. *Development* **123,** 1-36.

Haines,L., Neyt,C., Gautier,P., Keenan,D.G., Bryson-Richardson,R.J., Hollway,G.E., Cole,N.J., and Currie,P.D. (2004). Met and Hgf signaling controls hypaxial muscle and lateral line development in the zebrafish. *Development* **131,** 4857-4869.

Hamade,A., Deries,M., Begemann,G., Bally-Cuif,L., Genet,C., Sabatier,F., Bonnieu,A., and Cousin,X. (2006). Retinoic acid activates myogenesis in vivo through Fgf8 signalling. *Dev. Biol.* **289,** 127-140.

Hamanoue,M., Takemoto,N., Matsumoto,K., Nakamura,T., Nakajima,K., and Kohsaka,S. (1996). Neurotrophic effect of hepatocyte growth factor on central nervous system neurons in vitro. *J. Neurosci. Res.* **43,** 554-564.

Hashiya,N., Jo,N., Aoki,M., Matsumoto,K., Nakamura,T., Sato,Y., Ogata,N., Ogihara,T., Kaneda,Y., and Morishita,R. (2004). In vivo evidence of angiogenesis induced by transcription factor Ets-1: Ets-1 is located upstream of angiogenesis cascade. *Circulation* **109,** 3035-3041.

Hayashi,K. and Ozawa,E. (1995). Myogenic cell migration from somites is induced by tissue contact with medial region of the presumptive limb mesoderm in chick embryos. *Development* **121,** 661-669.

Hayashi,S., Morishita,R., Higaki,J., Aoki,M., Moriguchi,A., Kida,I., Yoshiki,S., Matsumoto,K., Nakamura,T., Kaneda,Y. et al. (1996). Autocrine-paracrine effects of overexpression of hepatocyte growth factor gene on growth of endothelial cells. *Biochem. Biophys. Res. Commun.* **220,** 539-545.

Helmbacher,F., Dessaud,E., Arber,S., deLapeyriere,O., Henderson,C.E., Klein,R., and Maina,F. (2003). Met signaling is required for recruitment of motor neurons to PEA3-positive motor pools. *Neuron* **39,** 767-777.

Herter,S., Piper,D.E., Aaron,W., Gabriele,T., Cutler,G., Cao,P., Bhatt,A.S., Choe,Y., Craik,C.S., Walker,N. et al. (2005). Hepatocyte growth factor is a preferred in vitro substrate for human hepsin, a membrane-anchored serine protease implicated in prostate and ovarian cancers. *Biochem. J.* **390,** 125-136.

Heymann,S., Koudrova,M., Arnold,H., Koster,M., and Braun,T. (1996). Regulation and function of SF/HGF during migration of limb muscle precursor cells in chicken. *Dev. Biol.* **180,** 566-578.

Hofmann,M., Schuster-Gossler,K., Watabe-Rudolph,M., Aulehla,A., Herrmann,B.G., and Gossler,A. (2004). WNT signaling, in synergy with T/TBX6, controls Notch signaling by regulating Dll1 expression in the presomitic mesoderm of mouse embryos. *Genes Dev.* **18,** 2712-2717.

Hogan,B.L. and Kolodziej,P.A. (2002). Organogenesis: molecular mechanisms of tubulogenesis. *Nat. Rev. Genet.* **3,** 513-523.

Horiguchi,N., Takayama,H., Toyoda,M., Otsuka,T., Fukusato,T., Merlino,G., Takagi,H., and Mori,M. (2002). Hepatocyte growth factor promotes hepatocarcinogenesis through c-Met autocrine activation and enhanced angiogenesis in transgenic mice treated with diethylnitrosamine. *Oncogene* **21,** 1791-1799.

Hornstein,E. and Tabin,C.J. (2005). Developmental biology: asymmetrical threat averted. *Nature* **435,** 155-156.

Hu,Z., Evarts,R.P., Fujio,K., Marsden,E.R., and Thorgeirsson,S.S. (1993). Expression of hepatocyte growth factor and c-met genes during hepatic differentiation and liver development in the rat. *Am. J. Pathol.* **142,** 1823-1830.

Hukriede,N., Fisher,D., Epstein,J., Joly,L., Tellis,P., Zhou,Y., Barbazuk,B., Cox,K., Fenton-Noriega,L., Hersey,C. et al. (2001). The LN54 radiation hybrid map of zebrafish expressed sequences. *Genome Res.* **11,** 2127-2132.

Hukriede,N.A., Joly,L., Tsang,M., Miles,J., Tellis,P., Epstein,J.A., Barbazuk,W.B., Li,F.N., Paw,B., Postlethwait,J.H. et al. (1999). Radiation hybrid mapping of the zebrafish genome. *Proc. Natl. Acad. Sci. U. S. A* **96,** 9745-9750.

Hussain,S.Z., Sneddon,T., Tan,X., Micsenyi,A., Michalopoulos,G.K., and Monga,S.P. (2004). Wnt impacts growth and differentiation in ex vivo liver development. *Exp. Cell Res.* **292,** 157-169.

Iulianella,A., Melton,K.R., and Trainor,P.A. (2003). Somitogenesis: breaking new boundaries. *Neuron* **40,** 11-14.

Iwazawa,T., Shiozaki,H., Doki,Y., Inoue,M., Tamura,S., Matsui,S., Monden,T., Matsumoto,K., Nakamura,T., and Monden,M. (1996). Primary human fibroblasts induce diverse tumor invasiveness: involvement of HGF as an important paracrine factor. *Jpn. J. Cancer Res.* **87,** 1134-1142.

Jeffers,M., Fiscella,M., Webb,C.P., Anver,M., Koochekpour,S., and Vande Woude,G.F. (1998). The mutationally activated Met receptor mediates motility and metastasis. *Proc. Natl. Acad. Sci. U. S. A* **95,** 14417-14422.

Jeffers,M., Rong,S., and Woude,G.F. (1996). Hepatocyte growth factor/scatter factor-Met signaling in tumorigenicity and invasion/metastasis. *J. Mol. Med.* **74,** 505-513.

Jiang,S.T., Chuang,W.J., and Tang,M.J. (2000a). Role of fibronectin deposition in branching morphogenesis of Madin-Darby canine kidney cells. *Kidney Int.* **57,** 1860-1867.

Jiang,Y.J., Aerne,B.L., Smithers,L., Haddon,C., Ish-Horowicz,D., and Lewis,J. (2000b). Notch signalling and the synchronization of the somite segmentation clock. *Nature* **408,** 475-479.

Johnson,M., Koukoulis,G., Matsumoto,K., Nakamura,T., and Iyer,A. (1993). Hepatocyte growth factor induces proliferation and morphogenesis in nonparenchymal epithelial liver cells. *Hepatology* **17,** 1052-1061.

Karlstrom,R.O., Talbot,W.S., and Schier,A.F. (1999). Comparative synteny cloning of zebrafish you-too: mutations in the Hedgehog target gli2 affect ventral forebrain patterning. *Genes Dev.* **13,** 388-393.

Kataoka,H., Itoh,H., and Koono,M. (2002a). Emerging multifunctional aspects of cellular serine proteinase inhibitors in tumor progression and tissue regeneration. *Pathol. Int.* **52,** 89-102.

Kataoka,H., Itoh,H., Nuki,Y., Hamasuna,R., Naganuma,S., Kitamura,N., and Shimomura,T. (2002b). Mouse hepatocyte growth factor (HGF) activator inhibitor type 2 lacking the first Kunitz domain potently inhibits the HGF activator. *Biochem. Biophys. Res. Commun.* **290,** 1096-1100.

Kataoka,H., Shimomura,T., Kawaguchi,T., Hamasuna,R., Itoh,H., Kitamura,N., Miyazawa,K., and Koono,M. (2000). Hepatocyte growth factor activator inhibitor type 1 is a specific cell surface binding protein of hepatocyte growth factor activator (HGFA) and regulates HGFA activity in the pericellular microenvironment. *J. Biol. Chem.* **275,** 40453-40462.

Kato,M., Yoshimura,S., Kokuzawa,J., Kitajima,H., Kaku,Y., Iwama,T., Shinoda,J., Kunisada,T., and Sakai,N. (2004). Hepatocyte growth factor promotes neuronal differentiation of neural stem cells derived from embryonic stem cells. *Neuroreport* **15,** 5-8.

Kawaguchi,T., Qin,L., Shimomura,T., Kondo,J., Matsumoto,K., Denda,K., and Kitamura,N. (1997). Purification and cloning of hepatocyte growth factor activator inhibitor type 2, a Kunitz-type serine protease inhibitor. *J. Biol. Chem.* **272,** 27558-27564.

Kawakami,Y., Raya,A., Raya,R.M., Rodriguez-Esteban,C., and Belmonte,J.C. (2005). Retinoic acid signalling links left-right asymmetric patterning and bilaterally symmetric somitogenesis in the zebrafish embryo. *Nature* **435,** 165-171.

Kawaida,K., Matsumoto,K., Shimazu,H., and Nakamura,T. (1994). Hepatocyte growth factor prevents acute renal failure and accelerates renal regeneration in mice. *Proc. Natl. Acad. Sci. U. S. A* **91,** 4357-4361.

Kelly,P.D., Chu,F., Woods,I.G., Ngo-Hazelett,P., Cardozo,T., Huang,H., Kimm,F., Liao,L., Yan,Y.L., Zhou,Y. et al. (2000). Genetic linkage mapping of zebrafish genes and ESTs. *Genome Res.* **10,** 558-567.

Khwaja,A., Lehmann,K., Marte,B.M., and Downward,J. (1998). Phosphoinositide 3-kinase induces scattering and tubulogenesis in epithelial cells through a novel pathway. *J. Biol. Chem.* **273,** 18793-18801.

Kimmel,C.B., Ballard,W.W., Kimmel,S.R., Ullmann,B., and Schilling,T.F. (1995). Stages of embryonic development of the zebrafish. *Dev. Dyn.* **203,** 253-310.

Kimmel,C.B., Warga,R.M., and Schilling,T.F. (1990). Origin and organization of the zebrafish fate map. *Development* **108,** 581-594.

Kirchhofer,D., Peek,M., Lipari,M.T., Billeci,K., Fan,B., and Moran,P. (2005). Hepsin activates pro-hepatocyte growth factor and is inhibited by hepatocyte growth factor activator inhibitor-1B (HAI-1B) and HAI-2. *FEBS Lett.* **579,** 1945-1950.

Kitadokoro,K., Tsuzuki,H., Okamoto,H., and Sato,T. (1994). Crystal structure analysis of a serine proteinase from Streptomyces fradiae at 0.16-nm resolution and molecular modeling of an acidic-amino-acid-specific proteinase. *Eur. J. Biochem.* **224,** 735-742.

Klinowska,T.C., Soriano,J.V., Edwards,G.M., Oliver,J.M., Valentijn,A.J., Montesano,R., and Streuli,C.H. (1999). Laminin and beta1 integrins are crucial for normal mammary gland development in the mouse. *Dev. Biol.* **215,** 13-32.

Kmiecik,T.E., Keller,J.R., Rosen,E., and Vande Woude,G.F. (1992). Hepatocyte growth factor is a synergistic factor for the growth of hematopoietic progenitor cells. *Blood* **80,** 2454-2457.

Knapik,E.W. (2000). ENU mutagenesis in zebrafish--from genes to complex diseases. *Mamm. Genome* **11,** 511-519.

Koibuchi,N., Kaneda,Y., Taniyama,Y., Matsumoto,K., Nakamura,T., Ogihara,T., and Morishita,R. (2004). Essential role of HGF (hepatocyte growth factor) in blood formation in Xenopus. *Blood* **103,** 3320-3325.

Kokuzawa,J., Yoshimura,S., Kitajima,H., Shinoda,J., Kaku,Y., Iwama,T., Morishita,R., Shimazaki,T., Okano,H., Kunisada,T. et al. (2003). Hepatocyte growth factor promotes proliferation and neuronal differentiation of neural stem cells from mouse embryos. *Mol. Cell Neurosci.* **24,** 190-197.

Komschlies,K.L., Grzegorzewski,K.J., and Wiltrout,R.H. (1995). Diverse immunological and hematological effects of interleukin 7: implications for clinical application. *J. Leukoc. Biol.* **58,** 623-633.

Koochekpour,S., Jeffers,M., Rulong,S., Taylor,G., Klineberg,E., Hudson,E.A., Resau,J.H., and Vande Woude,G.F. (1997). Met and hepatocyte growth factor/scatter factor expression in human gliomas. *Cancer Res.* **57,** 5391-5398.

Krasnoselsky,A., Massay,M.J., DeFrances,M.C., Michalopoulos,G., Zarnegar,R., and Ratner,N. (1994). Hepatocyte growth factor is a mitogen for Schwann cells and is present in neurofibromas. *J. Neurosci.* **14,** 7284-7290.

Kuba,K., Matsumoto,K., Date,K., Shimura,H., Tanaka,M., and Nakamura,T. (2000). HGF/NK4, a four-kringle antagonist of hepatocyte growth factor, is an angiogenesis inhibitor that suppresses tumor growth and metastasis in mice. *Cancer Res.* **60,** 6737-6743.

Kumar,S. and Hedges,S.B. (1998). A molecular timescale for vertebrate evolution. *Nature* **392,** 917-920.

Kwok,C., Korn,R.M., Davis,M.E., Burt,D.W., Critcher,R., McCarthy,L., Paw,B.H., Zon,L.I., Goodfellow,P.N., and Schmitt,K. (1998). Characterization of whole genome radiation hybrid mapping resources for non-mammalian vertebrates. *Nucleic Acids Res.* **26,** 3562-3566.

Lai,L., Chen,F., McKenna,S., and Goldschneider,I. (1998). Identification of an IL-7-associated pre-pro-B cell growth-stimulating factor (PPBSF). II. PPBSF is a covalently linked heterodimer of IL-7 and a Mr 30,000 cofactor. *J. Immunol.* **160,** 2280-2286.

Lai,L. and Goldschneider,I. (2001). Cutting edge: Identification of a hybrid cytokine consisting of IL-7 and the beta-chain of the hepatocyte growth factor/scatter factor. *J. Immunol.* **167,** 3550-3554.

Lai,L., Zeff,R.A., and Goldschneider,I. (2006). A recombinant single-chain IL-7/HGFbeta hybrid cytokine induces juxtacrine interactions of the IL-7 and HGF (c-Met) receptors and stimulates the proliferation of CFU-S12, CLPs, and pre-pro-B cells. *Blood* **107,** 1776-1784.

Lam,S.H., Wu,Y.L., Vega,V.B., Miller,L.D., Spitsbergen,J., Tong,Y., Zhan,H., Govindarajan,K.R., Lee,S., Mathavan,S. et al. (2006). Conservation of gene expression signatures between zebrafish and human liver tumors and tumor progression. *Nat. Biotechnol.* **24,** 73-75.

Lamszus,K., Jin,L., Fuchs,A., Shi,E., Chowdhury,S., Yao,Y., Polverini,P.J., Laterra,J., Goldberg,I.D., and Rosen,E.M. (1997). Scatter factor stimulates tumor growth and tumor angiogenesis in human breast cancers in the mammary fat pads of nude mice. *Lab Invest* **76,** 339-353.

Lamszus,K., Schmidt,N.O., Jin,L., Laterra,J., Zagzag,D., Way,D., Witte,M., Weinand,M., Goldberg,I.D., Westphal,M. et al. (1998). Scatter factor promotes motility of human glioma and neuromicrovascular endothelial cells. *Int. J. Cancer* **75,** 19-28.

Larionov,A., Krause,A., and Miller,W. (2005). A standard curve based method for relative real time PCR data processing. *BMC. Bioinformatics.* **6,** 62.

Lawson,N.D. and Weinstein,B.M. (2002). In vivo imaging of embryonic vascular development using transgenic zebrafish. *Dev. Biol.* **248,** 307-318.

Le Douarin,N.M., Houssaint,E., Jotereau,F.V., and Belo,M. (1975). Origin of hemopoietic stem cells in embryonic bursa of Fabricius and bone marrow studied through interspecific chimeras. *Proc. Natl. Acad. Sci. U. S. A* **72,** 2701-2705.

Lee,S.L., Dickson,R.B., and Lin,C.Y. (2000). Activation of hepatocyte growth factor and urokinase/plasminogen activator by matriptase, an epithelial membrane serine protease. *J. Biol. Chem.* **275,** 36720-36725.

Levkowitz,G., Waterman,H., Ettenberg,S.A., Katz,M., Tsygankov,A.Y., Alroy,I., Lavi,S., Iwai,K., Reiss,Y., Ciechanover,A. et al. (1999). Ubiquitin ligase activity and tyrosine phosphorylation underlie suppression of growth factor signaling by c-Cbl/Sli-1. *Mol. Cell* **4,** 1029-1040.

Li,G., Schaider,H., Satyamoorthy,K., Hanakawa,Y., Hashimoto,K., and Herlyn,M. (2001). Downregulation of E-cadherin and Desmoglein 1 by autocrine hepatocyte growth factor during melanoma development. *Oncogene* **20,** 8125-8135.

Lin,C.Y., Anders,J., Johnson,M., and Dickson,R.B. (1999). Purification and characterization of a complex containing matriptase and a Kunitz-type serine protease inhibitor from human milk. *J. Biol. Chem.* **274,** 18237-18242.

Liu,Y. (1998). The human hepatocyte growth factor receptor gene: complete structural organization and promoter characterization. *Gene* **215,** 159-169.

Lock,L.S., Maroun,C.R., Naujokas,M.A., and Park,M. (2002). Distinct recruitment and function of Gab1 and Gab2 in Met receptor-mediated epithelial morphogenesis. *Mol. Biol. Cell* **13,** 2132-2146.

Maina,F., Casagranda,F., Audero,E., Simeone,A., Comoglio,P.M., Klein,R., and Ponzetto,C. (1996). Uncoupling of Grb2 from the Met receptor in vivo reveals complex roles in muscle development. *Cell* **87,** 531-542.

Maina,F., Hilton,M.C., Andres,R., Wyatt,S., Klein,R., and Davies,A.M. (1998). Multiple roles for hepatocyte growth factor in sympathetic neuron development. *Neuron* **20,** 835-846.

Maina,F., Hilton,M.C., Ponzetto,C., Davies,A.M., and Klein,R. (1997). Met receptor signaling is required for sensory nerve development and HGF promotes axonal growth and survival of sensory neurons. *Genes Dev.* **11,** 3341-3350.

Maina,F. and Klein,R. (1999). Hepatocyte growth factor, a versatile signal for developing neurons. *Nat. Neurosci.* **2,** 213-217.

Malicki,J.J., Pujic,Z., Thisse,C., Thisse,B., and Wei,X. (2002). Forward and reverse genetic approaches to the analysis of eye development in zebrafish. *Vision Res.* **42,** 527-533.

Maroun,C.R., Naujokas,M.A., Holgado-Madruga,M., Wong,A.J., and Park,M. (2000). The tyrosine phosphatase SHP-2 is required for sustained activation of extracellular signal-regulated kinase and epithelial morphogenesis downstream from the met receptor tyrosine kinase. *Mol. Cell Biol.* **20,** 8513-8525.

Mars,W.M., Kim,T.H., Stolz,D.B., Liu,M.L., and Michalopoulos,G.K. (1996). Presence of urokinase in serum-free primary rat hepatocyte cultures and its role in activating hepatocyte growth factor. *Cancer Res.* **56,** 2837-2843.

Mars,W.M., Zarnegar,R., and Michalopoulos,G.K. (1993). Activation of hepatocyte growth factor by the plasminogen activators uPA and tPA. *Am. J. Pathol.* **143,** 949-958.

Martin,T.A., Harding,K.G., and Jiang,W.G. (1999). Regulation of angiogenesis and endothelial cell motility by matrix-bound fibroblasts. *Angiogenesis.* **3,** 69-76.

Martin,T.A., Mansel,R., and Jiang,W.G. (2001). Hepatocyte growth factor modulates vascular endothelial-cadherin expression in human endothelial cells. *Clin. Cancer Res.* **7,** 734-737.

Matsuda-Hashii,Y., Takai,K., Ohta,H., Fujisaki,H., Tokimasa,S., Osugi,Y., Ozono,K., Matsumoto,K., Nakamura,T., and Hara,J. (2004b). Hepatocyte growth factor plays roles in the induction and autocrine maintenance of bone marrow stromal cell IL-11, SDF-1 alpha, and stem cell factor. *Exp. Hematol.* **32,** 955-961.

Matsumoto,K. and Nakamura,T. (1996). Emerging multipotent aspects of hepatocyte growth factor. *J. Biochem. (Tokyo)* **119,** 591-600.

Matsumoto,K., Tajima,H., Hamanoue,M., Kohno,S., Kinoshita,T., and Nakamura,T. (1992). Identification and characterization of "injurin," an inducer of expression of the gene for hepatocyte growth factor. *Proc. Natl. Acad. Sci. U. S. A* **89,** 3800-3804.

Maulik,G., Kijima,T., Ma,P.C., Ghosh,S.K., Lin,J., Shapiro,G.I., Schaefer,E., Tibaldi,E., Johnson,B.E., and Salgia,R. (2002a). Modulation of the c-Met/hepatocyte growth factor pathway in small cell lung cancer. *Clin. Cancer Res.* **8,** 620-627.

Maulik,G., Madhiwala,P., Brooks,S., Ma,P.C., Kijima,T., Tibaldi,E.V., Schaefer,E., Parmar,K., and Salgia,R. (2002b). Activated c-Met signals through PI3K with dramatic effects on cytoskeletal functions in small cell lung cancer. *J. Cell Mol. Med.* **6,** 539-553.

Maulik,G., Shrikhande,A., Kijima,T., Ma,P.C., Morrison,P.T., and Salgia,R. (2002c). Role of the hepatocyte growth factor receptor, c-Met, in oncogenesis and potential for therapeutic inhibition. *Cytokine Growth Factor Rev.* **13,** 41-59.

McKenna,S.D., Chen,F., Lai,L., and Goldschneider,I. (1998). Identification of an IL-7-associated pre-pro-B cell growth-stimulating factor (PPBSF). I. Production of the non-IL-7 component by bone marrow stromal cells from IL-7 gene-deleted mice. *J. Immunol.* **160,** 2272-2279.

Medico,E., Gentile,A., Lo,C.C., Williams,T.A., Gambarotta,G., Trusolino,L., and Comoglio,P.M. (2001). Osteopontin is an autocrine mediator of hepatocyte growth factor-induced invasive growth. *Cancer Res.* **61,** 5861-5868.

Michalopoulos,G., Houck,K.A., Dolan,M.L., and Leutteke,N.C. (1984). Control of hepatocyte replication by two serum factors. *Cancer Res.* **44,** 4414-4419.

Miyazawa,K., Shimomura,T., Kitamura,A., Kondo,J., Morimoto,Y., and Kitamura,N. (1993). Molecular cloning and sequence analysis of the cDNA for a

human serine protease reponsible for activation of hepatocyte growth factor. Structural similarity of the protease precursor to blood coagulation factor XII. *J. Biol. Chem.* **268,** 10024-10028.

Miyazawa,K., Tsubouchi,H., Naka,D., Takahashi,K., Okigaki,M., Arakaki,N., Nakayama,H., Hirono,S., Sakiyama,O., Takahashi,K. et al. (1989). Molecular cloning and sequence analysis of cDNA for human hepatocyte growth factor. *Biochem. Biophys. Res. Commun.* **163,** 967-973.

Mizuno,K., Higuchi,O., Ihle,J.N., and Nakamura,T. (1993). Hepatocyte growth factor stimulates growth of hematopoietic progenitor cells. *Biochem. Biophys. Res. Commun.* **194,** 178-186.

Mizuno,K., Inoue,H., Hagiya,M., Shimizu,S., Nose,T., Shimohigashi,Y., and Nakamura,T. (1994). Hairpin loop and second kringle domain are essential sites for heparin binding and biological activity of hepatocyte growth factor. *J. Biol. Chem.* **269,** 1131-1136.

Montesano,R., Matsumoto,K., Nakamura,T., and Orci,L. (1991a). Identification of a fibroblast-derived epithelial morphogen as hepatocyte growth factor. *Cell* **67,** 901-908.

Moriyama,T., Kataoka,H., Kawano,H., Yokogami,K., Nakano,S., Goya,T., Uchino,H., Koono,M., and Wakisaka,S. (1998). Comparative analysis of expression of hepatocyte growth factor and its receptor, c-met, in gliomas, meningiomas and schwannomas in humans. *Cancer Lett.* **124,** 149-155.

Muller,M., Morotti,A., and Ponzetto,C. (2002). Activation of NF-kappaB is essential for hepatocyte growth factor-mediated proliferation and tubulogenesis. *Mol. Cell Biol.* **22,** 1060-1072.

Mullins,M.C. (1999). Embryonic axis formation in the zebrafish. *Methods Cell Biol.* **59,** 159-178.

Nabeshima,K., Shimao,Y., Inoue,T., Itoh,H., Kataoka,H., and Koono,M. (1998). Hepatocyte growth factor/scatter factor induces not only scattering but also cohort migration of human colorectal-adenocarcinoma cells. *Int. J. Cancer* **78,** 750-759.

Nagashima,M., Hasegawa,J., Kato,K., Yamazaki,J., Nishigai,K., Ishiwata,T., Asano,G., and Yoshino,S. (2001). Hepatocyte growth factor (HGF), HGF activator, and c-Met in synovial tissues in rheumatoid arthritis and osteoarthritis. *J. Rheumatol.* **28,** 1772-1778.

Naka,D., Ishii,T., Yoshiyama,Y., Miyazawa,K., Hara,H., Hishida,T., and Kidamura,N. (1992). Activation of hepatocyte growth factor by proteolytic conversion of a single chain form to a heterodimer. *J. Biol. Chem.* **267,** 20114-20119.

Nakagami,H., Morishita,R., Yamamoto,K., Taniyama,Y., Aoki,M., Matsumoto,K., Nakamura,T., Kaneda,Y., Horiuchi,M., and Ogihara,T. (2001). Mitogenic and antiapoptotic actions of hepatocyte growth factor through ERK, STAT3, and AKT in endothelial cells. *Hypertension* **37,** 581-586.

Nakagami,H., Morishita,R., Yamamoto,K., Taniyama,Y., Aoki,M., Yamasaki,K., Matsumoto,K., Nakamura,T., Kaneda,Y., and Ogihara,T. (2002). Hepatocyte growth factor prevents endothelial cell death through inhibition of bax translocation from cytosol to mitochondrial membrane. *Diabetes* **51,** 2604-2611.

Nakamura,T., Nawa,K., and Ichihara,A. (1984). Partial purification and characterization of hepatocyte growth factor from serum of hepatectomized rats. *Biochem. Biophys. Res. Commun.* **122,** 1450-1459.

Nakamura,T., Nishizawa,T., Hagiya,M., Seki,T., Shimonishi,M., Sugimura,A., Tashiro,K., and Shimizu,S. (1989). Molecular cloning and expression of human hepatocyte growth factor. *Nature* **342,** 440-443.

Nakamura,T., Teramoto,H., and Ichihara,A. (1986). Purification and characterization of a growth factor from rat platelets for mature parenchymal hepatocytes in primary cultures. *Proc. Natl. Acad. Sci. U. S. A* **83,** 6489-6493.

Nakamura,Y., Morishita,R., Higaki,J., Kida,I., Aoki,M., Moriguchi,A., Yamada,K., Hayashi,S., Yo,Y., Matsumoto,K. et al. (1995a). Expression of local hepatocyte growth factor system in vascular tissues. *Biochem. Biophys. Res. Commun.* **215,** 483-488.

Nakashiro,K., Okamoto,M., Hayashi,Y., and Oyasu,R. (2000). Hepatocyte growth factor secreted by prostate-derived stromal cells stimulates growth of androgen-independent human prostatic carcinoma cells. *Am. J. Pathol.* **157,** 795-803.

Naldini,L., Tamagnone,L., Vigna,E., Sachs,M., Hartmann,G., Birchmeier,W., Daikuhara,Y., Tsubouchi,H., Blasi,F., and Comoglio,P.M. (1992). Extracellular proteolytic cleavage by urokinase is required for activation of hepatocyte growth factor/scatter factor. *EMBO J.* **11,** 4825-4833.

Naldini,L., Weidner,K.M., Vigna,E., Gaudino,G., Bardelli,A., Ponzetto,C., Narsimhan,R.P., Hartmann,G., Zarnegar,R., Michalopoulos,G.K. et al. (1991). Scatter factor and hepatocyte growth factor are indistinguishable ligands for the MET receptor. *EMBO J.* **10,** 2867-2878.

Namen,A.E., Lupton,S., Hjerrild,K., Wignall,J., Mochizuki,D.Y., Schmierer,A., Mosley,B., March,C.J., Urdal,D., and Gillis,S. (1988a). Stimulation of B-cell progenitors by cloned murine interleukin-7. *Nature* **333,** 571-573.

Namen,A.E., Schmierer,A.E., March,C.J., Overell,R.W., Park,L.S., Urdal,D.L., and Mochizuki,D.Y. (1988b). B cell precursor growth-promoting activity. Purification and characterization of a growth factor active on lymphocyte precursors. *J. Exp. Med.* **167,** 988-1002.

Nasevicius,A. and Ekker,S.C. (2000). Effective targeted gene 'knockdown' in zebrafish. *Nat. Genet.* **26,** 216-220.

Nguyen,L., Holgado-Madruga,M., Maroun,C., Fixman,E.D., Kamikura,D., Fournier,T., Charest,A., Tremblay,M.L., Wong,A.J., and Park,M. (1997). Association of the multisubstrate docking protein Gab1 with the hepatocyte growth

factor receptor requires a functional Grb2 binding site involving tyrosine 1356. *J. Biol. Chem.* **272,** 20811-20819.

Niranjan,B., Buluwela,L., Yant,J., Perusinghe,N., Atherton,A., Phippard,D., Dale,T., Gusterson,B., and Kamalati,T. (1995). HGF/SF: a potent cytokine for mammary growth, morphogenesis and development. *Development* **121,** 2897-2908.

Nishino,T., Hisha,H., Nishino,N., Adachi,M., and Ikehara,S. (1995). Hepatocyte growth factor as a hematopoietic regulator. *Blood* **85,** 3093-3100.

Nobes,C.D. and Hall,A. (1995a). Rho, rac and cdc42 GTPases: regulators of actin structures, cell adhesion and motility. *Biochem. Soc. Trans.* **23,** 456-459.

Nobes,C.D. and Hall,A. (1995b). Rho, rac, and cdc42 GTPases regulate the assembly of multimolecular focal complexes associated with actin stress fibers, lamellipodia, and filopodia. *Cell* **81,** 53-62.

Noji,S., Tashiro,K., Koyama,E., Nohno,T., Ohyama,K., Taniguchi,S., and Nakamura,T. (1990). Expression of hepatocyte growth factor gene in endothelial and Kupffer cells of damaged rat livers, as revealed by in situ hybridization. *Biochem. Biophys. Res. Commun.* **173,** 42-47.

Novak,K.D., Prevette,D., Wang,S., Gould,T.W., and Oppenheim,R.W. (2000). Hepatocyte growth factor/scatter factor is a neurotrophic survival factor for lumbar but not for other somatic motoneurons in the chick embryo. *J. Neurosci.* **20,** 326-337.

O'Brien,L.E., Tang,K., Kats,E.S., Schutz-Geschwender,A., Lipschutz,J.H., and Mostov,K.E. (2004). ERK and MMPs sequentially regulate distinct stages of epithelial tubule development. *Dev. Cell* **7,** 21-32.

Otonkoski,T., Cirulli,V., Beattie,M., Mally,M.I., Soto,G., Rubin,J.S., and Hayek,A. (1996). A role for hepatocyte growth factor/scatter factor in fetal mesenchyme-induced pancreatic beta-cell growth. *Endocrinology* **137,** 3131-3139.

Otte,J.M., Kiehne,K., Schmitz,F., Folsch,U.R., and Herzig,K.H. (2000). C-met protooncogene expression and its regulation by cytokines in the regenerating pancreas and in pancreatic cancer cells. *Scand. J. Gastroenterol.* **35,** 90-95.

Park,M., Dean,M., Cooper,C.S., Schmidt,M., O'Brien,S.J., Blair,D.G., and Vande Woude,G.F. (1986). Mechanism of met oncogene activation. *Cell* **45,** 895-904.

Park,M., Dean,M., Kaul,K., Braun,M.J., Gonda,M.A., and Vande,W.G. (1987). Sequence of MET protooncogene cDNA has features characteristic of the tyrosine kinase family of growth-factor receptors. *Proc. Natl. Acad. Sci. U. S. A* **84,** 6379-6383.

Parker,M.H., Seale,P., and Rudnicki,M.A. (2003). Looking back to the embryo: defining transcriptional networks in adult myogenesis. *Nat. Rev. Genet.* **4,** 497-507.

Parr,C., Davies,G., Nakamura,T., Matsumoto,K., Mason,M.D., and Jiang,W.G. (2001). The HGF/SF-induced phosphorylation of paxillin, matrix adhesion, and

invasion of prostate cancer cells were suppressed by NK4, an HGF/SF variant. *Biochem. Biophys. Res. Commun.* **285,** 1330-1337.

Petrelli,A., Gilestro,G.F., Lanzardo,S., Comoglio,P.M., Migone,N., and Giordano,S. (2002). The endophilin-CIN85-Cbl complex mediates ligand-dependent downregulation of c-Met. *Nature* **416,** 187-190.

Pollack,A.L., Runyan,R.B., and Mostov,K.E. (1998). Morphogenetic mechanisms of epithelial tubulogenesis: MDCK cell polarity is transiently rearranged without loss of cell-cell contact during scatter factor/hepatocyte growth factor-induced tubulogenesis. *Dev. Biol.* **204,** 64-79.

Ponzetto,C., Bardelli,A., Zhen,Z., Maina,F., dalla,Z.P., Giordano,S., Graziani,A., Panayotou,G., and Comoglio,P.M. (1994). A multifunctional docking site mediates signaling and transformation by the hepatocyte growth factor/scatter factor receptor family. *Cell* **77,** 261-271.

Postlethwait,J.H. and Talbot,W.S. (1997). Zebrafish genomics: from mutants to genes. *Trends Genet.* **13,** 183-190.

Postlethwait,J.H., Woods,I.G., Ngo-Hazelett,P., Yan,Y.L., Kelly,P.D., Chu,F., Huang,H., Hill-Force,A., and Talbot,W.S. (2000). Zebrafish comparative genomics and the origins of vertebrate chromosomes. *Genome Res.* **10,** 1890-1902.

Postlethwait,J.H., Yan,Y.L., Gates,M.A., Horne,S., Amores,A., Brownlie,A., Donovan,A., Egan,E.S., Force,A., Gong,Z. et al. (1998). Vertebrate genome evolution and the zebrafish gene map. *Nat. Genet.* **18,** 345-349.

Potempa,S. and Ridley,A.J. (1998). Activation of both MAP kinase and phosphatidylinositide 3-kinase by Ras is required for hepatocyte growth factor/scatter factor-induced adherens junction disassembly. *Mol. Biol. Cell* **9,** 2185-2200.

Pourquie,O. (2003). The segmentation clock: converting embryonic time into spatial pattern. *Science* **301,** 328-330.

Powell,E.M., Mars,W.M., and Levitt,P. (2001). Hepatocyte growth factor/scatter factor is a motogen for interneurons migrating from the ventral to dorsal telencephalon. *Neuron* **30,** 79-89.

Purdie,K.J., Whitley,G.S., Johnstone,A.P., and Cartwright,J.E. (2002). Hepatocyte growth factor-induced endothelial cell motility is mediated by the upregulation of inducible nitric oxide synthase expression. *Cardiovasc. Res.* **54,** 659-668.

Qin,L., Denda,K., Shimomura,T., Kawaguchi,T., and Kitamura,N. (1998). Functional characterization of Kunitz domains in hepatocyte growth factor activator inhibitor type 2. *FEBS Lett.* **436,** 111-114.

Reifers,F., Bohli,H., Walsh,E.C., Crossley,P.H., Stainier,D.Y., and Brand,M. (1998). Fgf8 is mutated in zebrafish acerebellar (ace) mutants and is required for maintenance of midbrain-hindbrain boundary development and somitogenesis. *Development* **125,** 2381-2395.

Reisinger,K., Kaufmann,R., and Gille,J. (2003). Increased Sp1 phosphorylation as a mechanism of hepatocyte growth factor (HGF/SF)-induced vascular endothelial growth factor (VEGF/VPF) transcription. *J. Cell Sci.* **116,** 225-238.

Risau,W. (1997). Mechanisms of angiogenesis. *Nature* **386,** 671-674.

Rosen,E.M., Meromsky,L., Setter,E., Vinter,D.W., and Goldberg,I.D. (1990). Smooth muscle-derived factor stimulates mobility of human tumor cells. *Invasion Metastasis* **10,** 49-64.

Royal,I. and Park,M. (1995a). Hepatocyte growth factor-induced scatter of Madin-Darby canine kidney cells requires phosphatidylinositol 3-kinase. *J. Biol. Chem.* **270,** 27780-27787.

Rubin,J.S., Chan,A.M., Bottaro,D.P., Burgess,W.H., Taylor,W.G., Cech,A.C., Hirschfield,D.W., Wong,J., Miki,T., Finch,P.W. et al. (1991). A broad-spectrum human lung fibroblast-derived mitogen is a variant of hepatocyte growth factor. *Proc. Natl. Acad. Sci. U. S. A* **88,** 415-419.

Sachs,M., Weidner,K.M., Brinkmann,V., Walther,I., Obermeier,A., Ullrich,A., and Birchmeier,W. (1996). Motogenic and morphogenic activity of epithelial receptor tyrosine kinases. *J. Cell Biol.* **133,** 1095-1107.

Sadler,K.C., Amsterdam,A., Soroka,C., Boyer,J., and Hopkins,N. (2005). A genetic screen in zebrafish identifies the mutants vps18, nf2 and foie gras as models of liver disease. *Development* **132,** 3561-3572.

Sadler,K.C., Krahn,K.N., Gaur,N.A., and Ukomadu,C. (2007). Liver growth in the embryo and during liver regeneration in zebrafish requires the cell cycle regulator, uhrf1. *Proc. Natl. Acad. Sci. U. S. A* **104,** 1570-1575.

Saelman,E.U., Keely,P.J., and Santoro,S.A. (1995). Loss of MDCK cell alpha 2 beta 1 integrin expression results in reduced cyst formation, failure of hepatocyte growth factor/scatter factor-induced branching morphogenesis, and increased apoptosis. *J. Cell Sci.* **108 (Pt 11),** 3531-3540.

Salgia,R., Li,J.L., Lo,S.H., Brunkhorst,B., Kansas,G.S., Sobhany,E.S., Sun,Y., Pisick,E., Hallek,M., Ernst,T. et al. (1995). Molecular cloning of human paxillin, a focal adhesion protein phosphorylated by P210BCR/ABL. *J. Biol. Chem.* **270,** 5039-5047.

Santos,O.F., Barros,E.J., Yang,X.M., Matsumoto,K., Nakamura,T., Park,M., and Nigam,S.K. (1994). Involvement of hepatocyte growth factor in kidney development. *Dev. Biol.* **163,** 525-529.

Sattler,M., Pisick,E., Morrison,P.T., and Salgia,R. (2000). Role of the cytoskeletal protein paxillin in oncogenesis. *Crit Rev. Oncog.* **11,** 63-76.

Sattler,M. and Salgia,R. (1998). Role of the adapter protein CRKL in signal transduction of normal hematopoietic and BCR/ABL-transformed cells. *Leukemia* **12,** 637-644.

Saucier,C., Papavasiliou,V., Palazzo,A., Naujokas,M.A., Kremer,R., and Park,M. (2002). Use of signal specific receptor tyrosine kinase oncoproteins reveals that pathways downstream from Grb2 or Shc are sufficient for cell transformation and metastasis. *Oncogene* **21,** 1800-1811.

Saxen,L. and Sariola,H. (1987). Early organogenesis of the kidney. *Pediatr. Nephrol.* **1,** 385-392.

Schaeper,U., Gehring,N.H., Fuchs,K.P., Sachs,M., Kempkes,B., and Birchmeier,W. (2000). Coupling of Gab1 to c-Met, Grb2, and Shp2 mediates biological responses. *J. Cell Biol.* **149,** 1419-1432.

Schaller,M.D. and Sasaki,T. (1997). Differential signaling by the focal adhesion kinase and cell adhesion kinase beta. *J. Biol. Chem.* **272,** 25319-25325.

Schmid,B., Furthauer,M., Connors,S.A., Trout,J., Thisse,B., Thisse,C., and Mullins,M.C. (2000). Equivalent genetic roles for bmp7/snailhouse and bmp2b/swirl in dorsoventral pattern formation. *Development* **127,** 957-967.

Schmidt,C., Bladt,F., Goedecke,S., Brinkmann,V., Zschiesche,W., Sharpe,M., Gherardi,E., and Birchmeier,C. (1995). Scatter factor/hepatocyte growth factor is essential for liver development. *Nature* **373,** 699-702.

Schulte-Merker,S. (2000). Zebrafish functional genomics. Interview by Joanne Wixon. *Yeast* **17,** 232-234.

Seki,T., Hagiya,M., Shimonishi,M., Nakamura,T., and Shimizu,S. (1991). Organization of the human hepatocyte growth factor-encoding gene. *Gene* **102,** 213-219.

Selden,C., Jones,M., Wade,D., and Hodgson,H. (1990). Hepatotropin mRNA expression in human foetal liver development and in liver regeneration. *FEBS Lett.* **270,** 81-84.

Sengupta,S., Gherardi,E., Sellers,L.A., Wood,J.M., Sasisekharan,R., and Fan,T.P. (2003). Hepatocyte growth factor/scatter factor can induce angiogenesis independently of vascular endothelial growth factor. *Arterioscler. Thromb. Vasc. Biol.* **23,** 69-75.

Shih,J. and Fraser,S.E. (1996). Characterizing the zebrafish organizer: microsurgical analysis at the early-shield stage. *Development* **122,** 1313-1322.

Shimomura,T., Denda,K., Kitamura,A., Kawaguchi,T., Kito,M., Kondo,J., Kagaya,S., Qin,L., Takata,H., Miyazawa,K. et al. (1997). Hepatocyte growth factor activator inhibitor, a novel Kunitz-type serine protease inhibitor. *J. Biol. Chem.* **272,** 6370-6376.

Shimomura,T., Kondo,J., Ochiai,M., Naka,D., Miyazawa,K., Morimoto,Y., and Kitamura,N. (1993). Activation of the zymogen of hepatocyte growth factor activator by thrombin. *J. Biol. Chem.* **268,** 22927-22932.

Shimomura,T., Miyazawa,K., Komiyama,Y., Hiraoka,H., Naka,D., Morimoto,Y., and Kitamura,N. (1995). Activation of hepatocyte growth factor by two homologous proteases, blood-coagulation factor XIIa and hepatocyte growth factor activator. *Eur. J. Biochem.* **229,** 257-261.

Shimomura,T., Ochiai,M., Kondo,J., and Morimoto,Y. (1992). A novel protease obtained from FBS-containing culture supernatant, that processes single chain form hepatocyte growth factor to two chain form in serum-free culture. *Cytotechnology* **8,** 219-229.

Sonnenberg,E., Meyer,D., Weidner,K.M., and Birchmeier,C. (1993). Scatter factor/hepatocyte growth factor and its receptor, the c-met tyrosine kinase, can mediate a signal exchange between mesenchyme and epithelia during mouse development. *J. Cell Biol.* **123,** 223-235.

Soriano,J.V., Pepper,M.S., Nakamura,T., Orci,L., and Montesano,R. (1995). Hepatocyte growth factor stimulates extensive development of branching duct-like structures by cloned mammary gland epithelial cells. *J. Cell Sci.* **108 (Pt 2),** 413-430.

Spix,J.K., Chay,E.Y., Block,E.R., and Klarlund,J.K. (2007). Hepatocyte growth factor induces epithelial cell motility through transactivation of the epidermal growth factor receptor. *Exp. Cell Res.*

Stainier,D.Y. (2001). Zebrafish genetics and vertebrate heart formation. *Nat. Rev. Genet.* **2,** 39-48.

Stainier,D.Y. (2002). A glimpse into the molecular entrails of endoderm formation. *Genes Dev.* **16,** 893-907.

Stella,M.C. and Comoglio,P.M. (1999b). HGF: a multifunctional growth factor controlling cell scattering. *Int. J. Biochem. Cell Biol.* **31,** 1357-1362.

Stern,C.D., Ireland,G.W., Herrick,S.E., Gherardi,E., Gray,J., Perryman,M., and Stoker,M. (1990). Epithelial scatter factor and development of the chick embryonic axis. *Development* **110,** 1271-1284.

Stickney,H.L., Barresi,M.J., and Devoto,S.H. (2000). Somite development in zebrafish. *Dev. Dyn.* **219,** 287-303.

Stoker,M., Gherardi,E., Perryman,M., and Gray,J. (1987). Scatter factor is a fibroblast-derived modulator of epithelial cell mobility. *Nature* **327,** 239-242.

Streit,A., Sockanathan,S., Perez,L., Rex,M., Scotting,P.J., Sharpe,P.T., Lovell-Badge,R., and Stern,C.D. (1997). Preventing the loss of competence for neural induction: HGF/SF, L5 and Sox-2. *Development* **124,** 1191-1202.

Streit,A., Stern,C.D., Thery,C., Ireland,G.W., Aparicio,S., Sharpe,M.J., and Gherardi,E. (1995). A role for HGF/SF in neural induction and its expression in Hensen's node during gastrulation. *Development* **121,** 813-824.

Tabata,M.J., Kim,K., Liu,J.G., Yamashita,K., Matsumura,T., Kato,J., Iwamoto,M., Wakisaka,S., Matsumoto,K., Nakamura,T. et al. (1996). Hepatocyte

growth factor is involved in the morphogenesis of tooth germ in murine molars. *Development* **122,** 1243-1251.

Tajbakhsh,S., Rocancourt,D., Cossu,G., and Buckingham,M. (1997). Redefining the genetic hierarchies controlling skeletal myogenesis: Pax-3 and Myf-5 act upstream of MyoD. *Cell* **89,** 127-138.

Takai,K., Hara,J., Matsumoto,K., Hosoi,G., Osugi,Y., Tawa,A., Okada,S., and Nakamura,T. (1997). Hepatocyte growth factor is constitutively produced by human bone marrow stromal cells and indirectly promotes hematopoiesis. *Blood* **89,** 1560-1565.

Takayama,H., La Rochelle,W.J., Anver,M., Bockman,D.E., and Merlino,G. (1996). Scatter factor/hepatocyte growth factor as a regulator of skeletal muscle and neural crest development. *Proc. Natl. Acad. Sci. U. S. A* **93,** 5866-5871.

Talbot,W.S. and Hopkins,N. (2000a). Zebrafish mutations and functional analysis of the vertebrate genome. *Genes Dev.* **14,** 755-762.

Tamura,S., Sugawara,T., Tokoro,Y., Taniguchi,H., Fukao,K., Nakauchi,H., and Takahama,Y. (1998). Expression and function of c-Met, a receptor for hepatocyte growth factor, during T-cell development. *Scand. J. Immunol.* **47,** 296-301.

Tashiro,K., Hagiya,M., Nishizawa,T., Seki,T., Shimonishi,M., Shimizu,S., and Nakamura,T. (1990). Deduced primary structure of rat hepatocyte growth factor and expression of the mRNA in rat tissues. *Proc. Natl. Acad. Sci. U. S. A* **87,** 3200-3204.

Thery,C., Sharpe,M.J., Batley,S.J., Stern,C.D., and Gherardi,E. (1995). Expression of HGF/SF, HGF1/MSP, and c-met suggests new functions during early chick development. *Dev. Genet.* **17,** 90-101.

Thien,C.B. and Langdon,W.Y. (2001). Cbl: many adaptations to regulate protein tyrosine kinases. *Nat. Rev. Mol. Cell Biol.* **2,** 294-307.

Tomita,N., Morishita,R., Taniyama,Y., Koike,H., Aoki,M., Shimizu,H., Matsumoto,K., Nakamura,T., Kaneda,Y., and Ogihara,T. (2003). Angiogenic property of hepatocyte growth factor is dependent on upregulation of essential transcription factor for angiogenesis, ets-1. *Circulation* **107,** 1411-1417.

Tuck,A.B., Park,M., Sterns,E.E., Boag,A., and Elliott,B.E. (1996). Coexpression of hepatocyte growth factor and receptor (Met) in human breast carcinoma. *Am. J. Pathol.* **148,** 225-232.

Turner,C.E. (2000a). Paxillin and focal adhesion signalling. *Nat. Cell Biol.* **2,** E231-E236.

Turner,C.E. (2000b). Paxillin interactions. *J. Cell Sci.* **113 Pt 23,** 4139-4140.

Uehara,Y., Minowa,O., Mori,C., Shiota,K., Kuno,J., Noda,T., and Kitamura,N. (1995). Placental defect and embryonic lethality in mice lacking hepatocyte growth factor/scatter factor. *Nature* **373,** 702-705.

van,A.J., Sehgal,S., Kukes,A., Brady,C., Barasch,J., Yang,J., and Huan,Y. (2001). Activation of hepatocyte growth factor (HGF) by endogenous HGF activator is required for metanephric kidney morphogenesis in vitro. *J. Biol. Chem.* **276,** 15099-15106.

Van,B.E., Witzenbichler,B., Chen,D., Silver,M., Chang,L., Schwall,R., and Isner,J.M. (1998). Potentiated angiogenic effect of scatter factor/hepatocyte growth factor via induction of vascular endothelial growth factor: the case for paracrine amplification of angiogenesis. *Circulation* **97,** 381-390.

van,d., V, Taher,T.E., Keehnen,R.M., Smit,L., Groenink,M., and Pals,S.T. (1997). Paracrine regulation of germinal center B cell adhesion through the c-met-hepatocyte growth factor/scatter factor pathway. *J. Exp. Med.* **185,** 2121-2131.

Vermot,J., Gallego,L.J., Fraulob,V., Niederreither,K., Chambon,P., and Dolle,P. (2005). Retinoic acid controls the bilateral symmetry of somite formation in the mouse embryo. *Science* **308,** 563-566.

Vermot,J. and Pourquie,O. (2005). Retinoic acid coordinates somitogenesis and left-right patterning in vertebrate embryos. *Nature* **435,** 215-220.

Wan,H., He,J., Ju,B., Yan,T., Lam,T.J., and Gong,Z. (2002). Generation of two-color transgenic zebrafish using the green and red fluorescent protein reporter genes gfp and rfp. *Mar. Biotechnol. (NY)* **4,** 146-154.

Wang,R., Ferrell,L.D., Faouzi,S., Maher,J.J., and Bishop,J.M. (2001). Activation of the Met receptor by cell attachment induces and sustains hepatocellular carcinomas in transgenic mice. *J. Cell Biol.* **153,** 1023-1034.

Wang,X., DeFrances,M.C., Dai,Y., Pediaditakis,P., Johnson,C., Bell,A., Michalopoulos,G.K., and Zarnegar,R. (2002). A mechanism of cell survival: sequestration of Fas by the HGF receptor Met. *Mol. Cell* **9,** 411-421.

Wang,X., Zhou,Y., Kim,H.P., Song,R., Zarnegar,R., Ryter,S.W., and Choi,A.M. (2004). Hepatocyte growth factor protects against hypoxia/reoxygenation-induced apoptosis in endothelial cells. *J. Biol. Chem.* **279,** 5237-5243.

Ward,A.B., Warga,R.M., and Prince,V.E. (2007). Origin of the zebrafish endocrine and exocrine pancreas. *Dev. Dyn.* **236,** 1558-1569.

Ward,A.C. and Lieschke,G.J. (2002). The zebrafish as a model system for human disease. *Front Biosci.* **7,** d827-d833.

Weidner,K.M., Arakaki,N., Hartmann,G., Vandekerckhove,J., Weingart,S., Rieder,H., Fonatsch,C., Tsubouchi,H., Hishida,T., Daikuhara,Y. et al. (1991). Evidence for the identity of human scatter factor and human hepatocyte growth factor. *Proc. Natl. Acad. Sci. U. S. A* **88,** 7001-7005.

Weidner,K.M., Behrens,J., Vandekerckhove,J., and Birchmeier,W. (1990). Scatter factor: molecular characteristics and effect on the invasiveness of epithelial cells. *J. Cell Biol.* **111,** 2097-2108.

Weidner,K.M., Di,C.S., Sachs,M., Brinkmann,V., Behrens,J., and Birchmeier,W. (1996). Interaction between Gab1 and the c-Met receptor tyrosine kinase is responsible for epithelial morphogenesis. *Nature* **384,** 173-176.

Weidner,K.M., Sachs,M., and Birchmeier,W. (1993). The Met receptor tyrosine kinase transduces motility, proliferation, and morphogenic signals of scatter factor/hepatocyte growth factor in epithelial cells. *J. Cell Biol.* **121,** 145-154.

Weimar,I.S., Miranda,N., Muller,E.J., Hekman,A., Kerst,J.M., de Gast,G.C., and Gerritsen,W.R. (1998). Hepatocyte growth factor/scatter factor (HGF/SF) is produced by human bone marrow stromal cells and promotes proliferation, adhesion and survival of human hematopoietic progenitor cells (CD34+). *Exp. Hematol.* **26,** 885-894.

Weinstein,B.M., Stemple,D.L., Driever,W., and Fishman,M.C. (1995). Gridlock, a localized heritable vascular patterning defect in the zebrafish. *Nat. Med.* **1,** 1143-1147.

Weisberg,E., Sattler,M., Ewaniuk,D.S., and Salgia,R. (1997). Role of focal adhesion proteins in signal transduction and oncogenesis. *Crit Rev. Oncog.* **8,** 343-358.

Wells,J.M. and Melton,D.A. (1999). Vertebrate endoderm development. *Annu. Rev. Cell Dev. Biol.* **15,** 393-410.

Westerfield,M., Doerry,E., and Douglas,S. (1999a). Zebrafish in the Net. *Trends Genet.* **15,** 248-249.

Westerfield,M., Doerry,E., Kirkpatrick,A.E., and Douglas,S.A. (1999b). Zebrafish informatics and the ZFIN database. *Methods Cell Biol.* **60,** 339-355.

Wojta,J., Kaun,C., Breuss,J.M., Koshelnick,Y., Beckmann,R., Hattey,E., Mildner,M., Weninger,W., Nakamura,T., Tschachler,E. et al. (1999b). Hepatocyte growth factor increases expression of vascular endothelial growth factor and plasminogen activator inhibitor-1 in human keratinocytes and the vascular endothelial growth factor receptor flk-1 in human endothelial cells. *Lab Invest* **79,** 427-438.

Wojta,J., Nakamura,T., Fabry,A., Hufnagl,P., Beckmann,R., McGrath,K., and Binder,B.R. (1994). Hepatocyte growth factor stimulates expression of plasminogen activator inhibitor type 1 and tissue factor in HepG2 cells. *Blood* **84,** 151-157.

Wolff,C., Roy,S., and Ingham,P.W. (2003). Multiple muscle cell identities induced by distinct levels and timing of hedgehog activity in the zebrafish embryo. *Curr. Biol.* **13,** 1169-1181.

Wong,V., Glass,D.J., Arriaga,R., Yancopoulos,G.D., Lindsay,R.M., and Conn,G. (1997). Hepatocyte growth factor promotes motor neuron survival and synergizes with ciliary neurotrophic factor. *J. Biol. Chem.* **272,** 5187-5191.

Woods,I.G., Kelly,P.D., Chu,F., Ngo-Hazelett,P., Yan,Y.L., Huang,H., Postlethwait,J.H., and Talbot,W.S. (2000). A comparative map of the zebrafish genome. *Genome Res.* **10,** 1903-1914.

Woods,I.G., Wilson,C., Friedlander,B., Chang,P., Reyes,D.K., Nix,R., Kelly,P.D., Chu,F., Postlethwait,J.H., and Talbot,W.S. (2005). The zebrafish gene map defines ancestral vertebrate chromosomes. *Genome Res.* **15,** 1307-1314.

Woolf,A.S., Kolatsi-Joannou,M., Hardman,P., Andermarcher,E., Moorby,C., Fine,L.G., Jat,P.S., Noble,M.D., and Gherardi,E. (1995). Roles of hepatocyte growth factor/scatter factor and the met receptor in the early development of the metanephros. *J. Cell Biol.* **128,** 171-184.

Xiao,G.H., Jeffers,M., Bellacosa,A., Mitsuuchi,Y., Vande Woude,G.F., and Testa,J.R. (2001). Anti-apoptotic signaling by hepatocyte growth factor/Met via the phosphatidylinositol 3-kinase/Akt and mitogen-activated protein kinase pathways. *Proc. Natl. Acad. Sci. U. S. A* **98,** 247-252.

Xiaorui Wang. (2006/2007). Characterization of Hepatocyte Growth Factor (HGF) and its receptor c-met in zebrafish (Danio Rerio) embryonic development.

Xin,X., Yang,S., Ingle,G., Zlot,C., Rangell,L., Kowalski,J., Schwall,R., Ferrara,N., and Gerritsen,M.E. (2001). Hepatocyte growth factor enhances vascular endothelial growth factor-induced angiogenesis in vitro and in vivo. *Am. J. Pathol.* **158,** 1111-1120.

Yamamoto,K., Morishita,R., Hayashi,S., Matsushita,H., Nakagami,H., Moriguchi,A., Matsumoto,K., Nakamura,T., Kaneda,Y., and Ogihara,T. (2001). Contribution of Bcl-2, but not Bcl-xL and Bax, to antiapoptotic actions of hepatocyte growth factor in hypoxia-conditioned human endothelial cells. *Hypertension* **37,** 1341-1348.

Yamamoto,Y., Livet,J., Pollock,R.A., Garces,A., Arce,V., deLapeyriere,O., and Henderson,C.E. (1997). Hepatocyte growth factor (HGF/SF) is a muscle-derived survival factor for a subpopulation of embryonic motoneurons. *Development* **124,** 2903-2913.

Yang,X.M. and Park,M. (1993). Expression of the met/hepatocyte growth factor/scatter factor receptor and its ligand during differentiation of murine P19 embryonal carcinoma cells. *Dev. Biol.* **157,** 308-320.

Yang,X.M. and Park,M. (1995). Expression of the hepatocyte growth factor/scatter factor receptor tyrosine kinase is localized to epithelia in the adult mouse. *Lab Invest* **73,** 483-491.

Yang,X.M., Vogan,K., Gros,P., and Park,M. (1996). Expression of the met receptor tyrosine kinase in muscle progenitor cells in somites and limbs is absent in Splotch mice. *Development* **122,** 2163-2171.

Yang,Y., Spitzer,E., Meyer,D., Sachs,M., Niemann,C., Hartmann,G., Weidner,K.M., Birchmeier,C., and Birchmeier,W. (1995). Sequential requirement of hepatocyte growth factor and neuregulin in the morphogenesis and differentiation of the mammary gland. *J. Cell Biol.* **131,** 215-226.

Yant,J., Buluwela,L., Niranjan,B., Gusterson,B., and Kamalati,T. (1998). In vivo effects of hepatocyte growth factor/scatter factor on mouse mammary gland development. *Exp. Cell Res.* **241,** 476-481.

Yao,P., Zhan,Y., Xu,W., Li,C., Yue,P., Xu,C., Hu,D., Qu,C.K., and Yang,X. (2004). Hepatocyte growth factor-induced proliferation of hepatic stem-like cells depends on activation of NF-kappaB. *J. Hepatol.* **40,** 391-398.

Yi,S., Chen,J.R., Viallet,J., Schwall,R.H., Nakamura,T., and Tsao,M.S. (1998). Paracrine effects of hepatocyte growth factor/scatter factor on non-small-cell lung carcinoma cell lines. *Br. J. Cancer* **77,** 2162-2170.

Yu,C.Z., Hisha,H., Li,Y., Lian,Z., Nishino,T., Toki,J., Adachi,Y., Inaba,M., Fan,T.X., Jin,T. et al. (1998). Stimulatory effects of hepatocyte growth factor on hemopoiesis of SCF/c-kit system-deficient mice. *Stem Cells* **16,** 66-77.

Yu,Y. and Merlino,G. (2002). Constitutive c-Met signaling through a nonautocrine mechanism promotes metastasis in a transgenic transplantation model. *Cancer Res.* **62,** 2951-2956.

Zaret,K.S. (2002). Regulatory phases of early liver development: paradigms of organogenesis. *Nat. Rev. Genet.* **3,** 499-512.

Zarnegar,R. and Michalopoulos,G. (1989). Purification and biological characterization of human hepatopoietin A, a polypeptide growth factor for hepatocytes. *Cancer Res.* **49,** 3314-3320.

Zarnegar,R. and Michalopoulos,G.K. (1995). The many faces of hepatocyte growth factor: from hepatopoiesis to hematopoiesis. *J. Cell Biol.* **129,** 1177-1180.

Zeng,Q., Chen,S., You,Z., Yang,F., Carey,T.E., Saims,D., and Wang,C.Y. (2002). Hepatocyte growth factor inhibits anoikis in head and neck squamous cell carcinoma cells by activation of ERK and Akt signaling independent of NFkappa B. *J. Biol. Chem.* **277,** 25203-25208.

Zhang,Y.W., Su,Y., Volpert,O.V., and Vande Woude,G.F. (2003). Hepatocyte growth factor/scatter factor mediates angiogenesis through positive VEGF and negative thrombospondin 1 regulation. *Proc. Natl. Acad. Sci. U. S. A* **100,** 12718-12723.

Zhong,T.P., Kaphingst,K., Akella,U., Haldi,M., Lander,E.S., and Fishman,M.C. (1998). Zebrafish Genomic Library in Yeast Artificial Chromosomes. *Genomics* **48,** 136-138.

Zon,L.I. (1995). Developmental biology of hematopoiesis. *Blood* **86,** 2876-2891.

Zorn,A.M. and Mason,J. (2001). Gene expression in the embryonic Xenopus liver. *Mech. Dev.* **103,** 153-157.